



Improving the metal-on-metal hip prosthesis

A study of wear

James Kenneth Lord

**This thesis is submitted in partial fulfilment of the requirements for the
Degree of Doctor of Philosophy**

**Newcastle University
School of Mechanical and Systems Engineering**

August 2012

Abstract

Hip arthroplasty is an increasingly prevalent intervention, aimed at reducing pain and restoring function to patients suffering from common musculoskeletal diseases such as arthritis. Metal-on-metal (MoM) hip replacements were intended to be low-wear alternatives to conventional metal-on-polyethylene prostheses. Recent data has shown that revision rates for most MoM prostheses have not been as low as predicted and are not consistent across all models. Many failures result from complications arising from wear debris. Accurately quantifying wear has proved difficult.

Using a co-ordinate measuring machine, a method for measuring the wear of ex-vivo MoM hip prostheses was developed and validated as accurate to within 0.5mm^3 . The method was applied to bearing surfaces and, where available, the internal tapers of femoral heads. Overall, 143 MoM hip explants were measured (95 resurfacings, 48 total hip replacements). Median total wear rates were $4.17\text{mm}^3/\text{year}$ (mean=11.52, range= $0.30\text{--}87.28\text{mm}^3/\text{year}$), notably higher than most simulator estimates of $1\text{--}2\text{mm}^3/\text{million cycles}$. Large differences were noted between different models of MoM hip.

Time in vivo correlated with wear volume (SRCC=0.387, $p<0.001$) but not wear rate (SRCC=-0.086, $p=0.169$) suggesting that the prostheses wore at an unchanging rate through their lifetime. Acetabular cup inclination and anteversion correlated with wear volume (SRCC=0.414 and 0.233) and wear rate (SRCC=0.353 and 0.231, all $p<0.001$). Wear scars were consistently seen at the rim of the acetabular cup. The distance between these scars and the rim inversely correlated with volume (SRCC=-0.387, $p<0.001$) and rate (SRCC=-0.357, $p<0.001$). Patient blood metal ion levels were elevated (median $10.20\mu\text{g/ml Cr}$, $9.73\mu\text{g/ml Co}$) and correlated with wear volume ($p<0.001$).

Surface roughness measurements were taken on the bearing surfaces and theoretical lubrication regimes (λ -ratio) calculated. There was an inverse correlation between worn λ -ratio and wear volume ($p=0.038$).

Through these findings, recommendations are made for optimising future designs of hip prosthesis to minimise wear.

Dedication

To my dear wife, Sarah. For your continued support and for uprooting your life to the U.K. while I completed this work. Without you, I might never have had the impetus to write the following pages.

Acknowledgements

First and foremost, I must thank my supervisor, Professor Tom Joyce. Without Tom's support and guidance, this thesis would not have been possible. Not only did Tom first involve me in the study of hip prostheses, he has spent countless hours helping me to develop both my research and my writing.

I must also acknowledge the work of Drs David Langton and Tony Nargol. Besides sourcing a large number of the explants on which this work is based, the guidance of experienced orthopaedic surgeons has been invaluable. I would not have understood the clinical aspects of this work had they not been the ones to teach me. I particularly want to thank Dr Langton for teaching me how to operate the co-ordinate measuring machine, without which I would not have been able to collect the data contained herein.

There have been countless members of staff and fellow research students in this department who have taken time to show me various operating methods and analysis techniques. They are too numerous to name, but two stand out. Mr Harry Grigg, for teaching me to use the ZYGO NewView 5000 interferometer and for sharing his knowledge of Matlab programming and Mr Richard Morris for answering my endless questions on statistical analysis.

Finally, I wish to thank the Engineering and Physical Sciences Research Council for funding my involvement in this work.

Table of contents

List of figures	vi
List of tables	x
List of abbreviations	xii
List of symbols	xiv
Chapter 1. Introduction	1
1.1 The natural hip joint	1
1.1.1 <i>Structure</i>	1
1.1.2 <i>What can go wrong?</i>	4
1.2 Hip arthroplasty	6
1.2.1 <i>The prostheses</i>	6
1.3 Aims and objectives	12
1.4 Thesis outline	12
Chapter 2. Background and Literature Review	14
2.1 Survivorship of hip arthroplasty	14
2.2 Potential failure modes	21
2.2.1 <i>Loosening</i>	22
2.2.2 <i>Infection</i>	22
2.2.3 <i>Avascular necrosis</i>	23
2.2.4 <i>Fracture</i>	23
2.2.5 <i>Wear</i>	24
2.3 Measuring wear	26
2.3.1 <i>In vivo</i>	26
2.3.2 <i>In vitro</i>	27
2.3.3 <i>Ex vivo</i>	29
2.4 What might affect wear?	32
2.5 Summary	37
Chapter 3. Methods	39
3.1 Materials	39
3.2 Clinical data	39
3.3 Wear measurement	41
3.3.1 <i>Measurement procedure</i>	42
3.3.2 <i>Volumetric wear calculation</i>	46
3.3.3 <i>Validation</i>	52
3.3.4 <i>The wear scar</i>	53
3.4 Surface roughness	54
3.4.1 <i>Measurement procedure</i>	54
3.4.2 <i>Roughness parameters</i>	55
3.4.3 <i>Lubrication regime</i>	56
3.5 Analyses	57
Chapter 4. Results	59
4.1 Clinical data	59
4.2 Wear measurement validation	70
4.2.1 <i>Masterball</i>	70
4.2.2 <i>Gravimetric</i>	70
4.3 Retrieval analysis	74
4.3.1 <i>Wear</i>	74
4.3.2 <i>Surface roughness</i>	88
4.3.3 <i>Correlation</i>	96
Chapter 5. Discussion	99
5.1 Methodology	99

5.2 Clinical data	101
5.3 Wear	102
5.3.1 Duration in vivo	105
5.3.2 Acetabular cup orientation	106
5.3.3 Coverage arc and CPR distance	108
5.3.4 Component diameter	110
5.3.5 Radial clearance	112
5.3.6 Metal ion concentration	113
5.4 Simulators	114
5.5 Surface roughness and lubrication	116
5.6 The taper junction	123
Chapter 6. Conclusions and future work	126
6.1 Conclusions	126
6.2 Future work	129
References	132

List of figures

Figure 1.1: Bone structure of the hip joint. Image courtesy and copyright Primal Pictures Ltd.	2
Figure 1.2: Image of the acetabulum, showing the connections of the three supporting ligaments. Image courtesy and copyright Primal Pictures Ltd.	3
Figure 1.3: The main movements made at the hip joint. From left to right: abduction/adduction, flexion/extension, lateral rotation, medial rotation.....	4
Figure 1.4: An example of the Charnley Hip Prosthesis showing the angled femoral stainless steel stem, the 7/8” femoral head and the PE acetabular cup. 7	
Figure 1.5: The Pinnacle® acetabular cup system, with a metal lining, a 36mm CoCrMo femoral head and a titanium stem. Note the internal taper of the head, which connects to the trunnion at the proximal end of the stem.....	9
Figure 1.6: An image of a 51mm diameter Birmingham Hip Resurfacing (BHR) femoral head. Note the shorter stem and hollow interior section to allow the prosthesis to cap the natural femoral head.	10
Figure 2.1: Revision rate against years in vivo for four models of hip resurfacing, taken from the literature and compared with the mean revision rate/year found for MoP THR (solid line). Size of bubble indicates study cohort size (labelled). Take care to note that the scales are different for each graph. The solid black line represents the same data on all graphs.	19
Figure 2.2: Revision rate against years in vivo for two models of hip resurfacing and two models of MoM THR, taken from the literature and compared with the mean revision rate/year found for MoP THR (solid line). Size of bubble indicates study cohort size (labelled). Take care to note that the scales are different for each graph. The solid black line represents the same data on all graphs.	20
Figure 2.3: Retrieval rate for nine models of hip replacement taken from the literature (table 2.2) and averaged to give the mean retrieval rate per year, across all sources.....	21
Figure 2.4: Left: Radiographic image of a right-side THR prosthesis, with the inclination angle (IA) marked. Right: Model of a right-side acetabular cup at 45° inclination and (A) 0° anteversion, (B) 10° retroversion (tilted towards the posterior), (C) 10° anteversion (tilted towards the anterior).	32
Figure 2.5: A typical Stribeck curve, showing the transition from boundary to fluid-film lubrication.	34
Figure 2.6: Figure shows a simplified image of a resurfacing femoral head and acetabular cup, indicating a 2-dimensional hip contact force vector (blue arrow) and the CPR distance (red arc). It should be clear how reduced coverage arc, smaller radius and/or increased cup orientation reduces the CPR distance.	36
Figure 3.1: Acetabular inclination and version. θ : inclination angle, a: anteversion angle, b: alternative plane of reference.....	41
Figure 3.2: Samples were held in a chuck to prevent movement during the scanning process.	43
Figure 3.3: Left: Image of an internal taper, with the point of origin of the CMM scan marked (red cross). Right: Cross-section of an internal taper, with the point of origin marked (red dot).....	45
Figure 3.4: Examples of the CMM output for (left to right) a femoral head, acetabular cup, and femoral taper. Deep red represents the highest wear, while deep blue represents unworn surface. Colour scales represent deviation from the modal radius, where 100% = 20 μ m.	46
Figure 3.5: An example of the raw data produced from the CMM measurements.	46

Figure 3.6: Examples of the wireframe surfaces created in Matlab using the coordinate data from the CMM.	47
Figure 3.7: Examples of the histograms of measured radii created for a femoral head (left) and acetabular cup (right). Horizontal axis shows deviation between measured radius and calculated unworn radius (mm). Vertical axis shows number of points. Note the high concentration of points around the '0' marks (the original radius) and long tails representing wear. Note also that for femoral heads the tail is to the left, representing a reduction in radius after material loss. For the acetabular cups the tail is to the right, representing an increase in radius after material loss.	48
Figure 3.8: Calculation of the unworn radius, R_1 , at any height, Z_1 , for a femoral taper given a known radius at one end, R_0 .	49
Figure 3.9: Calculation of the area of any irregular quadrilateral.	50
Figure 3.10: Examples of the Matlab output for (left to right) the femoral head, acetabular cup, and femoral taper seen in figure 3.4. Deep red represents the highest wear, while deep blue represents unworn surface. Colour scales represent linear wear depth in mm.	51
Figure 3.11: Calculating the angle between the component centreline and the point of maximum wear depth.	54
Figure 4.1: Boxplot of the acetabular cup inclination angle for each model of hip prosthesis (left) and each diagnosis (right).	64
Figure 4.2: Boxplot of the acetabular cup anteversion angle for each model of hip prosthesis (left) and each diagnosis (right).	64
Figure 4.3: Boxplot of CPR distance for each model of hip prosthesis (top) and each revision diagnosis (bottom). CPR distance is individual to each prosthesis and depends on diameter and cup orientation, as well as coverage arc.	67
Figure 4.4: Boxplots of Cr and Co ion levels in the blood and serum for each model of hip prosthesis.	69
Figure 4.5: Boxplots of Cr and Co ion levels in the blood and serum for each retrieval diagnosis.	69
Figure 4.6: Histogram of the masterball scan. Distribution was evaluated and is Gaussian. Minimum point = $-1.2\mu\text{m}$. Maximum point = $+1.3\mu\text{m}$. Positive 'linear wear depth' indicates manufacturing form and the ability of the CMM wear measurement methodology to identify this. Calculated wear volume = 0.04mm^3 .	71
Figure 4.7: Errors in the Matlab volumetric wear calculation when compared with gravimetric methods for all four validation components. Each set of three measurement numbers (separated by gray vertical lines) corresponds to a level of material removal.	74
Figure 4.8: A comparison of the effect of changing the number of data points collected with the CMM. Images produced are from the 48mm ASR™ validation head when taking 1458 points (left), 5832 points (centre, current method) and 23328 points (right).	75
Figure 4.9: Linear wear depth, split by model of prosthesis (left) and by diagnosis for retrieval (right). Stacks show median depth and are split by contribution of heads and cups.	80
Figure 4.10: Median wear volumes for each model of prosthesis (left) and by diagnosis for retrieval (right). Stacks show total median wear volume and are split by contribution of heads, cups and tapers. Only THRs (ASR™ XL and Pinnacle®) have tapers.	80
Figure 4.11: Median wear rates for each model of prosthesis. Stacks show total median wear rate and are split by contribution of heads, cups and tapers.	84

Figure 4.12: Measured radial clearance, split by prosthesis model (left) and diagnosis for retrieval (right).	84
Figure 4.13: Location of maximum linear wear on femoral heads and acetabular cups, split by model of prosthesis (left) and by diagnosis for revision (right). Angles are relative to the centre point of each component.	86
Figure 4.14: Location of maximum linear wear on acetabular cups, in comparison to the rim of the cup split by model of prosthesis (left) and by diagnosis for revision (right).	86
Figure 4.15: Percentage of surface area worn on femoral heads and acetabular cups, split by model of prosthesis (left) and by diagnosis for revision (right).	87
Figure 4.16: Roughness measurements in the unworn regions of the femoral heads, split by model of prosthesis.	92
Figure 4.17: Roughness measurements in the worn regions of the femoral heads, split by model of prosthesis.	92
Figure 4.18: Roughness measurements in the unworn regions of the acetabular cups, split by model of prosthesis.	93
Figure 4.19: Roughness measurements in the worn regions of the acetabular cups, split by model of prosthesis.	93
Figure 4.20: Boxplots of unworn (left) and worn (right) λ -ratios, split by model of prosthesis (top) and diagnosis for retrieval (bottom).	95
Figure 5.1: Revision rate per year (taken from the literature in table 2.2) and median volumetric wear (measured in the present study) for all eight models of hip prosthesis considered.	103
Figure 5.2: The effects of inclination and anteversion on total bearing surface wear rate.	107
Figure 5.3: Coverage arc and measured volumetric wear for each of the eight models of hip prosthesis.	109
Figure 5.4: Coverage arc and CPR distance for each of the eight models of hip prosthesis.	109
Figure 5.5: Effect of cup inclination angle and component diameter on CPR distance for cup coverage arc of 180° and anteversion of 10°.	110
Figure 5.6: The effect of prosthesis diameter on bearing surface wear rate.	111
Figure 5.7: Radial clearance against wear volume for all 143 retrieved prostheses.	112
Figure 5.8: Blood metal ion concentrations per mm ³ of wear for 7 of the 8 models studied. Adept® (3.4µg/l per mm ³) has been left out to improve clarity.	114
Figure 5.9: Two- and three-dimensional images of the typical unworn surface of a BHR™ (top) and Conserve® + (bottom) femoral head. Note the apparent carbides protruding from the surface of the as-cast BHR, resulting in an initially higher RMS (0.016µm) than the Conserve® (0.008µm).	117
Figure 5.10: Images of the unworn regions of femoral heads of the 8 models of MoM hip prosthesis. From top to bottom: Left; Adept®, BHR™, Pinnacle® (all cast), Durom™ (wrought). Right; ASR™ (cast with heat treated cup), ASR™ XL, Conserve® +, Cormet™ (All heat treated following casting).	119
Figure 5.11: Images of the worn regions of femoral heads of the 8 models of MoM hip prosthesis. From top to bottom: Left; Adept®, BHR™, Pinnacle® (all cast), Durom™ (wrought). Right; ASR™ (cast with heat treated cup), ASR™ XL, Conserve® +, Cormet™ (All heat treated following casting).	120
Figure 5.12: Image of a Cormet™ femoral head exhibiting pitting (approximate depth 0.2µm), with narrow scratches of similar depth originating at some of the pits.	121

Figure 5.13: Median λ -ratios in the worn regions as a percentage of those in the unworn regions for as-cast (blue), heat-treated (red) and wrought (yellow) models.....	122
Figure 5.14: The effect on bearing surface wear rate of heat treating hip prostheses ($n = 84$) compared with as cast ($n = 41$) or wrought ($n = 5$) models.	122
Figure 5.15: Typical image of a worn femoral head internal taper with wear indicated by dark red. There is a clear demarcation at (C) between the unworn area (A) and the worn area (B).	125

List of tables

Table 1.1: Typical values of range of motion in a healthy human hip joint [2-4].	4
Table 1.2: The key design characteristics of six of the most common hip resurfacing brands.	11
Table 2.1: Revision rates for the four classifications of hip prostheses, taken from joint registries around the world.	16
Table 2.2: Revision rates for six common hip resurfacing brands, two common LHMOM THR brands, and MoP THR overall for comparison.	18
Table 2.3: Wear rates for MoM hip prostheses, measured from simulator studies. Ranges represent the difference between “steady-state” and “bedding-in” wear.	28
Table 2.4: Summary of previous CMM based volumetric wear calculations for explanted MoM hip prostheses.	30
Table 3.1: Detail of the 273 retrieved MoM hip prosthesis components analysed in this study, broken down by model.	40
Table 3.2: Detail of the 273 retrieved MoM hip prosthesis components analysed in this study, broken down by reason for revision surgery.	40
Table 4.1: Breakdown of the recorded clinical data by prosthesis model.	61
Table 4.2: Breakdown of implantation angle, contact point to rim (CPR) distance and patient metal ion levels at the time of revision surgery.	66
Table 4.3: Measurement of the ceramic masterball indicating the size of the errors in the presented wear measurement method. Note: actual size supplied with masterball; difference in radius of 0.4µm is within claimed accuracy of Legex 322 (0.9µm)	70
Table 4.4: Comparison of Matlab method to gravimetric method. Mean volume is the mean of the 3 measurements at each stage. Mean absolute error is the mean of the error of the 3 measurements. St. Dev. = Standard deviation.	72
Table 4.5: Comparison of Matlab method to gravimetric method. Mean volume is the mean of the 3 measurements at each stage. Mean absolute error is the mean of the error of the 3 measurements. St. Dev. = Standard deviation.	72
Table 4.6: Comparison of Matlab method to gravimetric method. Mean volume is the mean of the 3 measurements at each stage. Mean absolute error is the mean of the error of the 3 measurements. St. Dev. = Standard deviation.	73
Table 4.7: Comparison of Matlab method to gravimetric method. Mean volume is the mean of the 3 measurements at each stage. Mean absolute error is the mean of the error of the 3 measurements. St. Dev. = Standard deviation.	73
Table 4.8: The effect of changing the number of data points collected on the measured radius, maximum wear depth and wear volume. Wear volume recorded gravimetrically = 12.964mm ³ .	76
Table 4.9: Measured wear data, split by model of prosthesis.	79
Table 4.10: Measured diameter, prosthesis clearance and wear scar location and coverage, split by model of prosthesis.	83
Table 4.11: Surface roughness measurements in the unworn and worn regions of retrieved femoral heads and acetabular cups, split by model of prosthesis.	91
Table 4.12: Unworn and worn region λ-ratios, split by prosthesis model.	95
Table 4.13: Spearman’s Rank Correlation Coefficients (SRCC) between nine controllable factors and six measures of bearing surface wear. Significant positive correlations are highlighted in green. Significant negative correlations are highlighted in pink.	97

Table 4.14: Spearman’s Rank Correlation Coefficients (SRCC) between seven controllable factors and three measures of taper wear. Significant positive correlations are highlighted in green.98

List of abbreviations

- ALVAL:** Aseptic Lymphocytic Vasculitis Associated Lesions.
- AOA:** Australian Orthopaedic Association.
- AOA NJRR:** Australian Orthopaedic Association National Joint Replacement Registry.
- ARMD:** Adverse Reactions to Metal Debris.
- ASR:** Articular Surface Replacement.
- AVN:** Avascular Necrosis.
- BHR:** Birmingham Hip Resurfacing.
- BMI:** Body Mass Index.
- CJRR:** Canadian Joint Replacement Registry.
- CMM:** Co-ordinate Measuring Machine.
- CoCrMo:** Cobalt-Chromium-Molybdenum.
- CPR:** Contact Patch to Rim.
- EBRA:** Einzel-Bild-Roentgen-Analyse.
- GPS:** Geometrical product specifications.
- HHS:** Harris Hip Score.
- HRA:** Hip Resurfacing Arthroplasty.
- ICPMS:** Inductively Coupled Plasma Mass Spectrometry.
- ISO:** International Standards Organization.
- LHMoM:** Large Head Metal-on-Metal.
- MHRA:** Medicines and Healthcare Products Regulatory Agency.
- MoM:** Metal-on-Metal.
- MoP:** Metal-on-Polyethylene.
- NAR:** Norwegian Arthroplasty Register.
- NHS:** National Health Service.
- NICE:** National Institute for Clinical Excellence.
- NJR:** National Joint Registry for England and Wales.
- NZNJR:** New Zealand National Joint Registry.
- OHS:** Oxford Hip Score.
- PE:** Polyethylene.
- PMMA:** Polymethylmethacrylate.
- PTFE:** Polytetrafluoroethylene.
- SHAR:** Swedish Hip Arthroplasty Register.
- SRCC:** Spearman's Rank Correlation Coefficient.

THR: Total Hip Replacement.

U.K.: United Kingdom.

U.S.A: United States of America.

XLPE: Cross-Linked Polyethylene.

List of symbols

- A_W**: Worn surface area of component (mm^2).
- A_T**: Total surface area of component (mm^2).
- d**: Diameter (m).
- E**: Young's Modulus (Pa).
- E***: Equivalent elastic modulus (Pa).
- H**: Hardness (N/mm^2).
- h_{min}**: Minimum effective film thickness (m).
- L**: Sliding distance (mm).
- PV**: Peak-to-Valley distance (surface roughness) (μm).
- r**: Radius (mm).
- Ra**: Surface Roughness Average (μm).
- RMS**: Surface Root Mean Square Roughness (μm).
- Rsk**: Surface Skewness.
- R_x**: Equivalent Radius (m).
- u**: Entraining Velocity (ms^{-1}).
- V**: Wear volume (mm^3).
- w**: Load (N).
- η** : Viscosity ($Pa\ s$).
- ω** : Angular velocity (rad/s).
- θ** : Angle ($^\circ$).
- v**: Poisson's ratio.

Chapter 1. Introduction

This thesis is concerned with the science of artificial hip joint replacement. It looks specifically at the failure of some of the most contemporary models of hip prostheses and attempts to understand and explain the causes of failure. Through this, recommendations are made to minimise such failures in the future. The causes of hip prosthesis failure may be mechanical, surgical and/or biological in nature, and will be discussed in greater depth in Chapter 2, Background and Literature Review. However, as this is an engineering PhD, specific attention is given to the wear of hip prostheses and how wear affects performance and survivorship.

Before an in depth study may be undertaken, however, it is important to understand exactly what hip prostheses are and why they are used. In turn, knowledge of the natural hip joint is imperative. Only then is it possible to fully understand the complications that can lead to hip joint replacement surgery and the important features of the natural joint that a hip prosthesis must replicate in order to be successful. Following this will be a brief discussion of the history of hip replacement, along with the main concerns that led to the evolution and development of the latest designs.

1.1 The natural hip joint

The acetabulofemoral joint, commonly known as the hip joint, is formed where the femur meets the pelvic bone. Specifically, there is an articulation between the acetabulum of the pelvic bone and the femoral head (figure 1.1). It connects the lower limbs to the axial skeleton and is essential for both weight bearing and locomotion.

1.1.1 Structure

The following description of the structure of the hip joint is summarised from Gray's Anatomy for Students [1]. The pelvic bone is actually formed of three bones - the ischium, the pubis and the ilium - though these fuse into a single bone by adulthood. At the connection of these bones is the acetabulum, a deep cup-shaped cavity in the pelvic bone. The acetabulum is coated in a thin layer of hyaline cartilage, typically 1 – 7mm thick, which acts to separate the bony surfaces and provide a layer promoting low friction movement.

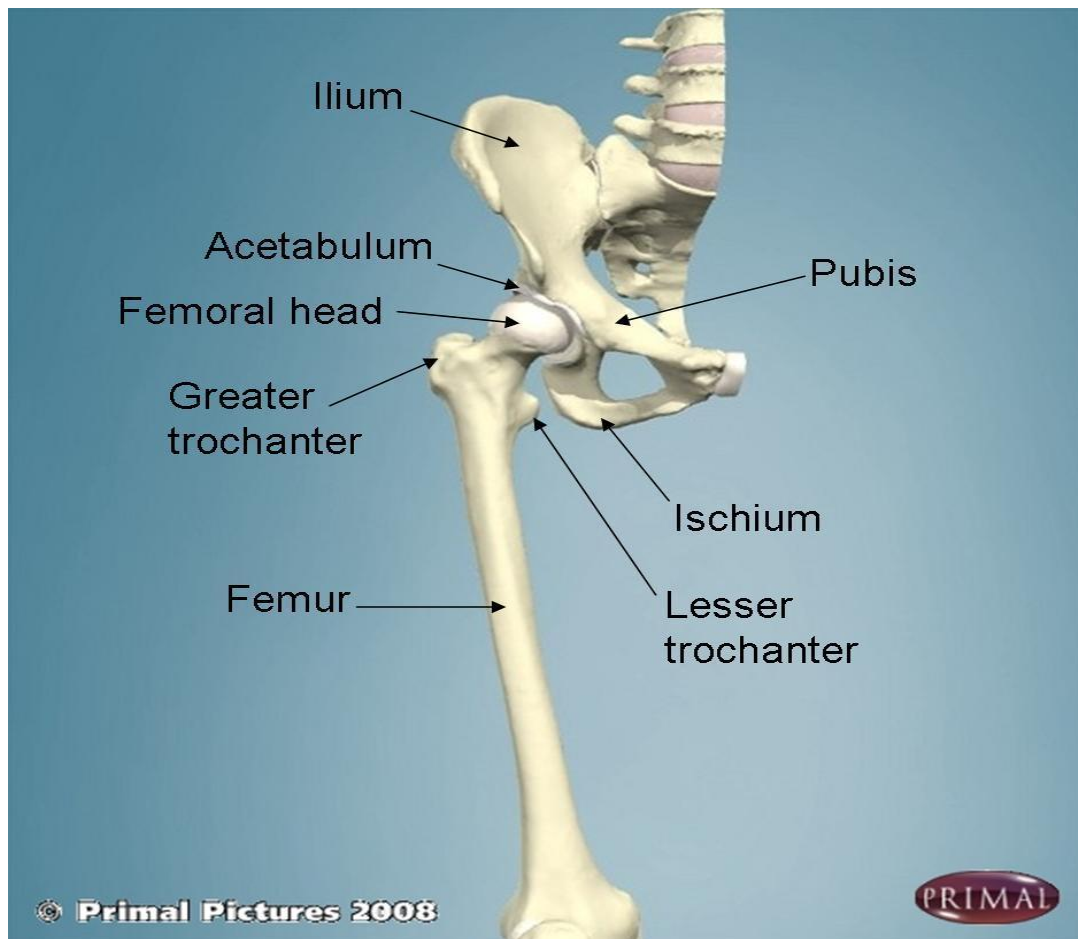


Figure 1.1: Bone structure of the hip joint. Image courtesy and copyright Primal Pictures Ltd.

The femur, or thigh bone, comprises a long shaft which joins to the acetabulum at the proximal end and the tibia at the knee joint at the distal end. At the proximal end, attachment sites for the muscles which move the hip joint are located on the greater and lesser trochanter (figure 1.1). There is a short projection of bone from the shaft known as the femoral neck. The angle of the femoral neck allows for increased range of motion at the hip joint without impingement of bones. Finally, the femoral neck ends in a roughly hemispherical shape, known as the femoral head. This is also coated in a thin layer of hyaline cartilage.

At the articular surface, the femoral head is covered by the acetabulum. A synovial membrane encloses the articulation and produces synovial fluid. Synovial fluid acts to lubricate the joint as well as remove substances from the articular cavity. Completely surrounding the hip joint is a joint capsule which attaches at the acetabulum and the femoral neck. In three places this joint

capsule thickens to form ligaments; the ischiofemoral ligament, the iliofemoral ligament and the pubofemoral ligament. These ligaments limit the movement of the hip joint and act to stabilise the joint (figure 1.2).

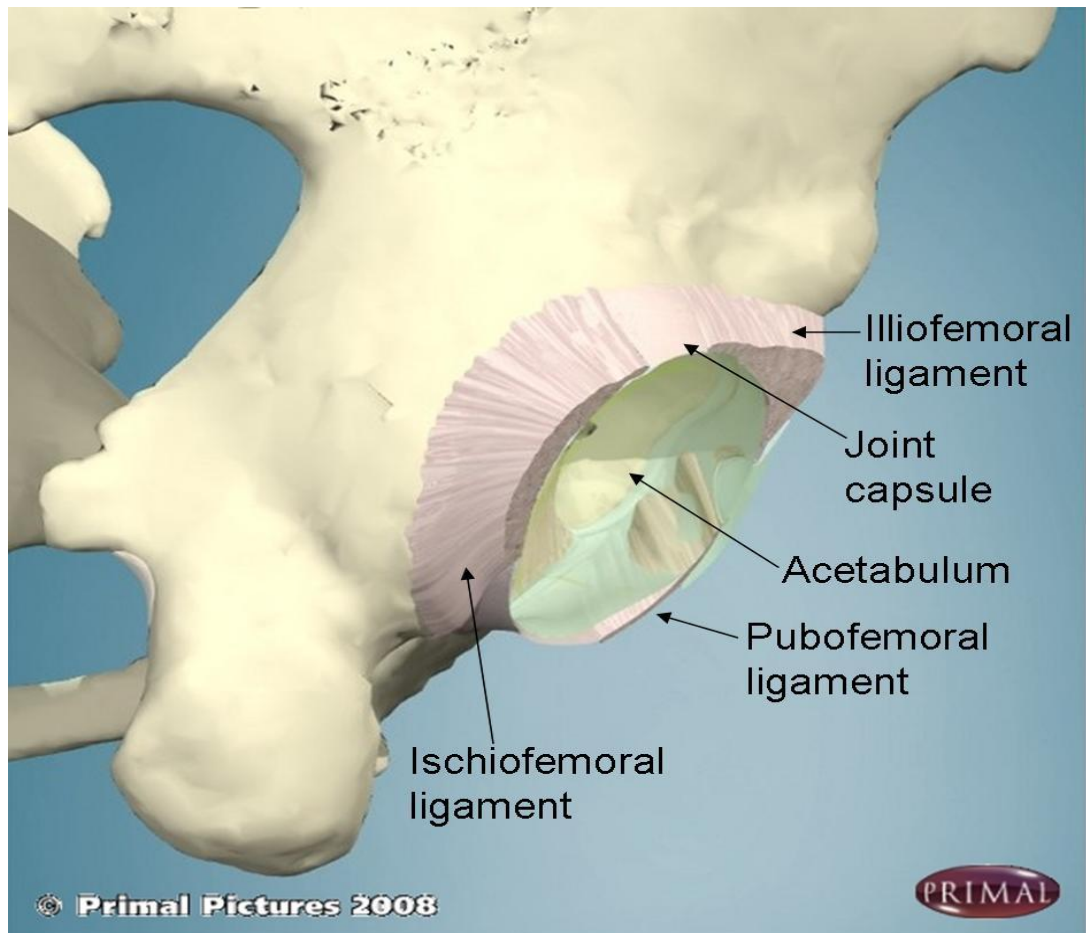


Figure 1.2: Image of the acetabulum, showing the connections of the three supporting ligaments. Image courtesy and copyright Primal Pictures Ltd.

The hip joint is known as a ball and socket joint, due to the shape of the articulating surfaces. This type of joint allows for movement in multiple directions and is therefore defined as multi-axial. Movements at the hip include flexion and extension, abduction and adduction, and medial and lateral rotation (figure 1.3). These movements are achieved by a series of muscles originating at the pelvis and inserting at the femur. Typical range of motion in a healthy human is shown in table 1.1 [2-4]

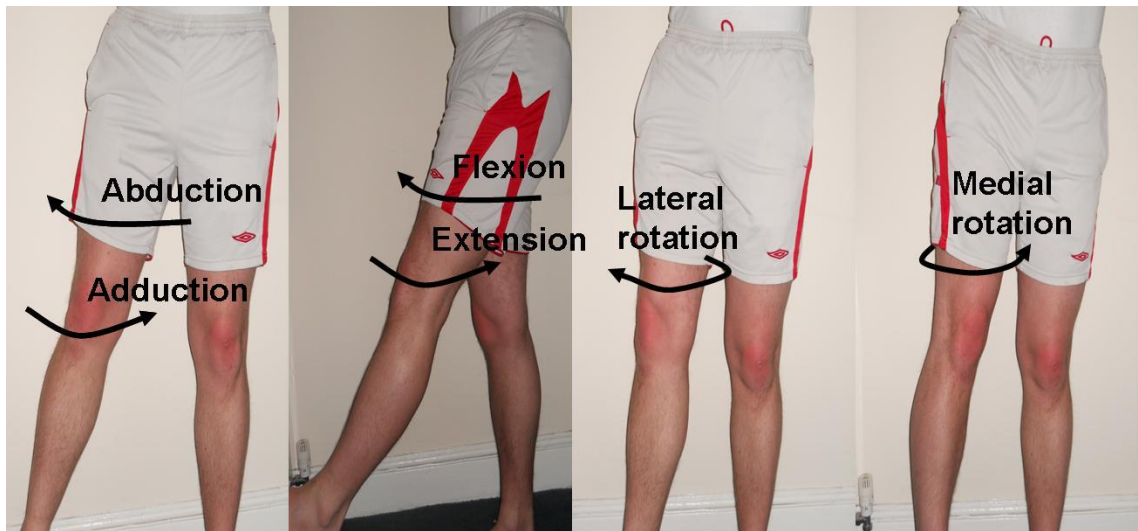


Figure 1.3: *The main movements made at the hip joint. From left to right: abduction/adduction, flexion/extension, lateral rotation, medial rotation.*

Flexion	Extension	Medial rotation	Lateral rotation	Abduction	Adduction
115° - 125°	10° - 30°	30° - 40°	30° - 45°	40° - 50°	30° - 35°

Table 1.1: *Typical values of range of motion in a healthy human hip joint [2-4].*

1.1.2 What can go wrong?

There are many possible complications that can arise at the hip joint and indicate a possible requirement for hip replacement. By far the most common indicator is osteoarthritis, accounting for 93% of procedures in the U.K. [5], 88.8% in Australia [6] and 85% in Sweden [7] in the most recent annual registries. Osteoarthritis occurs where there is a breakdown of the joint's cartilage. This is commonly due to erosion over time and, as such, is much more common in the elderly [8]. As well as age, genetics [8, 9] and high body mass index (BMI) [8, 10, 11] are considered risk factors and osteoarthritis is estimated by the National Health Service (NHS) to affect over 9 million people in the U.K. [12] (approximately 15% of the population [13]). It may also develop in younger patients as a result of unusually high activity levels [14] (e.g. professional athletes) or from trauma and injury [11]. The condition is degenerative and, whatever the cause, osteoarthritis can eventually lead to bone on bone articulation, as well as inflammation from cartilage debris [15]. It is also common for the affected joint to become less mobile as the osteoarthritis develops. Patients therefore commonly present with chronic pain and joint immobility, both of which severely impair the patient's quality of life. Although

initially attempts are made to treat the symptoms of osteoarthritis using measures such as painkillers and physiotherapy, the disease is progressive and may eventually require replacement of the affected joint [8].

A related disorder called rheumatoid arthritis [16, 17] is less common, but equally, if not more, debilitating. In this case the presenting symptoms are similar to osteoarthritis but they are caused by an autoimmune disease causing the body's immune system to attack its own tissue.

Other common reasons for hip replacement include fracture of the femoral neck and avascular necrosis (each accounting for 2% of hip arthroplasties in the U.K. in 2010 [5]). Fractures typically occur as a result of trauma, though this may be exacerbated by diseases such as osteoporosis [18], leading to decreased bone mass and therefore weakened bone. Fractures of the femoral neck are typically treated with internal fixation of the fracture using an orthosis such as bone screws. Although most fractures will heal with little long-term damage, complications can arise from poor re-alignment of the affected bone(s), infection or movement during healing. Given a healing time of up to 5 or 6 months [19, 20], during which time the affected area must remain immobile, along with the risk of complications, such fractures are sometimes treated with a hip replacement. This may be either at the initial surgery instead of implanting an orthosis, or after complications arise.

Avascular necrosis is caused by interrupted blood supply to the bone and leads to bone death. As well as occurring secondary to trauma, risk factors include use of corticosteroids, alcohol and smoking [21]. Avascular necrosis is progressive and patients again present with pain and immobility. Therefore, while early treatment may involve the avoidance of weight bearing, core decompression (an operation to reduce the pressure around the affected bone, allowing blood to flow more freely) [22, 23] and the transplantation of bone marrow [24, 25], hip replacement is typically necessary in the months or years following these procedures [25, 26].

1.2 Hip arthroplasty

As noted above, hip arthroplasty (the surgical replacement of the hip joint with an alternative material) may be carried out for a number of reasons. Whatever the primary diagnosis, however, the aims of hip arthroplasty remain the same. Broadly, these are to remove the pain associated with the above disorders and to restore movement at the damaged joint. Given the stated aims of treating pain and restoring motion, successful hip prostheses should attempt to recreate the shape and function of the natural hip joint to allow a similar range of pain-free motion.

Hip arthroplasty is an increasingly popular intervention. There were 76,759 such operations carried out in the U.K. in 2010 [5], a 6% increase from 2009 [27]. Of these, 7,852 operations were revision procedures, a revision 'burden' of 10.2%. From a second source, there were 35,996 hip replacement operations in Australia in the same time period [6], an increase of 3.6% from 2009 [28]. Revision operations accounted for 11.2% of these. In Sweden, there were 18,132 hip replacement operations in 2010. This was a 0.6% increase from 2009 and a 9.6% increase from 2008. Of the 18,132 operations in 2010, 2197 were revision procedures, a burden of 12.1% [7]. Tens of thousands of hip replacement operations are also reported in other countries across the world each year [29].

Given the large numbers of patients involved, it is essential that complications are kept to a minimum. Problems arising in hip prostheses are not only painful for the patient, but can necessitate expensive and time consuming follow-up and revision surgeries. Indeed, the American Academy of Orthopaedic Surgeons recently estimated that "a modest 2% decrease in the U.S. revision rate [of hip and knee replacements] would yield a savings of \$65.2 million in one year" [30].

1.2.1 The prostheses

Hip arthroplasty may be traced back over 100 years to the work of Themistocles Glück [31]. In 1891, Glück described the use of an ivory prosthesis that was fixed to the femur using nickel-plated screws. Many attempts at developing a successful hip prosthesis followed using a variety of materials, from acrylic [32]

to cobalt-chrome alloy [33] to stainless steel [34]. However, survivorship was often limited [35] and the modern prosthesis in a form that would be recognised today owes much to the work of John Charnley.

In the 1960s, Charnley developed what is now known as the Charnley Hip Prosthesis, a device consisting of a femoral component and an acetabular component (figure 1.4).



Figure 1.4: *An example of the Charnley Hip Prosthesis showing the angled femoral stainless steel stem, the 7/8" femoral head and the PE acetabular cup.*

The Charnley prosthesis was designed to completely replace a damaged hip joint and, as such, is known as a total hip replacement (THR). The single-piece femoral component was made of stainless steel and comprised a stem that was implanted into the femur with a roughly hemi-spherical ball atop the stem designed to replace the natural femoral head. The stem was similar in shape to a natural femur, including an angled protrusion to replicate the femoral neck. Amidst concerns that a larger femoral head would lead to a higher frictional torque at the bearing surface and also potentially produce more wear debris, Charnley opted for a relatively small diameter of 22.225mm ($\frac{7}{8}$ inch) [36]. The stainless steel stem was cemented in place. Recognising the need for a material "with a low coefficient of friction which at the same time could be tolerated in body tissue", the acetabular component was made of polytetrafluoroethylene (PTFE). Fixation of this cup was achieved by either

cement or press fit [36]. In this way the patients' damaged cartilage was removed and bone-on-bone contact was prevented, providing pain relief. Subsequent designs utilized a polyethylene cup instead of PTFE. Due to the polyethylene cup articulating against a steel head, this is an example of a metal-on-polyethylene (MoP) prosthesis. The metal and polymeric surfaces replaced not just the bone but also the removed hyaline cartilage. The basic ball and socket hip joint was recreated, allowing for reasonable range of motion. Charnley noted that recovery time was quick and that within a week patients would recover their preoperative range of motion [36]. In patients with severe arthritis, preoperative range of motion was low and postoperative values might not reach above 30°, but the motion was painless [36]. Studies have reported flexion of up to 110° using the Charnley prosthesis [37], close to the 115° – 125° seen in healthy hips.

Around the same time as Charnley was developing his MoP prosthesis, other designers were considering alternative bearing surfaces. Between 1956 and 1960, the first series of McKee-Farrar prostheses were implanted in Norwich, England [38]. At 41.275mm diameter (1⁵/₈ inch) the McKee-Farrar prosthesis was larger than the Charnley Hip Prosthesis and both the femoral head and acetabular cup were manufactured from cobalt-chromium alloy (CoCrMo). Earlier attempts had been made using an all stainless steel articulation, but these were found to loosen and require removal soon after implantation [38]. This was the first case of what would be recognised today as a metal-on-metal (MoM) hip prosthesis. Unlike the Charnley prosthesis, fixation was initially achieved using cobalt-chrome screws. However, following Charnley's success with polymethylmethacrylate (PMMA) cement in 1960, later McKee-Farrar prostheses were also fixed with cement.

Over the following decades, new hip prostheses were introduced. Often, such prostheses would offer slight variations on the existing designs with the intention of improving survivorship, easing surgery and/or improving patient recovery time and range of motion. Unlike earlier 'monoblock' designs, such as the Charnley and McKee-Farrar, 'modular' designs have femoral heads that are separate from the stems (although note that modular designs can also refer to acetabular cups where a different liner can be fitted into the cup shell). This

change potentially allows more customisation during surgery. Modular prostheses attach at the taper of the head and the trunnion of the stem (figure 1.5). One such contemporary prosthesis is the Pinnacle® Acetabular Cup System (DePuy Orthopaedics, Warsaw, IN, USA), the market leader in the U.K. in terms of uncemented hips with a market share of approximately 34% [5]. The Pinnacle® consists of a titanium alloy acetabular shell with a coverage arc of 180°. It may be fitted with a 36mm internal diameter liner made of CoCrMo, polyethylene or ceramic. The liner articulates against a femoral head, which again may be metal or ceramic, with a typical radial clearance between the components of 40-60µm [39].



Figure 1.5: *The Pinnacle® acetabular cup system, with a metal lining, a 36mm CoCrMo femoral head and a titanium stem. Note the internal taper of the head, which connects to the trunnion at the proximal end of the stem.*

Recent developments of MoM THR have seen an increase in diameter of the femoral component. These large head metal-on-metal (LHMoM) prostheses were intended to reduce the risk of dislocation [40, 41] and increase range of motion [42]. Further, larger femoral head diameters have been shown to improve lubrication and subsequently reduce wear rate in simulator studies of MoM hip replacements [43, 44]. Use of larger head sizes is increasing rapidly

and, defining large head as $\geq 36\text{mm}$, accounted for 28% of primary hip replacements in the U.K. in 2010, up from 14% in 2007 and just 1% in 2003 [5].

In the 1990s, a particularly different design was developed [45]. While previous hip prostheses were designed to completely replace the damaged joint, this new design was intended to replace only the articular surface. While the acetabular component of such designs remained largely the same as earlier prostheses, these so called hip resurfacing arthroplasties (HRA) consisted of a femoral component which, sitting atop a short stem, capped the femoral head rather than replacing it (figure 1.6).

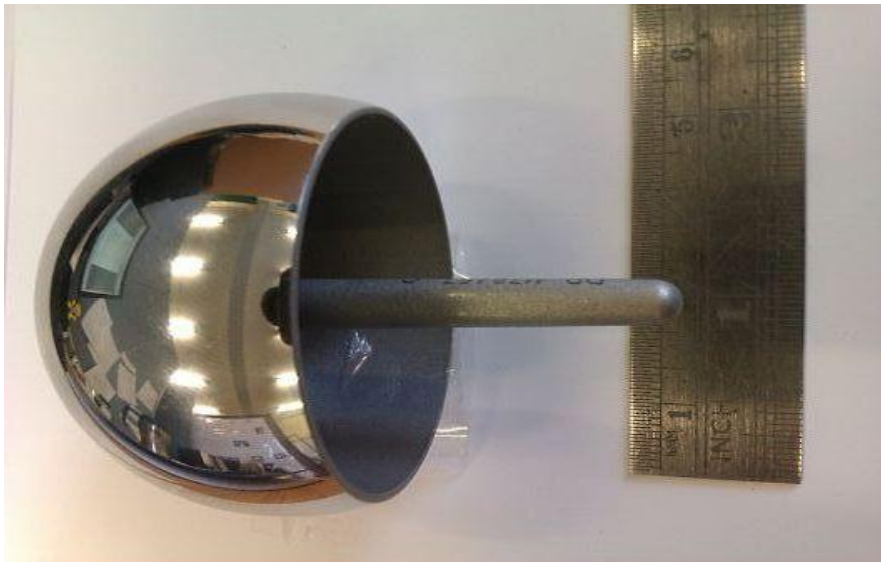


Figure 1.6: An image of a 51mm diameter Birmingham Hip Resurfacing (BHR) femoral head. Note the shorter stem and hollow interior section to allow the prosthesis to cap the natural femoral head.

Resurfacing the femoral head still provided a separation of bone-on-bone contact and subsequent pain relief and HRA was also thought to more closely replicate the natural hip joint [46]. Resurfacing is considered to offer other theoretical advantages over THR. These included preservation of femoral bone which would ease any revision operation [46, 47], improved function and greater range of motion [48-50], more physiological load transfer [51], and improved lubrication characteristics [52]. Further, the increase in head size associated with HRA decreased the risk of dislocations that had been associated with THR [48, 53]. Many different hip resurfacing prostheses are now available. Each device differs in size, shape and method of manufacture. The most popular designs and their key characteristics are outlined in table 1.2.

Prosthesis	Adept® [54]	Articular Surface Replacement™ (ASR) [55]	Birmingham Hip Resurfacing™ (BHR) [56]	Conserve® Plus (C+) [57]	Cormet™ [58]	Durom™ [54]
Manufacturer	Finsbury Orthopaedics	DePuy Orthopaedics	Smith & Nephew	Wright Medical	Corin	Zimmer
Approx. U.K. market share (%) [5]	9.8	9.2	50.8	3.6	11.2	5.0
Manufacturing method and treatment [51]	Cast	Cast HIP ¹ /SA ² cup	Cast	Cast HIP ¹ /SA ² head HIP ¹ /SA ² cup	Cast HIP ¹ /SA ² head HIP ¹ /SA ² cup	Wrought
Size range (mm)	Head: 40 – 58 Cup: 46 – 64	Head: 41 – 55 Cup: 46 – 64	Head: 38 – 58 Cup: 44 – 66	Head: 36 – 56 Cup: 44 – 64	Head: 40 – 56 Cup: 46 -64	Head: 38 – 60 Cup: 46 – 68
Radial clearance (µm) [51]	85	50	100	80	100	75
Coverage arc (°)	160	148 – 160	158 – 166	162 – 165	156 – 166	Up to 166

¹HIP = Hot isostatic pressurisation

²SA = Surface annealing

Table 1.2: *The key design characteristics of six of the most common hip resurfacing brands.*

Since 2003, HRA has accounted for approximately 7.1% of all hip arthroplasties carried out in the U.K. [5] and 6.8% of those in Australia [6]. Metal-on-Polyethylene THR prostheses are still the most common, enjoying an approximate market share of 59.9% of all hip prostheses implanted in the U.K. [5] and 51.2% in the U.S. [59], and now typically employing a variation known as cross-linked polyethylene (XLPE). Given these large numbers and their long history of usage a lot is known about the way they perform in the body (in vivo). The much shorter histories of most MoM hip prostheses, especially resurfacings, mean that there are still significant unanswered questions regarding their performance. This thesis is therefore concerned with the study of MoM THR and resurfacing hip prostheses, with comparisons drawn to previous studies of MoP where appropriate.

1.3 Aims and objectives

The aim of this study was to evaluate how factors within the control of engineers and surgeons affect the survivorship of MoM hip prostheses. Many complications leading to early revision have been linked to wear debris and wear is a primary focus of this study.

The first objective was to create and validate a quick, accurate, adaptable method of quantifying volumetric material loss of ex-vivo hip prostheses. The method needed to work for the bearing surfaces of both femoral heads and acetabular cups as well as at the interface of the tapers and trunnions, irrespective of component size or design.

The second objective was the measurement of a large sample set of ex-vivo hip prostheses, retrieved at revision surgery. Patient histories were collected, including data about the prosthesis used. Volumetric wear measurements were made and surface roughness was also measured on the bearing surface of the heads and cups. Links between a risk of increased wear and controllable variables related to the prosthesis and to surgery were sought.

1.4 Thesis outline

Chapter two, Background and Literature Review, looks more closely at the outcomes of hip arthroplasty. Reviews of survivorship are carried out with the

help of data from joint registries and peer-reviewed cohort studies. Current theories from the literature on failure modes are discussed, as are proposed solutions to such failures, which are taken both from clinical reviews and from simulator studies. Previous attempts at measuring wear of hip replacements, and the limitations of the methods used, are discussed before the current state of the art of hip replacement is outlined and unanswered questions posed.

Chapter three, Methods, focuses on the collection of data, related both to the patient demographic and to each hip prosthesis. The development and validation of the method used to calculate volumetric wear of ex-vivo hip prostheses is detailed, along with how the limitations from Chapter 2 were overcome. The methods used to measure surface roughness and analyse the collected data are also provided.

Chapter four, Results, begins with the results of the validation process of the volumetric wear calculator. Wear and roughness results from the measured hip prostheses are then given, followed by the results from correlation tests used to identify important factors affecting the wear of MoM hip prostheses.

Chapter five, Discussion, considers the findings of this study and the implications for future designs of artificial hip replacements. This is followed by an explanation of how the questions posed in Chapter two have been answered. The limitations of the study are also covered.

Chapter six, Conclusions and Future Work, draws together the salient conclusions from the study. Suggestions are given for carrying this work forward to further advance understanding of how artificial hip replacements can become more successful.

Chapter 2. Background and Literature Review

In order to judge the success of hip arthroplasty, several criteria should be discussed. On an individual level, functional scores such as the Harris Hip Score (HHS [60]) or Oxford Hip Score (OHS [61]) are used to assess the reduction in pain or the increase in physical activity after the operation. These are useful to demonstrate the benefits of hip arthroplasty.

However, this thesis is concerned not with individual improvements to a patient's quality of life but with the large scale survivorship of hip prostheses. Cohort studies and joint registries track this information, and allow for detailed analyses of large numbers of arthroplasties from which statistically significant conclusions may be drawn about the short and long term performance of different designs. Such methods are therefore useful in collating and quantifying outcomes, but do little to explain the gathered results.

This chapter will look at the results gathered from several large studies into survivorship and performance of hip arthroplasty. The main reasons given for revision will also be detailed, followed by a discussion of recent work attempting to understand the causes of failure.

2.1 Survivorship of hip arthroplasty

The truest test of any prosthesis is its performance in vivo. Survivorship of artificial hips has been extensively covered in national joint registries around the world. Additionally, cohort studies have reported on some designs of hip prostheses for periods of up to 40 years.

National joint registries allow for comparisons between large numbers of prostheses and have been established in several countries including the U.K. (National Joint Registry for England and Wales (NJR)), Australia (Australia Orthopaedic Association National Joint Replacement Registry (AOA NJRR)), Sweden (Swedish Hip Arthroplasty Register (SHAR)), Norway (Norwegian Arthroplasty Register (NAR)) and Canada (Canadian Joint Replacement Registry (CJRR)). There are some notable exceptions, in particular the United States of America.

Joint Registries aim to collate data on implant use and survivorship from their respective countries to give a large-scale overview. This can be a very powerful monitoring tool, but is not appropriate for drawing conclusions on the causation of any issues such as high revision rates. In the most established registries, the percentage of operations reported by hospitals can be in the high 90s [7], though for some registries it is typically in the 80s or below [5]. This can represent a significant amount of missing data. Additionally, there may be variations in patient demographics and survivorship results between countries. This has led to some calls for larger, multi-national registries [62, 63]. The majority of registries have only been active for 8-10 years (the exception being the SHAR, active since 1979). Therefore, it may be some time before any medium to long-term complications are detected. Finally, not all registries provide the same level of detail [63]. Some present survivorship for different bearing surface combinations, while others break this down further into individual models. As will be seen, significant variations can exist between models of prosthesis. Combining all models utilising the same bearing surface can lead to misleading conclusions on the suitability of that material combination if a minority of prostheses are performing poorly.

Considering first material combinations, MoP survival rates can be as high as 88% after more than 30 years in vivo [64]. The 5 and 10 year revision rates for MoP hip prostheses are around 2.6 – 3.6% and 7.1% respectively [5, 6]. The National Institute for Clinical Excellence (NICE) has recommended that both THR and HRA prostheses should achieve revision rates of less than 10% after 10 years in vivo [65].

The NJR quotes revision rates for MoM THR of 7.26% after 5 years and 13.61% after 7 years [5]. Rates for MoM resurfacing hip prostheses after 5 and 7 years were 8.48% and 11.81% respectively. As a group, therefore, these have not met the NICE recommendation. Table 2.1 provides the revision rates for MoP, MoM, resurfacing and LHMoM hip prostheses taken from various joint registries.

Prosthesis type	Registry [Reference]	Cohort size	Time to follow- up (years)	Revision rate (%)
MoP	NJR [5]	Up to 179,838	5	2.59
	NJR [5]	Up to 179,838	7	3.44
	AOA [6]	13,270	5	3.6
	AOA [6]	668	10	7.1
MoM (head diameter <36mm)	NJR [5]	21,917	5	4.74
	AOA [6]	4,791	5	3.91
Resurfacing	NJR [5]	Up to 21,242	5	8.48
	NJR [5]	Up to 21,242	7	11.81
	AOA [6]	6,405	5	4.4
	AOA [6]	84	10	7.5
	SHAR [7]	1,772	9	7.7
LHMoM	NJR [5]	19,667	5	7.25
	AOA [6]	14,089	5	7.14

Table 2.1: Revision rates for the four classifications of hip prostheses, taken from joint registries around the world.

Records are further broken down to consider individual designs. Revision rates for the prostheses detailed in Section 1.2.1 are offered in Table 2.2. This data is presented in graphical form in figures 2.1 and 2.2.

Figure 2.3 shows the mean revision rate per year for all studies included in table 2.2, split by prosthesis model. Overall, MoP THR offers the lowest revision rates. Revision rates appear to be higher in MoM THR, MoM HRA and LHMoM. Higher revision rates from newer prostheses are a serious concern. The older, proven MoP prostheses appear to provide superior survival rates [66]. Why then have so many thousands of MoM prostheses been implanted around the world? As previously noted, revision surgery is a burden on the patient, the surgeon and the healthcare system. Minimising revision rates will benefit all three and so the focus of this thesis will be those prostheses with the highest revision rates, with MoM HRA and LHMoM prostheses being of particular interest.

Prosthesis	Lead author [Reference]	Year	Cohort size	Time to follow-up (years)	Revision rate (%)
Adept®	NJR [5]	2011	3,355	5	4.42
	AOA [6]	2011	415	3	1.9
ASR™ resurfacing	NJR [5]	2011	3,153	5	9.63
	AOA [6]	2011	1,167	7	13.0
	Langton [67]	2011	59	5	9.8
	Langton [68]	2011	418	6	25.0
	Siebel [69]	2006	300	0.5	2.7
	Bergeron [70]	2009	228	4.6	5.2
	Jameson [71]	2010	214	5	7
	Klein [72]	2008	115	1	11.3
	De Steiger [73]	2011	1167	5	10.9
	BHR™	NJR [5]	2011	17,366	5
AOA [6]		2011	9,678	10	6.3
Langton [67]		2011	1,922	10	1.5
Pollard [74]		2006	54	5 – 7	6
Steffen [75]		2008	302	5	4.2
Treacy [76]		2005	144	5	2
Treacy [77]		2011	144	10	6.5
Carrothers [78]		2010	5000	7	3.7
Carrothers [78]		2010	5000	10	4.7
Khan [79]		2009	679	8	4.3
Rahman [80]		2010	329	9	3.5
Aulakh [81]		2010	202	7.5	3.65
De Smet [82]		2005	252	5	1.1
Witzleb [83]	2008	300	2	2	
Conserve® +	NJR [5]	2011	1,247	5	8.35
	Langton [67]	2011	961	5	< 1.0
	Amstutz [84]	2008	1000	5	4.8
	Amstutz [85]	2010	100	10	11.5
	Beaulé [86]	2009	116	3.2	1.9
	Kim [87]	2008	200	2.6	7.0
	Mont [88]	2007	1016	2.8	5.8

Prosthesis	Author	Year	Cohort size	Time to follow-up (years)	Revision rate (%)
Cormet™	NJR [5]	2011	3,844	5	6.30
	AOA [6]	2011	363	7	11.1
	Killampalli [89]	2009	100	2	0
	Stulberg [90]	2008	337	2	7.1
Durom™	NJR [5]	2011	1,726	5	6.35
	AOA [6]	2011	837	7	9.6
	Berton [91]	2010	100	4.8	7.6
	Gravius [92]	2009	82	2.4	2.4
	Lei [93]	2010	90	2.3	1.1
	Swank [94]	2009	128	1	1.9
	Vendittoli [95]	2010	109	4.7	5.5
ASR™ XL	NJR [5]	2011	2,540	5	11.34
	Langton [68]	2011	87	6	48.8
	Bernthal [96]	2012	70	3	17.1
	De Steiger [73]	2011	4406	5	9.3
Pinnacle® (MoM)	Engh [97]	2009	131	5.6	2.0
	Kindsfater [98]	2010	95	7	2.2
MoP	NJR [5]	2011	179,838	5	2.59
	AOA [6]	2011	13,270	5	3.6
	AOA [6]	2011	668	10	7.1
	Pollard [74]	2006	54	5 – 7	8
	Wroblewski [64]	2009	110	32	11.8

Table 2.2: Revision rates for six common hip resurfacing brands, two common LHMOM THR brands, and MoP THR overall for comparison.

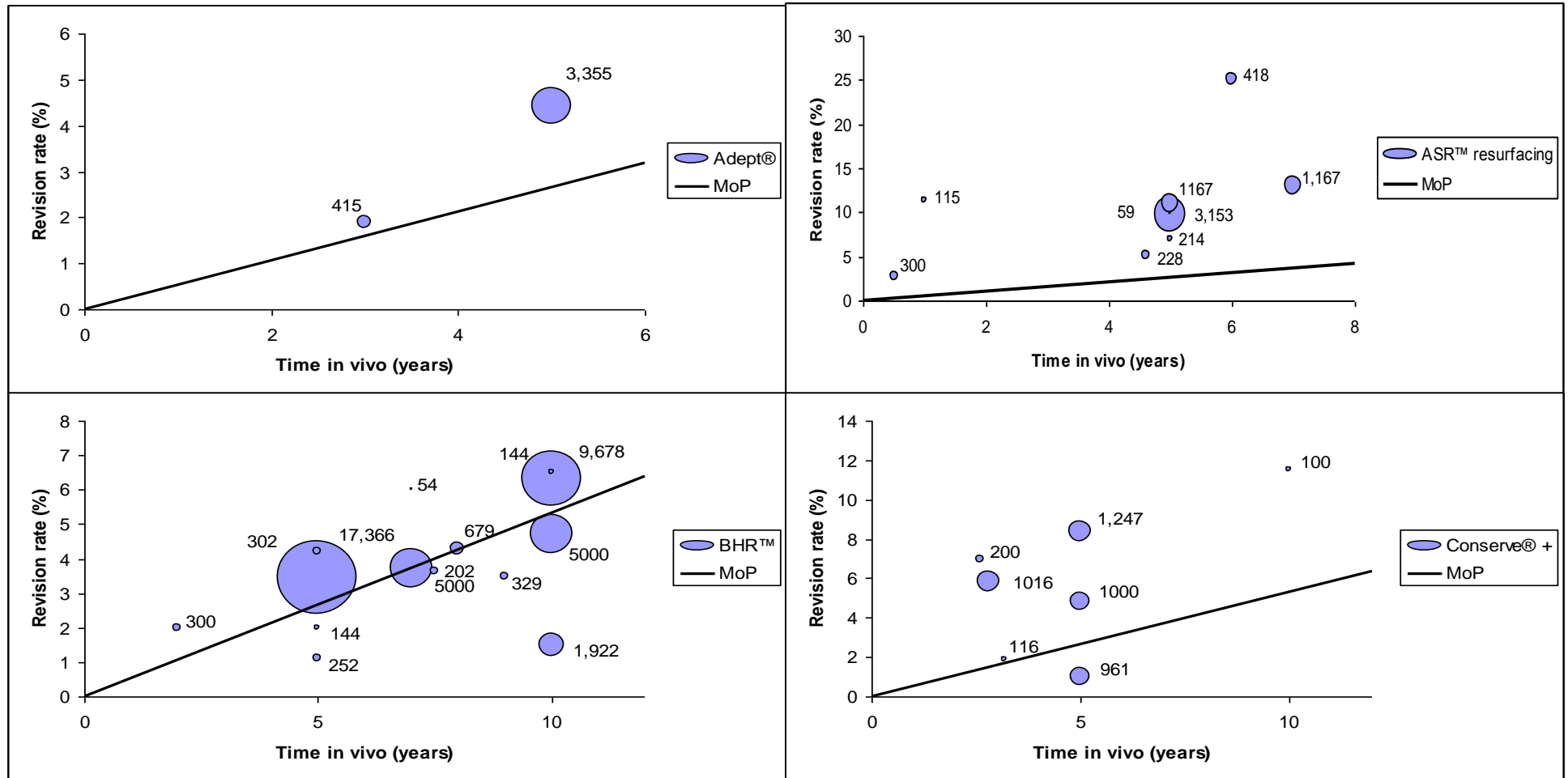


Figure 2.1: Revision rate against years in vivo for four models of hip resurfacing, taken from the literature and compared with the mean revision rate/year found for MoP THR (solid line). Size of bubble indicates study cohort size (labelled). Take care to note that the scales are different for each graph. The solid black line represents the same data on all graphs.

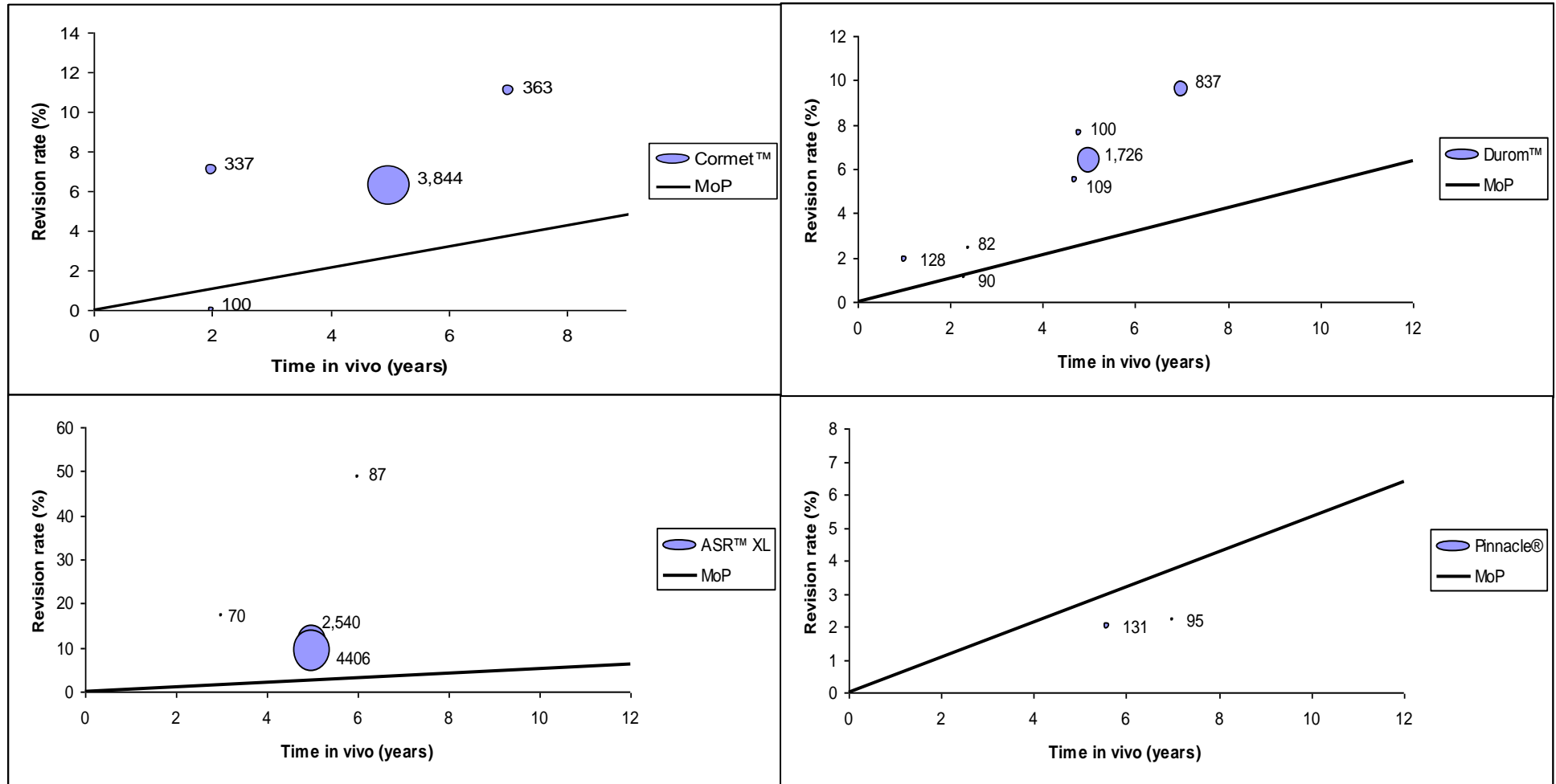


Figure 2.2: Revision rate against years in vivo for two models of hip resurfacing and two models of MoM THR, taken from the literature and compared with the mean revision rate/year found for MoP THR (solid line). Size of bubble indicates study cohort size (labelled). Take care to note that the scales are different for each graph. The solid black line represents the same data on all graphs.

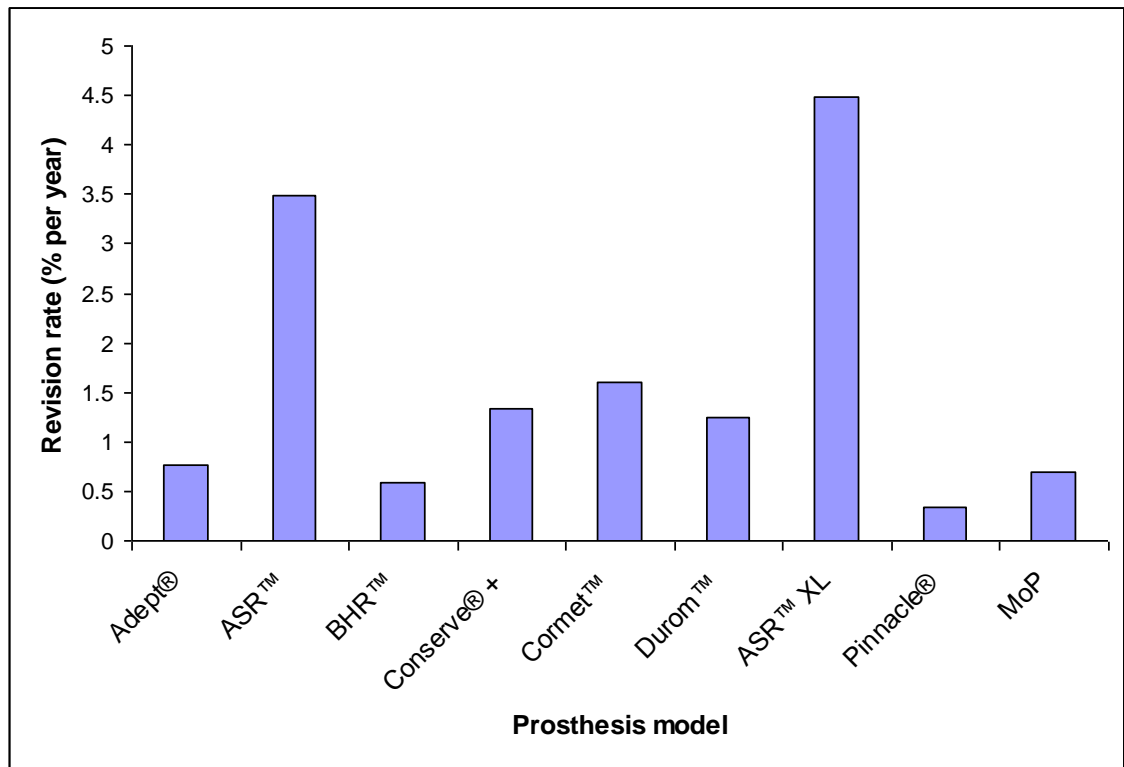


Figure 2.3: Retrieval rate for nine models of hip replacement taken from the literature (table 2.2) and averaged to give the mean retrieval rate per year, across all sources.

Within each group, there are some prostheses that outperform others. This disparity has not gone unnoticed and, in 2010, the ASR™ was recalled from the market in both its resurfacing and XL forms [99]. There are however many tens of thousands of patients potentially still at risk from this prosthesis and there are important design lessons that can still be learned from this, and other, models. The Durom™ too was withdrawn in the U.S. in 2008 [100] and the MITCH MoM hip was recalled internationally in 2012 [101, 102]. Why should prostheses apparently so similar in nature perform at such different levels? Is it the device or may surgeon or patient factors be more important? A thorough understanding of the factors affecting and necessitating revision of these prostheses is vital. Careful control of such factors will allow for lower revision rates in future implants.

2.2 Potential failure modes

As mentioned in Chapter 1, Introduction, failure of a prosthesis can be disastrous for the patient. A poorly performing prosthesis can commonly result in iatrogenic conditions (adverse conditions arising from a treatment) which, in many cases, do more harm than good. Despite the generally high survival rates

reported above, some devices do still require revision. Early failure is commonly related to surgical issues such as infection or avascular necrosis. Loosening of one or both components, which may be related to long-term wear debris generation, is the primary cause of late failure [5, 6].

2.2.1 Loosening

Loosening of the prosthesis was an indication in 45% of all hip revision surgeries carried out in the U.K. in 2010 [5]. Given an overall revision 5-year revision rate of 3.5% and assuming a similar proportion in recent years, the five-year revision rate due to loosening would be 1.6%. This would tally well with the ten-year revision rate due to loosening of 3.9% reported by the AOA [6].

Amstutz et al reported on 600 Conserve® Plus prostheses and found a revision rate due to loosening of up to 7.7% after a maximum of nine years [103]. Kim et al reported on a multicentre trial of 200 Conserve® Plus devices. After a mean follow up of 20 months, 14 revisions were noted (7%) of which 10 (5%) were due to component loosening [87]. Berton et al also reported 5% revision due to loosening at 4.8 years follow up in their study of 100 Durom™ prostheses [91]. Metal-on-metal revision rates as low as 0.6% - 2.0% due to loosening after 3 - 5 years have been reported [78, 84].

2.2.2 Infection

Another leading cause of revision surgery is infection of the wound following the primary surgery. Revision for infection can result in an increase in the number of hospital visits and length of stay compared with, for example, aseptic loosening [104]. Infections are thought to account for around 13% of all revisions in the U.K. [5] and 15% in the U.S. [105].

The NJR reported a five-year revision rate due to infection of 0.55% for all hip replacements, and 0.64% for hip resurfacings in the most recent annual report [5]. At ten years, the AOA reported a revision rate of 1.4% due to infection for all MoM hip replacements, and 0.6% for hip resurfacings [6]. Studies of other databases have reported similar findings. In a study of 42,665 THRs reported in the New Zealand National Joint Registry (NZNJR) between 1996 and 2006, Hooper et al reported a revision rate due to infection of 0.34% [106]. Ong et al

reported on a sample of 39,929 THRs from the U.S. Medicare program between 1997 and 2006 and found a revision rate of 1.63% due to infection within two years after primary surgery. The rate between two and ten years dropped to 0.59% [105]. Similar five and ten year revision rates due to infection of 1-2% have been reported in cohort studies of hip resurfacings [85, 91].

2.2.3 Avascular necrosis

Also related to surgery, avascular necrosis (AVN) is another potential complication. Although hip arthroplasty is sometimes used to combat AVN, there are some cases where the presence of a prosthesis interrupts the blood supply to the bone. During surgery, some interruption to the femoral head blood supply is not uncommon, although the extent of this interruption can vary [107]. A posterior surgical approach has been identified as a risk factor for decreased blood flow, although other approaches also decrease blood supply [108, 109]. As discussed in Chapter 1, Introduction, AVN is progressive and leads to the weakening and destruction of bone. All other things being equal, weaker bones are more susceptible to fracture.

2.2.4 Fracture

In the first few weeks and months following surgery, fracture of the femoral neck is the most common reason for revision amongst resurfacing devices [27, 28], although fractures do still occur later. For example, Marker et al reported an overall fracture risk of 2.5% at a mean follow-up of 44 months, with half of these occurring in the first 12 months after surgery and the remainder later [110]. Several causes have been speculated for femoral neck fracture including surgical notching of the femoral neck and varus placement, both of which increase the stresses on the femur [111, 112]. Risk factors identified include female gender [110, 111], high Body Mass Index (BMI) [110] and surgeon learning curve [110, 113], though the latter opinion has been disputed [111]. The key issue is the ability of the bone to withstand the load being applied to it. Females typically have smaller bones than males and a notch will weaken the bone. High BMI increases the load applied. For this reason, AVN has been associated with an increased risk of femoral neck fracture [107].

Several clinical studies have demonstrated the incidence of failure due to femoral neck fracture to be between 0.7% and 2.5% [75, 76, 110, 111, 113-115], and the 2010 AOA arthroplasty registry records the overall risk of fracture at 9 years as 2.6%, though the incidence increases rapidly in the first year after surgery and only very slightly thereafter [28]. The same source records cumulative revision rates for resurfacing devices in the same time frame as 7.2%. As such, fractures represent a significant percentage of overall resurfacing failures (35.6%).

2.2.5 Wear

Finally, and perhaps most significantly, complications arise from the wear debris originating where surfaces articulate. In traditional MoP THR, it is the polyethylene (PE) that predominantly (if not exclusively) wears. The generation of PE particles due to wear is now well known to adversely affect survivorship. Long-term PE wear has been linked to osteolysis, an inflammatory reaction involving bone resorption [116-119]. Submicron particles produced through wear migrate to the periprosthetic tissue [120]. This initiates a foreign body response, whereby osteoclasts (the major bone-resorptive cell responsible for the regulation of bone mass) are activated by PE debris [121, 122].

Polyethylene debris is typically in the size range of 0.1 – 1.0 μ m [123-126], which is key in activating osteoclasts [122]. Osteolysis, in turn, leads to implant loosening as the bone supporting the implant is resorbed.

With metal on metal (MoM) devices, polyethylene debris is clearly not a concern. However, despite the reduction in wear volumes reported in laboratory tests [127] (discussed in section 2.3.2) these devices do still wear. Whether osteolysis plays a role in implant loosening of MoM implants is open to debate. Metal debris is typically of the order of 40nm in size [128, 129], well outside of the most reactive 0.1 – 1.0 μ m range for polyethylene particles [122]. However, some studies have shown evidence of osteolysis following MoM hip replacement [85, 130-132]. Although a number of studies have also reported no evidence of osteolysis following MoM hip implantation, it is worth noting again that there are very few long-term studies for contemporary MoM hip replacements and that, in MoP prostheses, osteolysis is most prevalent in long-term implants. Laboratory tests have shown that MoM wear particles in the size

range of those found in vivo are capable of activating osteolytic cells [129]. The authors noted that, as with PE debris, the reaction to CoCr debris can vary by patient and that higher wear implants are more likely to provoke an osteolytic response, due to a higher number of wear particles.

It has been suggested that the number of wear particles generated with each step could be tens, or even hundreds, of times greater in MoM prostheses than MoP [133]. A typical MoP prosthesis wearing at $100\text{mm}^3/\text{year}$ produces in the region of 5×10^{11} PE particles per year [134-136], while metal particles from a MoM prosthesis may be as numerous as $67 - 2500 \times 10^{11}$ per year [133].

As metal debris is generated, Cr and Co ions are given off. These ions are detectable in the blood and urine of patients and have been shown to increase following MoM hip arthroplasty [137]. The Medicines and Healthcare products Regulatory Agency (MHRA) has issued guidance on metal ion levels in the patient. Above a concentration of $7\mu\text{g/l}$ (equivalent to 7 parts per billion or 119nmol/l cobalt and 134.5nmol/l chromium) [138] further investigation is advised. These values compare with $0.2 - 0.3\mu\text{g/l}$ (approximately 5nmol/L) in a healthy person without a MoM implant [139-141]. According to some studies, upwards of 20% of MoM patients currently exceed the $7\mu\text{g/l}$ level [142] for some models, in particular the ASR™ resurfacing [143]. The same study [143] found that only 6% of BHR™ and Conserve® + patients exceeded this level. Negative long term effects of exposure to metal debris have not been conclusively demonstrated, but there are concerns over studies reporting tissue damage. Some surgeons have noticed 'pseudotumours' at revision surgery [144]. These soft tissue masses have been postulated to be a result of a toxic reaction to particulate metal debris [145], but the exact cause is currently unknown [146]. Pseudotumour incidence as high as 39% after 4 years has been seen in MoM hip patients [147], and increased metal ion concentrations have been associated with an increased risk of pseudotumour development.

Aseptic lymphocytic vasculitis associated lesions (ALVAL) have been noted in the periprosthetic tissue at revision surgeries of MoM hips [132]. It is currently unknown if such lesions play a role in the failure of prostheses, or are simply an associated observation [67].

Another common observation is metallosis – the build-up of metal debris in the periprosthetic tissue. Risk factors for all of the above include female gender, smaller diameter components, high cup anteversion and obesity [148, 149]. There is evidence that the above reactions are all associated with sensitivity to metal debris [150]. As such, some authors across multiple research groups have adopted the umbrella term of adverse reactions to metal debris (ARMD) [48, 149, 151].

2.3 Measuring wear

This thesis is concerned primarily with wear related complications. Many authors have attempted to quantify the wear of hip prostheses. Maximum linear wear depth has previously been used as a quantification of wear [131, 152]. Although linear wear depth gives an indication, it does not account for variable wear across the component surface and could easily lead to confusing results. Take, for example a 40mm diameter hemi-spherical femoral head. The surface area of this head, A , depends on the radius, r , such that

$A = 2\pi r^2 = 2\pi * 400 \approx 2513\text{mm}^2$. If this component had been worn to a depth of $5\mu\text{m}$ across 35% of its surface, the total volumetric wear would be $2513 * 0.35 * 0.005 = 4.4\text{mm}^3$. This same component worn to a depth of $10\mu\text{m}$ across 10% of its surface would have 2.5mm^3 of wear. Thus, the $5\mu\text{m}$ example could be classified as half as worn, despite producing almost twice as much debris. Since the true amount of wear debris entering the body is a primary concern, an accurate method of assessing volumetric wear is vital.

2.3.1 In vivo

With MoP prostheses, the relatively high linear wear of the PE component meant that radiographs were an effective technique for estimating linear wear while the prosthesis was in vivo [153]. Measurements of wear in vivo allowed for the performance of the implant to be tracked over time with subsequent radiographs. Additionally, various formulae have been proposed for calculating volumetric wear from linear wear [154-156]. Even applying such calculations in vitro, volumetric errors were typically of the order of tens of cubic mm when compared with gravimetric [157] or fluid-displacement measures (whereby the component is submerged and the volume of fluid displaced recorded) [155]. However, with PE wear rates sometimes reaching over $100\text{mm}^3/\text{year}$ and total

PE volumes approaching 1000mm^3 [123], errors of $10 - 20\text{mm}^3$ represented a relatively small percentage error for MoP prostheses.

Radiographic estimation has shown linear resolution in the region of 0.055mm to 0.3mm [158]. This is particularly inaccurate for metal-on-metal prostheses where wear rates as low as 0.006mm/year ($6\mu\text{m/year}$) have been demonstrated [152].

2.3.2 *In vitro*

There are many simulator studies (*in vitro*) investigating the performance of MoM bearing combinations. Simulator testing involves a high number of cycles (typically several million) being applied to a joint, with volumetric wear commonly being calculated gravimetrically [159, 160]. There are international standards which “specify the relative angular movement between articulating components, the pattern of the applied force, the speed and duration of testing, the sample configuration and the test environment to be used for the wear testing of total hip-joint prostheses” (ISO 14242). A selection of such studies is presented in table 2.3. Wear rates range from $0.03 - 6.30\text{mm}^3/\text{million cycles}$ (mm^3/Mc).

One important concept in MoM simulator tests, particularly MoM resurfacings, is that of ‘bedding-in’ or ‘running-in’. Bedding-in is a phenomenon whereby the early wear rate (approximately during the first one million cycles) is relatively high. Following this is a ‘steady-state’ wear rate which is typically much smaller than the bedding-in rate [43, 161-163]. While this effect is well documented *in vitro*, it is not yet clear whether it occurs *in vivo*.

A common theme amongst the majority of simulator studies is a report of very low wear rates for MoM hip prostheses, particularly when compared with the $10-20\text{mm}^3/\text{Mc}$ typically seen in MoP simulator tests [164, 165]. However, simulator tests are often carried out with perfect prosthesis positioning, ample lubricant [166] and with simplified loading conditions [167]. In reality, surgeons often struggle to consistently achieve optimal implantation angles and improper acetabular cup orientation has been shown to have a negative effect on *in vivo* performance [168-172].

Lead author [Reference]	Nominal articulating diameter (mm)	Wear rate (mm ³ /Mc)
Smith [173]	16	4.85
Smith [173]	22.225	6.30
Smith [173]	28	0.54 – 1.62
Williams [174]	28	0.58
Firkins [175]	28	0.04 – 3.09
Fisher [176]	28	0.3 – 2.1
Ishida [177]	32	1.58
Goldsmith [178]	36	0.07
Dowson [179]	36	1 – 3
Williams [174]	39	1.61
Lee [162]	40	0.88 – 2.33
Heisel [161]	47	0.03 – 1.69
Li [180]	50	0.20 – 5.49
Vassiliou [163]	50	0.24 – 1.84
Lee [162]	56	0.47 – 1.15

Table 2.3: *Wear rates for MoM hip prostheses, measured from simulator studies. Ranges represent the difference between “steady-state” and “bedding-in” wear.*

In a hip simulator, Williams et al [174] showed that increasing the cup inclination angle from 45° to 55° resulted in an increase in wear rate from 0.58mm³/Mc to 1.61mm³/Mc for a 28mm diameter MoM prosthesis and from 1.61mm³/Mc to 8.99mm³/Mc for a 39mm diameter MoM hip prosthesis. Angadji et al [160] found that for cup inclination angles of 35°, 50° and 60° the steady state wear rate was 0.24mm³/Mc, 0.69mm³/Mc and 1.7mm³/Mc respectively.

Further, there has been some question over the appropriateness of the current standard (ISO 14242) for simulator testing when applied to MoM prostheses. Kamali et al [167] have suggested that a stop/start motion, a change in frequency from 1Hz to 0.5Hz, and alternating kinetic and kinematic profiles would provide a more physiologically relevant test protocol. When performing wear tests under these conditions, they found bedding-in wear rates of 8.4 – 11.5mm³/Mc and steady-state wear rates of 1.9 – 2.8mm³/Mc, much higher than the typical rates from table 2.2.

2.3.3 Ex vivo

In reality then, the truest assessment of wear will come from prostheses retrieved from the body (ex vivo). The gravimetric methods which are the gold standard of simulator work are clearly not practical with ex vivo prostheses, given the lack of a datum measurement. One alternative approach has been the measurement of the bearing surface of retrieved prostheses using co-ordinate measuring machines (CMMs).

There are a handful of studies offering ex vivo volumetric wear rates of MoM hip prostheses. In 1996, Kothari et al used a CMM to evaluate 22 retrieved McKee-Farrar total hip replacements [181]. Three hundred and twenty five points were measured on each sample and the 'accuracy' of the CMM used was $\pm 5\mu\text{m}$. Although accuracy in this context was not explicitly defined in this paper, it is reasonable to accept the definition offered in ISO 10360 "Geometrical product specifications (GPS) -- Acceptance and reverification tests for coordinate measuring machines (CMM)". Here accuracy is defined as the maximum permitted form error when a reference sphere is measured with 25 evenly distributed points [182]. With accuracy of $\pm 5\mu\text{m}$ and possible wear rates as low as $6\mu\text{m}/\text{year}$ as noted above, there is potential for large errors. Indeed, in 2006 Becker et al evaluated the influence of measurement accuracy in CMM based approaches and recommended a minimum accuracy of $\pm 2\mu\text{m}$ [183]. However a later study by the same authors comparing two CMMs (a "standard precision" $2.9\mu\text{m}$ and a "high precision" $0.8\mu\text{m}$) concluded that a high precision CMM was "essential for assessing wear in modern hard-on-hard bearings" [184]. Becker et al examined retrieved 28mm MoM THRs and these were all femoral heads with no acetabular cups examined [184].

Morlock et al reported in 2006 on a CMM based volumetric wear measurement methodology [185]. This method was then used in 2008 to report on 267 retrieved hip resurfacing components (although wear data on only 58 components [including 26 pairs] was tabulated in the paper) [172]. The CMM used by Morlock et al was said to be accurate to $\pm 3\mu\text{m}$. Bills et al published a CMM based volumetric wear measurement method in 2007 [186], as did Witzleb et al in 2009 [187]. Bills et al stated that most average CMMs have an accuracy of approximately $3\mu\text{m}$ and as such would not be accurate enough for

useful volumetric measurements of hard-on-hard orthopaedic bearings [186]. Both Bills et al and Witzleb et al used CMMs with accuracy of $\pm 1\mu\text{m}$, but the methods were applied to small numbers of retrievals (4 and 10 components respectively). Neither set of authors gave the articulating diameters of the hip components they measured. This retrieval and measurement data is summarised in table 2.4.

Perhaps most importantly, of the above publications, only Morlock et al [185] and Becker et al [184] provided any data on the accuracy of their calculations. Morlock et al claimed errors for volumetric calculations within 8% when applying their method to a simulated data set, though data was not offered to support this claim. Because the data set was simulated, this error value is only for the calculation of wear and does not indicate errors arising from their CMM measurements or from differentiating between manufacturing tolerance and wear. Becker et al showed percentage error for the high precision CMM decreasing from approximately 15% to 2% when linear wear depths were increased from $3\mu\text{m}$ to $15\mu\text{m}$. The standard precision CMM varied from 55% to 10% errors across the same range. However, neither Morlock et al nor Becker et al offered their actual volumetric wear and so it is not possible to quantify these percentage errors in terms of mm^3 .

Lead author [Reference]	Year	Number of components measured	CMM accuracy (μm)	Number of points taken	Size of errors
Kothari [181]	1996	22 pairs	± 5	325	Not given
Bills [186]	2007	2 pairs	± 1	Not given	Not given
Morlock [172]	2008	58 (inc. 26 pairs)	± 3	Not given	Up to 8%
Witzleb [187]	2009	10 (inc. 2 pairs)	± 1	1297	Not given
Becker [184]	2009	44 femoral heads	± 0.8 & ± 2.9	15960	Max. 15% & 55%
Morris [188]	2011	16 cups	± 20	200,000	Max 40%
Carmignato [189]	2011	9 femoral heads	± 1	17,827	3.4mm^3
Bills [190]	2012	6 pairs	± 1.3	236,400	1.859mm^3

Table 2.4: Summary of previous CMM based volumetric wear calculations for explanted MoM hip prostheses.

Morris et al reported on the application of a CMM based volumetric wear measurement to in vitro tested acetabular cups, taking 200,000 data points

using a CMM accurate to $20\mu\text{m}$, 25x greater than the $0.8\mu\text{m}$ accuracy recommended by Becker et al. Differences of up to 40% were reported between gravimetric and CMM methods [188], though it was claimed this was due to wear away from the bearing surface being recorded gravimetrically but not by the CMM.

Carmignato et al published a study discussing the importance of uncertainty in CMM based methods [189]. For ceramic heads of 28 – 32mm diameter, they found uncertainty values of $3.0 - 3.4\text{mm}^3$. After artificially wearing the components to a mean of 158.4mm^3 (range $83.7 - 303.9\text{mm}^3$), the difference in volume between the CMM and gravimetric measurements was a mean of 1.9mm^3 (range $0.3 - 2.9\text{mm}^3$). This was considered a “good agreement” by the authors, given the high volumes. However, typical wear volumes may only be of the order of a few cubic mm, many times smaller than those in this study. Further reduction in volumetric error is desirable.

In 2012, Bills et al published a description of a CMM based method for measuring volumetric wear, and its inherent uncertainty [190]. Their method involved measuring a series of points on the component's surface and constructing a solid object by linearly connecting these points. The volume of this object was calculated and compared with the volume of an ideal sphere of the same radius. The authors claimed an uncertainty overall of 1.859mm^3 when collecting 236,400 data points using a CMM accurate to $1.3\mu\text{m}$. Of greater consequence was the large volumetric systematic error of the method, which could only be significantly reduced when the number of points measured was increased. For example, when 8000 points were simulated on a 50mm diameter hemisphere the error in their volumetric calculation was 24.746mm^3 . This is a significant volume, possibly many times that found from an ex vivo component. It is important to note that again this was done using a simulated data set and thus expresses error only in the calculation of component volume, ignoring the real-world uncertainties of measurements. The authors themselves suggest that the error contribution for this calculation stage “should be kept below 1mm^3 and ideally below 0.5mm^3 ” [190]. Only when upwards of 300,000 points were taken did the volumetric error approach values within 0.5mm^3 .

2.4 What might affect wear?

As noted in Section 1.3, the key concern of this thesis is a deeper understanding of how wear (and therefore the associated risk of early failure) is affected by factors within the control of engineers and surgeons.

In 1978, Lewinnek et al proposed a 'safe' zone for acetabular cup orientation in the body for MoP hip prostheses [53]. They specifically looked at inclination (the degree to which the cup is inclined, relative to the transverse axis) and anteversion (the degree to which the cup is rotated forwards, relative to the coronal plane) angles (figure 2.4).

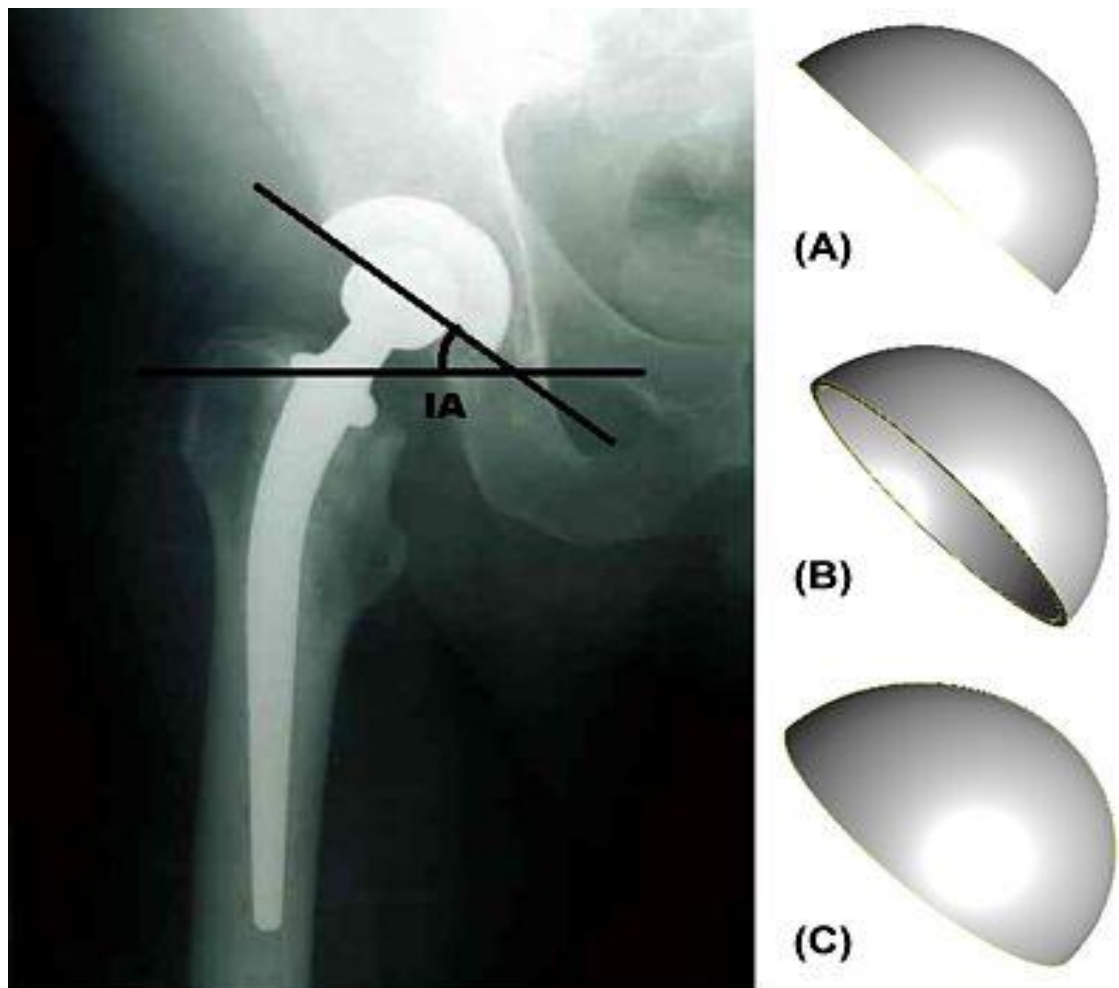


Figure 2.4: Left: Radiographic image of a right-side THR prosthesis, with the inclination angle (IA) marked. Right: Model of a right-side acetabular cup at 45° inclination and (A) 0° anteversion, (B) 10° retroversion (tilted towards the posterior), (C) 10° anteversion (tilted towards the anterior).

This safe zone, $40^{\circ} \pm 10^{\circ}$ inclination and $15^{\circ} \pm 10^{\circ}$ anteversion, was specified to reduce the risk of dislocation following hip arthroplasty with an increase from

1.5% to 6.1% dislocation outside of this range. Similar values are commonly quoted by manufacturers as the recommended implantation angles. In MoM prostheses, high inclination angle has been correlated with lower functional scores [91], higher revision rates [91, 172] and an increase in the concentration of patient Cr and Co ion levels [168, 170]. The same is also true of anteversion [149, 172].

Patient demographics have also been shown to influence the outcome of MoM hip replacement. Younger patients tend to be at a greater risk of revision surgery [5, 6, 191], as do females [5, 6, 78, 113] although it has been suggested that female gender itself is not a risk factor but that females are more likely to receive smaller prostheses [192]. Appropriate patient selection has been considered a very important factor in achieving lower revision rates [50, 114, 193], though ideally hip prostheses should be made as robust as possible to be successful and effective in as many people as possible.

In Section 2.1, a disparity in performance between different models of hip resurfacing and different models of LHMOM THRs was noted. Given the huge sample sizes taken, particularly in national joint registries, it is reasonable to assume that all models are subject to similar variations in patient demographics, surgeon experience and implantation angles. This suggests then that design differences play an important role in the performance of prostheses.

In vitro, large component diameter and reduced diametral clearance between head and cup have been shown to promote the most beneficial lubrication regime [43, 194-196]. In vivo, however, reduced clearance has been theorised to lead to an increased risk of edge loading [197, 198] (and subsequently higher wear [172]), as well as an increased risk of wear if the acetabular component is deformed during implantation [170, 199]. Reducing the clearance between the head and the cup increases the size of the contact area. Under otherwise equal conditions, a larger contact area will necessarily mean that contact occurs closer to the cup rim, thereby increasing the risk of edge-loading.

One useful tool for demonstrating the combined effect of head diameter (d) and clearance (c_d) is the Stribeck curve [43, 200] (figure 2.5). As well as these two

variables, lubricant viscosity (η), angular velocity at the joint ($\bar{\omega}$) and mean cyclic load (w) all affect the Stribeck curve. These can then be plotted against the friction coefficient (μ).

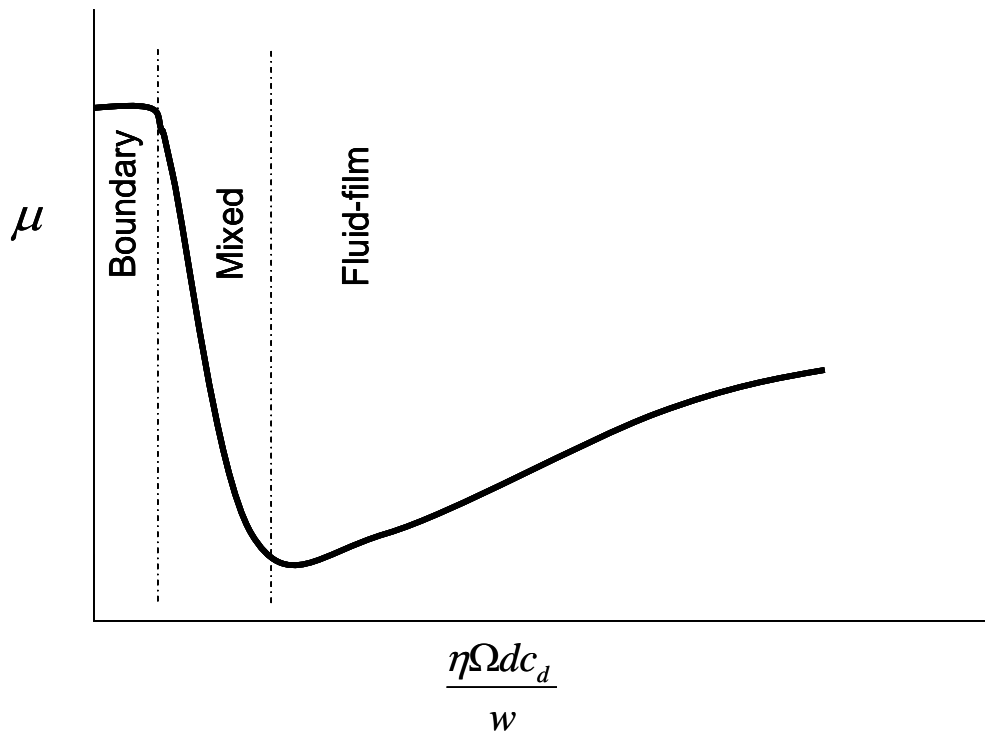


Figure 2.5: A typical Stribeck curve, showing the transition from boundary to fluid-film lubrication.

Hamrock and Dowson took this further [201] by extending the work of Johnson et al [202] to calculate the minimum effective film thickness (h_{\min}) and lambda-ratio (λ -ratio) of MoM hip prostheses [43]. Although this work was applicable only to materials of low elastic modulus (which CoCrMo is not), the principles can be extended to CoCrMo prostheses if some criteria are met. Most importantly, the lubricant must not change viscosity under pressure (which synovial fluid does not) and the contact area between the components must be wide in relation to the lubricant film thickness (which is the case here). The Hamrock-Dowson equation allows for calculation of the minimum effective film thickness (h_{\min}) from:

$$\frac{h_{\min}}{R_x} = 2.80 \left(\frac{\eta u}{E^* R_x} \right)^{0.65} \left(\frac{w}{E^* R_x^2} \right)^{-0.21}$$

Here, R_x is the equivalent radius (m), η is the lubricant viscosity (Pa s), u is the entraining velocity (ms^{-1}), E^* is the equivalent elastic modulus (Pa) and w is the load (N). Entraining velocity, u , varies with head diameter according to the formula:

$$u = \frac{\omega d}{4}$$

Here, ω is angular velocity (rad/s) and d is head diameter (m). Equivalent elastic modulus, E^* , depends on the material properties Young's modulus, E , and Poisson's ratio, ν , such that:

$$E^* = \frac{E}{1 - \nu^2}$$

The lambda ratio was then calculated from:

$$\lambda = \frac{h_{\min}}{[(R_{a1})^2 + (R_{a2})^2]^{0.5}}$$

Where subscript 1 refers to the femoral head and subscript 2 refers to the acetabular cup.

In agreement with lubrication theory, smaller diameter resurfacings have been shown to perform less well in vivo, with increases in patient metal ion levels [170] and revision rates evident [71, 113]. However, these results from hip resurfacing prostheses should be interpreted with caution. Increasing the diameter of THRs (as in LHMOM THR) has produced very poor survivorship, with revision rates of anywhere from 10 – 50% at 3 – 6 years [5, 68, 96, 149, 203]. Can biotribology help to explain this apparent contradiction? If fluid-film lubrication is not maintained and there is contact between the head and cup, the volumetric wear can be estimated by the Archard wear equation [204], typically written as:

$$V = \frac{KWL}{H}$$

Where V is the wear volume (mm^3), W is the load (N), L is the sliding distance (mm), K is a dimensionless constant and H is the hardness of the softest surface (N/mm^2). Under otherwise identical conditions, a larger diameter prosthesis will have a larger sliding distance. Therefore, assuming some contact between head and cup (i.e. fluid-film lubrication is not maintained), larger diameter prostheses will produce greater wear volumes.

Langton et al have claimed that the most important feature of the MoM hip prosthesis when predicting performance is the arc of acetabular cover, due to the increased risk of 'rim loading' or 'edge loading' of the cup [67]. Specifically, Langton et al proposed a measurement of the 'contact patch to rim' (CPR) distance [171]. This is the distance between the rim of the cup and the hip contact force vector and it depends not only on the coverage arc of the cup, but also on the diameter and implantation angles (figure 2.6). They found a significant inverse relationship between CPR distance and patient metal ion concentrations, with the risk of high ion levels increasing over time [171]. Models with lower coverage arcs are more susceptible to producing high volumes of metal ions than models with higher coverage arcs, given identical implantation angles.

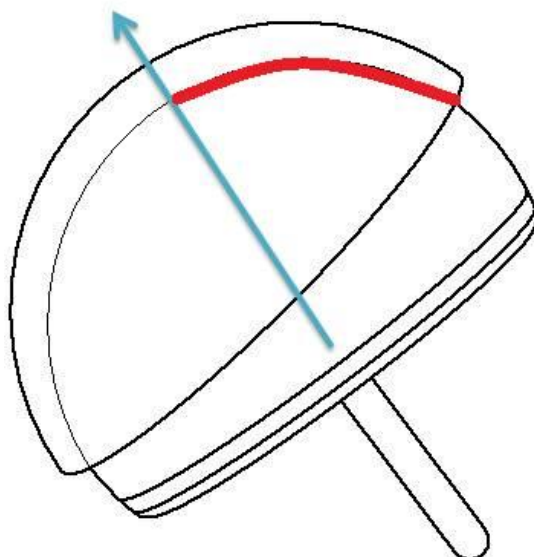


Figure 2.6: Figure shows a simplified image of a resurfacing femoral head and acetabular cup, indicating a 2-dimensional hip contact force vector (blue arrow) and the CPR distance (red arc). It should be clear how reduced coverage arc, smaller radius and/or increased cup orientation reduces the CPR distance.

2.5 Summary

Whilst a largely successful intervention, MoM hip arthroplasty has not achieved the success that was hoped for - revision rates are often higher than MoP prostheses. There is however substantial variation in performance between different models of seemingly very similar MoM prostheses. As well as patient selection and the ability to achieve optimum implantation angle of the acetabular cup, there appear to be design differences which affect survivorship. A deeper understanding of these will allow similar issues to be avoided in future.

Head diameter and clearance both affect the dominant lubrication regime. Theoretical calculations of this regime can be carried out for ex vivo hip prostheses. How does this regime change during the lifetime of a prosthesis? Is there evidence of “bedding-in” in vivo, indicated by an increase in the λ -ratio?

Acetabular cup orientation, effective coverage arc and CPR distance have all been shown to have an effect on survivorship and/or increase patient metal ion levels. If they can also be proven to be linked to an increase in wear volumes, this would help to explain adverse reactions when cup orientation is sub-optimal and CPR distance is low.

There has been concern that simulators do not currently provide an appropriately accurate simulation of real life conditions. Are the low wear rates seen in simulators for MoM hip prostheses achieved in vivo? Wear measurements of a large number of ex vivo samples could be compared with simulator studies to see if similar rates are achieved in vivo.

Ex vivo data provides only an ‘end-point’ snapshot of performance. In vivo wear data was achievable radiographically to reasonable accuracy for MoP prostheses given the high wear rates and could be used to provide ongoing performance data. This was a very useful tool which is not available for MoM prostheses. A method of assessing the wear of MoM prostheses, perhaps through a surrogate measure, would be extremely useful. It has been shown that metal wear leads to metal debris which leads to an increase in metal ion concentrations in the patient. It has been suggested that metal ion levels could be used as a surrogate measure of wear in vivo [205]. Is there a correlation

between wear volume and metal ion concentrations? Can a measurement of patient ion levels be used to estimate the volumetric wear?

A 'safe' level of metal ion concentration of $7\mu\text{g/l}$ has been published by the MHRA. Is this guidance reasonable, or do complications arise at lower ion concentrations? It is vitally important that any complications are caught early and diagnosed correctly to cause the minimum amount of discomfort and damage to the patient.

Complications arising from wear account for a significant number of early failures of MoM hips. There is some evidence of high concentrations of metal debris leading to osteolysis. Given that osteolysis will inevitably weaken the bone, osteolysis may increase the risk of fracture [206]. Previously fracture has been thought of as a predominantly surgical issue. Might high wear rates also be implicated in femoral neck fractures?

An accurate, quick and repeatable method for measuring wear of ex vivo samples is imperative. Current CMM based methods struggle to achieve accuracy within several cubic mm. For MoM prostheses, this is not accurate enough. A value of 0.5mm^3 has been suggested by Bills et al as a suitable accuracy for the calculation of wear using a simulated data set [190]. Realistically, given simulator study wear rates often around $1 - 2\text{mm}^3/\text{Mc}$, accuracy of 0.5mm^3 could be a reasonable value for the entire measurement process on real, ex vivo components.

Chapter 3. Methods

This chapter will explain the methods employed to answer the questions posed in Chapter 2, Background and Literature Review. The collection of clinical data will be discussed first, including information about patient demographics and the prostheses explanted. The method of volumetric wear measurement will follow, along with the validation procedure. Measurements of surface roughness are then described. Finally, the data analysis process is presented and the statistical test justified. Research Ethics Committee approval was obtained for all work carried out (REC/09/H0905/41).

3.1 Materials

One hundred and forty three (143) femoral heads and one hundred and thirty (130) acetabular cups were obtained from revision surgery of MoM hip prostheses. Of these, forty-eight heads and forty-seven cups (forty-seven mating pairs) were from total hip replacements of one of two models (Pinnacle® and ASR™ XL). All Pinnacle® cups in this study were fitted with CoCrMo liners and articulated against CoCrMo femoral heads. Throughout this thesis, 'Pinnacle®' will be used to refer to this MoM head/cup pair. The remaining ninety-five heads and eighty-three cups (eighty-three mating pairs) were from hip resurfacing prostheses of one of six models (Adept®, ASR™, BHR™, Conserve® Plus, Cormet™ and Durom™). The median nominal articulating diameter was 45mm (range 36 – 57mm) and the components were retrieved after a median duration in vivo of 39months (range 2 – 102 months). A breakdown by prosthesis model is given in table 3.1.

3.2 Clinical data

At the time of retrieval, key information about each prosthesis was recorded in collaboration with the various hospitals that made their retrieved prostheses available for study. A diagnosis was made by the operating surgeon on the reason for retrieval. Diagnoses were diverse, but fell broadly into four groups:

1. Fracture of the femoral neck. This was exclusive to hip resurfacing prostheses and was treated by revision to a total hip replacement. Fractures were considered either early (2 – 7 months in vivo) or late (20 – 62 months in vivo).

2. Adverse reactions to metal debris (ARMD) [149]. This umbrella terms describes joint failures associated with pain, metallosis (a build up of metal debris in the periprosthetic tissue [148]), aseptic lymphocytic vasculitis-associated lesions (ALVAL) [146] and/or effusion (an abnormal collection of fluid) of the hip.
3. Implant loosening. This may commonly also be related to wear debris and osteolysis/bone resorption [207, 208].
4. Surgical. This included infection and avascular necrosis (AVN).

A complete breakdown of the number of retrievals following diagnosis of each condition is provided in table 3.2.

Prosthesis	Type	Number of heads	Number of cups	Mean nominal articulating diameter (range) (mm)	Mean duration in vivo (months) (range)
Pinnacle®	THR	26	26	36 (36 – 36)	37 (12 – 91)
Adept®	HRA	2	2	51 (50 – 52)	52 (42 – 62)
ASR™	HRA	61	54	47 (41 – 55)	41 (2 – 96)
ASR™ XL	THR	22	22	47 (41 – 57)	41 (11 – 68)
BHR™	HRA	16	14	44 (38 – 50)	42 (3 – 89)
Conserve® +	HRA	3	3	46 (42 – 52)	17 (6 – 30)
Cormet™	HRA	5	5	46 (40 – 48)	63 (6 – 102)
Durom™	HRA	8	4	48 (42 – 52)	44 (2 – 98)

Table 3.1: Detail of the 273 retrieved MoM hip prosthesis components analysed in this study, broken down by model.

Diagnosis	Number of femoral heads	Number of acetabular cups
ARMD	118	117
Early fracture	9	2
Late fracture	6	3
Loosening	4	4
Surgical	6	4

Table 3.2: Detail of the 273 retrieved MoM hip prosthesis components analysed in this study, broken down by reason for revision surgery.

Patient age and gender were recorded, as was the length of time between implantation and retrieval of the prosthesis. The model of prosthesis and nominal diameter were also recorded, including the type of stem used (where applicable for THR).

Radiographs taken following implantation were used to assess the inclination and anteversion angles of the acetabular component (figure 3.1). This was done by an orthopaedic surgeon working at Newcastle University using Einzel-Bild-Roentgen-Analyse (EBRA, University of Innsbruck, Innsbruck, Austria) software [170, 209]. Concentrations of Cr and Co ions in serum and whole blood were recorded immediately prior to retrieval using Inductively Coupled Plasma Mass Spectrometry (ICPMS) [210] in a blinded analysis at the Biochemistry Department of the Royal Surrey County Hospital, Guildford, United Kingdom.

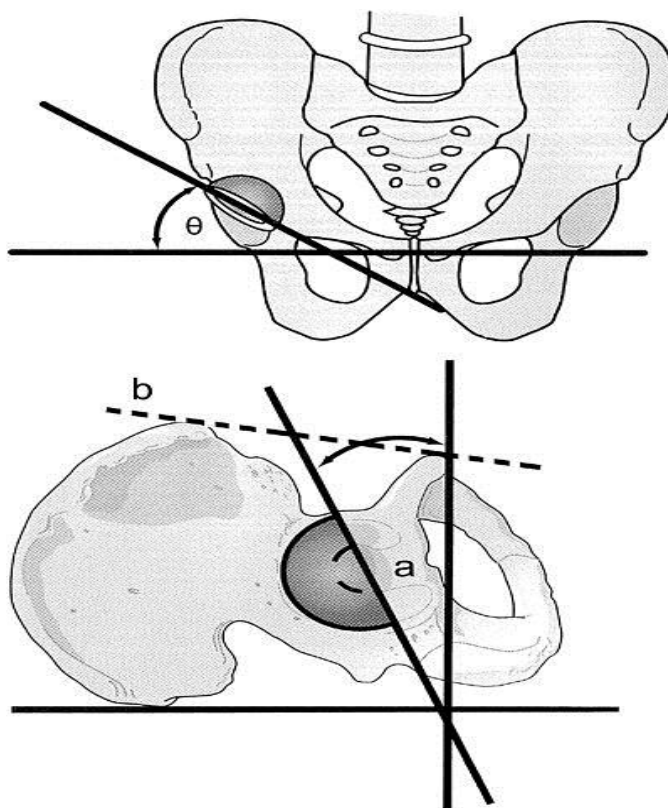


Figure 3.1: Acetabular inclination and version. θ : inclination angle, a : anteversion angle, b : alternative plane of reference.

3.3 Wear measurement

With so many complications of hip arthroplasty being linked to wear debris, an accurate assessment of the amount of wear is imperative. As discussed in Chapter 2, Background and Literature Review, many of the methods employed

to measure wear of MoP hip prostheses are not viable in MoM prostheses due to the significant reduction in wear. Further, many current methods analyse only linear wear depths whereas wear volumes will provide greater insights.

With the aid of a dedicated Mitutoyo LEGEX322 Co-ordinate Measuring Machine (CMM), a method of calculating volumetric wear was developed [143, 211]. This CMM used a contact stylus to collect three dimensional co-ordinate data from the surface of a sample. This data was then compared with projected data for an ideal, unworn surface in order to evaluate the material loss over the lifetime of the prosthesis.

3.3.1 Measurement procedure

Following retrieval, explants were soaked in 10% formalin for one week before being rinsed thoroughly in water and stored anonymously in a temperature controlled environment ($22^{\circ}\text{C} \pm 0.2^{\circ}\text{C}$). Prior to measurement, all surfaces were cleaned using acetone and a lint-free cloth in order to remove any remaining loose deposits and minimise spurious measurements and the CMM configuration was calibrated using a ceramic masterball. A 5mm diameter ruby (Al_2O_3) ball fixed to a 50mm carbon fibre stem was used to collect measurements. Femoral heads were held in place by their stem using a self-centring three-jawed chuck to prevent movement during the scanning process (figure 3.2). Acetabular cups were held in a clay mould to remove any risk of the chuck deforming the cups.

Although the general measurement approach was the same for all components, variations were necessary to account for the different component shapes and typical wear patterns of femoral heads, acetabular cups and femoral tapers. Thus, three different program types were written in MCOSMOS, the Mitutoyo CMM software. These in turn varied in their exact specification depending on the diameter of the component being measured.

The first step was to define a co-ordinate origin – a point from which all measurements would be taken. For the partially spherical femoral heads and acetabular cups, the origin was defined at the centre of the

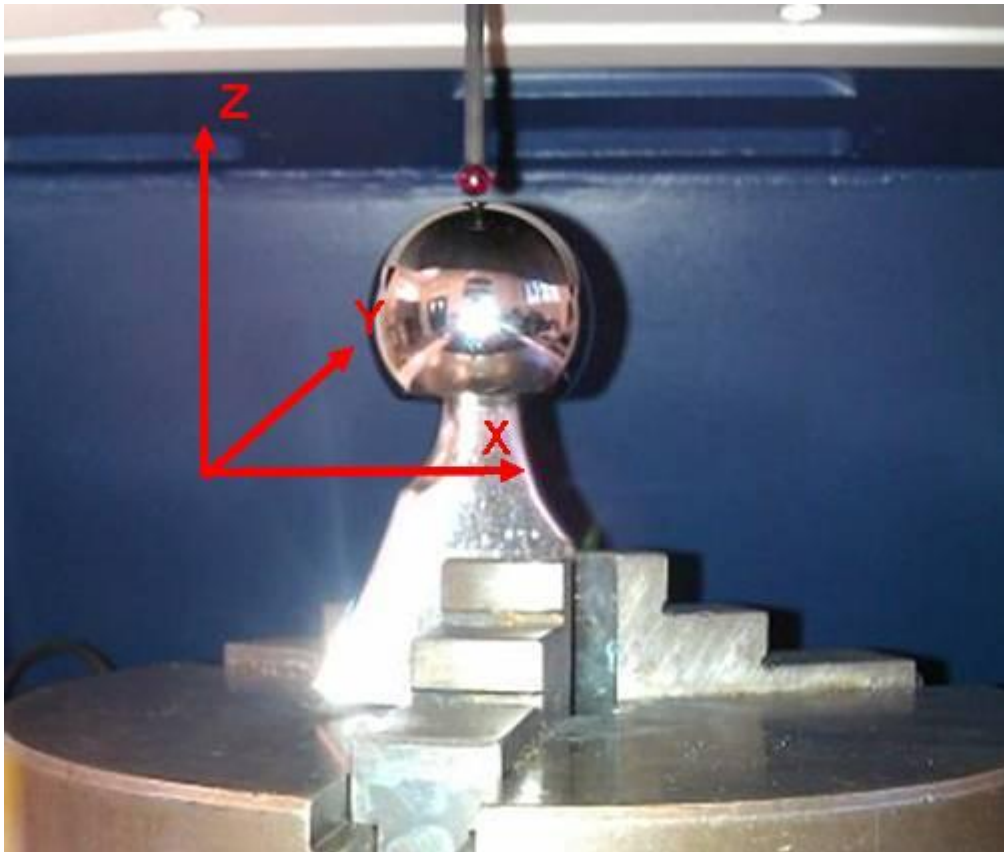


Figure 3.2: *Samples were held in a chuck to prevent movement during the scanning process.*

imaginary full sphere. For optimum accuracy, the program aimed to identify this origin from as wide an area of the articulating surface as possible. For femoral components, four points were taken at 90° intervals around the full 360° of the equator in the X-Y plane. Three further points were taken in the Z-X plane at 25° intervals. From these seven points a sphere was projected. The sphericity, defined here as the maximum deviation in radius at any point from that of an ideal sphere of the same size, was calculated. If the sphericity of this initial sphere was found to be within 2µm (within the manufacturing tolerance found by scanning new, unused components) then a Cartesian co-ordinate system was defined with the origin set according to the centre of this sphere. If the sphericity was outside of the 2µm tolerance, for example due to one of the measurements being taken within a worn area of the component, then, using the MCOSMOS software, the coordinate system was rotated by 10° about the z axis and the process repeated until a suitably unworn area was located. In the rare event of the method failing to find a satisfactory form after 36 passes, the area over which the points were taken was restricted to a 300° area around the equator with the aim being to minimise the probability of contacting a worn area. Even in

highly worn components, wear is typically localised and this adjustment always proved to be successful in allowing a spherical origin to be found.

For acetabular cups, the process was identical to that of the femoral program except that areas within 30° of the rim of the cup were not used in the calculation of the sphere. This decision was based on the principle that in most heavily worn cups, the wear is located primarily at the rim of the cup, a result which has also been reported elsewhere [172, 174, 212]. The procedure described above provided a rapid methodology to determine the approximate centre of the sphere.

To determine the definitive centre of the sphere, 100 points were taken in the YZ plane moving from equator to equator for the femoral heads but limited to a 120 degree scan about the pole in the case of the acetabular cups (for reasons described above). The coordinate system was then rotated 22.5° about the z axis and the process repeated seven times, so that a total of 800 points were taken. From this point on, the CMM was used in 'scanning' mode. That is, the CMM did not break contact with the sample being scanned until the co-ordinate system was rotated; all 100 points were collected in a single pass. Any points which were calculated to be greater than 2µm deviation from the initial spherical form, as determined from the initial seven points, were discarded as they were unlikely to represent the original surface and so could not be used. All other points were retained and used in the calculation of the second sphere. The centre of the second sphere was then taken as the definitive origin. This method was developed on the principle that even heavily worn samples typically show a sharply demarcated transition between worn and unworn areas. Points taken over worn areas are highly likely to be much greater than 2µm in deviation from the original calculated form and are not used to determine the definitive origin.

For the internal tapers of the femoral heads, the origin was defined at the centre of the flat circle at the proximal end of the taper (figure 3.3). The heads were overturned and held in position so the larger diameter of the taper was uppermost. Initially the bearing surface was scanned in order to determine an origin using the centre of the part-spherical head. Next, 20 equispaced linear traces were made in the ZX plane. Out of these 20 traces, those which were

found to have deviations from straightness of less than 1.5 microns were used to calculate the angle of the cone and also the Z axis of the coordinate system. The value of 1.5 microns was chosen as the limit as sterile, unused samples (n = 3) were found to have surface deviations below this value.

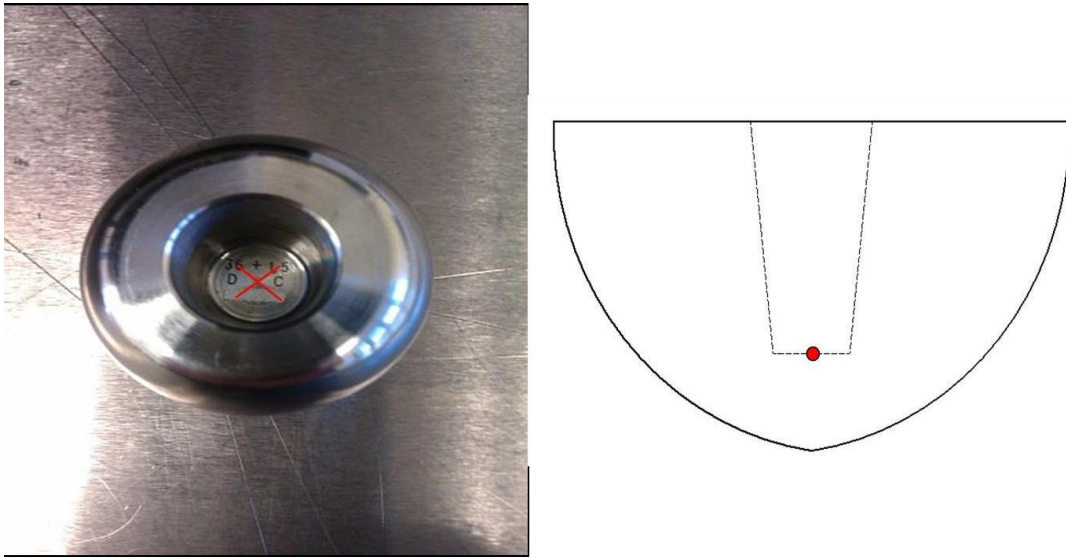


Figure 3.3: *Left: Image of an internal taper, with the point of origin of the CMM scan marked (red cross). Right: Cross-section of an internal taper, with the point of origin marked (red dot).*

With the origin defined, the measurements were taken. For femoral heads, scans were taken every 5° around the circumference, starting 5mm below the equator and converging on the pole. Data was collected every 0.3mm along each scan. This allowed for between 6048 and 7128 data points to be collected for each head, depending on the articulating diameter. Acetabular cup scans were also taken at 5° intervals and began at the lip of each cup. This allowed for between 3024 to 4104 data points for each cup. At each point the 3-dimensional position was recorded in Cartesian co-ordinates, relative to the centre of the sample. This number of points was decided on to provide an appropriate distribution across the surface, without unnecessarily extending the time taken (a full head, cup and taper set could be scanned within one hour).

For the femoral tapers, thirty linear scans were carried out in the ZX plane, with the coordinate system rotating through 12° each time. Depending on the length of the cone, between 1000 and 2000 points were recorded for each internal taper. Figure 3.4 shows typical CMM outputs for a 36mm femoral head, its taper and the mating acetabular cup.

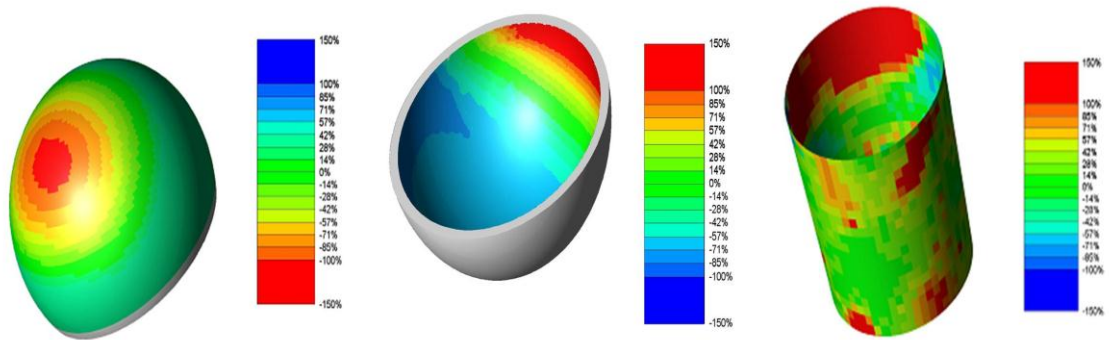


Figure 3.4: Examples of the CMM output for (left to right) a femoral head, acetabular cup, and femoral taper. Deep red represents the highest wear, while green/blue represents unworn surface. Colour scales represent deviation from the modal radius, where 100% = 20µm.

3.3.2 Volumetric wear calculation

While the CMM was capable of providing linear wear depth information, a more powerful system was required to calculate volumetric wear. Raw data was taken from the CMM in the form of an ASCII file and was imported into Matlab (The Mathworks, Inc.). Figure 3.5 shows the start of a typical ASCII file.

```

Head 361 - Notepad
File Edit Format View Help
UL; Auto Store
CS;1.000000;0.000000;0.000000;0.000000;1.000000;0.000000;0.000000;1.000000;0.000000;0.000000;0.000000;0.000000;
EB;SF;1; ;Freeform surface,
MM;SF;0.050000;-0.050000;SheetOffset=0.000000;Pos=0;MeanTol=1;PosLbl=;Restrict=;
PR;0.000000;
MP;-17.651141;-0.010532;-3.542546;0.981749;0.000000;0.190183;Mark=1;;;
MM;SF;0.050000;-0.050000;SheetOffset=0.000000;Pos=0;MeanTol=1;PosLbl=;Restrict=;
PR;0.000000;
MP;-17.732978;0.001006;-3.094659;0.985568;-0.000000;0.169277;Mark=1;;;
MM;SF;0.050000;-0.050000;SheetOffset=0.000000;Pos=0;MeanTol=1;PosLbl=;Restrict=;
PR;0.000000;
MP;-17.804949;0.000354;-2.647330;0.989129;0.000000;0.147052;Mark=1;;;
MM;SF;0.050000;-0.050000;SheetOffset=0.000000;Pos=0;MeanTol=1;PosLbl=;Restrict=;
PR;0.000000;
MP;-17.866651;-0.000332;-2.194946;0.992477;0.000000;0.122429;Mark=1;;;
MM;SF;0.050000;-0.050000;SheetOffset=0.000000;Pos=0;MeanTol=1;PosLbl=;Restrict=;
PR;0.000000;
MP;-17.916735;0.000508;-1.741126;0.995298;-0.000000;0.096859;Mark=1;;;
MM;SF;0.050000;-0.050000;SheetOffset=0.000000;Pos=0;MeanTol=1;PosLbl=;Restrict=;
PR;0.000000;
MP;-17.955498;-0.000295;-1.280444;0.997461;0.000000;0.071215;Mark=1;;;
MM;SF;0.050000;-0.050000;SheetOffset=0.000000;Pos=0;MeanTol=1;PosLbl=;Restrict=;
PR;0.000000;
MP;-17.982301;-0.000286;-0.824903;0.998922;-0.000000;0.046410;Mark=1;;;
MM;SF;0.050000;-0.050000;SheetOffset=0.000000;Pos=0;MeanTol=1;PosLbl=;Restrict=;
PR;0.000000;
MP;-17.997958;-0.000477;-0.363899;0.999752;-0.000000;0.022283;Mark=1;;;
MM;SF;0.050000;-0.050000;SheetOffset=0.000000;Pos=0;MeanTol=1;PosLbl=;Restrict=;
PR;0.000000;
MP;-18.002867;-0.004372;0.102397;0.999986;-0.000000;-0.005337;Mark=1;;;
MM;SF;0.050000;-0.050000;SheetOffset=0.000000;Pos=0;MeanTol=1;PosLbl=;Restrict=;
PR;0.000000;

```

Figure 3.5: An example of the raw data produced from the CMM measurements.

The first step was to identify and retrieve the relevant data from such a file. The first three lines provide information about the machine set-up. Following this are three lines repeated for each measured point. The lines beginning 'MM' and

'PR' remain constant throughout the file. Thus, it was the 'MP' lines which contained the co-ordinate data. These lines contained 6 pieces of co-ordinate information. The first three were the X, Y and Z co-ordinates relative to the origin defined in section 3.2.1. The next three were these co-ordinates scaled between -1 and 1. By reading each line of the file into Matlab, the first three values from each line beginning 'MP' were stored in three vectors (X, Y, Z) of length L, where L is equivalent to the number of data points measured.

These vectors were then reorganised in matrices of size n by m, where n was the number of individual line scans performed (72 for heads and cups, 30 for tapers) and m was the number of points measured per scan, which varied according to component size.

Due to measuring a point every 0.3mm along a trace, it was occasionally possible for a trace to contain an extra point, for example if the length of the trace was increased due to a large wear patch. The method for shaping matrices meant that this would lead to inaccurate modelling and therefore inaccurate wear volumes. Therefore, Matlab was trained to recognise when this had occurred and automatically remove one point from the affected trace. The method of calculating volumetric wear (explained at the end of this section) meant that this procedure was valid and would not compromise the final calculation. The three matrices (X, Y, Z) were used to graphically recreate the measured surface. Each point was connected linearly to adjacent points to create a wireframe surface (figure 3.6).

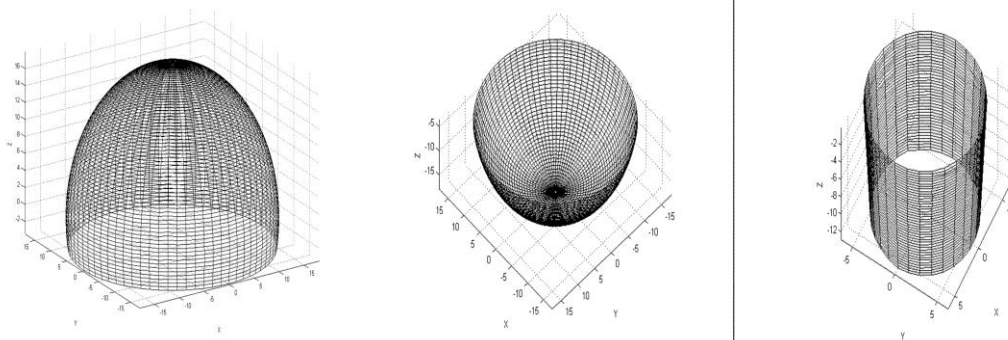


Figure 3.6: Examples of the wireframe surfaces created in Matlab using the co-ordinate data from the CMM.

In order to calculate linear wear depths, the distances from the measured points to the origin were compared with their original unworn equivalents. The method for heads and cups differed from the method for tapers due to the difference in shape. For heads and cups, the distance, r , from each measured point to the origin was calculated using the formula $r = \sqrt{X^2 + Y^2 + Z^2}$. These measured radii were presented on a histogram similar to those in figure 3.7. The median radius was determined and this was taken to be the original radius of the component. This was considered accurate as wear very rarely occurred over more than 50% of the surface and varied greatly in depth (and therefore in measured radius). Given the tight manufacturing tolerances of $\pm 2\mu\text{m}$, measurements of the unworn regions of components found a large number of points with the same radius. This gave each histogram a distinctive peak and elongated tail. The original radius was considered constant and so the difference between each measured radius and the original radius gave the linear wear depth at each point.

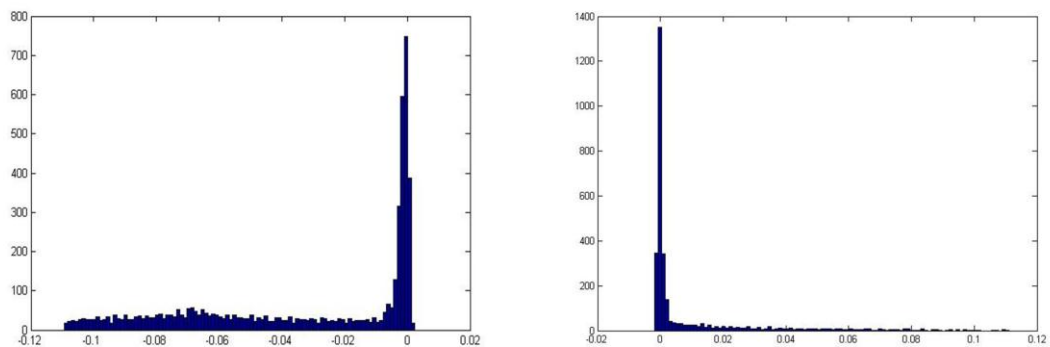


Figure 3.7: Examples of the histograms of measured radii created for a femoral head (left) and acetabular cup (right). Horizontal axis shows deviation between measured radius and calculated unworn radius (mm). Vertical axis shows number of points. Note the high concentration of points around the '0' marks (the original radius) and long tails representing wear. Note also that for femoral heads the tail is to the left, representing a reduction in radius after material loss. For the acetabular cups the tail is to the right, representing an increase in radius after material loss.

For tapers, the distance, r , from each measured point to the centreline of an ideal cone was calculated using the formula $r = \sqrt{X^2 + Y^2}$ where X and Y were the Cartesian co-ordinates perpendicular to the cone's centreline (the Z axis). This 'original' cone was positioned at the time of scanning (as described above), and all measurements were taken relative to it.

The expected distance from the centreline of this cone to each point if the cone were unworn was also calculated. This distance varied depending on the height at which the point was measured. This was accounted for simply by factoring in the 'Z' co-ordinate measured by the CMM. Given a known radius at one end of the taper, R_0 , the radius, R_1 , at any height, Z_1 , relative to that end was given by $R_1 = R_0 + Z_1 \tan \theta$, where θ is the angle of the taper as measured in section 3.2.1 (figure 3.8). The difference between expected distance and measured distance gave linear wear depths.

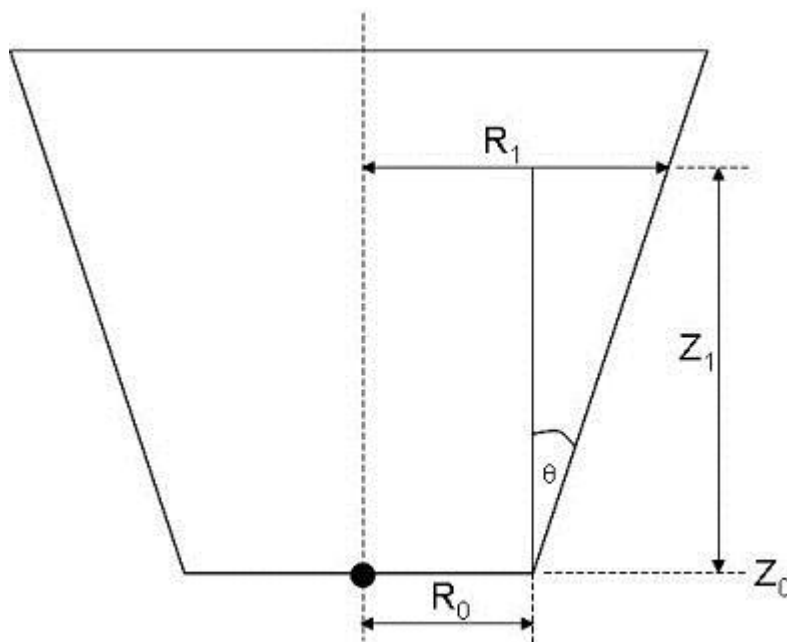


Figure 3.8: Calculation of the unworn radius, R_1 , at any height, Z_1 , for a femoral taper given a known radius at one end, R_0 .

In order to calculate volumetric wear, the area of each gridsquare was calculated. The length of the lines, l , defining each gridsquare was calculated by the formula $l = \sqrt{(X_2 - X_1)^2 + (Y_2 - Y_1)^2 + (Z_2 - Z_1)^2}$. This was repeated for each of the four lines – a, b, c, d, as well as for the diagonals p and q (figure 3.9). In reality, connections between data points were not linear but instead included a shallow arc due to the spherical nature of the component. It was possible to account for this, but doing so significantly increased processing time from under one second to roughly ten seconds and was found to change the calculated wear volume by less than 0.01mm^3 . Thus, the simplified (linear) calculation was used.

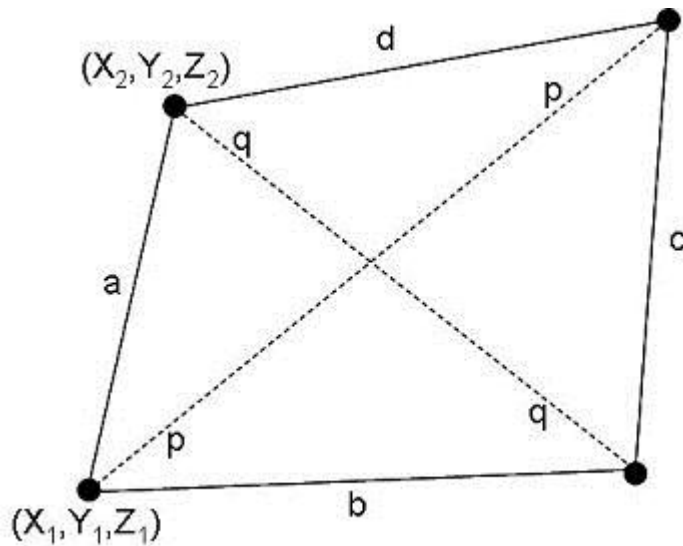


Figure 3.9: Calculation of the area of any irregular quadrilateral.

Each gridsquare formed a different irregular quadrilateral shape and so the following method was used to calculate the surface area. A value, s , was defined such that $s = (a + b + c + d) / 2$. The surface area of each gridsquare was calculated using Bretschneider's formula [213]:

$$Area = \sqrt{(s - a)(s - b)(s - c)(s - d) - \frac{1}{4}(ac + bd + pq)(ac + bd - pq)}$$

Then, the area was multiplied by the mean wear depth at the four corners defining the gridsquare. Multiplying the area by the depth yielded a volume of wear. The process was repeated for all gridsquares and the calculated volumes added together to give a total volumetric wear.

Finally, the wireframe model (figure 3.6) was coloured according to wear depth to provide a visual representation of the severity of the wear. Examples for the matching head, cup and taper from figure 3.4 are shown in figure 3.10.

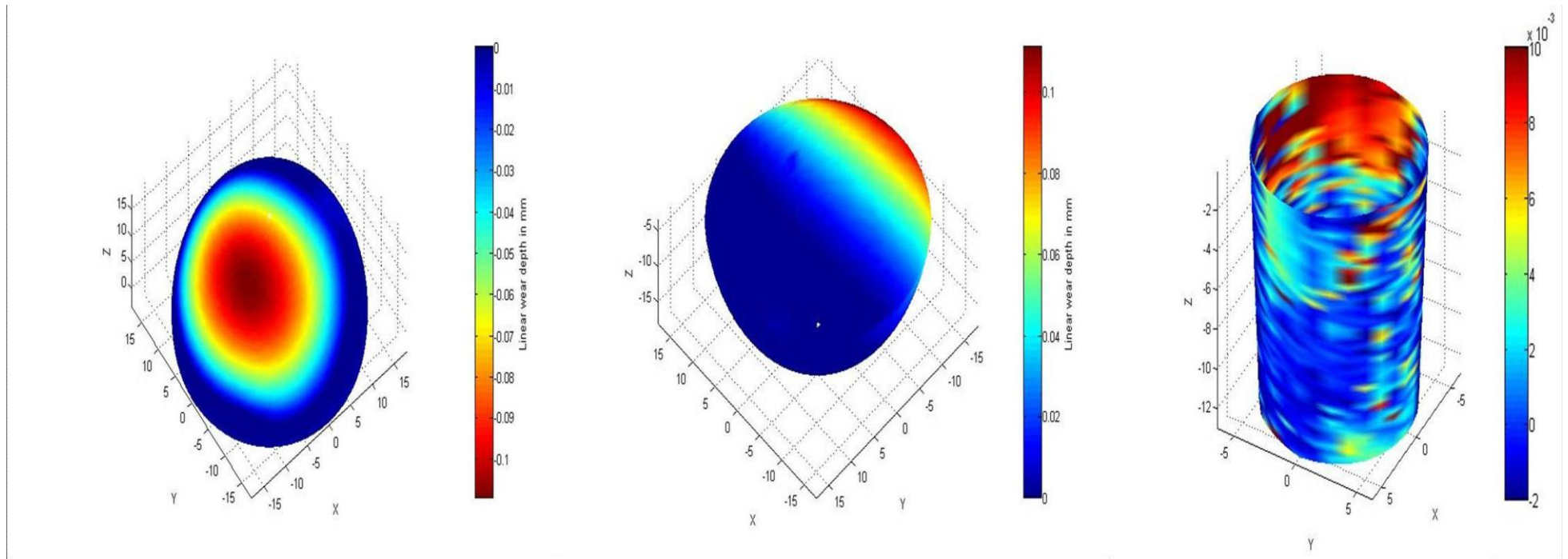


Figure 3.10: Examples of the Matlab output for (left to right) the femoral head, acetabular cup, and femoral taper seen in figure 3.4. Deep red represents the highest wear, while deep blue represents unworn surface. Colour scales represent linear wear depth in mm.

3.3.3 Validation

Validation of the above process for measuring volumetric wear of retrieved MoM hip prostheses was achieved with 3 unused metal hip prosthesis components (2 heads, 1 cup) and a ceramic calibration ball. First, a 19.9881mm diameter ceramic masterball was scanned and processed using the method described above. Due to the ceramic material and the tight manufacturing tolerances used for creating a masterball (within 0.5µm sphericity), this component was expected to show very little deviation in radii. It was unworn and therefore any volumetric “wear” measured was expected to be due to form error from manufacture rather than material removal.

Secondly, the method was validated against established gravimetric methodology using new femoral head and acetabular cup components. The components used were a 36mm nominal diameter Metasul® head (THR), a 48mm nominal diameter ASR™ XL (THR) head and a 46mm nominal diameter Conserve® Plus (resurfacing) acetabular cup, all manufactured from CoCrMo. Given the consistent partial-sphere shape across all models of hip prosthesis, it is reasonable to validate the method on one model and apply this to all models. In the same way the exact model (or combination of models) used in the validation process is of little consequence.

The samples were cleaned thoroughly in an acetone bath for 5 minutes. They were left to dry for one hour on a lint-free cloth and then weighed on a high precision scale (Denver Instrument, sensitivity 0.1 mg). The samples were weighed six times, and an average taken for each sample. Using a density for CoCrMo of 8.3g.cm⁻³ [214, 215] an initial volume of each sample was calculated to be used as a datum. The samples were also scanned using the CMM, so that the effect of form error on apparent “wear” could be evaluated.

The CoCrMo samples then had a quantity of material removed from their bearing surface to simulate wear. As the intention here was simply to remove material, sandpaper was used. In this way it was possible to produce a wear pattern of variable depth across the surface. Following material removal, the samples were cleaned to remove any debris, weighed, measured and analysed again using the CMM. Three scans were taken. The samples were removed

and replaced between scans in order to assess repeatability of measurements for a given sample. More material was then removed from the samples and the process of gravimetric and dimensional (CMM) measurements repeated. In total there were three stages of material removal, with three scans taken at each stage. The volumetric wear calculated from each scan was compared with the volume of material lost determined by the gravimetric method. This comparison was done to test accuracy of the CMM measurement methodology as volumetric wear increased. It was assumed that volumes obtained gravimetrically represented the 'gold standard' (for a CoCrMo component, a change in weight of 0.1mg was equivalent to a volumetric change of 0.012mm³) and the accuracy of the CMM method was assessed against the gravimetric method. This process was also carried out on the internal taper of the new Metasul® head. This was done after all testing was complete on the bearing surface to avoid confusion of results.

Finally, to validate the number of data points used, the 48mm femoral head was measured again (three times) using four times the number of points and once more (three times) using one quarter the number of points.

3.3.4 The wear scar

In addition to volumetric material loss, more detail about the size and location of the wear scar was sought. In section 3.2.2, volumetric wear was calculated by multiplying the area of each gridsquare by the mean wear depth at the four corners. In the same way, by calculating the area of all gridsquares and adding them together the total surface area of the component, A_T , was calculated. Then, by considering only those gridsquares with wear depth greater than 2µm (the typical manufacturing tolerance from section 3.3.1), the worn surface area, A_W , was calculated. This was then expressed as a percentage of the total surface

area by the formula $\frac{A_W}{A_T} * 100$.

The location of the wear scar was defined by the angle between the centre point of the part-spherical component and the point of maximum wear depth, M. The length, l , and height, h , of this point were calculated relative to origin by

$l = \sqrt{X^2 + Y^2}$ and $h = Z$ (Figure 3.11). Then the angle, $\theta = a \tan\left(\frac{h}{l}\right)$. The angle

relative to the component centreline, φ , was then calculated by $\varphi = 90 - \theta$. Thus, wear centred on the pole returned an angle, φ , close to zero. Wear at the rim of a cup returned an angle of around 70° - 75° (depending on the arc of cover) while wear centred on the rim of the head could reach around 110° from the centreline.

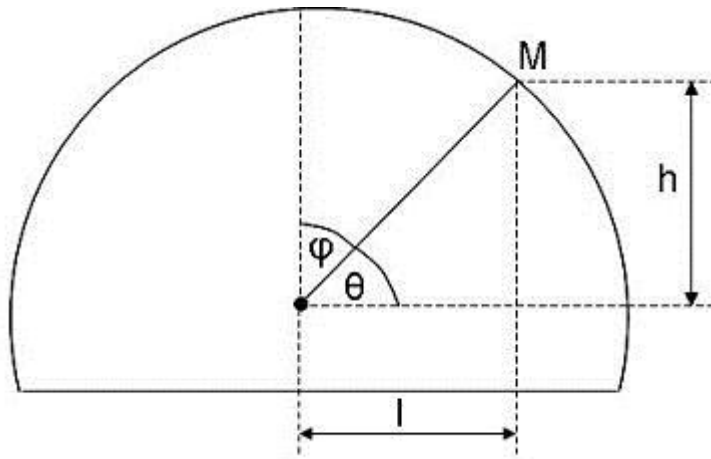


Figure 3.11: Calculating the angle between the component centreline and the point of maximum wear depth.

3.4 Surface roughness

Surface roughness measurements were made on the articulating surfaces of the femoral heads and acetabular cups. Using the output of the wear measurement process (figure 3.10) a worn and unworn region was identified on each component and surface roughness measurements were focused in these two distinct regions. Since the unworn region had, by definition, suffered no wear it is reasonable to assume that this region also did not roughen. Therefore, the unworn region allowed a measurement of initial surface roughness, since such a measurement was unavailable prior to implantation. Measurements in the worn region provided a means for assessing the change in roughness over time and how this change may have affected the operation of the prosthesis, in particular in terms of a change in lubrication regime.

3.4.1 Measurement procedure

The surface of each component was cleaned again with acetone prior to measurement. Surface roughness of the femoral heads was measured using a ZYGO NewView 5000 interferometer [216], a non-contact light-based machine accurate to the nearest nanometre [217, 218]. In total, fifty measurements were taken for each head, twenty-five in each of the worn and unworn regions

identified in section 3.4. Due to the inconsistencies in size and shape of the wear scar across different samples, no single set of points could be defined for taking the measurements on all samples. Therefore measurements were made at the operator's discretion and all attempts were made to represent the entirety of each region.

A 10x magnification objective was used, in addition to the 2x magnification of the NewView 5000. Each measurement contained approximately 76000 data points in an area 0.317mm by 0.238mm (0.075mm²) from which surface roughness data was extracted.

The ZYGO method was not practical for the acetabular cups, due to the microscope objective being too large to fit far enough inside the concave curvature. Cup roughness measurements were therefore performed using a Form Talysurf 50e (Taylor Hobson, Leicester, United Kingdom) contact stylus, accurate to the nearest 10nm [219, 220]. The use of such a dual device measurement for femoral heads and acetabular cups has been employed previously [221]. Wear measurements had highlighted the rim of the cups as areas of interest and so measurements were taken every 10° at the rim of each cup, giving a total of 36 measurements. A cut-off length of 0.25mm was selected. Sensitivity of the Talysurf was 10nm.

3.4.2 Roughness parameters

For each measurement, four different roughness parameters were recorded [222]:

1. Peak to Valley (PV). The distance between the highest and lowest points on the surface. This gives the maximum size of defects in the scan area.
2. Root Mean Square (RMS). The square root of the mean of the height differences squared. This gives a value for deviation in the surface height and accounts for both positive and negative variation (peaks and valleys).
3. Skewness (Rsk). A measure of whether the surface is dominated by peaks (positive skew) or valleys (negative skew). A surface with negative skew is indicative of a series of valleys and, in this application, wear.

4. Roughness average (Ra). The arithmetic average of the absolute height deviations.

3.4.3 Lubrication regime

There are three basic lubrication regimes. Most preferable is fluid-film lubrication [127], in which the bearing surfaces are separated by a thin film of lubricant. Keeping the surfaces separated minimises wear. Least preferable is boundary lubrication, in which the surfaces are in constant contact. This increases friction between the components in contact which subsequently increases risk of wear [223]. Mixed lubrication is also recognised, a combination of fluid film and boundary which is most common in hip prostheses and the lubrication regime can vary during gait [194].

The minimum effective film thickness (h_{\min}) outlined by Dowson [43], was calculated using a modified version of the Hamrock-Dowson equation [196] described in Section 2.4 as:

$$\frac{h_{\min}}{R_x} = 2.80 \left(\frac{\eta u}{E^* R_x} \right)^{0.65} \left(\frac{w}{E^* R_x^2} \right)^{-0.21}$$

Where R_x is the equivalent radius (m), η is the lubricant viscosity (Pa s), u is the entraining velocity (ms⁻¹), E^* is the equivalent elastic modulus (Pa) and w is the load (N).

Values for synovial lubricant viscosity ($\eta = 0.0025$ Pa s), load ($w = 2500$ N), Young's modulus ($E = 210$ GPa), Poisson's ratio ($\nu = 0.3$) and angular velocity ($\omega = 1.5$ rad/s) were taken from the scientific literature [196, 224]. All other values were measured directly.

Ra measurements were then used to calculate the lambda ratio from:

$$\lambda = \frac{h_{\min}}{[(R_{a1})^2 + (R_{a2})^2]^{0.5}}$$

Where subscript 1 refers to the femoral head and subscript 2 refers to the acetabular cup.

3.5 Analyses

Differences between models of hip prosthesis were analysed. In order to determine the correct statistical tests, all variables were tested for normality. Then differences in design, patient and clinical factors were analysed using the Kruskal Wallace test evaluated to the 95% confidence level ($P=0.05$). If differences were identified, the Mann Whitney test evaluated to the 95% confidence level ($P=0.05$) was used to determine for which models those differences existed. Factors studied were:

- Patient
 - Age
 - Gender
- Clinical
 - Reason for revision
 - Acetabular cup inclination angle
 - Acetabular cup anteversion angle
- Design
 - Coverage arc
 - Contact point to rim (CPR) distance
 - Radial clearance
 - Component diameter

Secondly, differences in measures of performance between components and between models were analysed, again using the Kruskal Wallace test and followed up with the Mann Whitney test, both evaluated to the 95% confidence level ($P=0.05$). Factors studied were:

- Rate of linear wear
- Rate of volumetric wear
- Percentage of surface area worn
- Location of deepest wear
- Metal ion levels
- Duration in vivo
- Lubrication regime

Finally, factors were sought which had a significant effect on wear rate. This was achieved using Friedman's test evaluated to the 95% confidence level ($P=0.05$) and all patient, clinical and design factors were considered. Lubrication regime was also considered at this stage.

Two further considerations were of interest. Firstly, whether lubrication regime was well maintained from the time of implantation (unworn region) to the time of revision (worn region) of the prosthesis and secondly, whether there was a correlation between wear and metal ion levels. Both of these were tested using Spearman's rank correlation coefficient evaluated to the 95% confidence level ($P=0.05$).

Chapter 4. Results

This chapter presents the results obtained during the study. It begins with the basic summary statistics of the clinical data. This is followed by the results of the validation study and then the summary statistics of the wear and surface roughness data. Finally, the significant factors correlating with wear are identified and the results of the correlation tests between wear and metal ion concentrations are detailed.

All results were assessed for normality. It was found that none of the results were normally distributed. Therefore, non-parametric statistical methods were used as these make no assumptions about the normality of data. Similarly, when reporting on averages of data sets, the median was the most appropriate description. Given the widespread reporting of means in other studies, mean values have also been included to ease comparison.

4.1 Clinical data

Data about the patients and prostheses used is presented in table 4.1. There were 143 revisions in 143 patients. In 130 cases, both the femoral head and acetabular cup was analysed. In the remaining 13 cases, the cup was not revised. The most common diagnosis for revision was adverse reaction to metal debris (ARMD), which accounted for 115 of the 143 revisions (80.4%). Other reasons for revision were 9 early femoral neck fractures (2 – 7months, 6.3%), 9 surgical complications such as infection or avascular necrosis (6.3%), 6 late femoral neck fractures (20 – 62months, 4.2%) and 4 cases of implant loosening (2.8%). Ninety-four of the patients were female (65.7%). The median patient age was 56 years (range 30 – 73 years). Patients who initially had a hip resurfacing prosthesis were significantly younger than those with a total hip replacement ($p < 0.001$). The median ages were 52 and 62 years respectively (range 30 – 69 years and 50 – 73 years respectively). Overall there were 95 hip resurfacing prostheses analysed (66.4%) and 48 total hip replacements (33.6%). The most common model analysed was the ASR™ with 61 retrievals (42.7%). This was followed by the Pinnacle® (26, 18.2%), ASR™ XL (22, 15.4%), BHR™ (16, 11.2%), Durom™ (8, 5.6%), Cormet™ (5, 3.5%), Conserve® Plus (3, 2.1%) and Adept® (2, 1.4%).

Model	Number retrieved	Diagnosis	Gender	Age (years)	Duration in vivo (months)	Nominal diameter (mm)	Stem type
Adept®	2 Heads 2 Cups	2 ARMD	1 Female 1 Male	Median: 58 Mean: 58 Range: 56 - 60	Median: 52 Mean: 52 Range: 42 - 62	Median: 51 Mean: 51 Range: 50 - 52	-
ASR™	61 Heads 54 Cups	49 ARMD 4 Early fracture 5 Late fracture 3 Surgical	38 Female 23 Male	Median: 51 Mean: 52 Range: 35 - 67	Median: 42 Mean: 41 Range: 2 - 96	Median: 46 Mean: 47 Range: 41 - 55	-
BHR™	16 Heads 14 Cups	11 ARMD 1 Early fracture 1 Late fracture 1 Loosening 2 Surgical	14 Female 2 Male	Median: 47 Mean: 46 Range: 30 - 63	Median: 32 Mean: 42 Range: 3 - 89	Median: 44 Mean: 44 Range: 38 - 50	-
Conserve® +	3 Heads 3 Cups	1 ARMD 1 Early fracture 1 Surgical	2 Female 1 Male	Median: 53 Mean: 53 Range: 51 - 54	Median: 14 Mean: 17 Range: 6 - 30	Median: 44 Mean: 46 Range: 42 - 52	-
Cormet™	5 Heads 5 Cups	3 ARMD 1 Loosening 1 Surgical	1 Female 4 Male	Median: 56 Mean: 56 Range: 55 - 57	Median: 72 Mean: 63 Range: 6 - 102	Median: 48 Mean: 46 Range: 40 - 48	-
Durom™	8 Heads 5 Cups	4 ARMD 3 Early fracture 1 Surgical	5 Female 3 Male	Median: 61 Mean: 60 Range: 49 - 69	Median: 34.5 Mean: 44 Range: 2 - 98	Median: 48 Mean: 48 Range: 42 - 52	-

Model	Number retrieved	Diagnosis	Gender	Age (years)	Duration in vivo (months)	Nominal diameter (mm)	Stem type
All resurfacing	95 Heads 83 Cups	70 ARMD	61 Female 34 Male	Median: 52	Median: 42	Median: 46	-
		9 Early fracture		Mean: 53	Mean: 42	Mean: 46	
		6 Late fracture		Range: 30 - 69	Range: 2 - 102	Range: 38 - 55	
		2 Loosening 8 Surgical					
ASR™ XL	22 Heads 22 Cups	21 ARMD	13 Female	Median: 59	Median: 48	Median: 46	11 Corail 11 S-ROM
		1 Surgical	9 Male	Mean: 60	Mean: 41	Mean: 47	
				Range: 50 - 73	Range: 11 - 68	Range: 41 - 57	
Pinnacle®	26 Heads 25 Cups	24 ARMD	20 Female	Median: 64	Median: 36.5	Median: 36	18 Corail 8 S-ROM
		2 Loosening	6 Male	Mean: 64	Mean: 37	Mean: 36	
				Range: 59 - 71	Range: 12 - 91	Range: 36 - 36	
All THR	48 Heads 47 Cups	45 ARMD	33 Female	Median: 62	Median: 37	Median: 36	29 Corail 19 S-ROM
		2 Loosening	15 Male	Mean: 62	Mean: 39	Mean: 41	
		1 Surgical		Range: 50 - 73	Range: 11 - 91	Range: 36 - 57	
All retrievals	143 Heads 130 Cups	115 ARMD	94 Female 49 Male	Median: 56	Median: 39	Median: 45	29 Corail 19 S-ROM
		9 Early fracture		Mean: 55	Mean: 41	Mean: 45	
		6 Late fracture		Range: 30 - 73	Range: 2 - 102	Range: 36 - 57	
		4 Loosening					
		9 Surgical					

Table 4.1: Breakdown of the recorded clinical data by prosthesis model.

The median duration in vivo was 39 months (range 2 – 102 months). Overall, resurfacing models were in vivo slightly longer (median 42 months, range 2 – 102 months) than total hip replacements (median 37 months, range 11 – 91 months). This difference was not significant ($p = 0.473$). Early fracture retrievals were revised after the shortest time (median 2.5 months, range 2 – 7 months). Surgical (median 37 months, range 16 – 72 months), ARMD (median 42 months, range 8 – 96 months), late fracture (median 46 months, range 20 – 62 months) and loosening (median 55.5 months, range 12 – 99 months) revisions survived longer.

The median nominal diameter was 45mm (range 36 – 57mm). Resurfacing models (median 46mm, range 38 – 55mm) were the same size as ASR™ XL prostheses (median 46mm, range 41 – 57mm) and both were larger than the Pinnacle® prostheses (all 36mm). This difference was significant ($p < 0.001$ in both cases). Loosened components tended to be of smaller diameter (median 41mm, range 36 – 48mm) than surgical (median 45mm, range 38 – 48mm), ARMD (median 45mm, range 36 – 57mm), early fracture (median 49mm, range 42 – 54mm) and late fracture (median 49mm, range 46 – 52mm).

Only two models of stem were used (both manufactured by DePuy as both of the THRs analysed were manufactured by DePuy). The Corail was the most common stem, used with 29 total hip replacements (60.4%). The remaining 19 used S-ROM stems (39.6%). There was a difference in the angle of the femoral taper, depending on which stem was used ($p < 0.001$). For Corail stems, the median taper angle was 5.6379° (range $5.5710^\circ - 5.7983^\circ$). For S-ROM stems, the median taper angle was 5.9817° (range $5.9200^\circ - 6.0256^\circ$).

Further clinical data is presented in table 4.2. The median cup inclination (48.85° , range $22.85^\circ - 76.04^\circ$) and anteversion (17.04° , range $0.00^\circ - 40.00^\circ$) angles were close to the commonly recommended angles of 45° and 15° respectively [55, 56, 225]. The median cup inclination angle for resurfacing prostheses was 49.39° (range $22.85^\circ - 75.00^\circ$). The median anteversion angle was 18.72° (range $0.00^\circ - 40.00^\circ$). For total hip replacements, the median cup inclination angle was 46.88° (range $34.76^\circ - 76.04^\circ$). The median anteversion angle was 14.92° (range $0.00^\circ - 39.90^\circ$).

Figures 4.1 and 4.2 show the inclination and anteversion angles for each model and each diagnosis. At 50.53°, (range 28.50° - 72.53°) the ASR™ cup inclination angle was slightly higher than the recommended 45° angle ($p < 0.001$), but within a reasonable range. The median Adept® inclination angle was low at 29.85° (range 26.93° - 32.77°). This was not significantly different from the recommended 45° ($p = 0.371$), though this is due in large part to the small number of Adept® samples ($n = 2$). The ASR™ anteversion angle was also high at 20.66° (range 0.00° - 39.30°, $p < 0.001$), but again within a reasonable range. Compared with the recommended 15° the median Durom (7.72°, range 0.00° - 30.00°) and Cormet (7.87°, range 0.00° - 16.49°) anteversion angles were low, but not significantly so ($p = 0.401$ and $p = 0.106$ respectively).

Early fracture (median 41.50°, range 35.67 – 56.92°) and surgical (median 41.83°, range 38.00 – 60.30°) revisions were associated with lower inclination angles. Higher inclination angles were seen in loosening (median 46.88°, range 44.52 – 48.06°), ARMD (median 49.39°, range 26.93 – 72.53°) and late fracture (median 55.05°, range 41.72 – 60.03°). The lowest anteversion angles were seen in early fracture (median 10.77°, range 0.00 – 28.87°) and loosened (median 11.62°, range 5.00 – 16.97°). Higher anteversion angles were seen in surgical (median 16.75°, range 5.32 – 18.71°), ARMD (median 18.00°, range 1.50 – 39.30°) and late fracture (median 25.55°, range 12.00 – 31.31°) retrievals.

The median contact point to rim (CPR) distance was 12.06mm (range 1.14mm – 25.48mm). Overall, the total hip replacements had a larger CPR distance (median 12.78mm, range 1.14mm – 19.28mm) than the resurfacings (median 11.04mm, range 1.16mm – 25.48mm), though this difference was not significant ($p = 0.403$). The CPR distance was smallest for the ASR™ resurfacing (median 9.78mm, range 1.16mm – 18.89mm) and largest for the Adept® (median 21.81mm, range 18.65mm – 24.96mm).

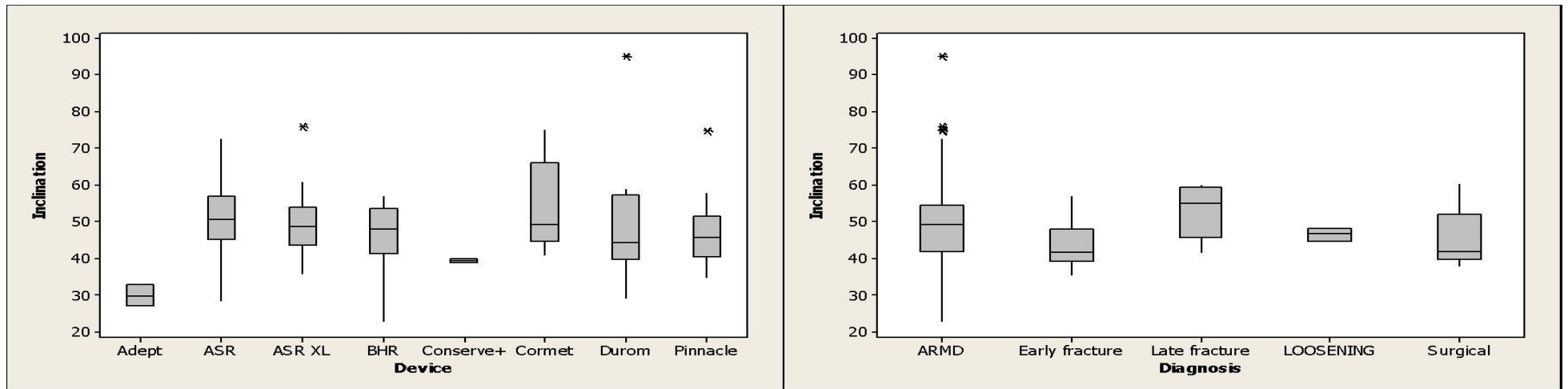


Figure 4.1: Boxplot of the acetabular cup inclination angle for each model of hip prosthesis (left) and each diagnosis (right).

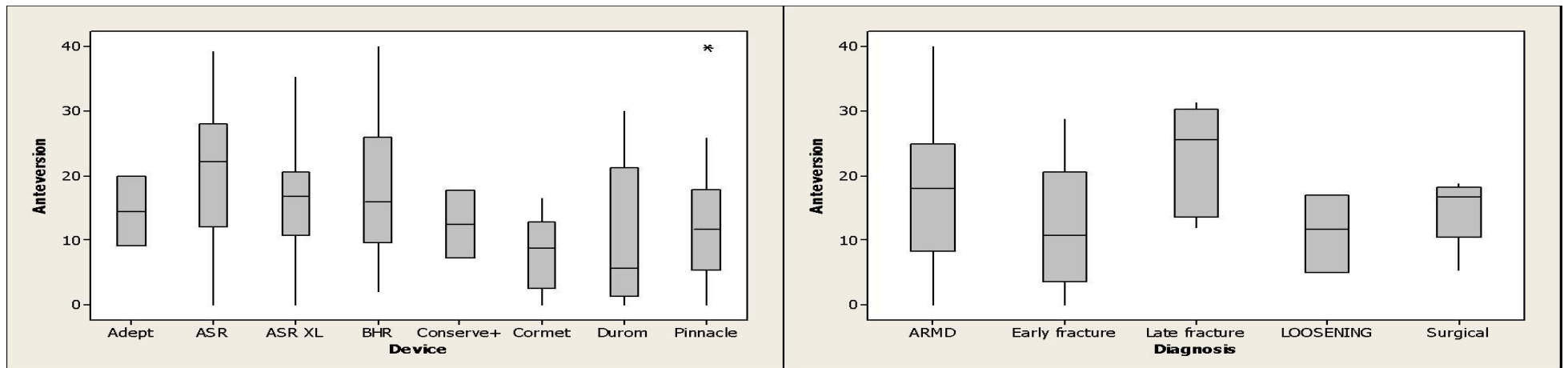


Figure 4.2: Boxplot of the acetabular cup anteversion angle for each model of hip prosthesis (left) and each diagnosis (right).

Model	Inclination (°)	Anteversión (°)	CPR distance (mm)	Blood Cr (µg/l)	Blood Co (µg/l)	Serum Cr (µg/l)	Serum Co (µg/l)
Adept®	Median: 29.85	Median: 14.52	Median: 21.81	Median: 10.91	Median: 5.80	Median: 10.35	Median: 6.31
	Mean: 29.85	Mean: 14.52	Mean: 21.81	Mean: 10.91	Mean: 5.80	Mean: 10.35	Mean: 6.31
	Range: 26.93 – 32.77	Range: 9.13 – 19.91	Range: 18.65 – 24.96	Range: 10.50 – 11.32	Range: 5.63 – 5.97	Range: 9.94 – 10.76	Range: 5.45 – 7.17
ASR™	Median: 50.53	Median: 22.10	Median: 9.78	Median: 17.60	Median: 21.30	Median: 23.50	Median: 19.80
	Mean: 50.55	Mean: 20.66	Mean: 9.92	Mean: 25.21	Mean: 48.69	Mean: 35.94	Mean: 44.39
	Range: 28.50 – 72.53	Range: 0 – 39.30	Range: 1.16 – 18.89	Range: 1.61 – 77.50	Range: 0.77 – 271.00	Range: 2.96 – 115.00	Range: 0.98 – 228.00
BHR™	Median: 47.82	Median: 15.99	Median: 12.86	Median: 6.435	Median: 7.55	Median: 6.34	Median: 8.20
	Mean: 45.99	Mean: 17.76	Mean: 13.23	Mean: 15.58	Mean: 24.20	Mean: 19.50	Mean: 27.06
	Range: 22.85 – 56.92	Range: 2.00 – 40.00	Range: 5.99 – 19.05	Range: 0.78 – 67.08	Range: 1.44 – 109.74	Range: 1.61 – 67.08	Range: 1.93 – 120.36
Conserve® +	Median: 39.39	Median: 12.40	Median: 18.60	Median: 1.90	Median: 1.00	Median: 1.90	Median: 1.00
	Mean: 39.39	Mean: 12.40	Mean: 18.60	Mean: 1.90	Mean: 1.00	Mean: 1.90	Mean: 1.00
	Range: 38.72 – 40.06	Range: 7.14 – 17.66	Range: 13.29 – 22.43	Range: 0.69 – 3.06	Range: 0.34 – 1.95	Range: 1.02 – 2.48	Range: 0.41 – 1.45
Cormet™	Median: 49.24	Median: 8.75	Median: 16.32	Median: 4.45	Median: 4.03	Median: 21.19	Median: 37.84
	Mean: 54.01	Mean: 7.87	Mean: 16.49	Mean: 10.69	Mean: 18.25	Mean: 23.16	Mean: 46.70
	Range: 40.91 – 75.00	Range: 0 – 16.49	Range: 14.17 – 19.17	Range: 4.45 – 23.16	Range: 4.03 – 16.70	Range: 7.15 – 34.54	Range: 8.43 – 60.29
Durom™	Median: 42.93	Median: 5.32	Median: 17.59	Median: 7.64	Median: 12.53	Median: 11.09	Median: 8.37
	Mean: 44.2	Mean: 7.72	Mean: 18.08	Mean: 8.94	Mean: 13.14	Mean: 13.71	Mean: 16.41
	Range: 29.21 – 59.00	Range: 0 – 30.00	Range: 8.19 – 25.48	Range: 2.37 – 15.43	Range: 5.69 – 21.17	Range: 5.46 – 23.47	Range: 4.48 – 37.19
All resurfacing	Median: 49.39	Median: 18.72	Median: 11.04	Median: 13.36	Median: 17.88	Median: 19.70	Median: 18.60
	Mean: 48.80	Mean: 18.14	Mean: 11.78	Mean: 22.69	Mean: 42.69	Mean: 32.95	Mean: 41.38
	Range: 22.85 – 75.00	Range: 0 – 40.00	Range: 1.16 – 25.48	Range: 0.78 – 77.50	Range: 0.77 – 271.00	Range: 1.61 – 115.00	Range: 0.98 – 228.00
ASR™ XL	Median: 48.84	Median: 16.89	Median: 11.01	Median: 8.94	Median: 10.09	Median: 11.08	Median: 10.80
	Mean: 49.36	Mean: 16.38	Mean: 11.57	Mean: 13.32	Mean: 17.87	Mean: 16.35	Mean: 19.33
	Range: 35.90 – 76.04	Range: 0 – 35.26	Range: 4.44 – 19.28	Range: 3.35 – 75.50	Range: 0.77 – 124.00	Range: 2.99 – 105.00	Range: 0.98 – 149.00
Pinnacle®	Median: 45.70	Median: 11.65	Median: 13.39	Median: 7.32	Median: 5.45	Median: 6.27	Median: 7.14
	Mean: 46.52	Mean: 12.32	Mean: 12.98	Mean: 9.14	Mean: 8.87	Mean: 9.73	Mean: 9.39
	Range: 34.76 – 74.94	Range: 0 – 39.90	Range: 1.14 – 17.09	Range: 0.47 – 28.76	Range: 0.63 – 64.31	Range: 0.62 – 45.19	Range: 1.00 – 54.69

Model	Inclination (°)	Anteversion (°)	CPR distance (mm)	Blood Cr (µg/l)	Blood Co (µg/l)	Serum Cr (µg/l)	Serum Co (µg/l)
All THR	Median: 46.88	Median: 14.92	Median: 12.78	Median: 8.48	Median: 5.85	Median: 8.39	Median: 7.66
	Mean: 47.85	Mean: 14.21	Mean: 12.24	Mean: 11.06	Mean: 13.01	Mean: 12.86	Mean: 14.08
	Range: 34.76 – 76.04	Range: 0 – 39.90	Range: 1.14 – 19.28	Range: 0.47 – 75.50	Range: 0.63 – 124.00	Range: 0.62 – 105.00	Range: 0.98 – 149.00
All retrievals	Median: 48.85	Median: 17.04	Median: 12.06	Median: 10.20	Median: 9.73	Median: 12.00	Median: 10.80
	Mean: 48.48	Mean: 16.82	Mean: 11.92	Mean: 18.39	Mean: 31.71	Mean: 24.91	Mean: 30.46
	Range: 22.85 – 76.04	Range: 0 – 40.00	Range: 1.14 – 25.48	Range: 0.47 – 77.50	Range: 0.63 – 271.00	Range: 0.62 – 115.00	Range: 0.98 – 228.00

Table 4.2: Breakdown of implantation angle, contact point to rim (CPR) distance and patient metal ion levels at the time of revision surgery.

The lowest CPR distances were seen in late fracture retrievals (median 8.52mm, range 5.56 – 18.42mm). The next lowest were ARMD (median 11.31mm, range 1.14 – 24.96mm), followed by surgical (median 14.50mm, range 7.72 – 17.49mm), early fracture (median 14.96mm, range 10.50 – 22.32mm) and loosened (median 15.92mm, range 13.61 – 18.22mm) retrievals. A boxplot of CPR distance for each model of prosthesis and each revision diagnosis is shown in figure 4.3.

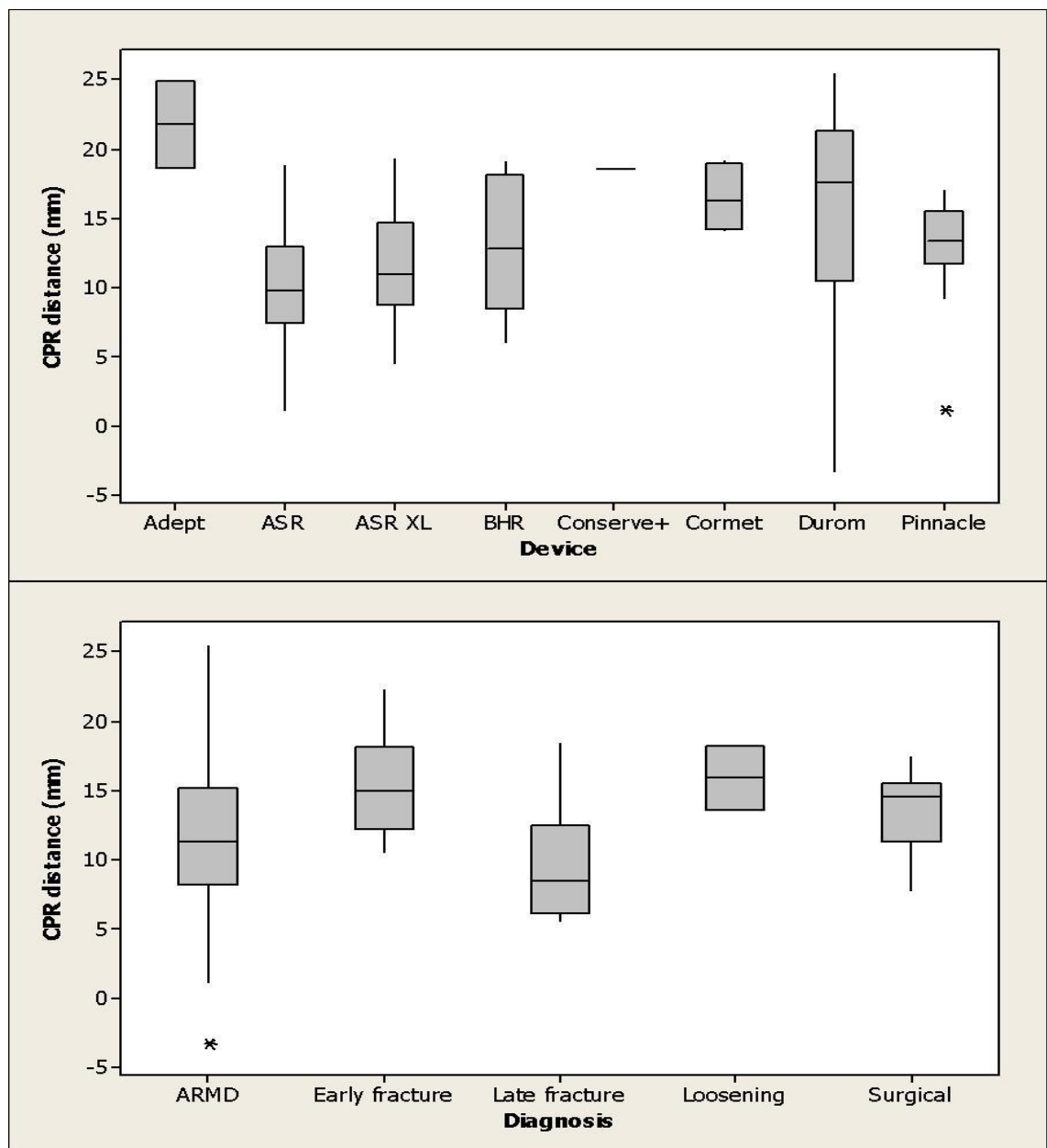


Figure 4.3: Boxplot of CPR distance for each model of hip prosthesis (top) and each revision diagnosis (bottom). CPR distance is individual to each prosthesis and depends on diameter and cup orientation, as well as coverage arc.

Since CPR distance can differ between devices with the same size and cup orientation, depending on coverage arc, this information was also assessed for

ASR™ resurfacings alone (since they constituted the largest group). Late fractures again had the lowest CPR distance (median 7.74mm, range 5.56 – 10.52mm). Retrievals following surgical complications had the largest (median 14.58mm, range 7.71 – 14.89mm). Median chromium ion levels were 10.25µg/l (range 0.47 – 77.50µg/l) in the blood and 12.25µg/l (range 0.62 – 115.00µg/l) in the serum. Median cobalt ion levels were 9.73µg/l (range 0.63 – 271.00µg/l) in the blood and 11.10µg/l (range 0.98 – 228.00µg/l) in the serum.

All measures of metal ion levels were higher in the resurfacings group than the total hip replacement group. In the whole blood, chromium ion levels were 58% higher in the resurfacing group (8.48µg/l vs. 13.36µg/l) and cobalt ion levels were 205% higher (5.85µg/l vs. 17.88µg/l). In the serum, chromium and cobalt ion levels were 134% (8.39µg/l vs. 19.70µg/l) and 143% (7.66µg/l vs. 18.60µg/l) higher respectively in the resurfacing group (all $p < 0.001$). Note, however, that these levels are heavily affected by the large number of ASR™ resurfacing patients with abnormally high metal ion levels. Other resurfacing patients did not suffer such high concentrations. Figure 4.4 shows a boxplot of chromium and cobalt ion levels in the whole blood and serum for each model of prosthesis individually. In all four measures, levels were highest in the ASR™. Mann Whitney analysis indicated that median blood Cr levels in ASR™ resurfacing patients (median 17.60µg/l) were significantly higher than in ASR™ XL (median 8.94µg/l, $p = 0.007$), BHR™ (median 6.44µg/l, $p = 0.041$), Durom™ (median 7.64µg/l, $p = 0.045$) and Pinnacle® (median 7.32µg/l, $p < 0.001$) patients. Blood Co levels in ASR™ resurfacing patients (median 21.30µg/l) were only significantly higher than the Pinnacle® patients (median 5.45µg/l, $p < 0.001$). In the serum, ASR™ resurfacing patient Cr levels (median 23.50µg/l) were significantly higher than ASR™ XL (median 11.08µg/l, $p = 0.010$) and Pinnacle® (median 6.27µg/l, $p < 0.001$) patients. ASR™ resurfacing serum Co levels (median 19.80µg/l) were also higher than ASR™ XL (median 10.80µg/l, $p = 0.040$) and Pinnacle® (median 7.14µg/l, $p < 0.001$) levels.

In terms of diagnosis, late fracture patients had the highest ion levels (figure 4.5). Mann Whitney analysis showed that blood Cr levels in ARMD patients (median 10.40µg/l) were significantly higher than in loosening (median 5.31µg/l, $p = 0.044$) and surgical (median 3.45µg/l, $p = 0.041$) retrievals. The same was

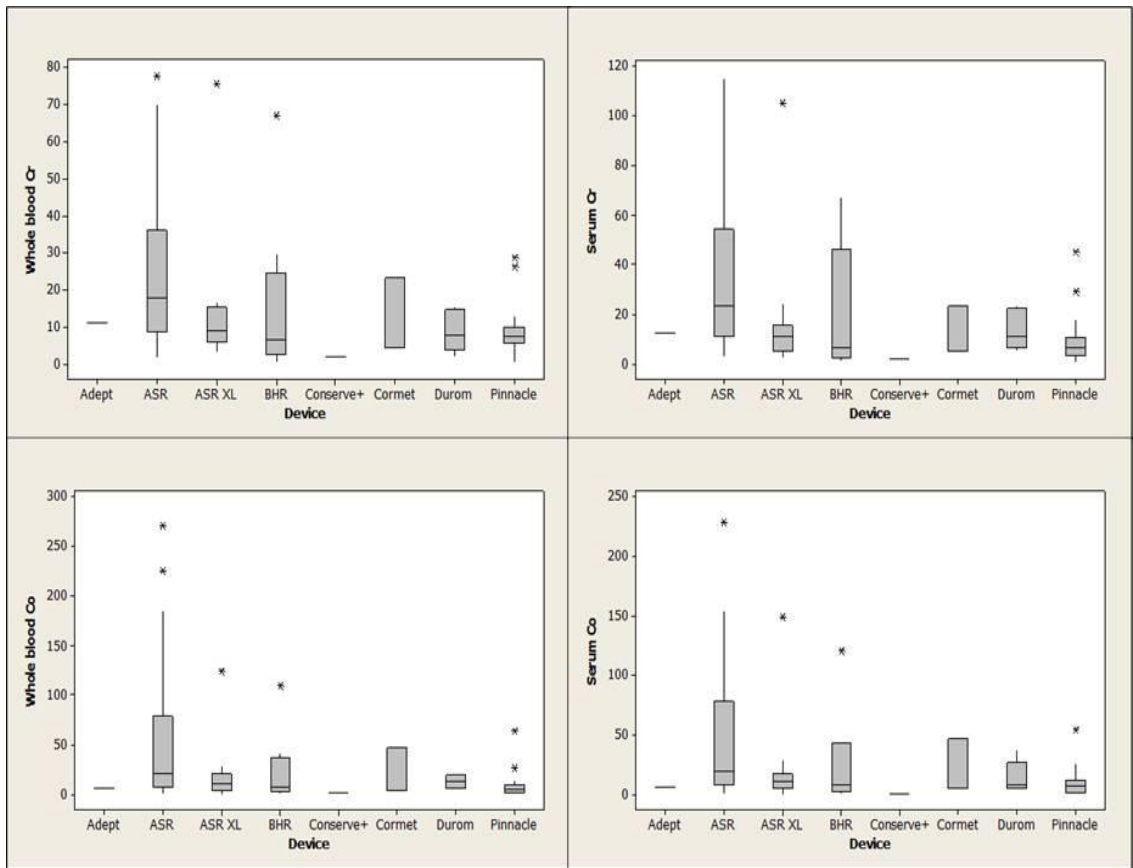


Figure 4.4: Boxplots of Cr and Co ion levels in the blood and serum for each model of hip prosthesis.

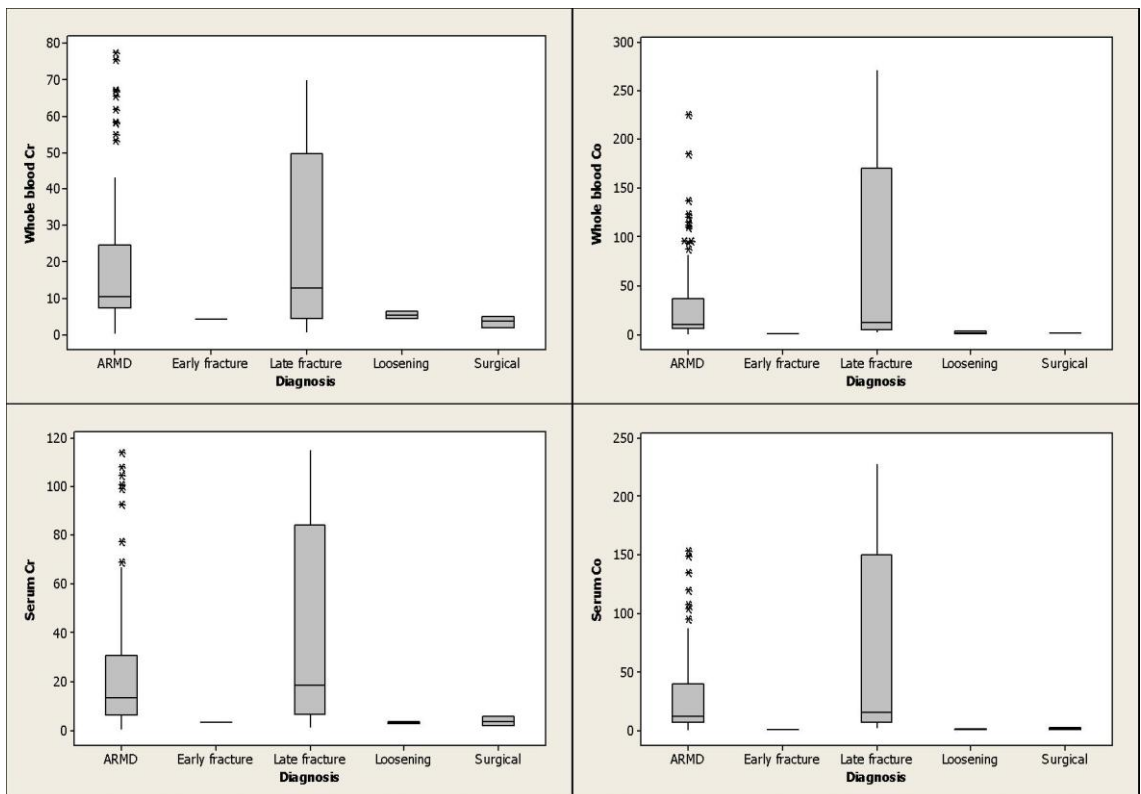


Figure 4.5: Boxplots of Cr and Co ion levels in the blood and serum for each retrieval diagnosis.

true for all other measures of metal ion concentrations. Despite higher median ion levels (e.g. blood Cr = 12.60µg/l), there were no significant differences between concentrations of Cr in late fracture components when compared with loosening and surgical related revisions. Levels of Co ions between these patients bordered on statistical significance ($0.074 < p < 0.081$).

4.2 Wear measurement validation

4.2.1 Masterball

The CMM method calculated a radius for the masterball of 9.9945mm. This is 0.4µm larger than the actual radius. This error is within the scanning limits of the CMM (accurate to within 0.9µm). The calculated “wear” volume was 0.04mm³. This is not actual wear but a combination of form error inherent in manufacture and measurement error. Moreover it is a trivial volume compared with those being measured on retrieved prostheses, typically of the order of 4.5 – 6.5mm³ per component as presented in section 4.3.

The results from the masterball measurements are summarised in Table 4.3. The measured radial deviations are presented as a histogram in Figure 4.6. The measurements were evaluated and provide a Gaussian distribution around the zero point, indicative of variations arising from a manufacturing process rather than from wear. Clearly no wear would be expected on such a masterball.

	Radius (mm)	Volume (mm ³)
Actual	9.9941	0
CMM	9.9945	0.04
Difference	0.0004	0.04

Table 4.3: Measurement of the ceramic masterball indicating the size of the errors in the presented wear measurement method. Note: actual size supplied with masterball; difference in radius of 0.4µm is within claimed accuracy of Legex 322 (0.9µm)

4.2.2 Gravimetric

Results of the gravimetric validation procedure are shown in Tables 4.4 – 4.7. The weight of material loss at each stage is presented and this is converted to a volume using the density for CoCrMo of 8.3g.cm⁻³ from section 3.3.3. The mean

Matlab calculations of original component radius, maximum linear wear depth and wear volume is presented from the three CMM scans at each level of material removal, along with the standard deviation of these values. Finally, the absolute error values of volumetric wear measurement were calculated and the mean presented. The maximum single error for any scan was 0.82mm^3 , occurring on the 40mm articulating diameter acetabular cup at the first stage of material removal. In this case the wear was underestimated as 2.75mm^3 , compared with 3.566mm^3 measured gravimetrically.

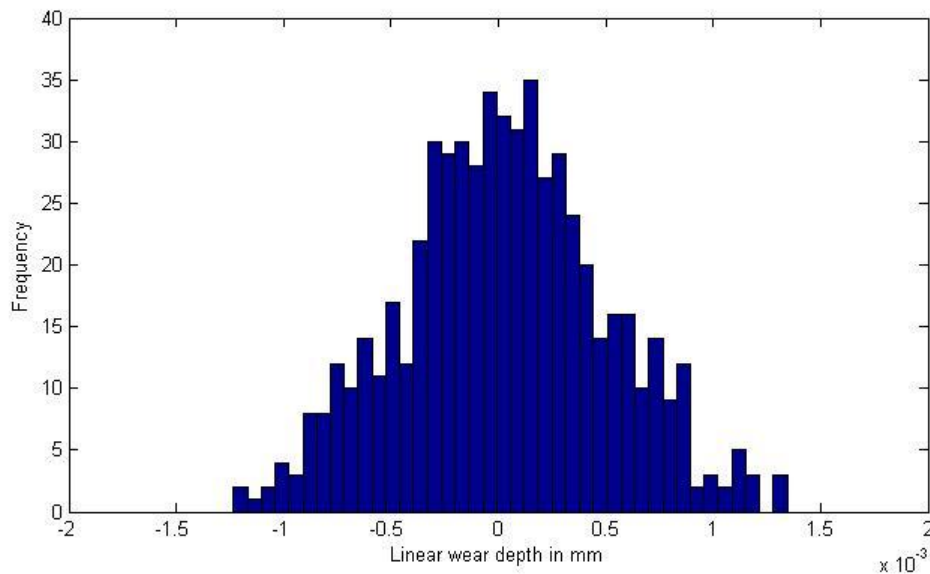


Figure 4.6: Histogram of the masterball scan. Distribution was evaluated and is Gaussian. Minimum point = $-1.2\mu\text{m}$. Maximum point = $+1.3\mu\text{m}$. Positive 'linear wear depth' indicates manufacturing form and the ability of the CMM wear measurement methodology to identify this. Calculated wear volume = 0.04mm^3 .

Figure 4.7 shows the errors in each Matlab measurement for all four validation components (two heads, one cup and one taper). Errors occurred as both under-estimates (21 measurements, 58%) and over-estimates (15 measurements, 42%) and there was a downward trend in volumetric error (mm^3) as wear increased. That is, as wear increased the Matlab method agreed more closely with the gravimetric method.

36mm Head	Material removal (mm³)		
	1st	2nd	3rd
Gravimetric – Weight/mg	42.0	84.1	128.6
Gravimetric converted to volume (mm ³)	5.060	10.133	15.494
Mean Matlab radius (mm) (±St. Dev.)	18.0055 (±0.0006)	18.0053 (±0.0005)	18.0058 (±0.0007)
Mean Matlab wear depth (µm) (±St. Dev.)	41.3 (±0.5)	47.8 (±0.2)	69.6 (±0.4)
Mean Matlab wear volume (mm ³) (±St. Dev.)	5.17 (±0.72)	9.82 (±0.51)	15.74 (±0.25)
Mean absolute Matlab error (mm ³)	0.54	0.50	0.24

Table 4.4: Comparison of Matlab method to gravimetric method. Mean volume is the mean of the 3 measurements at each stage. Mean absolute error is the mean of the error of the 3 measurements. St. Dev. = Standard deviation.

48mm Head	Material removal (mm³)		
	1st	2nd	3rd
Gravimetric – Weight/mg	29.9	75.0	107.6
Gravimetric converted to volume (mm ³)	3.602	9.036	12.964
Mean Matlab radius (mm) (±St. Dev.)	24.2521 (±0.0007)	25.2522 (±0.0003)	25.2533 (±0.0002)
Mean Matlab wear depth (µm) (±St. Dev.)	28.2 (±0.1)	53.0 (±0.4)	83.5 (±0.3)
Mean Matlab wear volume (mm ³) (±St. Dev.)	3.68 (±0.34)	9.19 (±0.24)	12.91 (±0.06)
Mean absolute Matlab error (mm ³)	0.24	0.22	0.05

Table 4.5: Comparison of Matlab method to gravimetric method. Mean volume is the mean of the 3 measurements at each stage. Mean absolute error is the mean of the error of the 3 measurements. St. Dev. = Standard deviation.

40mm Cup	Material removal (mm ³)		
	1st	2nd	3rd
Gravimetric – Weight/mg	29.6	53.8	91.2
Gravimetric converted to volume (mm ³)	3.566	6.482	10.988
Mean Matlab radius (mm) (±St. Dev.)	20.0621 (±0.0004)	20.0592 (±0.0005)	20.0613 (±0.0003)
Mean Matlab wear depth (µm) (±St. Dev.)	16.0 (±1.0)	131.0 (±1.4)	164.2 (±0.15)
Mean Matlab wear volume (mm ³) (±St. Dev.)	2.97 (±0.54)	6.52 (±0.23)	11.01 (±0.15)
Mean absolute Matlab error (mm ³)	0.49	0.17	0.11

Table 4.6: Comparison of Matlab method to gravimetric method. Mean volume is the mean of the 3 measurements at each stage. Mean absolute error is the mean of the error of the 3 measurements. St. Dev. = Standard deviation.

73

Taper	Material removal (mm ³)		
	1st	2nd	3rd
Gravimetric – Weight/mg	14.0	29.4	45.5
Gravimetric converted to volume (mm ³)	1.687	3.542	5.482
Mean Matlab taper angle (radians)	0.0988 (±0.0000)	0.0986 (±0.0000)	0.0987 (±0.0001)
Mean Matlab wear depth (µm) (±St. Dev.)	34.6 (±10.4)	85.7 (±3.3)	89.9 (±0.3)
Mean Matlab Volume (mm ³) (±St. Dev.)	1.57 (±0.31)	3.60 (±0.44)	5.41 (±0.07)
Mean absolute Matlab error (mm ³)	0.28	0.32	0.08

Table 4.7: Comparison of Matlab method to gravimetric method. Mean volume is the mean of the 3 measurements at each stage. Mean absolute error is the mean of the error of the 3 measurements. St. Dev. = Standard deviation.

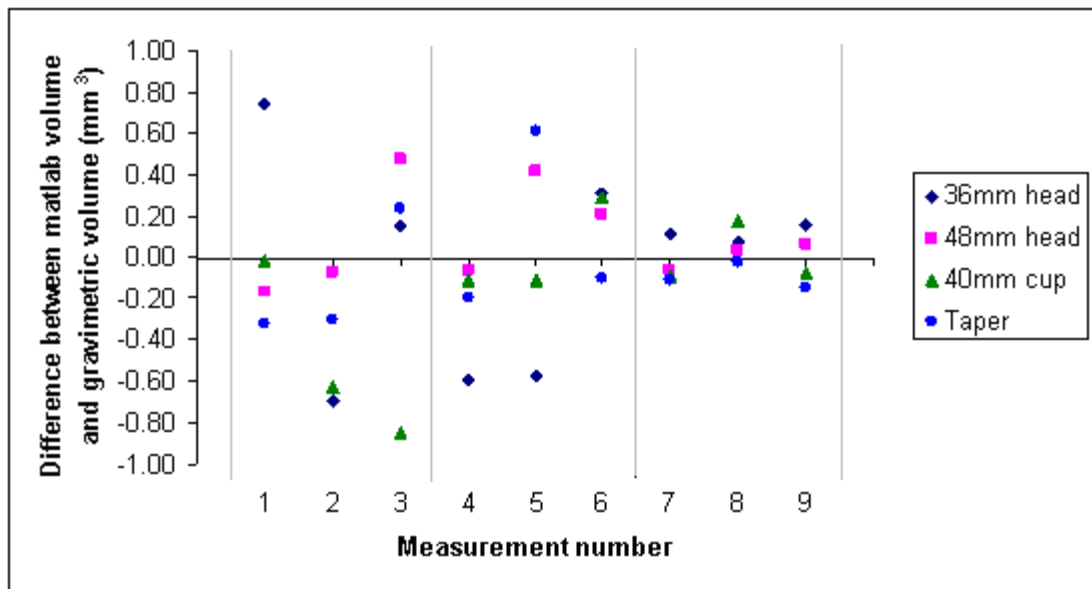


Figure 4.7: Errors in the Matlab volumetric wear calculation when compared with gravimetric methods for all four validation components. Each set of three measurement numbers (separated by gray vertical lines) corresponds to a level of material removal.

Table 4.8 shows the result of changing the number of data points collected.

Three sets of three measurements were taken on the 48mm ASR™ femoral head – one set using the method described in this thesis, one set collecting four times the number of data points and one set collecting a quarter of the data points. The effect of changing the number of points is also illustrated in figure 4.8. Note the very similar images produced by the current method and by quadrupling the number of data points. When the number of data points was quartered, a much more “angular” image was produced, due to the linear interpolation between points.

4.3 Retrieval analysis

4.3.1 Wear

Wear data was calculated using the CMM method presented in Section 3.3. This involved between 1000 – 2000 data points for each taper, 3024 – 4104 for each cup and 6048 – 7128 for each head. Linear wear depth (μm), wear volume (mm^3) and wear rate (mm^3/year) for all 143 retrievals are presented in table 4.9. The data is split by prosthesis model and by component type (head, cup or taper). The combined total values for all head and cup pairs are also provided.

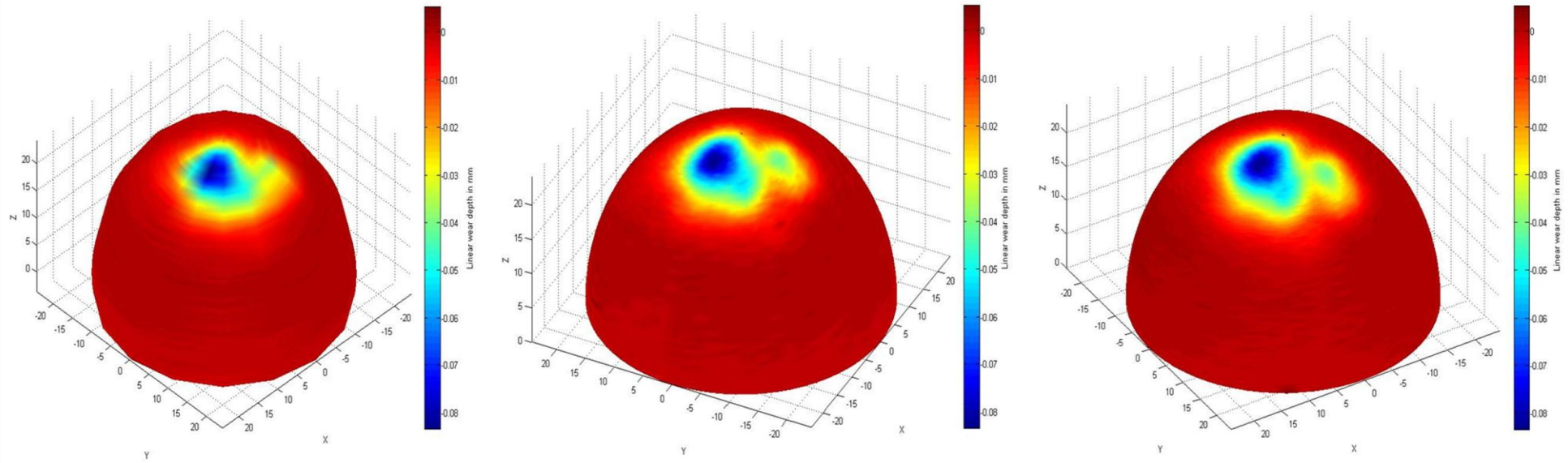


Figure 4.8: A comparison of the effect of changing the number of data points collected with the CMM. Images produced are from the 48mm ASR™ validation head when taking 1458 points (left), 5832 points (centre, current method) and 23328 points (right).

	Number of points measured		
	1458	5832 (current method)	23328
Radius (mm)	24.2527	24.2534	24.2525
	24.2526	24.2534	24.2527
	24.2528	24.2531	24.2526
Wear depth (μm)	83.9	83.4	84.2
	85.1	83.3	84.5
	83.7	83.9	84.3
Wear volume (mm^3)	14.07	12.84	13.04
	13.81	12.93	12.93
	13.78	12.96	12.94

Table 4.8: *The effect of changing the number of data points collected on the measured radius, maximum wear depth and wear volume. Wear volume recorded gravimetrically = 12.964mm³.*

Overall, linear wear on the cups (median 23.7 μm) was deeper than on the heads (median 15.0 μm). The ASR™ components showed a much greater combined wear depth (median 103.2 μm) than the other devices. The Adept® components showed the lowest overall wear depth (median 10.3 μm) (figure 4.9). Late fracture retrievals were associated with the highest linear wear depth (median 250.4 μm). Retrievals following ARMD (median 41.0 μm), loosening (median 19.2 μm) and surgical complications (median 12.6 μm) were associated with lower linear wear depths.

Femoral heads contributed a greater volume of wear (median 6.58mm³) than acetabular cups (median 4.53mm³). The ASR™ components wore more than any other model (median 28.58mm³ total wear). Adept® components wore the least (median 3.70mm³ total wear) (figure 4.10). Retrievals following late femoral neck fracture had the highest wear volumes (median 61.12mm³). Retrievals following ARMD (median 12.89mm³), early fracture (median 12.40mm³), loosening (median 5.79mm³) and surgical complications (median 5.63mm³) exhibited lower volumetric wear.

Model	Component depth (μm)	Total depth (μm)	Component volume (mm^3)	Total volume (mm^3)	Component rate (mm^3/year)	Total rate (mm^3/year)	
Adept®	Head	Median: 5.6 Mean: 5.6 Range: 4.3 – 6.8	Median: 10.3 Mean: 10.3 Range: 6.4 – 9.5	Median: 2.67 Mean: 2.67 Range: 2.16 – 3.18	Median: 3.70 Mean: 3.70 Range: 2.50 – 4.90	Median: 0.66 Mean: 0.66 Range: 0.42 – 0.91	Median: 0.94 Mean: 0.94 Range: 0.48 – 1.40
	Cup	Median: 4.4 Mean: 4.4 Range: 3.1 – 5.7		Median: 1.03 Mean: 1.03 Range: 0.34 – 1.72		Median: 0.28 Mean: 0.28 Range: 0.07 – 0.49	
ASR™	Head	Median: 27.8 Mean: 63.5 Range: 2.5 – 461.9	Median: 103.2 Mean: 197.2 Range: 8.1 – 1138.4	Median: 16.07 Mean: 37.23 Range: 0.56 – 326.88	Median: 28.58 Mean: 70.52 Range: 3.20 – 438.27	Median: 6.26 Mean: 10.23 Range: 0.22 – 48.76	Median: 9.61 Mean: 18.06 Range: 0.57 – 87.28
	Cup	Median: 60.0 Mean: 125.22 Range: 5.6 – 1014.6		Median: 8.98 Mean: 29.96 Range: 1.34 – 373.46		Median: 2.66 Mean: 8.04 Range: 0.35 – 68.84	
BHR™	Head	Median: 13.0 Mean: 29.6 Range: 1.2 – 193.3	Median: 30.4 Mean: 68.6 Range: 3.3 – 330.3	Median: 5.05 Mean: 14.11 Range: 0.30 – 99.67	Median: 8.68 Mean: 23.17 Range: 0.70 – 127.54	Median: 2.51 Mean: 7.39 Range: 0.13 – 65.33	Median: 6.38 Mean: 11.43 Range: 0.30 – 76.85
	Cup	Median: 12.7 Mean: 35.5 Range: 2.1 – 137.0		Median: 2.70 Mean: 7.53 Range: 0.40 – 34.76		Median: 1.53 Mean: 3.08 Range: 0.08 – 11.52	
Conserve® +	Head	Median: 9.7 Mean: 8.4 Range: 2.2 – 13.3	Median: 22.9 Mean: 37.0 Range: 6.2 – 82.0	Median: 4.69 Mean: 3.65 Range: 0.47 – 5.80	Median: 13.74 Mean: 11.06 Range: 1.90 – 17.55	Median: 4.02 Mean: 5.27 Range: 0.19 – 11.60	Median: 11.78 Mean: 15.88 Range: 0.76 – 35.10
	Cup	Median: 13.2 Mean: 28.6 Range: 4.0 – 68.7		Median: 9.05 Mean: 7.41 Range: 1.43 – 11.75		Median: 7.76 Mean: 10.61 Range: 0.57 – 23.50	

Model	Component depth (μm)	Total depth (μm)	Component volume (mm^3)	Total volume (mm^3)	Component rate (mm^3/year)	Total rate (mm^3/year)	
Cormet™	Head	Median: 23.1	Median: 9.95		Median: 3.72		
		Mean: 27.3	Mean: 13.11		Mean: 3.62	Median: 5.28	
	Range: 15.3 – 53.1	Median: 31.3	Range: 3.31 – 35.28	Median: 12.39	Range: 0.65 – 6.62	Mean: 4.77	
	Cup	Mean: 60.7	Mean: 2.44	Mean: 16.56	Median: 1.22	Range: 0.83 – 9.18	
Range: 20.2 – 191.7		Mean: 3.45	Range: 4.59 – 42.59	Mean: 1.15			
			Range: 1.28 – 7.31	Range: 0.18 – 2.56			
Durom™	Head	Median: 11.6	Median: 8.32		Median: 4.17		
		Mean: 21.3	Mean: 14.73		Mean: 10.63	Median: 4.21	
	Range: 5.1 – 49.9	Median: 62.5	Range: 1.70 – 32.22	Median: 23.70	Range: 2.22 – 40.98	Mean: 6.61	
	Cup	Mean: 79.4	Mean: 5.36	Mean: 38.49	Median: 1.07	Range: 3.63 – 14.38	
Range: 11.4 – 181.1		Mean: 20.54	Range: 5.85 – 100.69	Mean: 3.14			
			Range: 0.36 – 71.07	Range: 0.27 – 10.15			
All resurfacing	Head	Median: 20.0	Median: 9.95		Median: 4.54		
		Mean: 49.4	Mean: 28.39		Mean: 9.08	Median: 7.10	
	Range: 1.2 – 461.9	Median: 62.5	Range: 0.30 – 326.88	Median: 7.93	Range: 0.13 – 65.33	Mean: 15.16	
	Cup	Mean: 152.3	Mean: 5.84	Mean: 25.81	Median: 2.04	Range: 0.30 – 87.28	
Range: 3.3 – 1138.4		Mean: 23.03	Range: 0.30 – 373.46	Mean: 6.55			
			Range: 0.34 – 373.46	Range: 0.07 – 68.84			
ASR™ XL	Head	Median: 11.1	Median: 6.78		Median: 2.25		
		Mean: 20.2	Mean: 9.81		Mean: 3.31		
	Range: 2.9 – 162.9		Range: 0.75 – 75.53		Range: 0.34 – 13.33		
	Cup	Median: 15.9	Median: 29.0	Median: 4.06	Median: 12.92	Median: 1.07	Median: 3.37
		Mean: 44.4	Mean: 61.6	Mean: 7.88	Mean: 19.70	Mean: 2.56	Mean: 6.64
		Range: 9.1 – 518.1	Range: 1.57 – 52.41	Range: 3.64 – 128.60	Range: 0.66 – 10.51	Range: 1.09 – 27.86	
Taper	Median: 30.1		Median: 0.70		Median: 0.17		
	Mean: 28.7		Mean: 2.18		Mean: 0.78		
			Range: 0.10 – 9.29		Range: 0.05 – 4.95		

Model	Component depth (μm)	Total depth (μm)	Component volume (mm^3)	Total volume (mm^3)	Component rate (mm^3/year)	Total rate (mm^3/year)	
Pinnacle®	Head	Median: 9.1	Median: 3.26		Median: 1.32		
		Mean: 15.3	Mean: 6.07		Mean: 1.90		
		Range: 1.9 – 109.4	Range: 0.54 – 53.40		Range: 0.23 – 16.43		
	Cup	Median: 8.9	Median: 16.9	Median: 1.51	Median: 5.57	Median: 0.50	Median: 2.06
		Mean: 15.5	Mean: 30.7	Mean: 2.55	Mean: 9.29	Mean: 0.89	Mean: 2.99
		Range: 2.2 – 111.1	Range: 6.5 – 220.5	Range: 0.16 – 22.32	Range: 1.26 – 75.72	Range: 0.05 – 6.87	Range: 0.69 – 23.30
Taper	Median: 5.7		Median: 0.33		Median: 0.17		
	Mean: 12.2		Mean: 1.24		Mean: 0.36		
	Range: 1.4 – 67.3		Range: 0.05 – 6.70		Range: 0.02 – 1.75		
All THR	Head	Median: 9.8	Median: 4.19		Median: 1.43		
		Mean: 17.5	Mean: 7.78		Mean: 2.53		
		Range: 1.9 – 162.9	Range: 0.54 – 75.53		Range: 0.23 – 16.43		
	Cup	Median: 11.1	Median: 19.9	Median: 2.21	Median: 7.96	Median: 0.73	Median: 2.52
		Mean: 26.5	Mean: 43.8	Mean: 4.58	Mean: 13.69	Mean: 1.50	Mean: 4.48
		Range: 2.2 – 355.2	Range: 6.5 – 518.1	Range: 0.16 – 52.41	Range: 1.26 – 128.60	Range: 0.05 – 10.51	Range: 0.69 – 27.86
Taper	Median: 10.0		Median: 0.51		Median: 0.17		
	Mean: 17.5		Mean: 1.57		Mean: 0.50		
	Range: 1.4 – 68.1		Range: 0.05 – 9.29		Range: 0.02 – 4.95		
All retrievals	Head	Median: 15.0	Median: 6.58		Median: 2.80		
		Mean: 38.7	Mean: 21.47		Mean: 6.91		
		Range: 1.2 – 461.9	Range: 0.30 – 326.88		Range: 0.13 – 65.33		
	Cup	Median: 21.8	Median: 37.2	Median: 4.53	Median: 13.41	Median: 1.53	Median: 4.17
		Mean: 73.7	Mean: 114.8	Mean: 17.07	Mean: 40.22	Mean: 4.94	Mean: 11.52
		Range: 2.1 – 1014.6	Range: 3.3 – 1138.4	Range: 0.16 – 373.46	Range: 0.70 – 438.27	Range: 0.05 – 68.84	Range: 0.30 – 87.28
Taper	Median: 10.0		Median: 0.51		Median: 0.17		
	Mean: 17.5		Mean: 1.57		Mean: 0.50		
	Range: 1.4 – 68.1		Range: 0.05 – 9.29		Range: 0.02 – 4.95		

Table 4.9: Measured wear data, split by model of prosthesis.

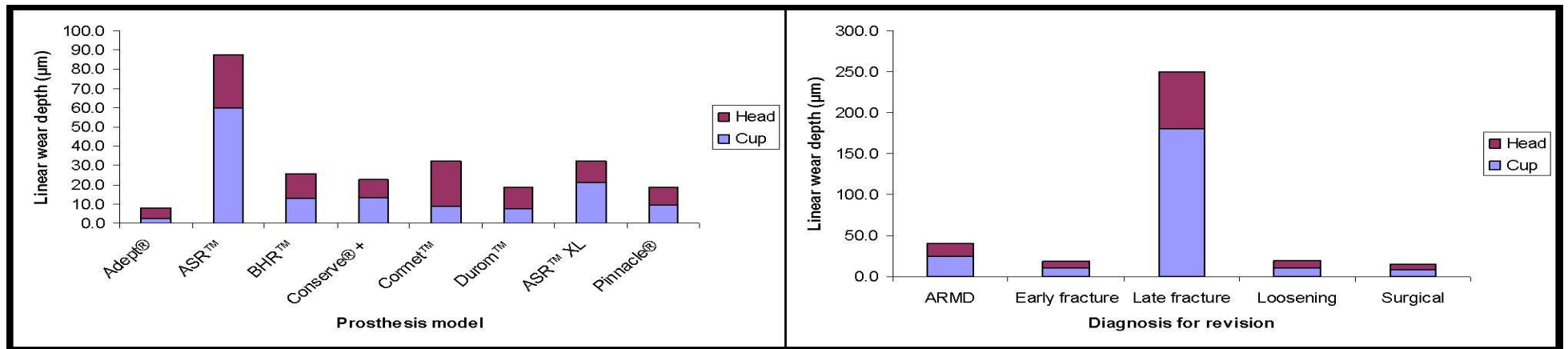


Figure 4.9: Linear wear depth, split by model of prosthesis (left) and by diagnosis for retrieval (right). Stacks show median depth and are split by contribution of heads and cups.

08

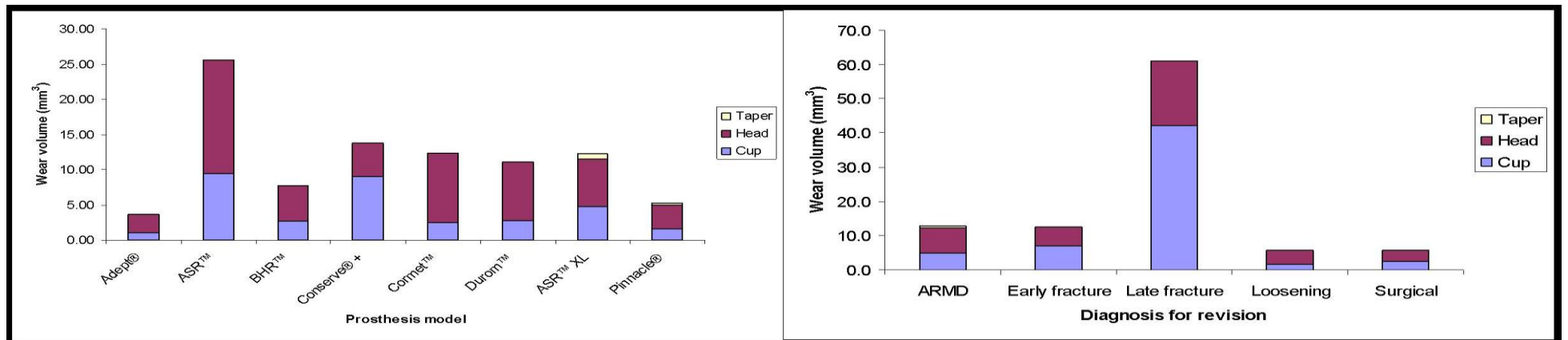


Figure 4.10: Median wear volumes for each model of prosthesis (left) and by diagnosis for retrieval (right). Stacks show total median wear volume and are split by contribution of heads, cups and tapers. Only THRs (ASR™ XL and Pinnacle®) have tapers.

Correspondingly, femoral heads also wore at a greater rate (median 2.80mm³/year) than acetabular cups (median 1.53mm³/year). The highest wear rate was seen on the Conserve® Plus (median 11.78mm³/year) and the lowest on the Adept® (median 0.94mm³/year). Early femoral neck fractures were associated with an extremely high wear rate (median 34.61mm³/year). Retrievals following late fracture (median 14.31mm³/year), ARMD (median 4.13mm³/year), loosening (median 1.33mm³/year) and surgical complications (median 1.12mm³/year) were all associated with lower wear rates (figure 4.11).

Measured diameter, radial clearance (µm), location of maximum wear depth relative to the component centre (°) and surface coverage of wear scar (%) are presented in table 4.10. The data is split by prosthesis model and by component type (head, cup or taper).

Figure 4.12 shows the measured clearance, split by prosthesis model and by diagnosis. The lowest radial clearances were seen in the ASR™ resurfacing (median 41.0µm) and ASR™ XL (median 37.6µm). The Cormet™ retrievals showed the greatest radial clearance (median 137.0µm). Retrievals following ARMD were associated with a lower clearance (median 42.3µm) while late fracture (median 43.8µm), surgical (median 66.3 µm), loosening (median 96.5µm) and early fracture (median 178.3µm) retrievals were associated with increasingly higher clearances. However, there were only 2 early fracture retrievals where the cup was also retrieved (and thus that clearance could be measured). These were one BHR™ and one Conserve® +. The Conserve® + that suffered early fracture had the largest clearance of all Conserve® + retrievals (222.2µm). The BHR™ had the second largest clearance of all BHR™ (134.4µm). Since different models employ markedly different clearances, this data was assessed for ASR™ resurfacings alone. In this case, retrievals following surgical complications had the lowest clearances (median 34.9µm), followed by ARMD (median 41.5µm) and late fractures (median 43.8µm).

Model	Measured diameter (mm)	Clearance (µm)	Wear location (°)	Wear coverage (% of surface area)
Adept®	Head Median: 50.8153 Mean: 50.8153 Range: 49.8180 – 51.8126	Median: 103.8 Mean: 103.8 Range: 98.2 – 109.4	Median: 35.9 Mean: 35.9 Range: 35.2 – 36.6	Median: 1.15 Mean: 1.15 Range: 0.00 – 2.29
	Cup Median: 51.0229 Mean: 51.0229 Range: 50.0368 – 52.0090		Median: 69.9 Mean: 69.9 Range: 66.4 – 73.3	Median: 0.00 Mean: 0.00 Range: 0.00 – 0.42
ASR™	Head Median: 45.5200 Mean: 46.3034 Range: 40.4986 – 54.4984	Median: 41.0 Mean: 41.99 Range: 20.1 – 138.4	Median: 34.8 Mean: 45.1 Range: 3.9 – 100.1	Median: 22.69 Mean: 22.94 Range: 0.00 – 73.52
	Cup Median: 45.5817 Mean: 46.2066 Range: 40.5448 – 54.5814		Median: 72.7 Mean: 72.3 Range: 65.2 – 77.1	Median: 19.93 Mean: 21.45 Range: 1.06 – 66.52
BHR™	Head Median: 43.8267 Mean: 43.9577 Range: 41.8412 – 51.7870	Median: 109.2 Mean: 118.1 Range: 78.0 – 237.6	Median: 25.4 Mean: 31.6 Range: 7.6 – 97.1	Median: 6.77 Mean: 12.21 Range: 0.00 – 44.37
	Cup Median: 44.0226 Mean: 44.2037 Range: 41.9984 – 50.0412		Median: 74.8 Mean: 65.5 Range: 16.9 – 78.6	Median: 5.78 Mean: 12.58 Range: 0.00 – 50.19
Conserve® +	Head Median: 43.9980 Mean: 45.9215 Range: 42.0056 – 51.7608	Median: 76.6 Mean: 121.7 Range: 66.3 – 222.2	Median: 44.8 Mean: 57.5 Range: 35.2 – 92.4	Median: 4.01 Mean: 4.19 Range: 0.00 – 8.57
	Cup Median: 44.1512 Mean: 46.1649 Range: 42.1382 – 52.2052		Median: 78.2 Mean: 78.4 Range: 77.8 – 79.1	Median: 13.69 Mean: 14.45 Range: 0.00 – 29.65
Cormet™	Head Median: 47.7738 Mean: 45.4168 Range: 40.0056 – 47.7918	Median: 137.0 Mean: 119.4 Range: 48.6 – 159.5	Median: 27.7 Mean: 31.1 Range: 24.1 – 39.3	Median: 16.46 Mean: 17.76 Range: 8.57 – 34.21
	Cup Median: 48.0174 Mean: 45.6556 Range: 40.1028 – 47.7918		Median: 78.9 Mean: 69.5 Range: 31.2 – 81.7	Median: 4.31 Mean: 4.96 Range: 0.00 – 11.78
Durom™	Head Median: 47.9837 Mean: 47.9547 Range: 41.9862 – 53.9812	Median: 109.1 Mean: 111.1 Range: 76.8 – 149.4	Median: 52.2 Mean: 57.1 Range: 0.2 – 102.3	Median: 11.69 Mean: 17.84 Range: 0.00 – 53.52
	Cup Median: 48.2117 Mean: 47.6476 Range: 42.1420 – 52.0248		Median: 78.6 Mean: 78.0 Range: 72.8 – 82.2	Median: 7.26 Mean: 13.25 Range: 0.00 – 38.48

Model	Measured diameter (mm)	Clearance (μm)	Wear location ($^{\circ}$)	Wear coverage (% of surface area)
All resurfacing	Head Median: 45.6639 Mean: 45.9930 Range: 40.0056 – 54.4984	Median: 43.7 Mean: 67.5 Range: 20.1 – 237.6	Median: 34.5 Mean: 43.3 Range: 0.2 – 102.3	Median: 17.77 Mean: 19.34 Range: 0.00 – 73.52
	Cup Median: 45.5849 Mean: 46.0125 Range: 40.1028 – 54.5814		Median: 72.8 Mean: 71.4 Range: 16.9 – 82.2	Median: 14.43 Mean: 17.75 Range: 0.00 – 66.52
ASR™ XL	Head Median: 45.9982 Mean: 46.7010 Range: 40.5100 – 56.4802	Median: 37.6 Mean: 40.6 Range: 14.6 – 91.5	Median: 38.7 Mean: 54.6 Range: 24.8 – 99.3	Median: 8.69 Mean: 9.53 Range: 0.00 – 27.36
	Cup Median: 46.0803 Mean: 46.7823 Range: 40.5636 – 56.5846		Median: 72.4 Mean: 66.3 Range: 3.0 – 76.8	Median: 10.43 Mean: 12.71 Range: 0.00 – 43.21
Pinnacle®	Head Median: 36.0053 Mean: 36.0029 Range: 35.9788 – 36.0156	Median: 45.0 Mean: 46.3 Range: 19.8 – 77.3	Median: 49.1 Mean: 66.9 Range: 28.8 – 104.2	Median: 5.30 Mean: 9.15 Range: 0.00 – 41.75
	Cup Median: 36.0956 Mean: 36.0934 Range: 36.0420 – 36.1370		Median: 77.0 Mean: 73.2 Range: 0.7 – 80.8	Median: 3.64 Mean: 6.50 Range: 0.00 – 36.01
All THR	Head Median: 36.0141 Mean: 40.9067 Range: 35.9788 – 56.4802	Median: 41.4 Mean: 43.7 Range: 14.6 – 91.5	Median: 41.3 Mean: 61.3 Range: 24.8 – 104.2	Median: 7.47 Mean: 10.72 Range: 0.00 – 40.04
	Cup Median: 36.1217 Mean: 40.9915 Range: 36.0420 – 56.5846		Median: 73.4 Mean: 70.1 Range: 0.7 – 80.8	Median: 7.47 Mean: 9.35 Range: 0.00 – 43.31
All retrievals	Head Median: 44.5188 Mean: 44.4142 Range: 35.9788 – 56.4802	Median: 42.8 Mean: 58.7 Range: 14.6 – 237.6	Median: 36.6 Mean: 49.3 Range: 0.2 – 104.2	Median: 11.62 Mean: 15.98 Range: 0.00 – 73.52
	Cup Median: 44.5840 Mean: 44.2259 Range: 36.0420 – 56.5846		Median: 72.9 Mean: 70.9 Range: 0.7 – 82.2	Median: 10.96 Mean: 14.65 Range: 0.00 – 66.52

Table 4.10: Measured diameter, prosthesis clearance and wear scar location and coverage, split by model of prosthesis.

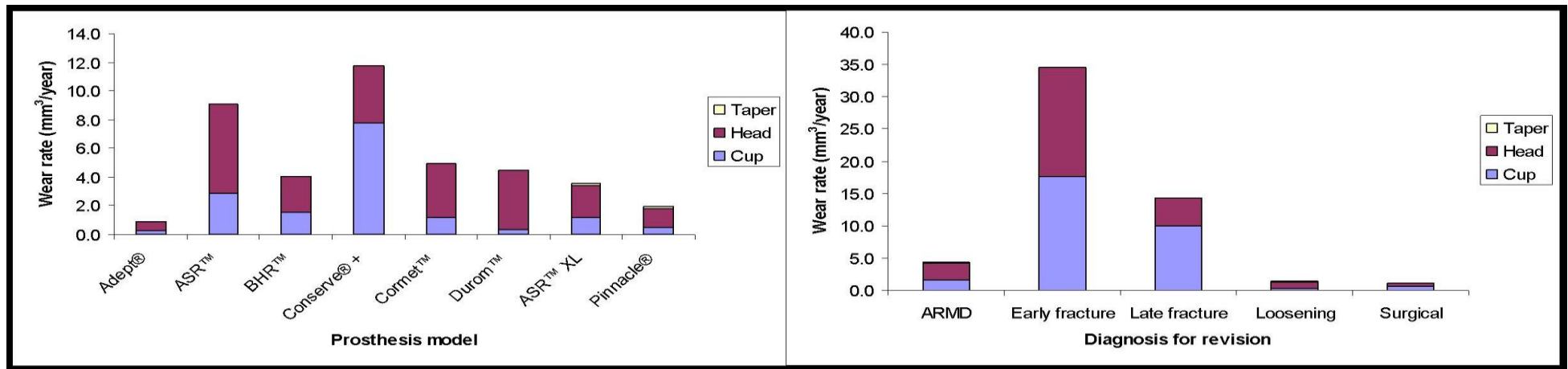


Figure 4.11: Median wear rates for each model of prosthesis. Stacks show total median wear rate and are split by contribution of heads, cups and tapers.

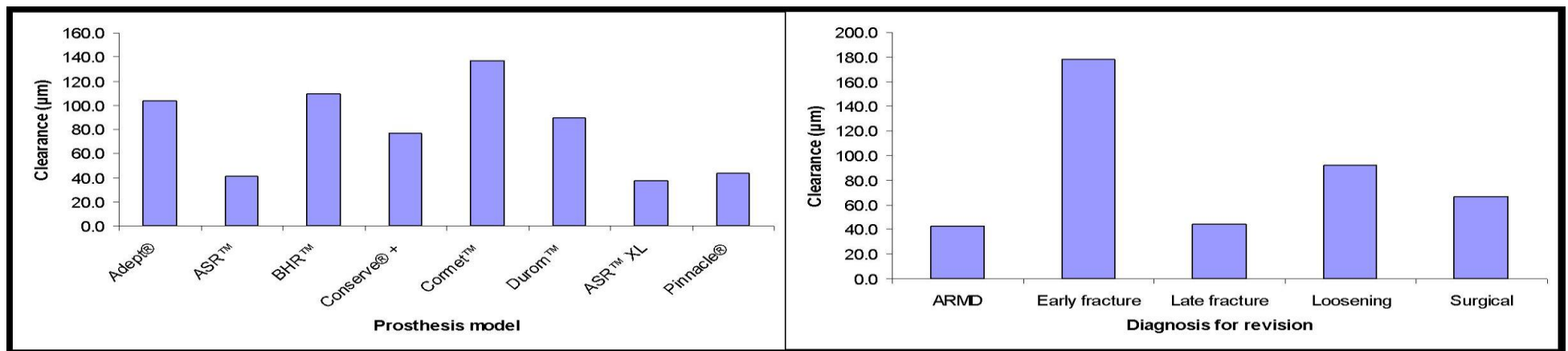


Figure 4.12: Measured radial clearance, split by prosthesis model (left) and diagnosis for retrieval (right).

Figure 4.13 shows the location of the maximum wear depth on the heads and cups, by angle relative to the component centre. For all models of prosthesis the median point of maximum cup wear was very close to the rim. The range of median values was 69.9° (Adept®) to 78.9° (Cormet™). For the heads, the BHR™ maximum wear was closest to the pole (median 25.4°) and the Durom™ the furthest (median 52.2°).

When compared with the coverage arc of each component (figure 4.14), Cormet™ prostheses wore closest to the rim (median 1.1° between rim and point of maximum wear depth). Pinnacle® prostheses wore furthest away (median 13.0°). Retrievals following late fracture were associated with cup wear closest to the rim (median 1.2°), followed by ARMD (median 2.6°), loosening (median 6.3°) and surgical complications (median 6.7°). Early neck fractures were worn further from the cup rim (median 58.8°), though with only two early fracture cups retrieved (39.8° and 77.8°) this should be interpreted with caution.

Figure 4.15 shows the median surface area coverage of the wear scar, as a percentage of the total surface area of the component. Overall, resurfacings had a larger wear scar on the heads (17.77% surface coverage) and cups (14.43% surface coverage) than the THRs (7.47% surface coverage for both heads and cups). Femoral heads tended to have a slightly higher surface area covered by the wear scar (median 11.62%) than acetabular cups (median 10.96%). The difference was not statistically significant ($p = 0.734$)

The ASR™ retrievals experienced the highest wear coverage on both the heads (median 22.69%) and the cups (median 19.93%). The lowest wear coverage was seen on the two Adept® retrievals, with 1.15% coverage on the heads and 0.21% on the cups. Coverage on the femoral heads was highest in late fracture retrievals (median 23.83%) and lowest following surgical complications (median 3.78%). Acetabular cup coverage was also highest following late femoral neck fracture (median 25.14%) and lowest following surgical complications (median 1.24%).

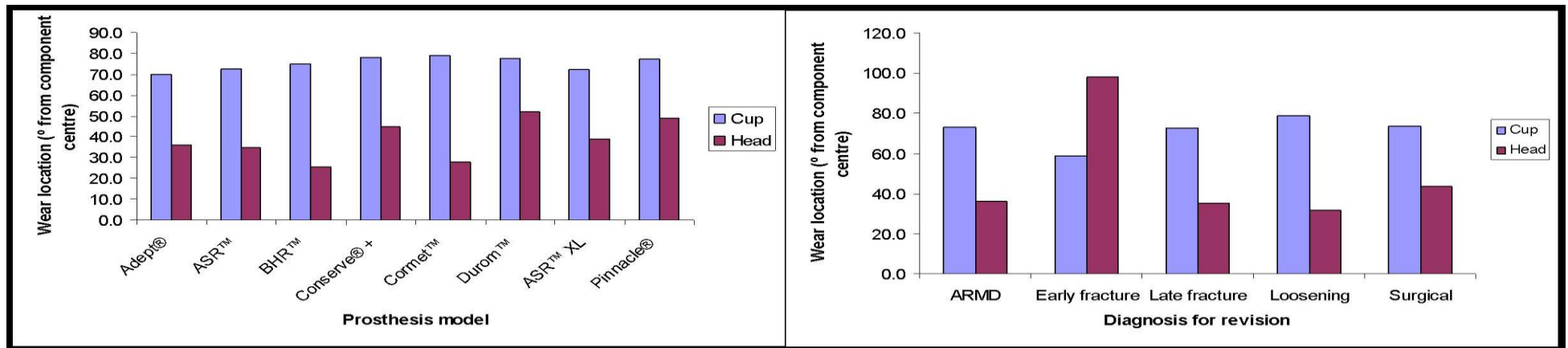


Figure 4.13: Location of maximum linear wear on femoral heads and acetabular cups, split by model of prosthesis (left) and by diagnosis for revision (right). Angles are relative to the centre point of each component.

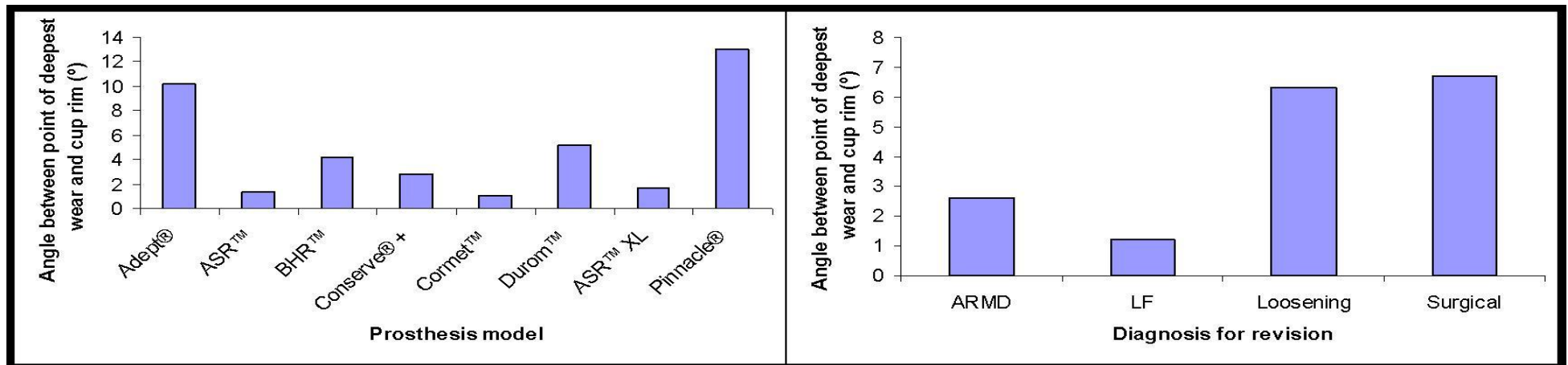


Figure 4.14: Location of maximum linear wear on acetabular cups, in comparison to the rim of the cup split by model of prosthesis (left) and by diagnosis for revision (right).

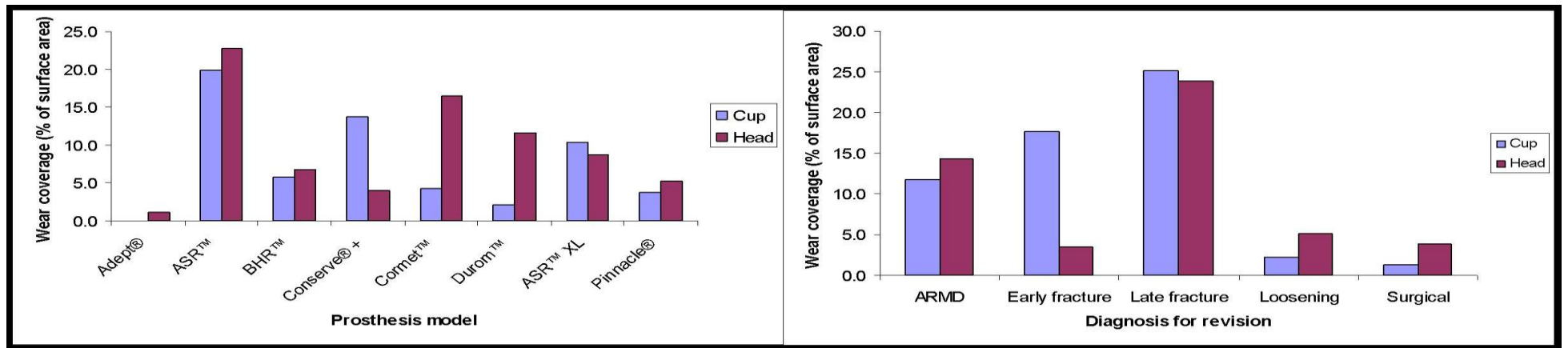


Figure 4.15: Percentage of surface area worn on femoral heads and acetabular cups, split by model of prosthesis (left) and by diagnosis for revision (right).

4.3.2 Surface roughness

Surface roughness values collected either by interferometry (heads) or contact profilometry (cups) are shown in table 4.11. This data was processed from 50 measurements on all 143 heads and 36 measurements on all 130 cups. Ra and RMS readings were very similar between heads and cups. Median values in the unworn regions were Ra = 0.008 μ m and RMS = 0.011 μ m for the heads and Ra= 0.01 μ m and RMS = 0.01 μ m for the cups. In the worn region, median values were Ra = 0.020 μ m and RMS = 0.035 μ m for the heads and Ra= 0.02 μ m and RMS = 0.03 μ m for the cups. These corresponded to a significant increase in roughness (all $p < 0.001$). Values of PV were also significantly higher in the worn regions than the unworn regions ($p < 0.001$). Rsk was significantly more negative in the worn regions ($p < 0.001$), indicative of a surface dominated by valleys.

In the unworn region, there were no significant differences between hip resurfacings and total hip replacements in Ra (median = 0.010 μ m for both, $p = 0.477$), RMS (median = 0.010 μ m for both, $p = 0.599$) or PV (median = 0.094 μ m and 0.080 μ m respectively, $p = 0.156$). There was a significant difference in Rsk (median = 0.160 and 0.280 respectively, $p < 0.001$).

In the worn region, there were significant differences in Ra (median = 0.024 μ m and 0.017 μ m respectively, $p = < 0.001$), RMS (median = 0.036 μ m and 0.030 μ m respectively, $p = < 0.001$) and PV (median = 0.479 μ m and 0.270 μ m respectively, $p = 0.048$) when comparing hip resurfacings to total hip replacements. There was no significant difference in Rsk ($p = 0.970$).

Figures 4.16 – 4.19 show boxplots of all measures of roughness in the unworn and worn regions for heads and cups.

		Surface roughness							
Model		Unworn region				Worn region			
		Ra (µm)	RMS (µm)	PV (µm)	Rsk	Ra (µm)	RMS (µm)	PV (µm)	Rsk
Adept®	Head	Median: 0.018	Median: 0.026	Median: 0.314	Median: 1.272	Median: 0.022	Median: 0.035	Median: 0.677	Median: -1.919
		Mean: 0.018	Mean: 0.026	Mean: 0.314	Mean: 1.272	Mean: 0.022	Mean: 0.035	Mean: 0.677	Mean: -1.919
		Range: 0.014 – 0.022	Range: 0.019 – 0.032	Range: 0.233 – 0.395	Range: 0.785 – 1.758	Range: 0.018 – 0.025	Range: 0.030 – 0.039	Range: 0.616 – 0.737	Range: -2.295 – -1.543
	Cup	Median: 0.01	Median: 0.01	Median: 0.10	Median: 0.20	Median: 0.04	Median: 0.05	Median: 0.21	Median: -2.12
		Mean: 0.01	Mean: 0.01	Mean: 0.10	Mean: 0.20	Mean: 0.04	Mean: 0.05	Mean: 0.21	Mean: -1.95
		Range: 0.01 – 0.01	Range: 0.01 – 0.01	Range: 0.08 – 0.12	Range: 0.13 – 0.27	Range: 0.02 – 0.05	Range: 0.04 – 0.06	Range: 0.16 – 0.25	Range: -3.01 – 0.01
ASR™	Head	Median: 0.006	Median: 0.009	Median: 0.130	Median: -0.167	Median: 0.027	Median: 0.047	Median: 1.009	Median: -2.391
		Mean: 0.008	Mean: 0.012	Mean: 0.188	Mean: -0.429	Mean: 0.042	Mean: 0.066	Mean: 1.052	Mean: -3.099
		Range: 0.002 – 0.053	Range: 0.002 – 0.082	Range: 0.033 – 1.295	Range: -7.770 – 1.747	Range: 0.006 – 0.167	Range: 0.010 – 0.248	Range: 0.239 – 2.844	Range: -16.1480.866
	Cup	Median: 0.01	Median: 0.01	Median: 0.05	Median: 0.17	Median: 0.02	Median: 0.03	Median: 0.11	Median: -3.84
		Mean: 0.01	Mean: 0.01	Mean: 0.09	Mean: 0.22	Mean: 0.02	Mean: 0.04	Mean: 0.18	Mean: -3.72
		Range: 0.01 – 0.01	Range: 0.01 – 0.01	Range: 0.03 – 1.30	Range: 0.07 – 0.96	Range: 0.01 – 0.09	Range: 0.02 – 0.25	Range: 0.06 – 2.60	Range: -4.92 – -1.04
BHR™	Head	Median: 0.021	Median: 0.028	Median: 0.334	Median: 1.078	Median: 0.030	Median: 0.038	Median: 0.764	Median: -2.201
		Mean: 0.020	Mean: 0.027	Mean: 0.357	Mean: 0.159	Mean: 0.040	Mean: 0.057	Mean: 0.960	Mean: -2.711
		Range: 0.008 – 0.046	Range: 0.011 – 0.035	Range: 0.058 – 0.678	Range: -4.543 – 2.000	Range: 0.004 – 0.145	Range: 0.013 – 0.198	Range: 0.245 – 2.496	Range: -8.465 – -0.141
	Cup	Median: 0.01	Median: 0.01	Median: 0.06	Median: 0.16	Median: 0.03	Median: 0.03	Median: 0.13	Median: -0.72
		Mean: 0.01	Mean: 0.01	Mean: 0.08	Mean: 0.17	Mean: 0.03	Mean: 0.04	Mean: 0.16	Mean: -0.55
		Range: 0.01 – 0.01	Range: 0.01 – 0.01	Range: 0.03 – 0.21	Range: 0.08 – 0.29	Range: 0.01 – 0.05	Range: 0.02 – 0.09	Range: 0.06 – 0.41	Range: -2.01 – 0.76
Conserve® +	Head	Median: 0.006	Median: 0.008	Median: 0.112	Median: -0.127	Median: 0.016	Median: 0.033	Median: 0.852	Median: -6.380
		Mean: 0.009	Mean: 0.013	Mean: 0.266	Mean: -0.767	Mean: 0.016	Mean: 0.029	Mean: 0.756	Mean: -5.350
		Range: 0.004 – 0.018	Range: 0.005 – 0.026	Range: 0.091 – 0.596	Range: -2.629 – 0.456	Range: 0.012 – 0.021	Range: 0.017 – 0.037	Range: 0.406 – 1.010	Range: -7.510 – -2.180
	Cup	Median: 0.01	Median: 0.01	Median: 0.08	Median: 0.17	Median: 0.02	Median: 0.04	Median: 0.16	Median: -3.12
		Mean: 0.01	Mean: 0.01	Mean: 0.07	Mean: 0.20	Mean: 0.02	Mean: 0.04	Mean: 0.14	Mean: -2.67
		Range: 0.01 – 0.01	Range: 0.01 – 0.01	Range: 0.03 – 0.10	Range: 0.16 – 0.26	Range: 0.01 – 0.03	Range: 0.02 – 0.05	Range: 0.06 – 0.19	Range: -3.87 – -0.14
Cornet™	Head	Median: 0.012	Median: 0.018	Median: 0.344	Median: -2.170	Median: 0.024	Median: 0.035	Median: 0.954	Median: -3.997
		Mean: 0.014	Mean: 0.020	Mean: 0.391	Mean: -2.261	Mean: 0.033	Mean: 0.060	Mean: 1.111	Mean: -4.225
		Range: 0.007 – 0.024	Range: 0.010 – 0.034	Range: 0.119 – 0.786	Range: -3.658 – -0.351	Range: 0.013 – 0.062	Range: 0.031 – 0.113	Range: 0.590 – 1.730	Range: -5.540 – -2.530
	Cup	Median: 0.01	Median: 0.01	Median: 0.09	Median: 0.40	Median: 0.04	Median: 0.07	Median: 0.18	Median: -1.45
		Mean: 0.01	Mean: 0.01	Mean: 0.15	Mean: 0.51	Mean: 0.06	Mean: 0.10	Mean: 0.30	Mean: -1.23
		Range: 0.01 – 0.01	Range: 0.01 – 0.01	Range: 0.06 – 0.31	Range: 0.16 – 1.08	Range: 0.02 – 0.03	Range: 0.03 – 0.24	Range: 0.11 – 0.62	Range: -2.14 – 0.31

		Surface roughness							
Model		Unworn region				Worn region			
		Ra (µm)	RMS (µm)	PV (µm)	Rsk	Ra (µm)	RMS (µm)	PV (µm)	Rsk
Durom™	Head	Median: 0.007	Median: 0.009	Median: 0.264	Median: 0.190	Median: 0.022	Median: 0.036	Median: 0.811	Median: -4.502
		Mean: 0.013	Mean: 0.015	Mean: 0.334	Mean: -1.050	Mean: 0.030	Mean: 0.042	Mean: 0.858	Mean: -4.051
		Range: 0.003 – 0.030	Range: 0.005 – 0.038	Range: 0.103 – 0.623	Range: -7.220 – 0.550	Range: 0.006 – 0.065	Range: 0.011 – 0.090	Range: 0.227 – 1.827	Range: -6.052 – -0.983
	Cup	Median: 0.01	Median: 0.01	Median: 0.04	Median: 0.13	Median: 0.02	Median: 0.03	Median: 0.08	Median: -3.03
		Mean: 0.01	Mean: 0.01	Mean: 0.06	Mean: 0.17	Mean: 0.02	Mean: 0.03	Mean: 0.11	Mean: -2.94
		Range: 0.01 – 0.01	Range: 0.01 – 0.01	Range: 0.02 – 0.12	Range: 0.12 – 0.25	Range: 0.01 – 0.03	Range: 0.01 – 0.05	Range: 0.04 – 0.24	Range: -3.74 – -2.13
All resurfacing	Head	Median: 0.009	Median: 0.012	Median: 0.164	Median: -0.118	Median: 0.025	Median: 0.041	Median: 0.943	Median: -2.764
		Mean: 0.011	Mean: 0.015	Mean: 0.242	Mean: -0.439	Mean: 0.039	Mean: 0.060	Mean: 1.005	Mean: -3.194
		Range: 0.002 – 0.053	Range: 0.002 – 0.082	Range: 0.033 – 1.295	Range: -7.770 – 2.000	Range: 0.004 – 0.167	Range: 0.010 – 0.248	Range: 0.227 – 2.844	Range: -16.148 – 0.866
	Cup	Median: 0.01	Median: 0.01	Median: 0.06	Median: 0.16	Median: 0.02	Median: 0.03	Median: 0.11	Median: -3.13
		Mean: 0.01	Mean: 0.01	Mean: 0.09	Mean: 0.23	Mean: 0.03	Mean: 0.04	Mean: 0.18	Mean: -2.91
		Range: 0.01 – 0.01	Range: 0.01 – 0.01	Range: 0.02 – 1.30	Range: 0.07 – 1.08	Range: 0.01 – 0.14	Range: 0.01 – 0.25	Range: 0.04 – 2.60	Range: -4.92 – 0.01
ASR™ XL	Head	Median: 0.006	Median: 0.007	Median: 0.104	Median: 0.546	Median: 0.019	Median: 0.036	Median: 0.879	Median: -2.977
		Mean: 0.008	Mean: 0.009	Mean: 0.142	Mean: 0.373	Mean: 0.032	Mean: 0.057	Mean: 1.001	Mean: -3.421
		Range: 0.002 – 0.013	Range: 0.002 – 0.019	Range: 0.013 – 0.369	Range: -2.889 – 2.245	Range: 0.009 – 0.125	Range: 0.013 – 0.177	Range: 0.228 – 3.161	Range: -11.669 – -0.513
	Cup	Median: 0.01	Median: 0.01	Median: 0.05	Median: 0.20	Median: 0.02	Median: 0.03	Median: 0.10	Median: -1.52
		Mean: 0.01	Mean: 0.01	Mean: 0.07	Mean: 0.21	Mean: 0.02	Mean: 0.03	Mean: 0.14	Mean: -1.61
		Range: 0.01 – 0.01	Range: 0.01 – 0.01	Range: 0.04 – 0.22	Range: 0.09 – 0.49	Range: 0.01 – 0.06	Range: 0.02 – 0.11	Range: 0.07 – 0.43	Range: -3.09 – 0.02
Pinnacle®	Head	Median: 0.010	Median: 0.014	Median: 0.164	Median: 0.803	Median: 0.014	Median: 0.021	Median: 0.554	Median: -2.521
		Mean: 0.010	Mean: 0.013	Mean: 0.174	Mean: 0.764	Mean: 0.016	Mean: 0.024	Mean: 0.537	Mean: -3.440
		Range: 0.002 – 0.020	Range: 0.003 – 0.026	Range: 0.051 – 0.465	Range: -1.247 – 1.645	Range: 0.004 – 0.099	Range: 0.005 – 0.130	Range: 0.069 – 1.246	Range: -11.079 – 1.128
	Cup	Median: 0.01	Median: 0.01	Median: 0.06	Median: 0.19	Median: 0.02	Median: 0.03	Median: 0.12	Median: -0.64
		Mean: 0.01	Mean: 0.01	Mean: 0.07	Mean: 0.21	Mean: 0.03	Mean: 0.04	Mean: 0.14	Mean: -0.77
		Range: 0.01 – 0.01	Range: 0.01 – 0.01	Range: 0.03 – 0.17	Range: 0.70 – 0.76	Range: 0.01 – 0.11	Range: 0.02 – 0.16	Range: 0.06 – 0.34	Range: -2.01 – 0.04
All THR	Head	Median: 0.008	Median: 0.011	Median: 0.153	Median: 0.761	Median: 0.016	Median: 0.026	Median: 0.590	Median: -2.851
		Mean: 0.008	Mean: 0.011	Mean: 0.160	Mean: 0.585	Mean: 0.023	Mean: 0.394	Mean: 0.750	Mean: -3.461
		Range: 0.002 – 0.020	Range: 0.002 – 0.026	Range: 0.043 – 0.465	Range: -2.889 – 2.245	Range: 0.004 – 0.125	Range: 0.005 – 0.177	Range: 0.069 – 3.161	Range: -11.669 – 1.128
	Cup	Median: 0.01	Median: 0.01	Median: 0.06	Median: 0.19	Median: 0.02	Median: 0.03	Median: 0.11	Median: -0.10
		Mean: 0.01	Mean: 0.01	Mean: 0.07	Mean: 0.21	Mean: 0.02	Mean: 0.04	Mean: 0.14	Mean: -1.17
		Range: 0.01 – 0.01	Range: 0.01 – 0.01	Range: 0.03 – 0.22	Range: 0.07 – 0.76	Range: 0.01 – 0.11	Range: 0.02 – 0.16	Range: 0.06 – 0.43	Range: 1.61 – 0.04

Model	Surface roughness								
	Unworn region				Worn region				
	Ra (μm)	RMS (μm)	PV (μm)	Rsk	Ra (μm)	RMS (μm)	PV (μm)	Rsk	
All retrievals	Head	Median: 0.008	Median: 0.011	Median: 0.159	Median: 0.415	Median: 0.020	Median: 0.035	Median: 0.814	Median: -2.764
		Mean: 0.010	Mean: 0.014	Mean: 0.215	Mean: -0.095	Mean: 0.034	Mean: 0.053	Mean: 0.920	Mean: -3.274
		Range: 0.002 – 0.053	Range: 0.002 – 0.082	Range: 0.033 – 1.295	Range: -7.770–2.245	Range: 0.004 – 0.167	Range: 0.005 – 0.248	Range: 0.069 – 3.161	Range: -16.148 – 1.128
	Cup	Median: 0.01	Median: 0.01	Median: 0.06	Median: 0.17	Median: 0.02	Median: 0.03	Median: 0.11	Median: -1.34
		Mean: 0.01	Mean: 0.01	Mean: 0.08	Mean: 0.22	Mean: 0.03	Mean: 0.04	Mean: 0.16	Mean: -2.29
		Range: 0.01 – 0.01	Range: 0.01 – 0.01	Range: 0.02 – 1.30	Range: 0.07 – 1.08	Range: 0.01 – 0.14	Range: 0.01 – 0.25	Range: 0.04 – 2.60	Range: -4.92 – 0.04

Table 4.11: *Surface roughness measurements in the unworn and worn regions of retrieved femoral heads and acetabular cups, split by model of prosthesis.*

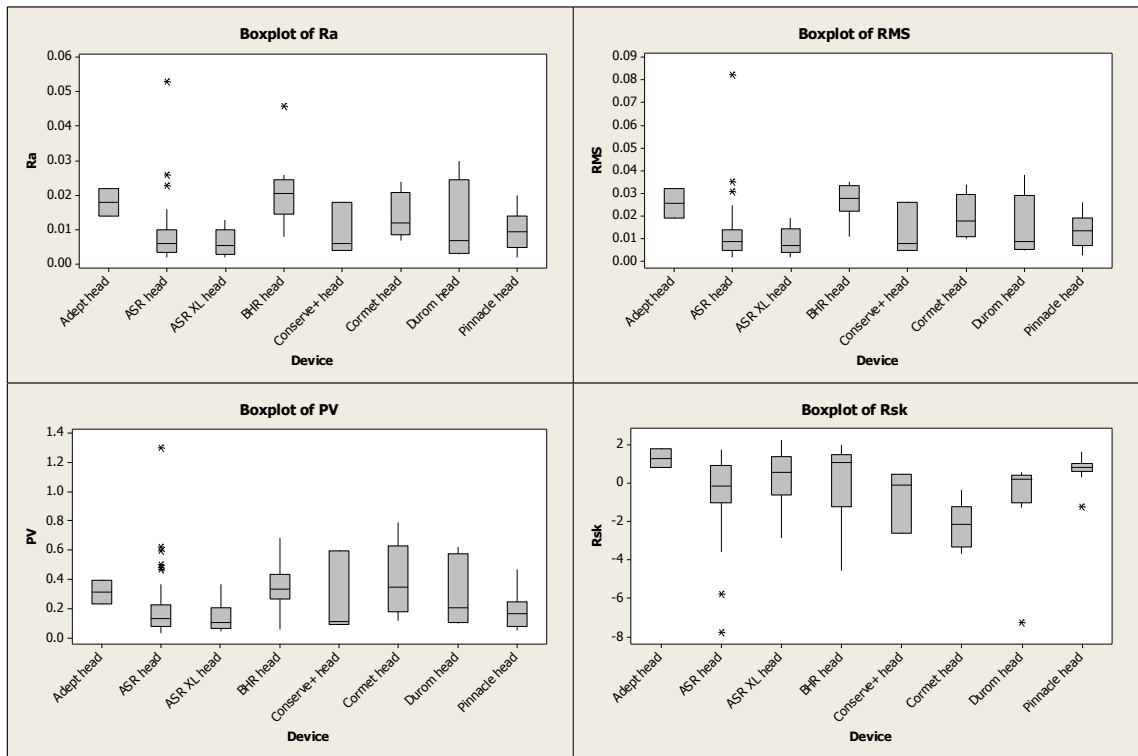


Figure 4.16: Roughness measurements in the unworn regions of the femoral heads, split by model of prosthesis.

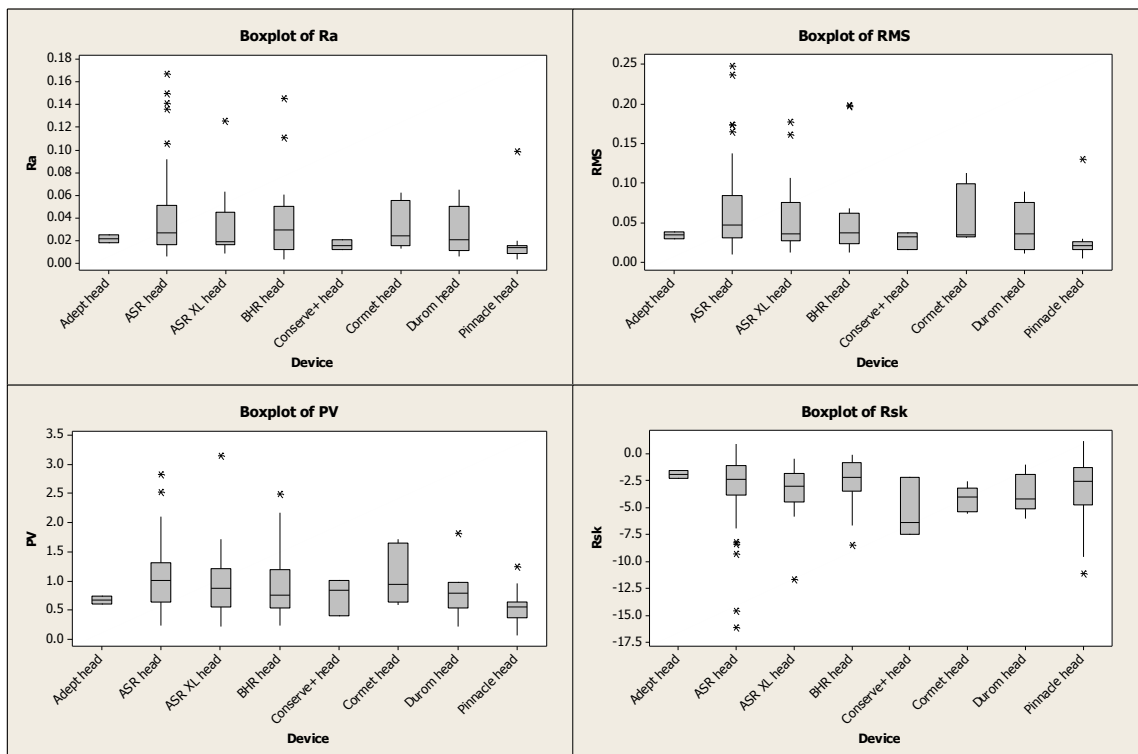


Figure 4.17: Roughness measurements in the worn regions of the femoral heads, split by model of prosthesis.

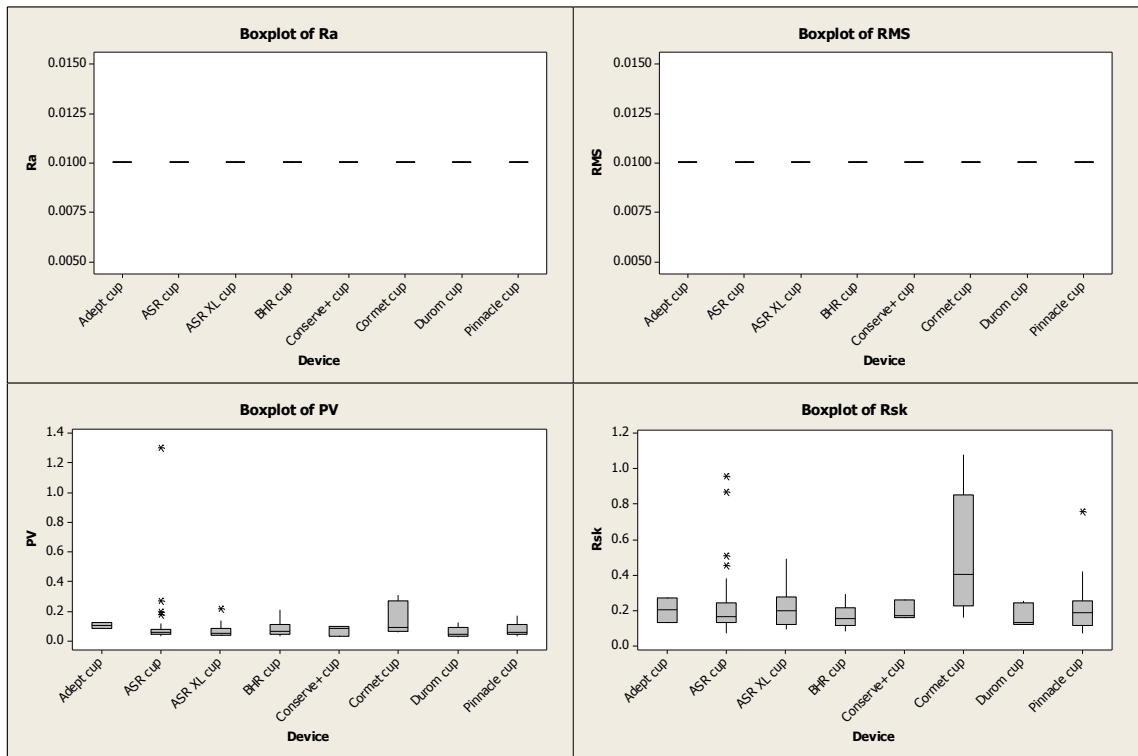


Figure 4.18: Roughness measurements in the unworn regions of the acetabular cups, split by model of prosthesis.

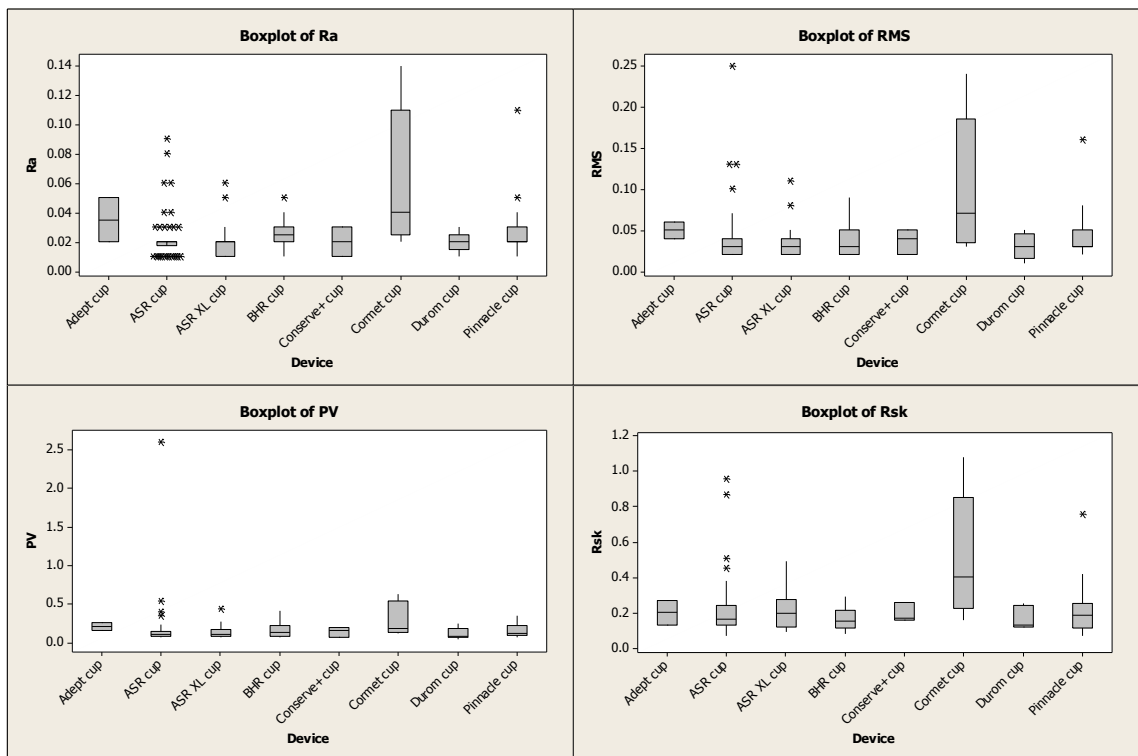


Figure 4.19: Roughness measurements in the worn regions of the acetabular cups, split by model of prosthesis.

Calculated lambda (λ) ratios in the unworn and worn regions are shown in table 4.12. The median λ -ratio in the unworn region was 3.33, indicative of fluid film lubrication. In the worn region it was 1.31, indicative of mixed lubrication. There were no significant differences between hip resurfacings and total hip replacements in unworn λ -ratio (3.69 and 3.00 respectively, $p = 0.768$) or in worn λ -ratio (1.20 and 1.40 respectively, $p = 0.079$).

In the unworn regions, the ASR™ XL had the highest λ -ratio (median 5.24) and the BHR™ had the lowest (median 1.20). The ASR™ maintained the highest λ -ratio in the worn regions at the time of retrieval (median 1.48) while the Cormet™ had the lowest (median 0.35) (figure 4.20).

Model	Unworn λ	Worn λ
Adept®	Median: 1.70	Median: 0.92
	Mean: 1.70	Mean: 0.92
	Range: 1.55 – 1.84	Range: 0.67 – 1.18
ASR™	Median: 4.72	Median: 1.48
	Mean: 4.64	Mean: 1.69
	Range: 1.33 – 7.77	Range: 0.29 – 5.31
BHR™	Median: 1.20	Median: 0.65
	Mean: 1.31	Mean: 0.82
	Range: 0.56 – 3.33	Range: 0.15 – 3.83
Conserve® +	Median: 2.75	Median: 0.94
	Mean: 2.22	Mean: 1.22
	Range: 0.97 – 2.95	Range: 0.69 – 2.03
Cormet™	Median: 1.39	Median: 0.35
	Mean: 1.58	Mean: 0.54
	Range: 0.94 – 2.38	Range: 0.16 – 1.22
Durom™	Median: 2.65	Median: 1.33
	Mean: 3.05	Mean: 2.12
	Range: 0.77 – 5.64	Range: 0.34 – 5.12
All resurfacing	Median: 3.69	Median: 1.20
	Mean: 3.65	Mean: 1.48
	Range: 0.56 – 7.77	Range: 0.15 – 5.31

Model	Unworn λ	Worn λ
ASR™ XL	Median: 5.24	Median: 1.80
	Mean: 5.32	Mean: 1.93
	Range: 2.63 – 12.05	Range: 0.55 – 4.23
Pinnacle®	Median: 2.31	Median: 1.25
	Mean: 2.28	Mean: 1.25
	Range: 1.27 – 3.31	Range: 0.21 – 2.35
All THR	Median: 3.00	Median: 1.40
	Mean: 3.67	Mean: 1.56
	Range: 1.27 – 12.05	Range: 0.21 – 4.23
All retrievals	Median: 3.33	Median: 1.31
	Mean: 3.66	Mean: 1.51
	Range: 0.56 – 12.05	Range: 0.15 – 5.31

Table 4.12: Unworn and worn region λ -ratios, split by prosthesis model.

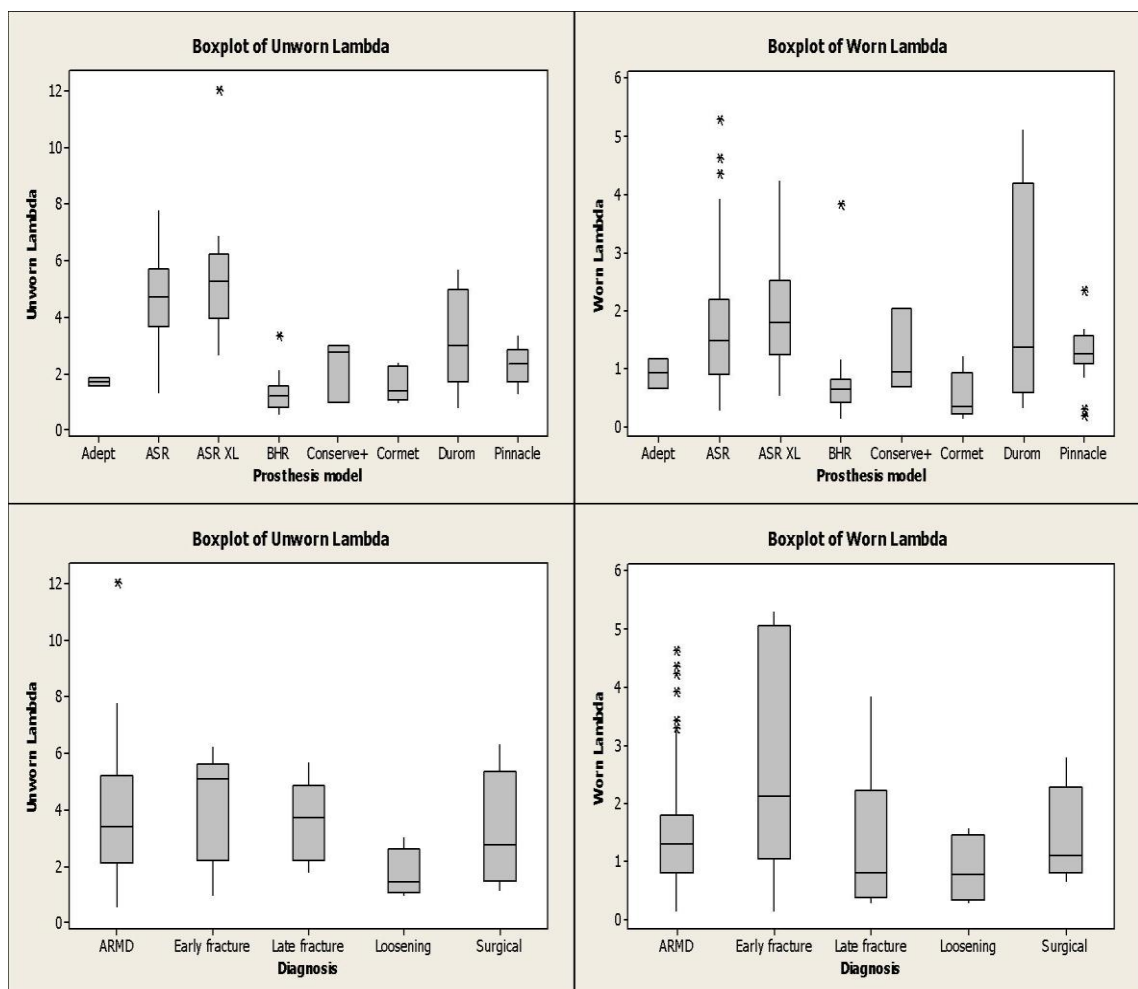


Figure 4.20: Boxplots of unworn (left) and worn (right) λ -ratios, split by model of prosthesis (top) and diagnosis for retrieval (bottom).

There were no significant differences in either unworn λ ($p = 0.218$) or worn λ ($p = 0.558$) by diagnosis for retrieval.

4.3.3 Correlation

All measures of bearing surface wear (linear depth, volume, volumetric rate and wear scar coverage) correlated with each other, with Spearman's Rank Correlation Coefficient (SRCC) of no less than 0.713 ($p < 0.001$ in all cases). Further, each measure of independent component wear correlated with the same measure of combined total wear, with SRCC of no less than 0.906 ($p < 0.001$ in all cases). All measures of taper wear also correlated with each other, with SRCC of no less than 0.745 ($p < 0.001$ in all cases). No significant correlation was found between bearing surface wear and taper wear ($p = 0.658$).

Table 4.13 details the SRCC and p-values for all measures of bearing surface wear (component depth, component volume, component volumetric rate, combine paired depth, combined paired volume and combined paired volumetric rate). Significant correlations are highlighted. Here, location of the wear scar refers to the angle between the point of maximum wear depth and the rim of the acetabular cup.

Inclination, anteversion and component radius all correlated with all measures of wear. Duration in vivo correlated with wear depth and wear volume, but not wear rate. All measures of wear were inversely correlated with CPR distance. Prostheses with wear closer to the cup rim were associated with higher measures of wear. Worn λ -ratios were found to inversely correlate with all measures apart from individual component wear rate. Unworn λ -ratios and clearance did not correlate with any measure of wear.

Table 4.14 details the SRCC and p-values for all measures of taper wear (depth, volume and rate). Duration in vivo correlated with wear depth and volume, but not wear rate. ASR™ XL devices showed greater taper wear (median 30.05 μm depth, 0.70 mm^3 volume) than Pinnacles® (5.67 μm , 0.31 mm^3 respectively). Finally, larger taper angles were correlated with greater taper wear depth, but not with wear volume or rate.

	Bearing surface wear measurement					
	Component depth	Component volume	Volumetric rate	Combined depth	Combined volume	Combined volumetric rate
Duration	0.368 (p<0.001)	0.360 (p<0.001)	-0.119 (p=0.051)	0.351 (p<0.001)	0.387 (p<0.001)	-0.086 (0.169)
Inclination	0.400 (p<0.001)	0.375 (p<0.001)	0.297 (p<0.001)	0.424 (p<0.001)	0.414 (p<0.001)	0.353 (p<0.001)
Anteversión	0.246 (p<0.001)	0.210 (p=0.001)	0.201 (p=0.001)	0.253 (p<0.001)	0.223 (p<0.001)	0.231 (p<0.001)
CPR	-0.427 (p<0.001)	-0.362 (p<0.001)	-0.305 (p<0.001)	-0.438 (p<0.001)	-0.387 (p<0.001)	-0.357 (p<0.001)
Radius	0.240 (p<0.001)	0.362 (p<0.001)	0.338 (p<0.001)	0.291 (p<0.001)	0.423 (p<0.001)	0.364 (p<0.001)
Clearance	-0.032 (p=0.603)	-0.012 (p=0.848)	-0.021 (p=0.733)	-0.021 (p=0.742)	0.007 (p=0.916)	-0.013 (p=0.838)
Location	-0.428 (p<0.001)	-0.527 (p<0.001)	-0.443 (p<0.001)	-0.398 (p<0.001)	-0.449 (p<0.001)	-0.394 (p<0.001)
Unworn λ	0.026 (p=0.762)	0.085 (p=0.313)	0.023 (p=0.191)	0.043 (p=0.178)	0.018 (p=0.206)	0.231 (p=0.008)
Worn λ	-0.301 (p<0.001)	-0.203 (p=0.015)	-0.104 (p=0.218)	-0.196 (p=0.025)	-0.182 (p=0.038)	-0.178 (p=0.044)

Table 4.13: Spearman's Rank Correlation Coefficients (SRCC) between nine controllable factors and six measures of bearing surface wear. Significant positive correlations are highlighted in green. Significant negative correlations are highlighted in pink.

	Taper wear measurement		
	Depth	Volume	Volumetric rate
Duration	0.539 (p<0.001)	0.440 (p<0.001)	0.148 (p=0.231)
Inclination	0.155 (p=0.159)	0.006 (p=0.963)	-0.027 (p=0.834)
Anteversión	-0.052 (p=0.637)	0.228 (p=0.065)	0.225 (p=0.073)
CPR	-0.124 (p=0.288)	-0.076 (p=0.565)	-0.082 (p=0.543)
Nominal diameter	0.473 (p<0.001)	0.320 (p=0.007)	0.240 (p=0.050)
Clearance	-0.070 (p=0.514)	0.022 (p=0.853)	0.006 (p=0.964)
Taper angle	0.410 (p<0.001)	0.085 (p=0.481)	0.095 (p=0.444)

Table 4.14: Spearman's Rank Correlation Coefficients (SRCC) between seven controllable factors and three measures of taper wear. Significant positive correlations are highlighted in green.

All measures of metal ions correlated highly with each other (SRCC of no less than 0.841, $p < 0.001$ in all cases) and with all measures of bearing surface wear (SRCC of no less than 0.667, $p < 0.001$ in all cases). There was also a significant correlation between unworn and worn λ -ratios (SRCC = 0.524, $p < 0.001$). Finally, it was noted that wear scar coverage increased with longer durations and correlated with all measures of wear while devices worn further from the rim of the cup survived longer in vivo (SRCC = 0.381, $p < 0.001$).

When considering ASR™ resurfacings alone, almost identical correlations were found for duration in vivo, inclination, CPR distance, radius and worn λ -ratio. It was also found that clearance correlated with all measures of wear (SRCC = 0.25 – 0.35, $0.001 < p < 0.038$). Anteversión was not found to correlate with any measure of wear, but did inversely correlate with the distance between the rim of the cup and the point of maximum wear (SRCC = -0.294, $p = 0.001$).

Chapter 5. Discussion

This chapter will discuss in more detail the findings from Chapter 4, Results. The implications of the work in this thesis on the future design and study of MoM hip prostheses will be covered, as will any limitations of the present study.

The accurate assessment of volumetric wear of ex vivo prostheses is central not only to this thesis, but to the research area in general. As such, the results of the validation study of the CMM based method will be discussed first. This will be followed by an assessment of the data collected including the clinical background, wear measurements and surface roughness data.

Finally, the controllable factors found to significantly correlate with wear volume will be looked at individually and suggestions for improvements will be made. Through such improvements and careful control of the identified factors, it is thought that wear (and the associated complications) can be reduced.

5.1 Methodology

As discussed in Chapter 2, Background and Literature Review, ex vivo wear of MoM hip prostheses has proved very difficult to measure accurately. Even with simulated data sets, most current methods struggle to achieve accuracy within a few cubic mm. Bills et al recommended that error should be kept within 0.5mm^3 , though they only achieved this with a simulated dataset of approximately 300,000 points. Collecting such a dataset on a CMM would be extremely time consuming.

In this study, a CMM based volumetric wear measurement was proposed and validated. Real datasets of up to approximately 7,000 data points were collected. The mean volumetric error was 0.28mm^3 (range $0.01 - 0.82\text{mm}^3$). While the present method marks a significant step forwards in the calculation of ex vivo wear measurement, it is expected that errors could be reduced even further by using a CMM with improved resolution (the resolution of the CMM in the present study was $0.8\mu\text{m}$). However, the current CMM is “high-accuracy” and achieves accuracy levels fit for the purpose of assessing ex vivo MoM hip prostheses.

Typically, error decreased as wear volume increased (figure 4.7). Overall, the mean error expressed as a percentage was 6.2%. Again, this dropped significantly as wear increased, from a mean of 11.4% at 3-5mm³ to a mean of 3.3% at 7-9mm³.

Given the relatively low number of data points collected, the present method was also quick (typically a complete head, cup and taper scan could be completed within an hour) allowing a large number of prostheses to be analysed in a short period of time. Other authors have expressed concerns about the inaccuracies introduced as the number of data points collected is reduced [189, 190]. The method employed in this study was tested using $\frac{1}{4}$ x and 4x the number of data points. As seen in section 4.2.2, the accuracy of the present method was very good and was not improved when the number of data points was quadrupled. Accuracy was negatively affected when the number of data points was quartered, although even then the mean error was 0.99mm³.

In the present study, the area of the measured surface was calculated, based on the summation of between 2952 and 7056 smaller areas (depending on the size of the component). This was multiplied by the linear wear depth to give a total wear volume. By avoiding the need to calculate the volume of the measured object, errors are reduced significantly. It should be noted that in the current study, scans were taken every 5° around the circumference regardless of component size. On larger components there are therefore slightly larger gaps between data points, particularly towards the equator. For example, the widest gap on a 43mm femoral head (where 6048 points were taken) would be 1.88mm. For a 53mm head (7128 points), this increased to 2.31mm. However, the size of each grid square is taken into account during volume calculation and so this difference in gap size did not significantly affect results, even in cases of high edge wear which was commonly seen on the acetabular components. This is evidenced not only by the high level of accuracy achieved, but also by the negligible change in accuracy when four times the number of data points were measured, representing a maximum gap size for a 53mm femoral head of 1.16mm.

In the present method, data points were connected linearly. Accuracy could be improved further by accounting for the small curvature of the surface between each data point. However, doing so did not make a significant difference to the result (less than 0.1mm^3) with the configuration detailed in this thesis, as discussed in section 3.3.2. Scanning time could be reduced by further limiting the number of data points, though fewer data points would result in an increase in error from this linear connection. When one quarter of the number of points was taken, scanning time was roughly halved but the error in wear volume calculation increased to around 1mm^3 , as shown in section 4.2.2. Accounting for the surface curvature in such a situation would help mitigate this. Fewer data points (and therefore larger gridsquares) would also mean a poorer definition of the wear scar, again increasing inaccuracies (figure 4.8). The current level of accuracy and time to complete a scan was deemed an acceptable compromise and both are significantly improved from previous studies. For example Bills et al's method when simulating 8,000 data points was accurate to around 25mm^3 [190]. This is almost 50x the accuracy of the present method, which uses up to 7,000 measured data points. Morris et al described their process as "fast, gaining results from four cups per day" [188]. Taking a day to be 8 hours, the present method is capable of 6x that rate.

In addition to measuring the volume of wear, the present method is capable of describing the size of the wear scar (surface area) and its location relative to the pole of the component. To the author's best knowledge, this is the first time such data has been offered. These two tools are extremely useful in understanding the mechanisms of wear – for example, the observation of rim wear on almost every acetabular cup. Although validation was not explicitly carried out on measuring the size of the wear scar, this was a part of the process for measuring the volumetric wear which was validated. It is reasonable to assume then that the measurements of the wear scar size achieve accuracy as good as or better than that of the volumetric wear calculation.

5.2 Clinical data

One hundred and forty-three hips were analysed, amongst the largest ex vivo studies ever performed. Eight different models were included in the study and were treated separately to reflect the fact that there are differences in survival

rates in vivo. Whilst considering individual models separately is a strength of the study, some models had only a small number of retrievals ($n = 2$ for the Adept®) which meant that statistically significant conclusions were hard to draw in such cases. Nevertheless, to the best of the author's knowledge this is the first such study to report on such a large number of models simultaneously and the data collected offers useful insights with real-world applications. Additionally the data has been collated at times to give results for 'all resurfacing' and 'all THR', giving much larger samples sizes (95 and 48 respectively).

One difficulty in collating the data is that compounding factors were introduced. This was particularly true for the THR group where only two models were considered. For this reason, tests were also carried out on the largest individual model group – the ASR™ resurfacing (61 hips). By comparing like for like, many compounding factors were mitigated. The same conclusions were drawn from this group as were drawn from the entire dataset.

5.3 Wear

Overall volumetric wear rates of $4.17\text{mm}^3/\text{year}$ were higher than rates typically offered by simulator studies (table 2.3) which are often in the region of $0.5 - 2\text{mm}^3/\text{million cycles}$ (taking one million cycles to be approximately equal to one year in vivo [226]). However, they were well within the $8.99\text{mm}^3/\text{million cycles}$ found by Williams et al for a 39mm MoM prosthesis with acetabular inclination of 55° [174]. Given the difficulties in accurately measuring volumetric wear of ex vivo MoM hip prostheses, such studies are rare in the literature. Morlock et al also found high wear rates for certain sub-groups of components, with mean wear rates for 14 rim-loaded heads and 15 rim-loaded cups of 8.69 and $15.88\text{mm}^3/\text{year}$ respectively [172]. Witzleb et al have reported on ten BHR™ explanted components (8 heads, 2 cups) which exhibited wear rates as high as $22.08\text{mm}^3/\text{year}$, with a mean of $3.36\text{mm}^3/\text{year}$ [187]. Given that this $3.36\text{mm}^3/\text{year}$ is for individual components, the overall BHR™ wear rate of $6.36\text{mm}^3/\text{year}$ in this study for heads and cups combined is remarkably similar.

Both linear and volumetric wear differed between models. The highest wear was seen on the ASR™ resurfacing. ASR™ retrievals had the largest wear scars on both heads and cups, and they wore very close to the cup rim. There

are several potential explanations for this that will be explored in subsequent sections. With the exceptions perhaps of the Durom™ and the ASR™ XL, the pattern of wear volumes across the models mimicked that of revision rates (figure 5.1), i.e. the highest wear volumes correlated with the highest revision rates.

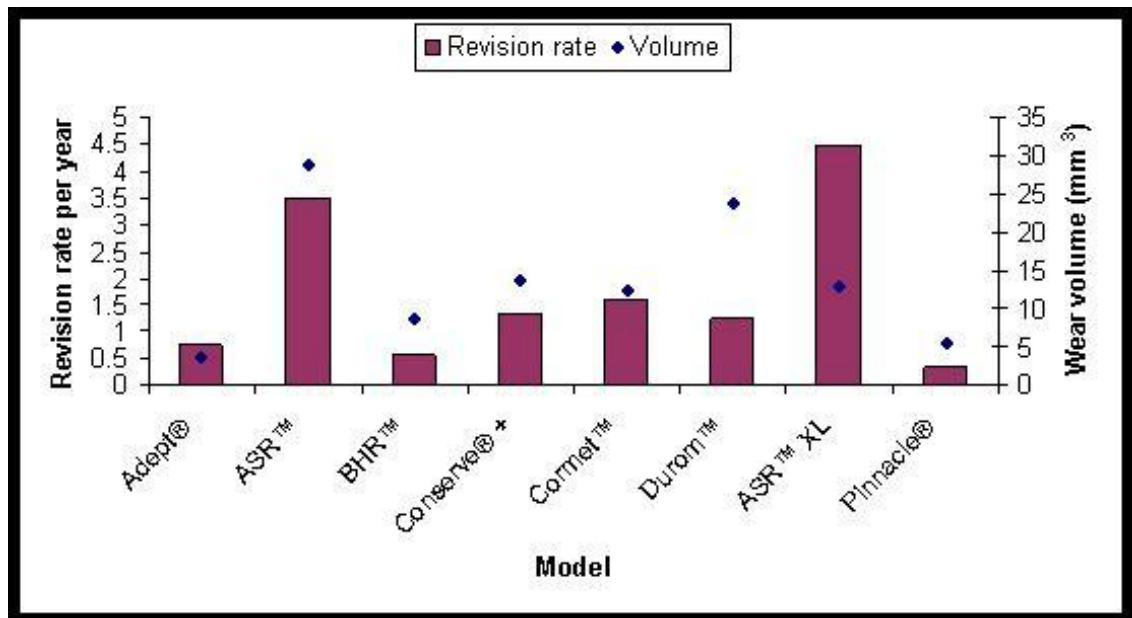


Figure 5.1: *Revision rate per year (taken from the literature in table 2.2) and median volumetric wear (measured in the present study) for all eight models of hip prosthesis considered.*

Given that the majority of prostheses in this study (80.4%) were revised due to ARMD, this link between wear volume and revision rate is perhaps not surprising but it does highlight the vital importance of wear (and thus biotribological studies) on the long-term performance of MoM hip prostheses. High wear is a serious concern and it needs to be minimised if the longevity of hip prostheses is to be improved, for the ultimate benefit of patients.

Revisions following late fracture were associated with extremely high wear depths (median 250.4 μ m, range 116.2 – 340.8 μ m) and volumes (median 61.12mm³, range 27.13 – 333.45mm³). Late fractures were also associated with wear closest to the cup rim (median 1.2^o), as well as the greatest surface wear scar coverage on both femoral heads (median 23.83% coverage) and acetabular cups (median 25.14%)

Other late fractures in the literature have been associated with gross metallosis [71, 149] or avascular necrosis [75, 76]. In all six cases of late fracture in the present study, bone loss at the femoral neck was noted at the time of revision. In four, there was evidence of joint effusion (a fluid build-up which, following MoM hip arthroplasty, is typically associated with metal debris [149]). Metal wear induced osteolysis leading to fracture is proposed here as the primary cause of prosthesis failure in these cases.

Wear following early fracture was less severe (median 12.40mm^3), but still many times what would be expected in a well functioning metal-on-metal prosthesis. Of particular concern was the short time in vivo (median 2.5months) meaning a high median wear rate of $34.61\text{mm}^3/\text{year}$. It could be claimed that, given the short duration in vivo, these prostheses were still in the bedding-in period. However, this wear rate is 3 – 4 times even the highest bedding-in wear rates ($8.99 - 11.5\text{mm}^3/\text{million cycles}$) in simulator studies with sub-optimal cup orientation [167, 174]. Although bone loss was only noted in one of the nine cases of early fracture, it is conceivable that such high wear in such a short period of time in vivo may contribute to the risk of neck fracture.

Retrievals following ARMD were associated with median wear volumes of 12.89mm^3 , very similar to early fracture retrievals but after significantly longer in vivo. Wear rates in the ARMD group of $4.13\text{mm}^3/\text{year}$, while lower than that amongst fractures, are significantly higher than the rates predicted by simulator studies (typically in the region of $0.5 - 2\text{mm}^3/\text{year}$). Given a median duration in vivo of 42months, the argument of bedding-in could not be applied to these retrievals. Wear occurred close to the cup rim (median 2.6° , further only than late fracture retrievals) and overall wear scar coverage was second only to late fractures. The close agreement in wear volumes between the ARMD group and the early fracture group provides further justification to the assertion that high early wear might play an important role in some early femoral neck fractures.

Loosening of MoM prostheses has typically been associated with long-term release of metal ions [227]. However, wear has been discredited as a cause in some cases of loosening [228] with metal hypersensitivity suggested instead [132, 229]. Patient metal ions in the loosening group of the present study were

elevated (median blood Cr = 5.31 μ g/l, Co = 1.10 μ g/l) and were within the MHRA 'safe' guidelines. In one study of MoM THR prostheses concluding that wear was not the cause of loosening, the mean wear rate was 2.2mm³/year [230], higher than the present rate of 1.33mm³/year in the loosened group. Given the low wear rate, metal hypersensitivity is a plausible explanation for the cases in the present study.

Prostheses retrieved following surgical complications were associated with the lowest values for all measures of wear, and wore furthest from the cup rim. This, combined with the fact that there is no evidence that the device itself was performing poorly, provides confidence that the surgical complication group can act as a baseline for well-performing prostheses in vivo. Median wear rates of 1.12mm³/year were similar to those from loosened prostheses (median 1.33mm³/year), providing further evidence that high wear may not have been a primary cause of loosening in this study.

There are of course causes behind high wear and many risk factors have been identified, including cup orientation and coverage arc, prosthesis diameter, clearance and surface roughness. These will be discussed below.

5.3.1 Duration in vivo

The median duration in vivo was 39 months, far shorter than the expected 10-20 years lifetime of hip prostheses. There were variations in time to revision depending on the failure mode. Early fractures were in vivo for the shortest amount of time (median 2.5months). Increasing durations were seen with surgical (median 37months), ARMD (median 42months), late fracture (median 46months) and loosening (median 55.5months) related revisions.

Previously, early fractures have been attributed to poor patient selection [110], surgeon inexperience [113] or surgical notching of the femoral neck [111]. All operations in the present study were carried out by an experienced surgeon and there was no evidence of surgical notching in any of the early fracture retrievals. Nothing unusual was noted in the patient age (median 62years) or gender (5 males, 4 females), or in the prosthesis diameter (median 49mm). The absence of the usual risk factors, coupled with the abnormally high wear (median

12.40mm³) of the early fracture retrievals indicates that failure in these cases may be wear related.

Loosening of MoM hip prostheses has been linked to long-term exposure to metal ions [227]. By definition, ARMD retrievals follow exposure to metal debris. A case has also been made for late fractures occurring secondary to metal debris. These conditions take time to develop, as evidenced by the longer durations in vivo.

In section 4.2.3, duration in vivo was found to correlate with both wear depth and wear volume across all components. A weaker inverse correlation between duration and component wear rate bordered on significant, but this was heavily influenced by the high wear rate of the early fracture retrievals. When considering only ARMD components, the correlations with wear depth and volume became more pronounced but there was no correlation between duration in vivo and component wear rate (SRCC = -0.018, $p = 0.784$) or total wear (SRCC = -0.019, $p = 0.775$).

This lack of correlation between duration in vivo and wear rate (SRCC = -0.086, $p = 0.169$) means that no evidence was found of the 'bedding-in' phenomenon seen in vitro. Indeed, the good correlation between wear volume and duration (SRCC = 0.387, $p < 0.001$) indicates a consistent wear rate through the prostheses' lifetime. Whilst there is strong evidence of a bedding-in period in vitro, there is reason to question its existence in vivo. It should be remembered though that all devices analysed here were failures and that their wear patterns might not represent all metal-on-metal hips implanted. Perhaps it is the failure of these devices to "recover" from the bedding-in period to a period of lower, steady-state wear that leads to the high wear rate and need for early revision surgery. Such "runaway" wear trends have been defined in vitro [159] and have been linked in vivo with smaller acetabular coverage arcs [231].

5.3.2 Acetabular cup orientation

Inclination and anteversion angles of the acetabular cup have been shown to affect survivorship and patient metal ion levels [91, 149, 168]. Typically, higher

implantation angles have been associated with poorer functional scores, higher revision rates and an increase in ion levels.

In the present study, median inclination and anteversion angles were 48.85° and 17.04° respectively. While these are consistent with the angles typically recommended by manufacturers, there was a large range in each case (inclination 22.85° – 76.04°, anteversion 0.00° - 40.00°). Across all models, higher inclination and anteversion angles correlated with an increase in both overall wear volume and overall wear rate. The correlation was stronger for inclination (SRCC = 0.414 and 0.353 for volume and rate respectively) than anteversion (SRCC = 0.223 and 0.231 respectively). Figure 5.2 shows the effect on total bearing surface wear rate of inclination and anteversion in this study. Low inclination is defined as <40°, good as 40° - 50° and high as >50°. Low anteversion is defined as <10°, good as 10° - 20° and high as >20°. While low angles did not increase the wear rate, there is an increased risk of higher wear if cup inclination and/or anteversion are high. This mimics the pattern of poorer performance with higher implantation angles noted above. This suggests that the creation of wear debris plays an important role in the failure of MoM hip prostheses, adding weight to the concept of ARMD failures.

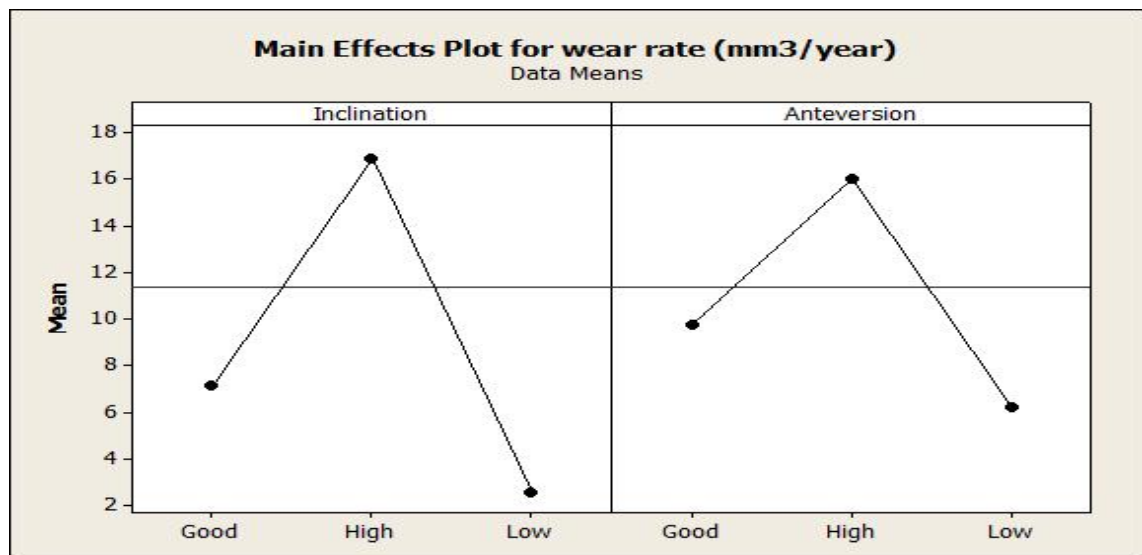


Figure 5.2: The effects of inclination and anteversion on total bearing surface wear rate.

As noted above, the vast majority of explanted cups were edge loaded. High cup orientation angles increase the risk of edge loading. Edge loading has previously been noted to significantly increase the wear rate [172]. It is

suggested here that this is the reason for the higher wear rates seen with higher implantation angles. Thus, proper implantation of the prosthesis is a critical issue for improving its longevity and it is recommended here that patients found to have sub-optimal positioning are subjected to regular follow-up. The definition of “sub-optimal” may depend on the model in question as some models (particularly those with shallower acetabular coverage arcs) are more susceptible to edge loading than others, given identical implantation angles.

The steepest inclination and anteversion angles were seen in the late femoral neck fractures. Neck fractures are a result of the bone’s inability to support the stresses being applied to it and steeper cup orientation increases these stresses [232, 233]. This, coupled with the high wear and subsequent weakening of the bone described above, is suggested as a primary cause of late femoral neck fracture.

5.3.3 Coverage arc and CPR distance

The acetabular coverage arc has also been noted to be important in predicting performance, perhaps the most important factor [67]. As with higher cup orientation angles, lower coverage arcs increase the risk of edge loading. Figure 5.3 shows the coverage arc for the eight models examined in this study, along with the median volumetric wear measured. Models with higher coverage arcs tended to be associated with lower volumetric wear.

Coverage arc and CPR distance are closely linked. Figure 5.4 shows these two measures for all eight models. Generally, as coverage arc increases, CPR distance increases and thus the risk of edge loading is decreased (assuming equal implantation angles and component diameters). Of course, in individual cases component diameter and implantation angle does make a difference. Figure 5.5 shows the effect of these factors on CPR distance.

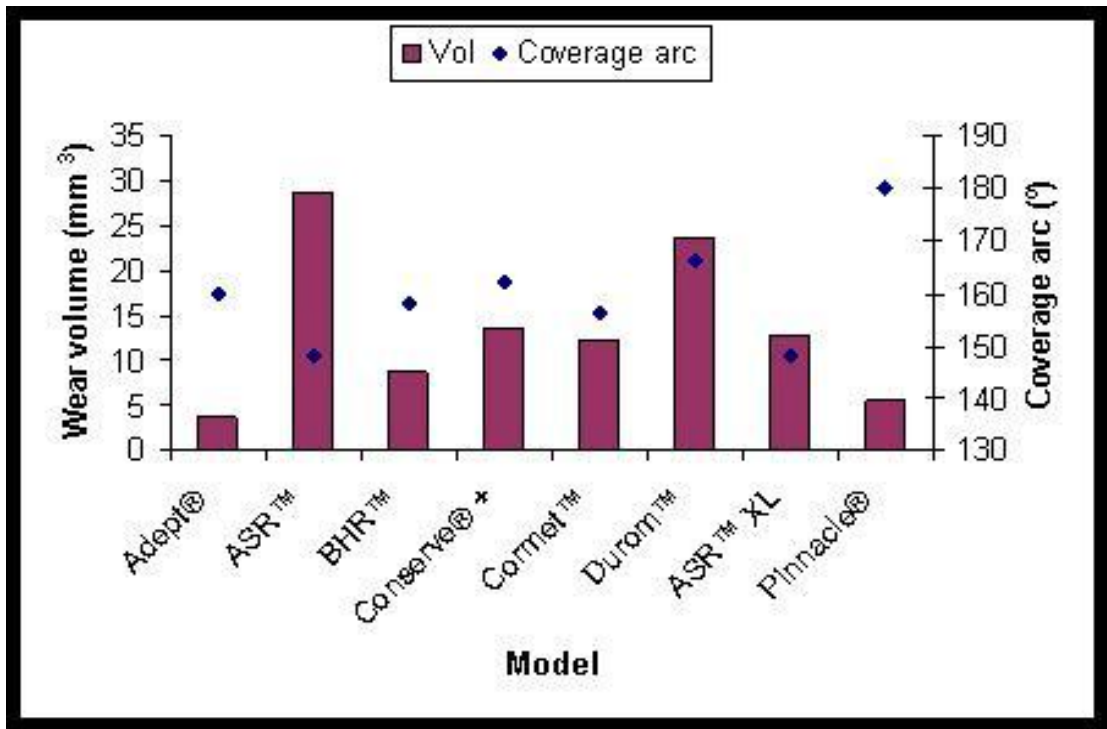


Figure 5.3: Coverage arc and measured volumetric wear for each of the eight models of hip prosthesis.

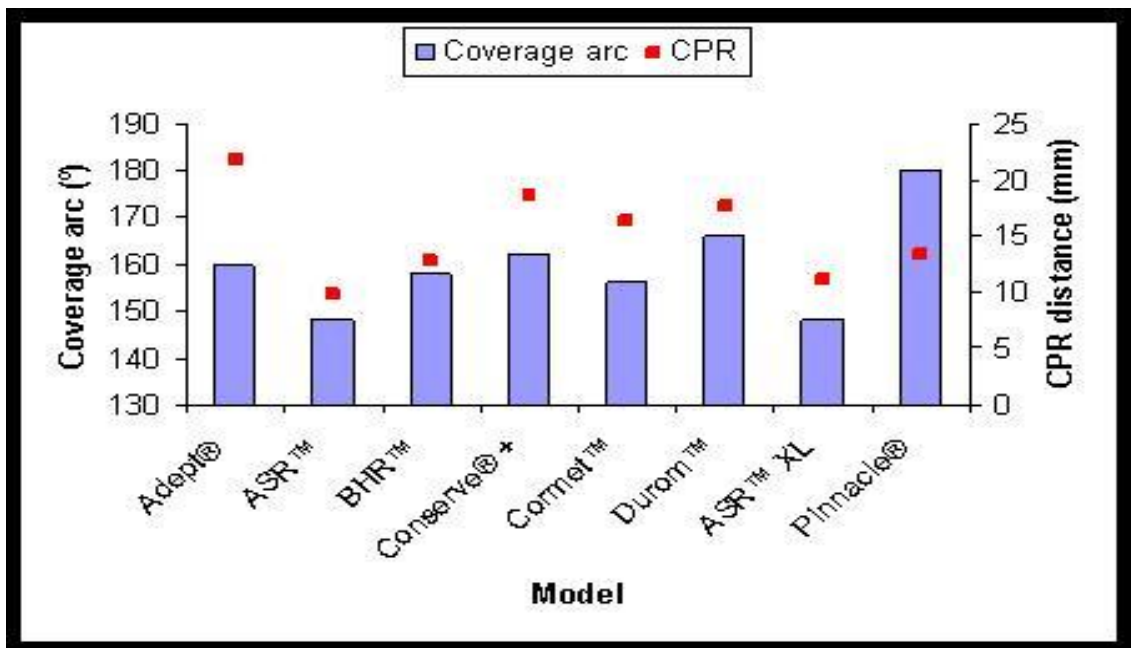


Figure 5.4: Coverage arc and CPR distance for each of the eight models of hip prosthesis.

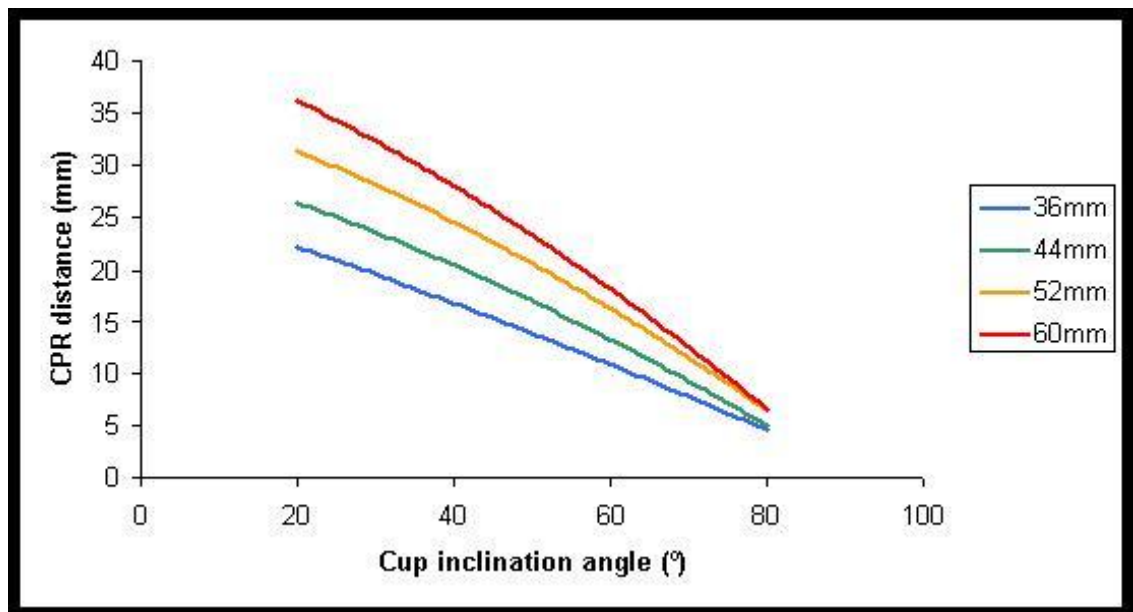


Figure 5.5: Effect of cup inclination angle and component diameter on CPR distance for cup coverage arc of 180° and anteversion of 10°.

In addition to increasing the risk of edge loading, CPR distance was found across all components to inversely correlate with wear rate (SRCC = -0.357) and wear volume (SRCC = -0.387). That is, as CPR distance increased, volumetric wear decreased. It has been suggested by Langton et al that a CPR distance greater than 10mm significantly reduces the risk of high metal ion levels [171]. Across all prostheses in this study, the median wear rate for CPR > 10mm was 3.46mm³/year, while for CPR < 10mm it was 8.19mm³/year (p = 0.003). While implantation angle will affect CPR distance, figure 5.4 shows that the cup coverage arc of each model (which is directly within the control of the manufacturer) plays a large role in defining the CPR distance for each individual prosthesis. Smaller arcs result in an increased risk of edge loading, higher wear and subsequent complications.

5.3.4 Component diameter

The smallest diameters were associated with prostheses revised for loosening (median 41mm). This supports previous work that suggests that smaller diameter is a risk factor in prosthesis loosening [113]. Prostheses revised following femoral neck fracture tended to be of a larger diameter than those revised for other reasons (median 49mm). As seen in figure 5.5, larger components increase the CPR distance of a prosthesis given otherwise identical conditions. However, they also create a larger surface area and larger

sliding distance. Under boundary lubrication, both of these would act to increase the amount of debris produced with each cycle (each step in the case of hip prostheses in vivo) and, as such, increase the overall wear rate.

Prosthesis radius correlated with all measures of wear in this study, indicating that larger devices are susceptible to larger wear volumes. Figure 5.6 shows the effect of prosthesis diameter on total bearing surface wear rate. Small prostheses are defined here as 36 – 41.99mm, medium as 42 – 47.99mm and large as 48mm diameter and above. Typically, larger devices are expected to promote a more favourable lubrication regime [194-196]. It was noted in the present study that head radius and λ -ratio were positively correlated in the unworn region (SRCC = 0.430, $p < 0.001$). However, this was not maintained in the worn region (SRCC = 0.018, $p = 0.835$).

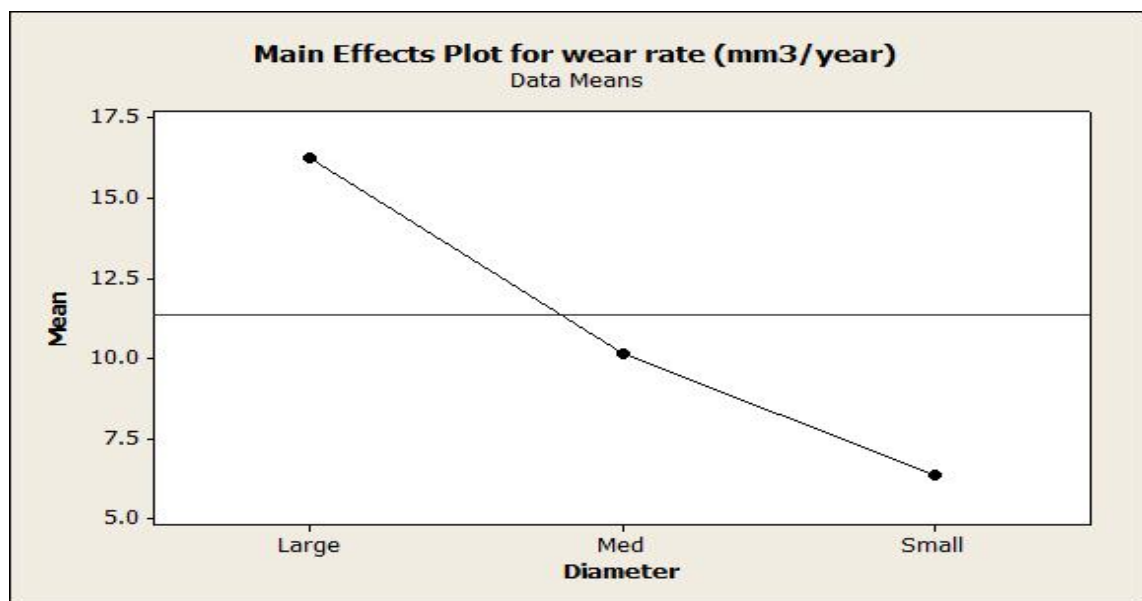


Figure 5.6: *The effect of prosthesis diameter on bearing surface wear rate.*

It is worth noting again that the present study looked only at failures. It is possible that many large-diameter MoM hip prostheses do maintain their fluid film lubrication regime. The fact remains though that the proposed benefits of larger prostheses are negated if the fluid film or mild-mixed lubrication regime is not maintained and that, in such situations, larger devices are susceptible to greater wear than smaller devices as governed by the Archard wear A [204] as explained in section 2.4.

5.3.5 Radial clearance

The largest clearances were seen in the two early neck fracture retrievals (134.4 μm and 222.2 μm). Such high clearances result in very low λ -ratios (1.14 and 0.97 – just either side of the border for boundary lubrication). The resulting boundary contact between the components can lead to high stresses and wear.

The lowest clearances were seen in the ARMD retrievals. Lower clearances increase the size of the contact area between the head and cup [197, 198, 234]. This increases the distribution of the contact force, resulting in lower pressure at each point. However, the increased contact area also reduces the distance from the contact patch to the cup rim, thereby increasing the risk of edge loading.

Although it has been suggested that clearances should be reduced as much as possible [43] there is clearly a practical limit to this. The present study showed no correlation between clearance and wear. This, perhaps, is because the two above factors counteract each other. There is a need to strike a balance between contact pressure and the risk of edge loading [234]. Figure 5.7 shows the clearance against wear volume for each retrieved hip prosthesis. Although many low clearance devices showed low wear volumes, there was a risk of high wear at low radial clearance (< 70 μm).

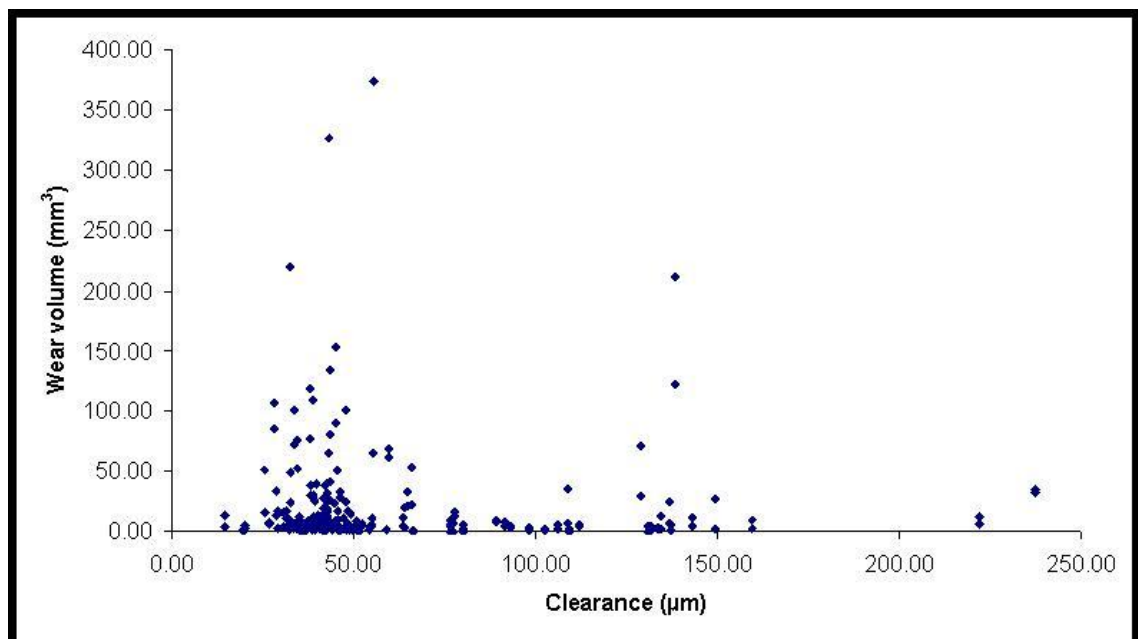


Figure 5.7: Radial clearance against wear volume for all 143 retrieved prostheses.

Radial clearances between 75 – 100 μ m were associated with the lowest risk of high wear volumes. This is within the approximate range of the Adept®, BHR™ and Cormet™ prostheses which were associated with the lowest wear amongst the hip resurfacings in this study. It is important to note that these models also have other design benefits over, for example, the ASR™ such as a larger coverage arc.

5.3.6 Metal ion concentration

Concentrations of metal ions in the patient were correlated strongly with wear volumes ($0.710 \leq \text{SRCC} \leq 0.817$, $p < 0.001$). Since these ion levels are detectable in the blood of patients, blood tests could be used as a surrogate measure of wear while the prosthesis is still in vivo.

Median metal ion concentrations in this study were higher than the 7 μ g/l ‘safe’ level offered by the MHRA (Cr = 10.20 μ g/l, Co = 9.73 μ g/l). However, fourteen patients of the 115 who suffered ARMD retrievals (12.2%), and all four revised for loosening, had both Cr and Co blood metal ion concentrations below 7 μ g/l.

The median levels for those eighteen patients revised below 7 μ g/l were 5.31 μ g/l Cr and 2.46 μ g/l Co. This calls into question the current ‘safe’ guideline level. In the absence of any clear reason for setting this level at 7 μ g/l [235] and given maximum concentrations of around 2 μ g/l following a well-functioning MoM hip replacement [236], there is reason to call for this level to be reduced to a maximum of 5 μ g/l for either Cr or Co. This ties in with the recent findings of Bosker et al that pseudotumour incidence increased fourfold when serum ion concentrations were greater than 5 μ g/l [147].

Differences in metal ion concentrations were noted between different models. However, with the exception of the Adept®, the concentrations of metal ions in the blood of patients (Cr + Co) were remarkably similar across all devices when normalised against wear volumes. The median values for all other resurfacings ranged from approximately 1.2 – 1.4 μ g/l for each mm³ of wear (figure 5.8). Such consistent agreement across resurfacing models may allow for the in vivo prediction of wear volumes using metal ion levels. Using this rate of ion release, a level of 5 μ g/l equates to 3.6 – 4.2mm³ of wear. Ion levels of 7 μ g/l equate to

5.0 – 5.8mm³. The ASR™ XL and Pinnacle® values were slightly higher at 1.5µg/l and 1.9µg/l respectively per mm³ of wear. It is interesting to note that the stemmed designs produced a greater number of ions per mm³ of wear and it has been suggested previously that tapers of LHMOM THA are a greater source of ions than bearing surface wear [237].

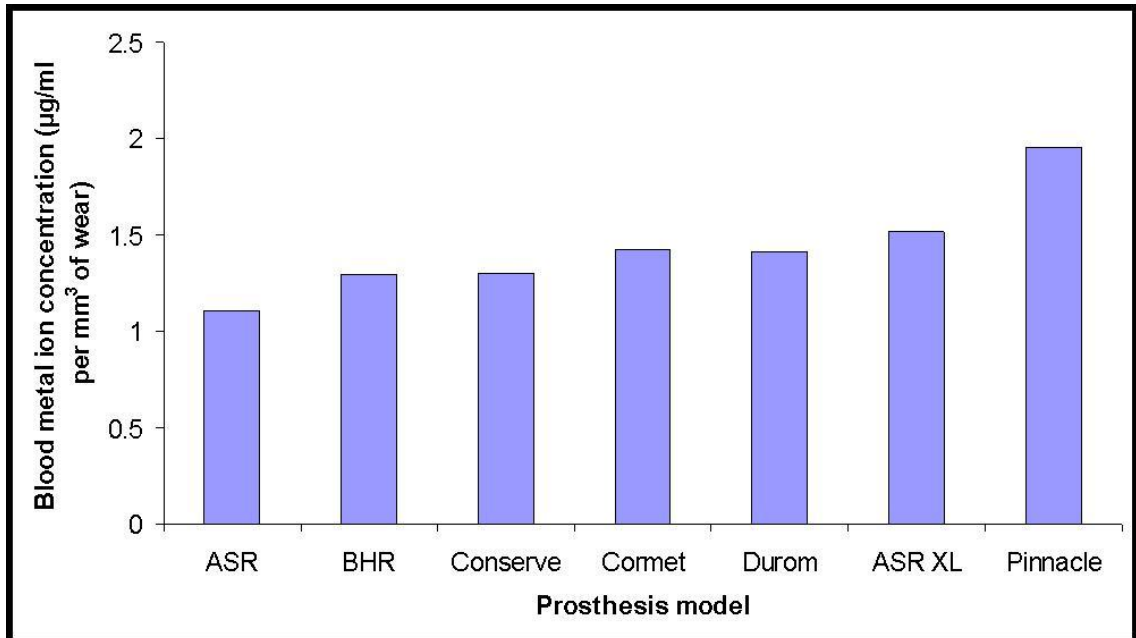


Figure 5.8: Blood metal ion concentrations per mm³ of wear for 7 of the 8 models studied. Adept® (3.4µg/l per mm³) has been left out to improve clarity.

It appears then that, for the models studied, wear is the primary factor governing ion release. Manufacturing method and subsequent heat treatment has been shown to affect the rate of metal ion release [167, 176]. The prostheses in the present study underwent a variety of heat treatments but all produced very similar concentrations of metal ions for each mm³ of wear. It is suggested here that the effect on ion release seen previously is a reflection of any changes in wear rate for heat treated prostheses when compared with non-heat treated models.

5.4 Simulators

Simulator studies typically calculate the steady-state wear rate of MoM hip prostheses to be less than 1 – 2mm³/million cycles (table 2.3). Even excluding the extremely high wear rates of the early neck fractures, the median wear rates of ex vivo prostheses in this study were 4.02mm³/year. The difference was more pronounced in some models, with the Conserve® + (median

11.78mm³/year) and ASR™ resurfacing (median 9.61mm³/year) in particular showing excessive wear rates. While median wear rates following surgical complications were only 1.12mm³/year, indicating the potential for “well-functioning” prostheses to approach the good results obtained in vitro, there is reason to question the suitability of current simulator testing in some situations.

In the tests by Williams et al [174], components were tested with the cup at 45° inclination, and then a second test was done with the cup at 55° inclination with the addition of microlateralization. At 45° inclination an overall wear rate of 1.61mm³/million cycles was reported, compared with 8.99mm³/million cycles at 55° inclination plus microlateralization. These values are much closer to those found in the present study.

Although the majority of prostheses were not implanted as steeply as 55° inclination – even the higher wearing devices – it is important to remember that a key issue in determining wear is the risk of edge loading. Steeper inclination angles increase this risk, but acetabular cup coverage arc is a key factor too. A 50mm hip prosthesis with a coverage arc of 160° (the upper limit of the ASR™) inclined at 45° has approximately the same CPR distance as an acetabular cup with a coverage arc of 180° inclined at 55° (both approximately 21mm) [234].

The opinion has been offered that current guidelines on testing hip prostheses (ISO 14242) are not physiologically relevant (i.e. they do not successfully recreate the loading profiles associated with in vivo conditions) and may lead to “an exaggerated lubrication regime, resulting in extremely low wear during the steady state phase in vitro” [167] when applied to MoM prostheses. The increased wear seen in vivo in this study, combined with the close agreement of wear rates here and in more physiologically relevant simulator tests, suggest that new guidance is needed to keep pace with the latest generation of hip prostheses. The effects of sub-optimal cup positioning and the difficulty surgeons face in consistently achieving optimum positioning (as evidenced by the large range in this study, using in vivo radiological measurements from multiple centres) suggest that new prostheses should be tested in sub-optimal positions to evaluate the risks, and effects, of edge-loading.

Such guidance should extend not only to academic research articles, but also to form one part of the testing of new prostheses prior to market release, which in Europe is currently performed “behind closed doors” by for-profit organisations known as notified bodies [238]. The MHRA, which oversees such notified bodies in the UK, has recently expressed concern that there may be discrepancies in the application of testing standards between notified bodies [239].

5.5 Surface roughness and lubrication

Surface roughness measurements were taken on all components in two distinct regions – worn and unworn. Measurements in the unworn region were intended to represent the surface roughness of the component before implantation. When compared with the unworn region, increased surface roughness was observed in the worn region of all prostheses, regardless of model or failure mode. However, increases were not consistent across all designs.

In the unworn region, median RMS values were very low for the ASR™ XL (0.007µm), Conserve® + (0.008µm), ASR™ resurfacing (0.009µm) and Durom™ (0.009µm). The Pinnacle® (0.014µm), Cormet™ (0.018µm), Adept™ (0.026µm) and BHR™ (0.026µm) all had higher median RMS values. However, with the exception of the Pinnacle® (0.021µm) and ASR™ resurfacing (0.047µm) prostheses, surface roughness in the worn zone was remarkably consistent across all devices ranging from RMS 0.033µm (Conserve® +) to 0.038µm (BHR™). Despite low initial roughness values for some models, they were unable to maintain such smooth surfaces in vivo.

As noted above, the ASR™ resurfacing prostheses roughened most in vivo. They also produced the greatest volume of wear. Smaller increases in roughness were seen on the ASR™ XL, Durom™, Conserve® + and Cormet™ prostheses and these increases were similar for these four designs (range 0.017µm to 0.029µm). Again, this is similar to the pattern of wear volumes, with these four designs producing similar volumes of wear to each other, but less than the ASR™. In keeping with this pattern, the BHR™, Adept® and Pinnacle® showed the smallest increases in surface roughness (0.010µm, 0.009µm and 0.007µm respectively). They also wore the least. Changes in

surface roughness appear then to be linked to wear. This is consistent with the literature [173, 196, 201]. However, it does not necessarily follow that devices that are initially rougher will wear more, as evidenced by the lower wear volumes of the Adept® and BHR™ prostheses which were initially the roughest but (alongside the Pinnacle®) produced the lowest wear volumes.

One key issue appears to be the microstructure of the device. As noted in Chapter 1, Introduction, all models apart from the Durom™ are manufactured by casting. The Durom is wrought. The ASR™, Conserve® + and Cormet™ prostheses are subsequently heat treated. Note again that these are the models that produced the highest wear and change in surface roughness despite achieving initially very low roughness values. As far back as 2003, a study of MoM hip resurfacing tribology by Cawley et al found that “[a]s cast materials were determined to have greater abrasive wear resistance when compared with single or multiple heat treated materials” [240]. This was because heat treatment reduced the size and spatial density of carbides – agglomerations of carbon with higher hardness than the surrounding material [161]. Similar results have been found by Kinbrum and Unsworth in 2008 [241] and by Kamali et al in 2010 [167]. Figure 5.9 shows typical images from the unworn region of a Conserve® + (heat treated) and BHR™ (as cast) femoral head.

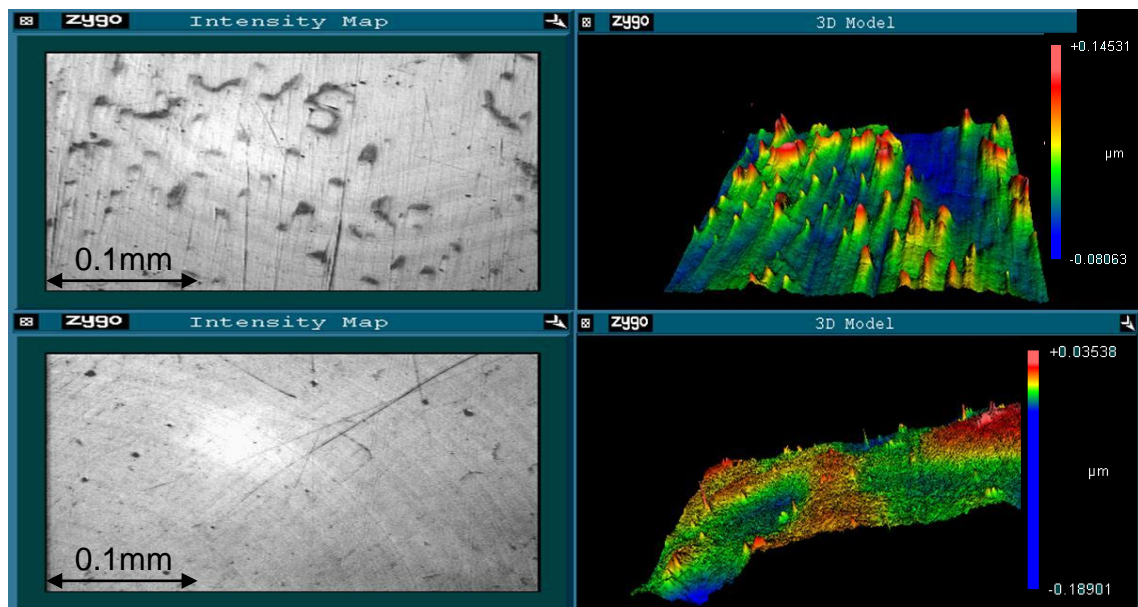


Figure 5.9: Two- and three-dimensional images of the typical unworn surface of a BHR™ (top) and Conserve® + (bottom) femoral head. Note the apparent carbides protruding from the surface of the as-cast BHR, resulting in an initially higher RMS ($0.016\mu\text{m}$) than the Conserve® ($0.008\mu\text{m}$).

The as-cast BHR™ showed a densely packed arrangement of protrusions, similar in appearance to the carbides discussed by Cawley et al, as did other as-cast prostheses. These are not present in the heat-treated Conserve® +. This is best demonstrated by the higher R_{sk} measurements for the BHR™, Adept® and Pinnacle® compared with the heat-treated models, indicative of a surface dominated by peaks rather than valleys. Whilst this initially meant that as-cast models had higher surface roughness, the carbide concentration gave improved wear resistance meaning that over time the heat treated models roughened (and wore) at a greater rate.

Figure 5.10 shows a typical three-dimensional representation of the unworn surface for all eight models of hip prosthesis in this study. The apparent carbides are clear in the as cast models, but are less common amongst the heat treated models, consistent with the description of Cawley et al.

Figure 5.11 shows typical representations of the worn areas of each model of prosthesis. Abrasive wear is apparent in all cases and was very commonly seen across all measured prostheses. Although abrasion was the most dominant wear mechanism, others were occasionally seen. Pitting was seen on all models apart from the wrought Durom, though it was much more frequently observed on the heat-treated femoral heads. Pitting has previously been attributed to carbide removal from the surface [242]. A consequence of pitting due to carbide removal is the potential for 3rd body wear as the relatively hard carbides are freed from the softer surface, resulting in deep scratches originating at the pits [161, 243]. This is consistent with the present findings (figure 5.12).

With the exception of three hip prostheses, λ -ratio decreased in the worn zone compared with the unworn zone. These three prostheses (all BHR™) were all low wear ARMD failures (mean $1.04\text{mm}^3/\text{year}$) with relatively high radial clearance (mean $132\mu\text{m}$) and were among the longest surviving prostheses in the study (mean 66 months). This small minority (2.1%) that became smoother over time might provide evidence of self-polishing in vivo, but the vast majority (97.9%) of prostheses in this study became rougher.

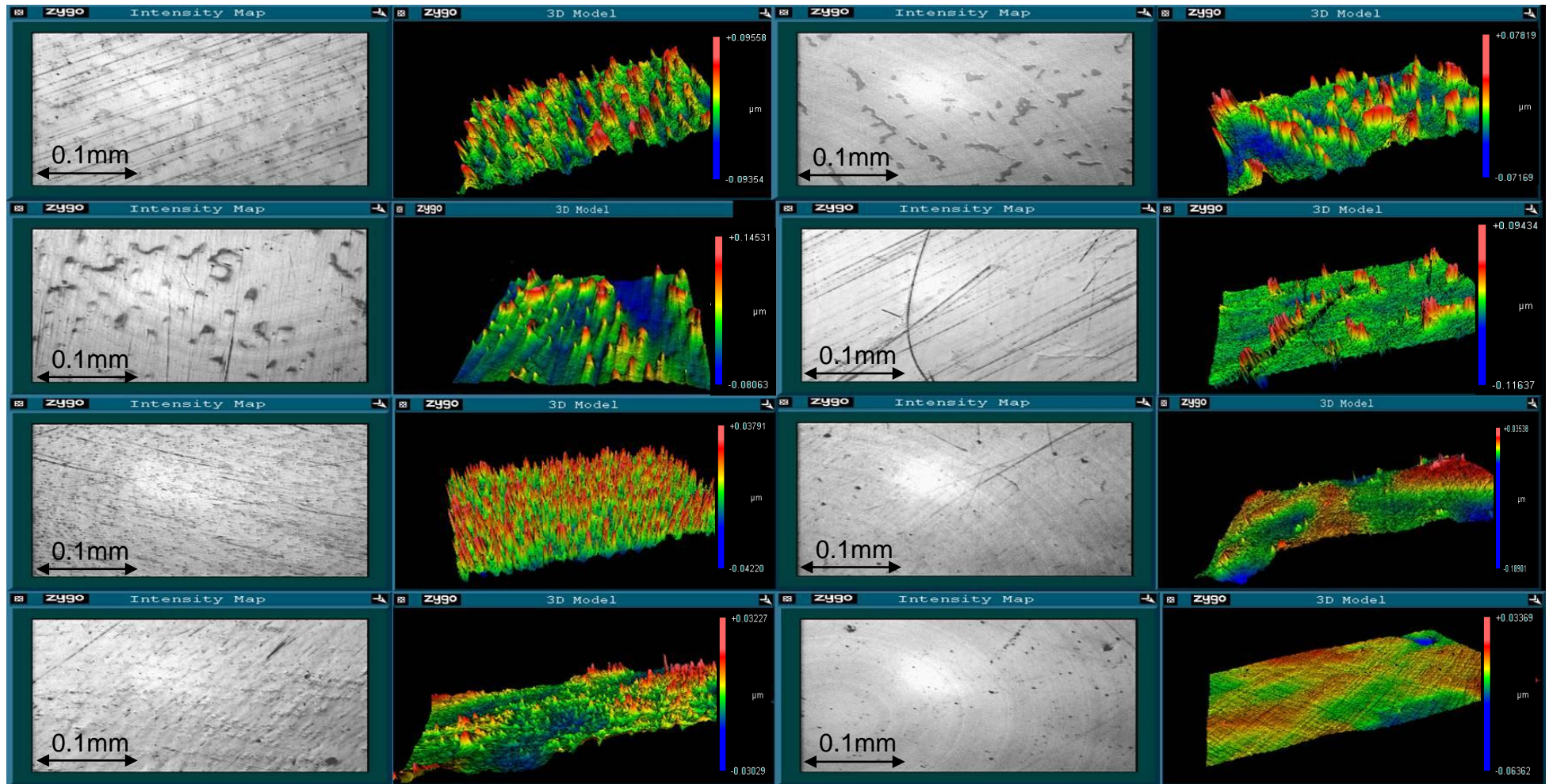


Figure 5.10: Images of the unworn regions of femoral heads of the 8 models of MoM hip prosthesis. From top to bottom: Left; Adept®, BHR™, Pinnacle® (all cast), Durom™ (wrought). Right; ASR™ (cast with heat treated cup), ASR™ XL, Conserve® +, Cormet™ (All heat treated following casting).

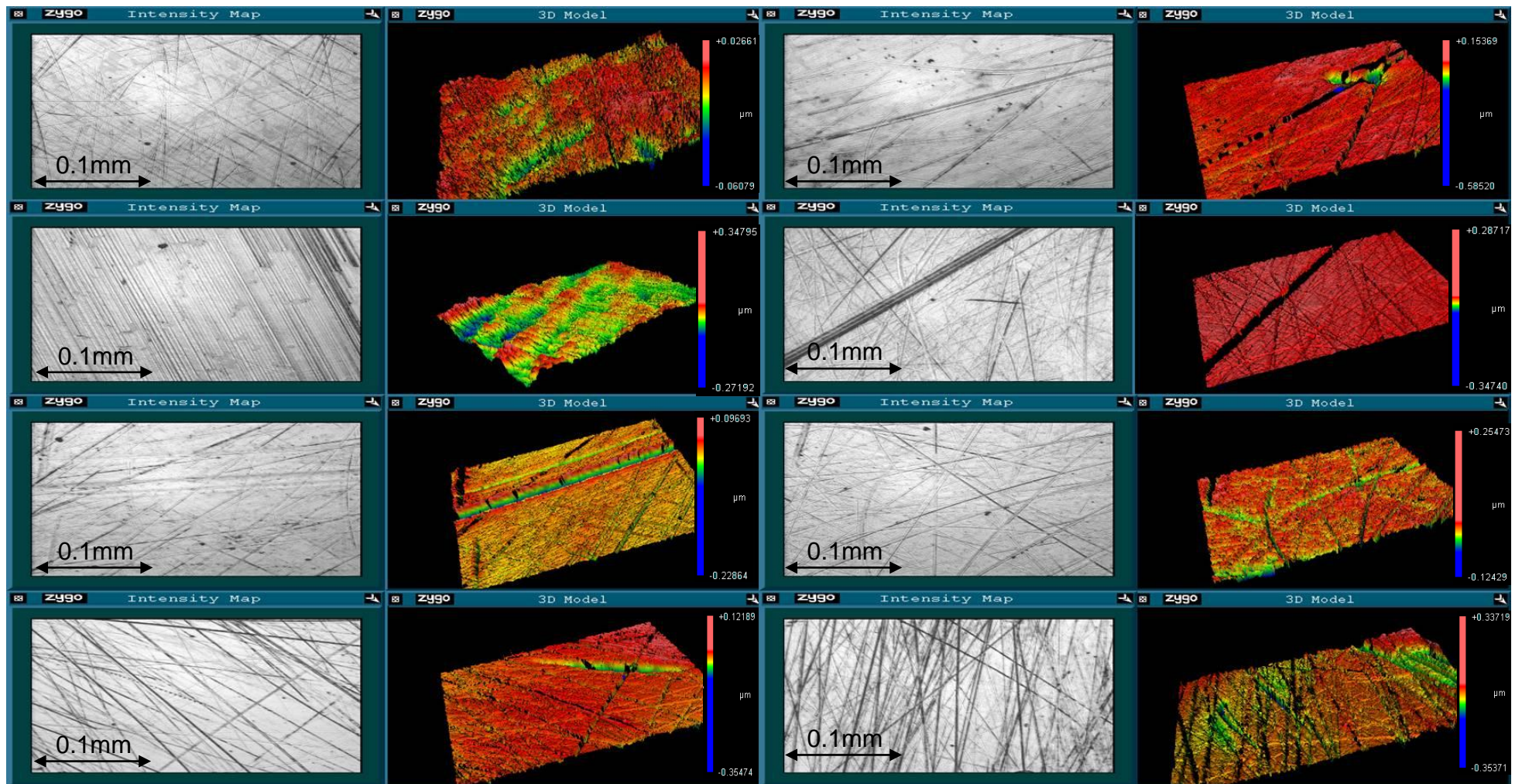


Figure 5.11: Images of the worn regions of femoral heads of the 8 models of MoM hip prosthesis. From top to bottom: Left; Adept®, BHR™, Pinnacle® (all cast), Durom™ (wrought). Right; ASR™ (cast with heat treated cup), ASR™ XL, Conserve® +, Cormet™ (All heat treated following casting).

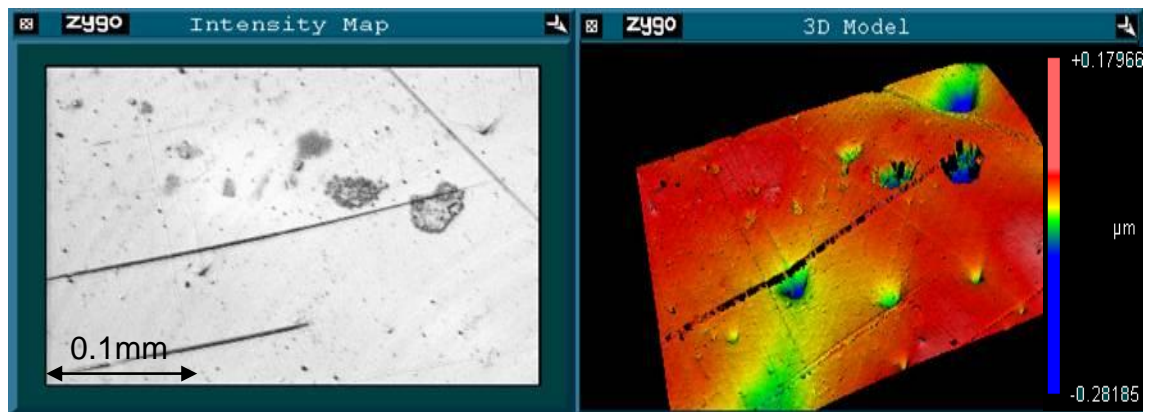


Figure 5.12: Image of a Cormet™ femoral head exhibiting pitting (approximate depth $0.2\mu\text{m}$), with narrow scratches of similar depth originating at some of the pits.

Again, it is difficult to extend the findings from these failed ex vivo prostheses to all well functioning in vivo prostheses – perhaps the inability to self-polish led to the high wear and early revision – but it is worth noting that even the prostheses revised for surgical complications did not show evidence of self-polishing. In keeping with the roughness results above, the ASR™ models had the highest λ -ratios in the unworn zone (5.24 and 4.64 for the ASR™ XL and resurfacing brands respectively). At 1.31, the BHR™ had the lowest. However, non heat-treated models were better able to maintain their λ -ratios, with the median λ -ratio in the worn regions around 54% of those in the unworn regions (figure 5.13). The wrought Durom™ also maintained approximately 50% of their unworn λ -ratio while the heat-treated models were only able to maintain between 25% (Cormet™) and 34% (ASR™ XL). In keeping with this, the effect of manufacturing method on total volumetric wear was significant ($p = 0.013$), with lower wear rates seen in the cast and wrought models than the heat treated models (figure 5.14). Having noted that, there was a positive correlation between unworn and worn λ -ratios, indicating that a prosthesis promoting a milder lubrication regime was better able to maintain that regime.

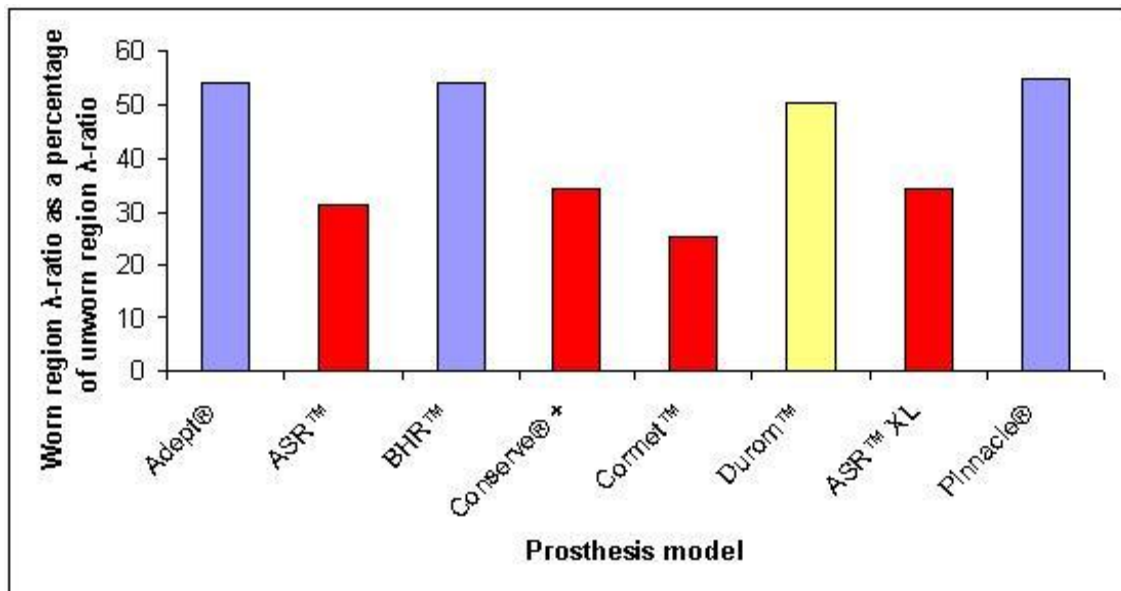


Figure 5.13: Median λ -ratios in the worn regions as a percentage of those in the unworn regions for as-cast (blue), heat-treated (red) and wrought (yellow) models.

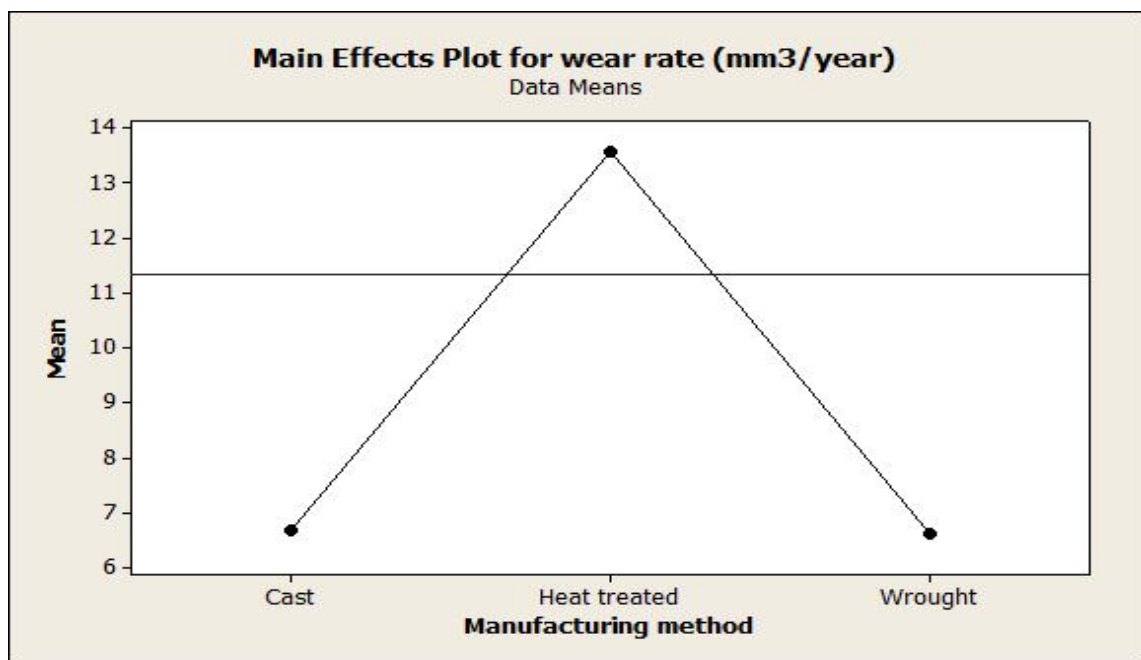


Figure 5.14: The effect on bearing surface wear rate of heat treating hip prostheses ($n = 84$) compared with as cast ($n = 41$) or wrought ($n = 5$) models.

Despite the better preservation of the lubrication regime, the median λ -ratios in the worn region of the Adept® and BHR™ were less than one, as were those of the Conserve®+ and Cormet™, indicating boundary lubrication. The remaining four designs of MoM hip had λ -ratios between 1.25 and 1.80, indicating mixed lubrication. It appears then that some models are more susceptible to degradations in the lubrication regime from fluid-film to mixed to boundary lubrication. Despite median worn λ -ratios indicating boundary lubrication, the

Adept® and BHR™ prostheses produced some of the lowest wear rates. However, it is important to remember that the size of the wear scar was smallest on these two models. Looking at the maximum linear wear depths (figure 4.9), the BHR™ in particular (median 13.0 μm) is similar to or greater than most other models. Only the ASR™ resurfacing showed significantly greater wear depth and the majority of that was on the heavily edge-loaded cups. Of the other models, only the Cormet™ showed greater wear depth on the heads (median 23.1 μm) and the worn λ -ratio of the Cormet™ (median 0.35) was lower than that of the BHR™ (median 0.65).

Although it initially seems counter-intuitive that the BHR™ should produce relatively little wear (median 8.68 mm^3) when compared with other resurfacings (only the Adept® wore less) with such a low λ -ratio, it is clear now that the wear in the worn region is relatively high. Because the worn region covers a smaller area (median 6.77% of the heads, 5.78% of the cups) than most other models (median 14.15% on the heads, 11.74% of the cups) however, the overall wear volume is still lower. This provides real ex vivo data to support the assertion in Chapter 2 that volumetric wear measurements provide a fuller picture than linear wear depths alone.

In terms of failure mode, the lowest worn λ -ratios were seen in the late fracture and loosened prostheses (λ -ratio < 1). Surgical and ARMD failures were slightly higher ($1 < \lambda$ -ratio < 1.5) and early fractures significantly so (λ -ratio > 2). This mimics the pattern of duration in vivo and likely reflects the increase in surface roughness (and subsequent degradation of the lubrication regime) over time.

5.6 The taper junction

As seen in Chapter 4, THRs also experience wear at the taper junction. Although often comparatively low (median 0.70 mm^3) when considered next to the bearing surface wear, taper wear is not insignificant. Wear depths up to 40 μm have been reported at the taper junction [234]. The maximum taper wear depth in this study was 68 μm (median 13.5 μm). The maximum volumetric wear was 9.29 mm^3 and this occurred in a prosthesis whose total combined bearing surface wear was 8.33 mm^3 (at a rate of 1.47 mm^3/year , comparable to the 1.12 mm^3/year found in retrievals secondary to surgical complications). Wear at

the taper junction can contribute a significant amount of the overall wear and, given that 46 of 48 (96%) of the THRs in this study failed secondary to ARMD, can therefore contribute to the risk of failure.

Previous studies have reported that early failure of large diameter MoM THRs did not correlate with acetabular cup orientation [96, 203] but did correlate with head size, with larger heads failing earlier [244]. This is consistent with the wear data reported in this study. Cup orientations, clearance and CPR distance were all found not to correlate with any measure of taper wear. Head radius, however, did. There was no correlation between bearing surface wear and taper wear.

ASR™ XL models suffered greater taper wear than Pinnacle® models, with the ASR™ XL / SROM stem combination in particular producing higher taper wear. Tapers mating with SROM stems had wider internal angles than those mating with Corail stems. Wider angles have been associated with an increase in micromotion at the taper junction [245] which in turn increases the risk of wear.

This centre has recently reported on a series of failed ASR™ XL and Pinnacle® THRs [246]. In that study a “togglng” effect occurring where the trunnion “locks-in” inside the taper was postulated as the primary cause of taper wear. This is consistent with the patterns of wear seen in the present study (figure 5.15), where there is a clear demarcation at the point where the trunnion locks-in. Corrosion has commonly been mentioned in conjunction with wear at the taper junction [203, 234]. Given the wear patterns, and the fact that similar material combinations have been used in smaller bearings with few reported ill-effects [247], it is suggested that this occurs secondary to mechanical wear [246].

High revision rates amongst large diameter MoM THRs have led to calls in the U.K. for them to no longer be implanted [244]. The wear data presented here offers some insights into the mechanisms of wear at the taper junction, and (unlike the bearing surface data which is often model specific) raises concerns that many thousands of prostheses employing similar taper/trunnion interfaces could be at risk.

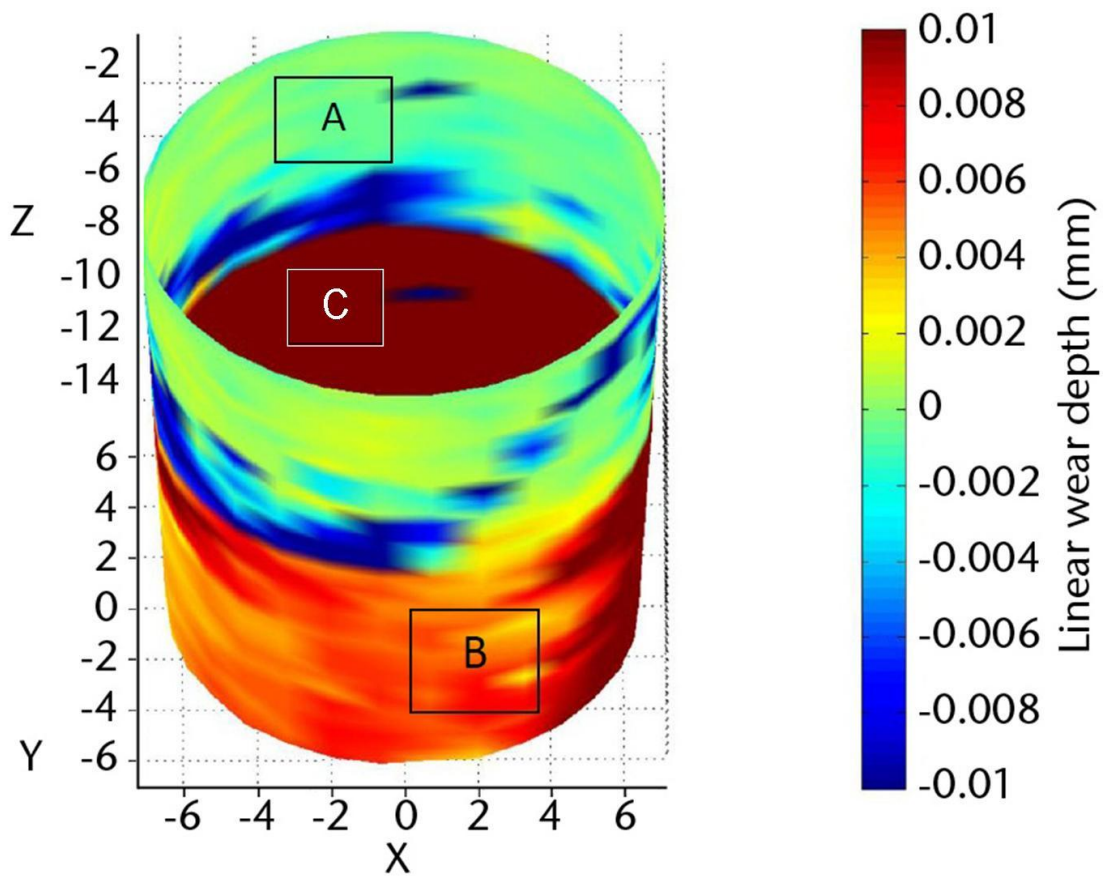


Figure 5.15: Typical image of a worn femoral head internal taper with wear indicated by dark red. There is a clear demarcation at (C) between the unworn area (A) and the worn area (B).

Chapter 6. Conclusions and future work

This chapter will briefly summarise the salient conclusions from the study, as well as provide suggestions for how the work could be taken forward in the future. This thesis has focused on the causes and mechanisms of failure of modern metal-on-metal hip prostheses. The novel measurement techniques described within have allowed for the quantification and classification of the wear of ex vivo prostheses.

This study has involved data from 143 such explants from one of eight contemporary designs. Reports on such large and diverse data sets are rare, and the present data set has allowed for the investigation of several important issues.

6.1 Conclusions

Wear assessment of MoM hip prostheses has proved difficult. Techniques that were effective for older MoP devices are not accurate enough for the lower wearing MoM models [155, 157, 158]. The methodology described in this thesis has proved to be an accurate repeatable method for measuring the wear of ex vivo MoM hip prostheses. Other attempts at achieving this goal in the literature have struggled to achieve satisfactory accuracy levels, even using simulated data sets [185, 189, 190]. The methods described here were validated against established gravimetric methods using real devices. The maximum error recorded was 0.82mm^3 , the overall mean error just 0.28mm^3 . This marks a significant improvement over other methods currently employed.

Wear appears to be a primary cause of failure in a large number of modern MoM hip prostheses. This is reflected in the strong correlation between wear volumes measured in this study and the revision rate of each model (figure 5.1). Not only is adverse reaction to metal debris of increasing concern, evidence has been presented here to suggest that, in the absence of any obvious cause such as surgical notching, femoral neck fracture may also be related to high wear.

It might initially seem reasonable to assume that all MoM hip prostheses would perform to similar standards. This is not the case. There are considerable differences in both the wear rate and revision rate [5-7] of modern MoM hip

prostheses. The models considered in this thesis are relatively new to the market and such patterns of wear and failure rates are still emerging. Given the wide variety of models on the market employing apparently very similar designs, the wide range of results is concerning. Small differences in design and manufacture of hip prostheses can have dramatic effects on their performance and it is unreasonable to suggest that just because one prosthesis is “similar” to another that they will perform to a similar standard. Such discrepancies have been seen before, such as the Capital 3M™ THR whose poor performance in the U.K eventually led to the creation of the NJR, on the recommendation of the Royal College of Surgeons [248] to provide a thorough monitoring tool.

One very important factor from a surgical point of view is the positioning of the acetabular cup. Manufacturers typically recommend very narrow bands for inclination and anteversion angles, often no more than 40° – 45° inclination and 10° – 15° [58] or 15° – 20° anteversion [55, 56]. Radiographic data in this study and others [148, 168, 171] has shown that surgeons struggle to consistently achieve such implantation angles. Even given a comparatively generous range of 45°±10° inclination and 15°±10° anteversion, 66 of the 143 prostheses (46%) in this multi-surgeon study were outside of this range for at least one of inclination or anteversion. Since this study looked only at failed devices, this number is not representative of all hip replacements but it does highlight the difficulty faced in achieving consistently optimal positioning. Steeper angles result in an increased risk of edge loading and higher wear.

Strongly linked to the risk of edge loading is the coverage arc of the acetabular cup [67]. All other factors being equal, a shallower cup will result in a decreased CPR distance. In this study, models with lower coverage arcs tended to be associated with higher wear volumes. Although there were good intentions behind the reduction in coverage arc in some modern designs, the subsequent reduction in CPR distance has led to complications. The 180° coverage arc employed in the Pinnacle® was associated with lower wear.

Although larger diameters have been shown in some studies of hip resurfacings to result in improved survivorship [194-196], large head MoM THRs have performed poorly [96, 203, 244, 246]. In this study, increased bearing diameters

were associated with higher wear. Initially this may seem to counter lubrication theory which states that increased diameters will promote a more favourable lubrication regime [201] which would be expected to reduce wear. However, in the unworn regions diameter correlated with λ -ratios indicating that larger diameter components did indeed promote a more favourable lubrication regime. This correlation was not present in the worn regions indicating a degradation of the lubrication regime over time. If the initial fluid-film or mild mixed lubrication shifts towards boundary contact, larger devices would be expected to produce higher wear as a result of their increased sliding distance. While large diameter resurfacings can perform more successfully than their smaller counterparts, maintaining at least a mild mixed lubrication regime is vital.

Clearance also strongly affects the lubrication regime [201]. Low clearances have been championed in the past as they promote the most beneficial conditions and distribute the contact stresses over a larger area [43]. However, it is important to note that low clearances also increase the size of the contact patch and decrease the CPR distance, as well as increasing the risk of contact between the head and cup if there is any deformation of the components [172, 198, 199]. The wear data in this study highlighted a decreased risk of high wear when radial clearance was in the region of 75 - 100 μ m.

Metal ion concentrations in patients, taken at the time of revision surgery, were found to strongly correlate with prosthesis wear volumes. As such, it is suggested that measurements of these ions taken via blood tests while the prosthesis is still in vivo can be used as a valid surrogate measure of wear and thus performance. The 'safe' level of metal ion concentrations stated in guidance from the MHRA is 7 μ g/ml [138]. Twelve percent of ARMD revisions in this study were necessary when patient ion levels were below this level (median 5.31 μ g/ml Cr). Additionally, ARMD complications have been shown to increase significantly when concentrations reach 5 μ g/ml [147]. Suggesting that further investigation is only necessary when levels reach 7 μ g/ml is false. A maximum of 5 μ g/ml is suggested here although, given that well functioning MoM hips result in levels of around 2 μ g/ml alongside the increased risk ARMD complications at and above 5 μ g/ml, perhaps prompting further investigation at levels of 4 μ g/ml would be more appropriate.

Although low surface roughness values promote better lubrication regimes [196, 201], models with initially low surface roughnesses were not able to maintain them. In addition, models with initially high surface roughness did not necessarily wear more. However, change in roughness over time was linked to the wear volume. In particular, models which were heat-treated following manufacture (the ASR™, Conserve® + and Cormet™) were associated with initially low surface roughness, but a rapid increase in roughness in the worn region as well as higher wear volumes than other models. Only three prostheses showed evidence of self-polishing (all low wear ARMD BHR™). Although it is unclear if this is true of all prostheses or just failures such as those analysed here, even “well functioning” devices retrieved following surgical complications did not show evidence of self-polishing.

Wear at the taper junction can contribute a significant amount of the overall wear volume. Given the high prevalence of ARMD failures amongst the THRs in this study (96% revised following ARMD), taper junction wear can also significantly increase the risk of failure. Consistent with previous studies, femoral head radius was one of the most important factors correlating with taper wear. Additionally, wider femoral taper angles were associated with greater wear depths which have previously been linked with an increase in micromotion and a toggling effect at the taper/trunnion interface [245, 246]. No evidence of corrosion was seen in this study and, given that similar material combinations have been used in smaller bearings with few ill-effects, it is suggested here that corrosion identified in other studies [203, 234, 249] occurs secondary to mechanical wear. Unlike the above factors linked to surface wear (which may pose a risk only in specific models) similar taper/trunnion interfaces are employed in many models of large diameter MoM THRs which could put several times more patients at risk than complications associated with a specific device, such as those associated with the withdrawn ASR™.

6.2 Future work

Despite the positive results achieved in this study, there is much follow-up work that could still be done. By its very nature, this study looked only at prostheses

that had failed. In order to establish a baseline for well-functioning hip prostheses, retrievals following surgical complications were analysed. Such retrievals showed no sign of abnormal wear and so were considered to be functioning normally. Nevertheless, these devices still failed. Ideally, a study of ex vivo prostheses that had not failed would be undertaken to examine the wear rate. This could only be achieved by examining prostheses retrieved from patients who had died from unrelated causes after receiving a MoM hip replacement.

In looking only at retrieved prostheses, this study did not include data from still functioning prostheses implanted as part of the same cohort. Given the wide range of centres involved in sourcing the explants, including this data would involve collating multiple cohorts. Doing so would allow comparison of revision rates to established databases such as the NJR. While wear data would clearly not be available for the still implanted prostheses, it has been shown in sections 4.2.3 and 5.3.6 that measures of metal ion concentrations can be used as surrogate measures. Additionally, comparisons of factors such as implantation angle, diameter and CPR distance could be made between the failed and still functioning groups. Further support would be added to the conclusions of this thesis if the well-functioning prostheses matched the criteria suggested here for minimising wear and extending survivorship.

Examining ex vivo prostheses allows for conclusions to be drawn from devices which have experienced the truest test – time in vivo. However, it also makes it difficult to separate factors of interest from each other, particularly when individual model groups are small. Simulator tests that isolate individual factors could be designed and run to help support or reject the conclusions drawn in this thesis. For example, the effect of clearance could be assessed by manufacturing a number of otherwise identical prostheses which operate with different clearances. According to section 5.3.5, lower wear volumes should be seen for radial clearances in the region of 75 – 100 μ m. Isolating factors in this way would allow for definitive recommendations to be made for future designs of MoM hip prostheses. Such experiments would also allow for the influence of each factor on the wear rate to be quantified and thus the “most important” factors to control could be identified.

This thesis has also highlighted some areas where improvements could be made. It is clear from this multicentre study that surgeons struggle to consistently achieve optimum implantation angles. Work on the design and manufacture of improved instrumentation to ease implantation and orientation could allow for a greater number of patients to receive optimally positioned prostheses, and experience the decreased wear and failure rates associated with this.

The wear rates measured in this study were significantly higher than those expected from simulator tests. Section 5.4 discussed the appropriateness of current testing protocols. Stricter tests, including those carried out at a range of acetabular cup orientations, would allow for an assessment to be made on the risk, and effect, of edge loading occurring for specific models. Patients found to be implanted with orientations associated with a higher risk of edge loading for their model of hip prosthesis could then be given regular follow-up assessments.

Finally, more physiologically relevant test protocols could allow for more realistic assessments of wear rates to be made. Even the prostheses retrieved following surgical complications in this study wore at a rate of $1.12\text{mm}^3/\text{year}$, at the top end of the majority of recent simulator tests (table 2.2). Applying such tests to all new models of hip prosthesis may well identify any design issues long before the prostheses are implanted in patients. Given that patterns of failure may take several years to develop and indentify in vivo, identifying and rectifying potential issues at this pre-implantation stage would help avoid unnecessary, expensive and potentially dangerous revision operations for many thousands of patients.

References

1. Drake, R.L., Vogl, A.W., and Mitchell, A.W.M., (2010). *Gray's Anatomy for Students*. Philadelphia, PA: Churchill Livingstone.: p. 512 - 533.
2. Incavo, S.J., Thompson, M.T., Gold, J.E., Patel, R.V., Icenogle, K.D., and Noble, P.C., *Which Procedure Better Restores Intact Hip Range of Motion: Total Hip Arthroplasty or Resurfacing? A Combined Cadaveric and Computer Simulation Study*. The Journal of Arthroplasty, 2011. **26**(3): p. 391-397.
3. Roaas, A.r. and Andersson, G.B.J., *Normal Range of Motion of the Hip, Knee and Ankle Joints in Male Subjects, 30 - 40 Years of Age*. Acta Orthopaedica, 1982. **53**(2): p. 205-208.
4. Roach, K.E. and Miles, T.P., *Normal Hip and Knee Active Range of Motion: The Relationship to Age*. Physical Therapy, 1991. **71**(9): p. 656-665.
5. NJR, *National Joint Registry Annual Report 2011*. 2011.
6. AOA, *Australian Orthopaedic Association Annual Report*. 2011.
7. Garellick, G., Kärrholm, J., Rogmark, C., and Herberts, P., *Swedish Hip Arthroplasty Register. Annual Report*. 2010.
8. *Osteoarthritis (April 2011)*. In *Arthritis Research UK*. Retrieved July 28, 2011, from http://www.arthritisresearchuk.org/arthritis_information/arthritis_types_syptoms/osteoarthritis.aspx#non.
9. Valdes, A.M., Spector, T.D., Tamm, A., Kisand, K., Doherty, S.A., Dennison, E.M., Mangino, M., Tamm, A., Kerna, I., Hart, D.J., Wheeler, M., Cooper, C., Lories, R.J., Arden, N.K., and Doherty, M., *Genetic variation in the SMAD3 gene is associated with hip and knee osteoarthritis*. Arthritis & Rheumatism, 2011. **62**(8): p. 2347-2352.
10. Holliday, K.L., McWilliams, D.F., Maciewicz, R.A., Muir, K.R., Zhang, W., and Doherty, M., *Lifetime body mass index, other anthropometric measures of obesity and risk of knee or hip osteoarthritis in the GOAL case-control study*. Osteoarthritis and Cartilage, 2011. **19**(1): p. 37-43.
11. Cooper, C., Inskip, H., Croft, P., Campbell, L., Smith, G., McLearn, M., and Coggon, D., *Individual Risk factors for Hip Osteoarthritis: Obesity, Hip Injury and Physical Activity*. American Journal of Epidemiology, 1998. **147**(6): p. 516-522.
12. *Arthritis*. In *NHS Conditions*. Retrieved April 19, 2012, from <http://www.nhs.uk/Conditions/Arthritis/Pages/Introduction.aspx>
13. *Office for National Statistics. Population Estimates for UK, England and Wales, Scotland and Northern Ireland, Population Estimates Timeseries 1971 to Current Year*. 2010.
14. Michaëlsson, K., Byberg, L., Ahlbom, A., Melhus, H.k., and Farahmand, B.Y., *Risk of Severe Knee and Hip Osteoarthritis in Relation to Level of Physical Exercise: A Prospective Cohort Study of Long-Distance Skiers in Sweden*. PLoS ONE, 2011. **6**(3): p. e18339.
15. Biswas, S.V., Iqbal, R., and Knight, S., (2008). *Muscles, Bones and Skin*. London: Mosby.
16. Fishman, P., Bar-Yehuda, S., and Borea, P.A., *Rheumatoid Arthritis: History, Molecular Mechanisms and Therapeutic Applications*. 2010, Springer Netherlands. p. 291-298.
17. Henderson, B., Edwards, J.C.W., and Pettipher, E.R., in *Mechanisms and Models in Rheumatoid Arthritis*. 1995, Academic Press: London. p. 3-24.
18. Kanis, J.A., Melton, L.J., Christiansen, C., Johnston, C.C., and Khaltaev, N., *The diagnosis of osteoporosis*. Journal of Bone and Mineral Research, 1994. **9**(8): p. 1137-1141.

19. Nikolaou, V.S., Efstathopoulos, N., Kontakis, G., Kanakaris, N.K., and Giannoudis, P.V., *The influence of osteoporosis in femoral fracture healing time*. *Injury*, 2009. **40**(6): p. 663-668.
20. Giannoudis, P.V., Furlong, A.J., Macdonald, D.A., and Smith, R.M., *Reamed against unreamed nailing of the femoral diaphysis: a retrospective study of healing time*. *Injury*, 1997. **28**(1): p. 15-18.
21. Edgar, C. and Einhorn, T.A., *Treatment of Avascular Necrosis of the Femoral Head With Drilling and Injection of Concentrated Autologous Bone Marrow*. *Techniques in Orthopaedics*, 2011. **26**(1): p. 2-8
10.1097/BTO.0b013e31820e6528.
22. Mont, M.A., Ragland, P.S., and Etienne, G., *Core Decompression of the Femoral Head for Osteonecrosis Using Percutaneous Multiple Small-Diameter Drilling*. *Clinical Orthopaedics and Related Research*, 2004. **429**: p. 131-138
10.1097/01.blo.0000150128.57777.8e.
23. Koo, K.H., Kim, R., Ko, G.H., Song, H.R., Jeong, S.T., and Cho, S.H., *Preventing collapse in early osteonecrosis of the femoral head. A randomised clinical trial of core decompression*. *J Bone Joint Surg Br*, 1995. **77-B**(6): p. 870-874.
24. Wen, Q., Ma, L., Chen, Y.P., Yang, L., Luo, W., and Wang, X.N., *Treatment of avascular necrosis of the femoral head by hepatocyte growth factor-transgenic bone marrow stromal stem cells*. *Gene Ther*, 2008. **15**(23): p. 1523-1535.
25. Wang, B.-L., Sun, W., Shi, Z.-C., Zhang, N.-F., Yue, D.-B., Guo, W.-S., Xu, S.-Q., Lou, J.-N., and Li, Z.-R., *Treatment of nontraumatic osteonecrosis of the femoral head with the implantation of core decompression and concentrated autologous bone marrow containing mononuclear cells*. *Archives of Orthopaedic and Trauma Surgery*, 2011. **130**(7): p. 859-865.
26. Steinberg, M.E., Larcom, P.G., Strafford, B., Hosick, W.B., Corces, A., Bands, R.E., and Hartman, K.E., *Core Decompression With Bone Grafting for Osteonecrosis of the Femoral Head*. *Clinical Orthopaedics and Related Research*, 2001. **386**: p. 71-78.
27. NJR, *National Joint Registry Annual Report 2010*. 2010.
28. AOA, *Australian Orthopaedic Association Annual Report*. 2010.
29. Bergen, H., *The Norwegian Arthroplasty Register. Annual Report June 2010*. 2010.
30. *American Joint Replacement Registry Project (2011) In American Academy of Orthopaedic Surgeons*. Retrieved July 28, 2011 from <http://www6.aaos.org/news/pemr/JointRegistry/JointRegistry.cfm>.
31. Rang, M., *Anthology of Orthopaedics*. 1966, Churchill Livingstone: Edinburgh, London, New York.
32. Judet, J. and Judet, R., *THE USE OF AN ARTIFICIAL FEMORAL HEAD FOR ARTHROPLASTY OF THE HIP JOINT*. *J Bone Joint Surg Br*, 1950. **32-B**(2): p. 166-173.
33. Thompson, F.R., *Vitallium intramedullary hip prosthesis - preliminary report*. *N.Y. State J Med*, 1952. **52**: p. 3011 - 3020.
34. Wiles, P., *The surgery of the osteo-arthritis hip*. *British Journal of Surgery*, 1958. **45**(193): p. 488-497.
35. Gomez, P.F. and Morcuende, J.A., *Early Attempts at Hip Arthroplasty: 1700s to 1950s*. *Iowa Orthopaedic Journal*, 2005. **25**: p. 25-29.
36. Charnley, J., *ARTHROPLASTY OF THE HIP: A New Operation*. *The Lancet*, 1961. **277**(7187): p. 1129-1132.

37. Obrant, K.J., Ringsberg, K., and Sanz-Ån, L., *Decreased abduction strength after Charnley hip replacement without trochanteric osteotomy*. Acta Orthopaedica, 1989. **60**(3): p. 305-307.
38. McKee, G.K. and Watson-Farrar, J., *REPLACEMENT OF ARTHRITIC HIPs BY THE McKEE-FARRAR PROSTHESIS*. J Bone Joint Surg Br, 1966. **48-B**(2): p. 245-259.
39. *K003523 - 510(k) Premarket Notification - DEPUY PINNACLE METAL-ON-METAL ACETABULAR CUP LINERS (2005)*. Retrieved March 27, 2012 from <http://www.orthopediclaw.com/Pinnacle-Hip-Implant-510k.pdf>.
40. Cuckler, J.M., Moore, K.D., Lombardi Jr, A.V., McPherson, E., and Emerson, R., *Large versus small femoral heads in metal-on-metal total hip arthroplasty*. The Journal of Arthroplasty, 2004. **19**(8, Supplement): p. 41-44.
41. Smith, T.M., Berend, K.R., Lombardi, A.V., Jr., Emerson, R.H., Jr., and Mallory, T.H., *Metal-on-Metal Total Hip Arthroplasty with Large Heads May Prevent Early Dislocation*. Clinical Orthopaedics and Related Research, 2005. **441**: p. 137-142 10.1097/01.bl0.0000193810.23706.73.
42. Matsushita, A., Nakashima, Y., Jingushi, S., Yamamoto, T., Kuraoka, A., and Iwamoto, Y., *Effects of the Femoral Offset and the Head Size on the Safe Range of Motion in Total Hip Arthroplasty*. The Journal of Arthroplasty, 2009. **24**(4): p. 646-651.
43. Dowson, D., *Tribological principles in metal-on-metal hip joint design*. Proceedings of the Institution of Mechanical Engineers, Part H: Journal of Engineering in Medicine, 2006. **220**(2): p. 161-171.
44. Dowson, D., Hardaker, C., Flett, M., and Isaac, G.H., *A hip joint simulator study of the performance of metal-on-metal joints: Part II: Design*. The Journal of Arthroplasty, 2004. **19**(8, Supplement): p. 124-130.
45. Clarke, I.C., Donaldson, T., Bowsher, J.G., Nasser, S., and Takahashi, T., *Current concepts of metal-on-metal hip resurfacing*. The Orthopedic clinics of North America, 2005. **36**(2): p. 143-62, viii.
46. Schmalzried, T.P., Fowble, V.A., Ure, K.J., and Amstutz, H.C., *Metal on Metal Surface Replacement of the Hip: Technique, Fixation, and Early Results*. Clinical Orthopaedics and Related Research, 1996. **329**: p. S106-S114.
47. Quesada, M.J., Marker, D.R., and Mont, M.A., *Metal-on-Metal Hip Resurfacing: Advantages and Disadvantages*. The Journal of Arthroplasty, 2008. **23**(7, Supplement 1): p. 69-73.
48. Macpherson, G. and Breusch, S., *Metal-on-metal hip resurfacing: a critical review*. Archives of Orthopaedic and Trauma Surgery, 2010: p. 1-10.
49. Gore, D.R., Murray, M.P., Gardner, G.M., and Sepic, S.B., *Hip function after total vs. surface replacement*. Acta Orthopaedica, 1985. **56**(5): p. 386-390.
50. Shimmin, A., Beaulé, P.E., and Campbell, P., *Metal-on-Metal Hip Resurfacing Arthroplasty*. J Bone Joint Surg Am, 2008. **90**(3): p. 637-654.
51. Heisel, C., Kleinhans, J., Menge, M., and Kretzer, J., *Ten different hip resurfacing systems: biomechanical analysis of design and material properties*. International Orthopaedics, 2009. **33**(4): p. 939-943.
52. Udofia, I.J. and Jin, Z.M., *Elastohydrodynamic lubrication analysis of metal-on-metal hip-resurfacing prostheses*. Journal of Biomechanics, 2003. **36**(4): p. 537-544.
53. Lewinnek, G.E., Lewis, J.L., Tarr, R., Compere, C.L., and Zimmerman, J.R., *Dislocations after total hip-replacement arthroplasties*. J Bone Joint Surg Am, 1978. **60**(2): p. 217-220.
54. Zimmer, *Durom Hip Resurfacing Surgical Technique*. 2008.
55. DePuy, *ASR™ Surgical Technique*. Cat no: 9998-02-280. 2006.

56. Smith&Nephew., *Birmingham Hip Resurfacing System™ Surgical Technique*. 2007.
57. Wright, *Conserve Plus Total Hip Resurfacing System. Surgical Technique*. 2006.
58. Corin, *Cormet Precision. Surgical Technique*. 2009.
59. Bozic, K.J., Kurtz, S., Lau, E., Ong, K., Chiu, V., Vail, T.P., Rubash, H.E., and Berry, D.J., *The Epidemiology of Bearing Surface Usage in Total Hip Arthroplasty in the United States*. J Bone Joint Surg Am, 2009. **91**(7): p. 1614-1620.
60. Harris, W.H., *Traumatic arthritis of the hip after dislocation and acetabular fractures: treatment by mold arthroplasty. An end-result study using a new method of result evaluation*. J Bone Joint Surg Am, 1969. **51**(4): p. 737-755.
61. Dawson, J., Fitzpatrick, R., Carr, A., and Murray, D., *Questionnaire on the Perceptions of Patients About Total Hip Replacement*. J Bone Joint Surg Br, 1996. **78-B**(2): p. 185-190.
62. Sedrakyan, A., Paxton, E.W., and Marinac-Dabic, D., *Stages and Tools for Multinational Collaboration: The Perspective from the Coordinating Center of the International Consortium of Orthopaedic Registries (ICOR)* J Bone Joint Surg Am, 2011. **9**(Suppl 3).
63. Havelin, L.I., Robertsson, O., Fenstad, A.M., Overgaard, S., Garellick, G., and Furnes, O., *A Scandinavian Experience of Register Collaboration: The Nordic Arthroplasty Register Association (NARA)* J Bone Joint Surg Am, 2011. **93**(Suppl 3).
64. Wroblewski, B.M., Siney, P.D., and Fleming, P.A., *Charnley low-frictional torque arthroplasty: FOLLOW-UP FOR 30 TO 40 YEARS*. J Bone Joint Surg Br, 2009. **91-B**(4): p. 447-450.
65. NICE, *Technology Appraisal Guidance - No. 44. Guidance on the use of metal on metal hip resurfacing arthroplasty*. 2002.
66. Anand, R., Graves, S.E., Steiger, R.N.d., Davidson, D.C., Ryan, P., Miller, L.N., and Cashman, K., *What Is the Benefit of Introducing New Hip and Knee Prostheses?* . J Bone Joint Surg Am, 2011. **9**(Suppl 3).
67. Langton, D.J., Joyce, T.J., Jameson, S.S., Lord, J., Van Orsouw, M., Holland, J.P., Nargol, A.V.F., and De Smet, K.A., *Adverse reaction to metal debris following hip resurfacing: THE INFLUENCE OF COMPONENT TYPE, ORIENTATION AND VOLUMETRIC WEAR*. J Bone Joint Surg Br, 2011. **93-B**(2): p. 164-171.
68. Langton, D.J., Jameson, S.S., Joyce, T.J., Gandhi, J.N., Sidaginamale, R., Mereddy, P., Lord, J., and Nargol, A.V.F., *Accelerating failure rate of the ASR total hip replacement*. J Bone Joint Surg Br, 2011. **93-B**(8): p. 1011-1016.
69. Siebel, T., Maubach, S., and Morlock, M., *Lessons learned from early clinical experience and results of 300 ASR® hip resurfacing implantations*. Proceedings of the Institution of Mechanical Engineers, Part H: Journal of Engineering in Medicine, 2006. **220**(2): p. 345-353.
70. Bergeron, S.G., Desy, N.M., Nikolaou, V.S., Debiparshad, K., and Antoniou, J., *The early results of metal-on-metal hip resurfacing - a prospective study at a minimum two-year follow-up*. Bull NYU Hosp Jt Dis., 2009. **67**(2): p. 132-4.
71. Jameson, S.S., Langton, D.J., and Nargol, A.V.F., *Articular Surface Replacement of the hip: a prospective single-surgeon series*. Journal of Bone & Joint Surgery, British Volume, 2010. **92-B**(1): p. 28-37.
72. Klein, M., Scherger, B., Bernd, H., and Ostermann, P.A., *Complications after hip resurfacing using the ASR prosthesis in patients with osteoarthritis*. Z Orthop Unfall., 2008. **146**(2): p. 179-84.

73. Steiger, R.N.d., Hang, J.R., Miller, L.N., Graves, S.E., and Davidson, D.C., *Five-Year Results of the ASR XL Acetabular System and the ASR Hip Resurfacing System: An Analysis from the Australian Orthopaedic Association National Joint Replacement Registry*. J Bone Joint Surg Am, 2011. **93**(24): p. 2287 - 93.
74. Pollard, T.C.B., Baker, R.P., Eastaugh-Waring, S.J., and Bannister, G.C., *Treatment of the young active patient with osteoarthritis of the hip: A FIVE- TO SEVEN-YEAR COMPARISON OF HYBRID TOTAL HIP ARTHROPLASTY AND METAL-ON-METAL RESURFACING*. J Bone Joint Surg Br, 2006. **88-B**(5): p. 592-600.
75. Steffen, R.T., Pandit, H.P., Palan, J., Beard, D.J., Gundle, R., McLardy-Smith, P., Murray, D.W., and Gill, H.S., *The five-year results of the Birmingham Hip Resurfacing arthroplasty: AN INDEPENDENT SERIES*. J Bone Joint Surg Br, 2008. **90-B**(4): p. 436-441.
76. Treacy, R.B.C., McBryde, C.W., and Pynsent, P.B., *Birmingham hip resurfacing arthroplasty: A minimum follow up of 5 years*. J Bone Joint Surg Br, 2005. **87-B**(2): p. 167-170.
77. Treacy, R.B.C., McBryde, C.W., Shears, E., and Pynsent, P.B., *Birmingham hip resurfacing: A MINIMUM FOLLOW-UP OF TEN YEARS*. J Bone Joint Surg Br, 2011. **93-B**(1): p. 27-33.
78. Carrothers, A.D., Gilbert, R.E., Jaiswal, A., and Richardson, J.B., *Birmingham hip resurfacing: The prevalence of failure*. Journal of Bone & Joint Surgery, British Volume, 2010. **92-B**(10): p. 1344-1350.
79. Khan, M., Kuiper, J.-H., Edwards, D., Robinson, E., and Richardson, J.B., *Birmingham Hip Arthroplasty: Five to Eight Years of Prospective Multicenter Results*. The Journal of Arthroplasty, 2009. **24**(7): p. 1044-1050.
80. Rahman, L., Muirhead-Allwood, S., and Alkinj, M., *What is the Midterm Survivorship and Function After Hip Resurfacing?* Clinical Orthopaedics and Related Research®, 2010. **468**(12): p. 3221-3227.
81. Aulakh, T., Rao, C., Kuiper, J.-H., and Richardson, J., *Hip resurfacing and osteonecrosis: results from an independent hip resurfacing register*. Archives of Orthopaedic and Trauma Surgery, 2010. **130**(7): p. 841-845.
82. De Smet, K., *Belgium experience with metal-on-metal surface arthroplasty*. Orthopedic Clinics of North America, 2005. **36**(2): p. 203-13.
83. Witzleb, W.C., Arnold, M., Krummenauer, F., Knecht, A., Ranisch, H., and Günther, K.P., *Birmingham Hip Resurfacing arthroplasty: short-term clinical and radiographic outcome*. Eur J Med Res., 2008. **13**(1): p. 39 - 46.
84. Amstutz, H. and Le Duff, M., *Eleven years of experience with metal-on-metal hybrid hip resurfacing: a review of 1000 conserve plus*. J Arthroplasty, 2008. **23**(6 Suppl 1): p. 8.
85. Amstutz, H.C., Le Duff, M.J., Campbell, P.A., Gruen, T.A., and Wisk, L.E., *Clinical and Radiographic Results of Metal-on-Metal Hip Resurfacing with a Minimum Ten-Year Follow-up*. J Bone Joint Surg Am, 2010. **92**(16): p. 2663-2671.
86. Beulé, P.E., Shim, P., and Banga, K., *Clinical Experience of Ganz Surgical Dislocation Approach for Metal-on-Metal Hip Resurfacing*. The Journal of Arthroplasty, 2009. **24**(6, Supplement): p. 127-131.
87. Kim, P.R., Beaulé, P.E., Laflamme, G.Y., and Dunbar, M., *Causes of Early Failure in a Multicenter Clinical Trial of Hip Resurfacing*. The Journal of Arthroplasty, 2008. **23**(6, Supplement): p. 44-49.
88. Mont, M.A., Seyler, T.M., Ulrich, S.D., Beaulé, P.E., Boyd, H.S., Grecula, M.J., Goldberg, V.M., Kennedy, W.R., Marker, D.R., Schmalzried, T.P., Sparling,

- E.A., Vail, T.P., and Amstutz, H.C., *Effect of Changing Indications and Techniques on Total Hip Resurfacing*. Clinical Orthopaedics and Related Research, 2007. **465**: p. 63-70 10.1097/BLO.0b013e318159dd60.
89. Killampalli, V.V., Hayes, A., Parsons, N., Costa, M.L., and Prakash, U., *Hip resurfacing using the trochanteric flip osteotomy*. Hip Int., 2009. **19**(2): p. 131-5.
 90. Stulberg, B.N., Trier, K.K., Naughton, M., and Zadzilka, J.D., *Results and lessons learned from a United States hip resurfacing investigational device exemption trial*. J Bone Joint Surg Am 2008. **90**(Suppl 3): p. 21 - 6.
 91. Berton, C., Girard, J., Krantz, N., and Migaud, H., *The Durom Large Diameter Head acetabular component: EARLY RESULTS WITH A LARGE-DIAMETER METAL-ON-METAL BEARING*. J Bone Joint Surg Br, 2010. **92-B**(2): p. 202-208.
 92. Gravius, S., Mumme, T., Weber, O., Berdel, P., and Wirtz, D.C., *Surgical principles and clinical experiences with the DUROM hip resurfacing system using a lateral approach*. Oper Orthop Traumatol., 2009. **21**(6): p. 586 - 601.
 93. Lei, M., Yang, S., Xu, W., Ye, S., Ze, R., and Fan, L., *Metal-on-metal total hip resurfacing arthroplasty for treatment of advanced osteonecrosis of femoral head in young and middle-aged patients*. Zhongguo Xiu Fu Chong Jian Wai Ke Za Zhi., 2010. **24**(3): p. 262-5.
 94. Swank, M.L. and Alkire, M.R., *Minimally invasive hip resurfacing compared to minimally invasive total hip arthroplasty*. Bull NYU Hosp Jt Dis. , 2009. **67**(2): p. 113-5.
 95. Vendittoli, P.A., Ganapathi, M., Roy, A.G., Lusignan, D., and Lavigne, M., *A comparison of clinical results of hip resurfacing arthroplasty and 28 mm metal on metal total hip arthroplasty: a randomised trial with 3-6 years follow-up*. Hip Int., 2010. **20**(1): p. 1 - 13.
 96. Bernthal, N.M., Celestre, P.C., Stavrakis, A.I., Ludington, J.C., and Oakes, D.A., *Disappointing Short-Term Results With the DePuy ASR XL Metal-on-Metal Total Hip Arthroplasty*. The Journal of Arthroplasty, 2012(0).
 97. Engh, C. and Ho, H., *Metal-on-Metal Hip Arthroplasty: Does Early Clinical Outcome Justify the Chance of an Adverse Local Tissue Reaction?* Clinical Orthopaedics and Related Research®, 2009. **468**(2): p. 406-412.
 98. Kindsfater, K.A., Sychterz Terefenko, C.J., Gruen, T.A., and Sherman, C.M., *Minimum 5-Year Results of Modular Metal-On-Metal Total Hip Arthroplasty*. The Journal of Arthroplasty, 2012. **27**(4): p. 545-550.
 99. MHRA, *Medical Device Alert: ASR™ hip replacement implants manufactured by DePuy International Ltd (MDA/2010/069)*. 2010.
 100. FDA. *Class 2 recall Durom cup. 2008 Sept 26. Retrieved on 25 July 2012 from <http://www.accessdata.fda.gov/scripts/cdrh/cfdocs/cfres/res.cfm?id=72744>*.
 101. MHRA, *Metal-on-metal (MoM) total hip replacements: MITCH TRH acetabular cups/MITCH TRH modular heads (Finsbury Orthopaedics) when implanted with uncemented Accolade femoral stems (Stryker Orthopaedics) (MDA/2012/016)*. 2012.
 102. *MITCH TRH Modular Heads Hazard alert. April 12, 2012. Retrieved on July 25, 2012 from <http://www.medsafe.govt.nz/hot/RecallActionNoticesNew/Stryker%20MITCH%20Recall%20notice.pdf>*.
 103. Amstutz, H.C., Le Duff, M.J., Campbell, P.A., and Dorey, F.J., *The Effects of Technique Changes on Aseptic Loosening of the Femoral Component in Hip Resurfacing. Results of 600 Conserve Plus With a 3 to 9 Year Follow-up*. The Journal of Arthroplasty, 2007. **22**(4): p. 481-489.

104. Bozic, K.J. and Ries, M.D., *The impact of infection after total hip arthroplasty on hospital and surgeon resource utilization*. J Bone Joint Surg Am, 2005. **87**(8): p. 6.
105. Ong, K.L., Kurtz, S.M., Lau, E., Bozic, K.J., Berry, D.J., and Parvizi, J., *Prosthetic Joint Infection Risk After Total Hip Arthroplasty in the Medicare Population*. The Journal of Arthroplasty, 2009. **24**(6, Supplement): p. 105-109.
106. Hooper, G.J., Rothwell, A.G., Stringer, M., and Frampton, C., *Revision following cemented and uncemented primary total hip replacement*. Journal of Bone & Joint Surgery, British Volume, 2009. **91-B**(4): p. 451-458.
107. Steffen, R.T., Smith, S.R., Urban, J.P.G., McLardy-Smith, P., Beard, D.J., Gill, H.S., and Murray, D.W., *The effect of hip resurfacing on oxygen concentration in the femoral head*. Journal of Bone & Joint Surgery, British Volume, 2005. **87-B**(11): p. 1468-1474.
108. Khan, A., Yates, P., Lovering, A., Bannister, G.C., and Spencer, R.F., *The effect of surgical approach on blood flow to the femoral head during resurfacing*. Journal of Bone & Joint Surgery, British Volume, 2007. **89-B**(1): p. 21-25.
109. Amarasekera, H.W., Costa, M.L., Foguet, P., Krikler, S.J., Prakash, U., and Griffin, D.R., *The blood flow to the femoral head/neck junction during resurfacing arthroplasty*. Journal of Bone & Joint Surgery, British Volume, 2008. **90-B**(4): p. 442-445.
110. Marker, D.R., Seyler, T.M., Jinnah, R.H., Delanois, R.E., Ulrich, S.D., and Mont, M.A., *Femoral Neck Fractures After Metal-on-Metal Total Hip Resurfacing: A Prospective Cohort Study*. The Journal of Arthroplasty, 2007. **22**(7, Supplement 1): p. 66-71.
111. Shimmin, A.J. and Back, D., *Femoral neck fractures following Birmingham hip resurfacing: A NATIONAL REVIEW OF 50 CASES*. J Bone Joint Surg Br, 2005. **87-B**(4): p. 463-464.
112. Davis, E.T., Olsen, M., Zdero, R., Waddell, J.P., and Schemitsch, E.H., *Femoral neck fracture following hip resurfacing*. Journal of Bone & Joint Surgery, British Volume, 2008. **90-B**(11): p. 1522-1527.
113. Amstutz, H.C., Beaulé, P.E., Dorey, F.J., Le Duff, M.J., Campbell, P.A., and Gruen, T.A., *Metal-on-Metal Hybrid Surface Arthroplasty: Two to Six-Year Follow-up Study*. J Bone Joint Surg Am, 2004. **86**(1): p. 28-39.
114. Beaulé, P.E.M.D., Dorey, F.J.P.H.D., LeDuff, M.M.A., Gruen, T.M.S., and Amstutz, H.C.M.D., *Risk Factors Affecting Outcome of Metal-on-Metal Surface Arthroplasty of the Hip*. SO - Clinical Orthopaedics & Related Research January 2004;418:87-93, 2010.
115. Cossey, A.J., Back, D.L., Shimmin, A., Young, D., and Spriggins, A.J., *The Nonoperative Management of Periprosthetic Fractures Associated With the Birmingham Hip Resurfacing Procedure*. The Journal of Arthroplasty, 2005. **20**(3): p. 358-361.
116. Dowd, J., Sychterz-Terefenko, C., Young, A.M., and Engh Sr, C.A., *Characterization of long-term femoral-head-penetration rates. Association with and prediction of osteolysis*. J Bone Joint Surg Br, 2000. **82**.
117. Orishimo, K.F., Claus, A.M., Sychterz-Terefenko, C., and Engh Sr, C.A., *Relationship between polyethylene wear and osteolysis in hips with a second-generation porous-coated cementless cup after seven years of follow-up*. J Bone Joint Surg Am, 2003. **85**(6).
118. Perez, R.E., Rodriguez, J.A., Deshmukh, R.G., and Ranawat, C.S., *Polyethylene wear and periprosthetic osteolysis in metal-backed acetabular components with cylindrical liners*. The Journal of Arthroplasty, 1998. **13**(1): p. 1-7.

119. Sochart, D.H., *Relationship of acetabular wear to osteolysis and loosening in total hip arthroplasty*. Clinical Orthopaedics and Related Research, 1999. **1**(363).
120. Zhu, Y.H., Chiu, K.Y., and Tang, W.M., *Polyethylene wear and osteolysis in total hip arthroplasty*. J Ortho Surg, 2001. **9**(1).
121. Amstutz, H., Campbell, P., Kossovsky, N., and Clarke, I.C., *Mechanism and clinical significance of wear debris-induced osteolysis*. Clinical Orthopaedics and Related Research, 1992. **276**(1).
122. Ingham, E. and Fisher, J., *The role of macrophages in osteolysis of total joint replacement*. Biomaterials, 2005. **26**(11): p. 1271-1286.
123. Tipper, J.L., Ingham, E., Hailey, J.L., Besong, A.A., Fisher, J., Wroblewski, B.M., and Stone, M.H., *Quantitative analysis of polyethylene wear debris, wear rate and head damage in retrieved Charnley hip prostheses*. Journal of Materials Science: Materials in Medicine, 2000. **11**(2): p. 117-124.
124. Jasty, M., Bragdon, C., Jiranek, W., Chandler, H., Maloney, W., and Harris, W.H., *Etiology of osteolysis around porous-coated cementless total hip arthroplasties*. Clinical Orthopaedics and Related Research, 1994(308): p. 111-26.
125. Minoda, Y., Kobayashi, A., Sakawa, A., Aihara, M., Tada, K., Sugama, R., Iwakiri, K., Ohashi, H., and Takaoka, K., *Wear particle analysis of highly crosslinked polyethylene isolated from a failed total hip arthroplasty*. Journal of Biomedical Materials Research Part B: Applied Biomaterials, 2008. **86B**(2): p. 501-505.
126. Richards, L., Brown, C., Stone, M.H., Fisher, J., Ingham, E., and Tipper, J.L., *Identification of nanometre-sized ultra-high molecular weight polyethylene wear particles in samples retrieved in vivo*. J Bone Joint Surg Br, 2008. **90-B**(8): p. 1106-1113.
127. Unsworth, A., *Tribology of artificial hip joints*. Proceedings of the Institution of Mechanical Engineers, Part J: Journal of Engineering Tribology, 2006. **220**(8): p. 711-718.
128. Firkins, P.J., Tipper, J.L., Saadatzadeh, M.R., Ingham, E., Stone, M.H., Farrar, R., and Fisher, J., *Quantitative analysis of wear and wear debris from metal-on-metal hip prostheses tested in a physiological hip joint simulator*. Bio-Medical Materials and Engineering, 2001. **11**(2): p. 143-157.
129. Brown, C., Fisher, J., and Ingham, E., *Biological effects of clinically relevant wear particles from metal-on-metal hip prostheses*. Proceedings of the Institution of Mechanical Engineers, Part H: Journal of Engineering in Medicine, 2006. **220**(2): p. 355-369.
130. Girard, J., Bocquet, D., Autissier, G., Fouilleron, N., Fron, D., and Migaud, H., *Metal-on-Metal Hip Arthroplasty in Patients Thirty Years of Age or Younger*. J Bone Joint Surg Am, 2010. **92**(14): p. 2419-2426.
131. Sieber, H.P., Rieker, C.B., and Kottig, P., *Analysis of 118 second-generation metal-on-metal retrieved hip implants*. J Bone Joint Surg Br, 1999. **81-B**(1): p. 46-50.
132. Willert, H.-G., Buchhorn, G.H., Fayyazi, A., Flury, R., Windler, M., Koster, G., and Lohmann, C.H., *Metal-on-Metal Bearings and Hypersensitivity in Patients with Artificial Hip Joints. A Clinical and Histomorphological Study*. J Bone Joint Surg Am, 2005. **87**(1): p. 28-36.
133. Doorn, P.F., Campbell, P.A., Worrall, J., Benya, P.D., McKellop, H.A., and Amstutz, H.C., *Metal wear particle characterization from metal on metal total hip replacements: Transmission electron microscopy study of periprosthetic tissues and isolated particles*. Journal of Biomedical Materials Research, 1998. **42**(1): p. 103-111.

134. Campbell, P., Ma, S., Schmalzried, T., and Amstutz, H.C., *Tissue digestion for wear debris particle isolation*. Journal of Biomedical Materials Research, 1994. **28**(4): p. 523-526.
135. Shanbhag, A.S., Jacobs, J.J., Black, J., Galante, J.O., and Glant, T.T., *Macrophage/particle interactions: Effect of size, composition and surface area*. Journal of Biomedical Materials Research, 1994. **28**(1): p. 81-90.
136. McKellop, H.A., Campbell, P., Park, S.H., Schmalzried, T.P., Grigoris, P., Amstutz, H.C., and Sarmiento, A., *The origin of submicron polyethylene wear debris in total hip arthroplasty*. Clinical Orthopaedics and Related Research, 1995(311): p. 3-20.
137. Back, D.L.F.E.D., Young, D.A.F., and Shimmin, A.J.F., *How Do Serum Cobalt and Chromium Levels Change after Metal-on-Metal Hip Resurfacing? [Article]*. SO - Clinical Orthopaedics & Related Research September 2005;438:177-181, 2005.
138. MHRA, *Medical Device Alert: All metal-on-metal (MoM) hip replacements (MDA/2012/008)* 2012.
139. Clarke, M.T., Lee, P.T.H., Arora, A., and Villar, R.N., *Levels of metal ions after small- and large-diameter metal-on-metal hip arthroplasty*. J Bone Joint Surg Br, 2003. **85-B**(6): p. 913-917.
140. Daniel, J., Ziaee, H., Pradhan, C., Pynsent, P.B., and McMinn, D.J.W., *Blood and urine metal ion levels in young and active patients after Birmingham hip resurfacing arthroplasty*. Journal of Bone & Joint Surgery, British Volume, 2007. **89-B**(2): p. 169-173.
141. Versieck, J. and Cornelis, R., *Normal levels of trace elements in human blood plasma or serum*. Analytica Chimica Acta, 1980. **116**(2): p. 217-254.
142. Antoniou, J., Zukor, D.J., Mwale, F., Minarik, W., Petit, A., and Huk, O., *Metal Ion Levels in the Blood of Patients After Hip Resurfacing: A Comparison Between Twenty-eight and Thirty-six-Millimeter-Head Metal-on-Metal Prostheses*. J Bone Joint Surg Am, 2008. **90**(Suppl 3).
143. Langton, D.J., Joyce, T.J., Mangat, N., Lord, J., Van Orsouw, M., Smet, K.D., and Nargol, A.V.F., *Reducing Metal Ion Release Following Hip Resurfacing Arthroplasty*. The Orthopedic clinics of North America, 2011. **42**(2): p. 169-180.
144. Daniel, J., Holland, J.P., Quigley, L., Sprague, S., and Bhandari, M., *Pseudotumors associated with total hip arthroplasty*. J Bone Joint Surg Am, 2012. **94**(1): p. 86-93.
145. Pandit, H., Glyn-Jones, S., McLardy-Smith, P., Gundle, R., Whitwell, D., Gibbons, C.L.M., Ostlere, S., Athanasou, N., Gill, H.S., and Murray, D.W., *Pseudotumours associated with metal-on-metal hip resurfacings*. J Bone Joint Surg Br, 2008. **90-B**(7): p. 847-851.
146. Kwon, Y.-M., Thomas, P., Summer, B., Pandit, H., Taylor, A., Beard, D., Murray, D.W., and Gill, H.S., *Lymphocyte proliferation responses in patients with pseudotumors following metal-on-metal hip resurfacing arthroplasty*. Journal of Orthopaedic Research, 2010. **28**(4): p. 444-450.
147. Bosker, B.H., Ettema, H.B., Boomsma, M.F., Kollen, B.J., Maas, M., and Verheyen, C.C.P.M., *High incidence of pseudotumour formation after large-diameter metal-on-metal total hip replacement*. Journal of Bone & Joint Surgery, British Volume, 2012. **94-B**(6): p. 755-761.
148. Ollivere, B., Darrah, C., Barker, T., Nolan, J., and Porteous, M.J., *Early clinical failure of the Birmingham metal-on-metal hip resurfacing is associated with metallosis and soft-tissue necrosis*. J Bone Joint Surg Br, 2009. **91-B**(8): p. 1025-1030.

149. Langton, D.J., Jameson, S.S., Joyce, T.J., Hallab, N.J., Natsu, S., and Nargol, A.V.F., *Early failure of metal-on-metal bearings in hip resurfacing and large-diameter total hip replacement: A CONSEQUENCE OF EXCESS WEAR*. J Bone Joint Surg Br, 2010. **92-B**(1): p. 38-46.
150. Korovessis, P., Petsinis, G., Repanti, M., and Repantis, T., *Metallosis after contemporary metal-on-metal total hip arthroplasty. Five to nine-year follow-up*. J Bone Joint Surg Am, 2006. **88**(6): p. 1183-91.
151. Haddad, F.S., Thakrar, R.R., Hart, A.J., Skinner, J.A., Nargol, A.V.F., Nolan, J.F., Gill, H.S., Murray, D.W., Blom, A.W., and Case, C.P., *Metal-on-metal bearings*. Journal of Bone & Joint Surgery, British Volume, 2011. **93-B**(5): p. 572-579.
152. McKellop, H.P., Park, S.-H.P., Chiesa, R.M.S., Doorn, P.M.D., Lu, B.M.S., Normand, P.B.S., Grigoris, P.M.D.P., and Amstutz, H.M.D., *In Vivo Wear of 3 Types of Metal on Metal Hip Prostheses During 2 Decades of Use*. Clinical Orthopaedics & Related Research Metal on Metal Hip Protheses: Past Performance and Future Directions, 1996. **329**(Supplement): p. S128-S140.
153. Barrack, R.L., Lavernia, C., Szuszczewicz, E.S., and Sawhney, J., *Radiographic wear measurements in a cementless metal-backed modular cobalt-chromium acetabular component*. The Journal of Arthroplasty, 2001. **16**(7): p. 820-828.
154. Wu, J.S.-S., Hsu, S.-L., and Chen, J.-H., *Wear patterns of, and wear volume formulae for, hemispherical acetabular cup liners*. Wear, 2009. **268**(3-4): p. 481-487.
155. Wu, J., Hsu, S.-L., and Chen, J.-H., *Evaluating the accuracy of wear formulae for acetabular cup liners*. Medical and Biological Engineering and Computing, 2009. **48**(2): p. 157-165.
156. Ilchmann, T., Reimold, M., and Müller-Schauenburg, W., *Estimation of the wear volume after total hip replacement: A simple access to geometrical concepts*. Medical Engineering & Physics, 2008. **30**(3): p. 373-379.
157. Mizoue, T., Yamamoto, K., Masaoka, T., Imakiire, A., Akagi, M., and Clarke, I.C., *Validation of acetabular cup wear volume based on direct and two-dimensional measurements: hip simulator analysis*. Journal of Orthopaedic Science, 2003. **8**(4): p. 491-499.
158. Charles, R.B., Henrik, M., Xunhua, Y., Rebecca, P., Johan, K., Niclas, B., Daniel, M.E., and William, H.H., *Experimental assessment of precision and accuracy of radiostereometric analysis for the determination of polyethylene wear in a total hip replacement model*. Journal of Orthopaedic Research, 2002. **20**(4): p. 688-695.
159. Bowsher, J.G., Clarke, I.C., Williams, P.A., and Donaldson, T.K., *What is a "Normal" wear pattern for metal-on-metal hip bearings?* Journal of Biomedical Materials Research Part B: Applied Biomaterials, 2009. **91B**(1): p. 297-308.
160. Angadji, A., Royle, M., Collins, S.N., and Shelton, J.C., *Influence of cup orientation on the wear performance of metal-on-metal hip replacements*. Proceedings of the Institution of Mechanical Engineers, Part H: Journal of Engineering in Medicine, 2009. **223**(4): p. 449-457.
161. Heisel, C., Streich, N., Krachler, M., Jakubowitz, E., and Kretzer, J.P., *Characterization of the Running-in Period in Total Hip Resurfacing Arthroplasty: An in Vivo and in Vitro Metal Ion Analysis*. J Bone Joint Surg Am, 2008. **90**(Supplement_3): p. 125-133.
162. Lee, R., Essner, A., and Wang, A., *Tribological Considerations in Primary and Revision Metal-on-Metal Arthroplasty*. J Bone Joint Surg Am, 2008. **90**(Supplement_3): p. 118-124.

163. Vassiliou, K., D Elfick, A., Scholes, S., and Unsworth, A., *The effect of 'running-in' on the tribology and surface morphology of metal-on-metal Birmingham hip resurfacing device in simulator studies*. Proceedings of the Institution of Mechanical Engineers, Part H: Journal of Engineering in Medicine, 2006. **220**(2): p. 269-277.
164. Bowsher, J.G. and Shelton, J.C., *A hip simulator study of the influence of patient activity level on the wear of crosslinked polyethylene under smooth and roughened femoral conditions*. Wear, 2001. **250**(1-12): p. 167-179.
165. Ries, M.D., Scott, M.L., and Jani, S., *Relationship Between Gravimetric Wear and Particle Generation in Hip Simulators: Conventional Compared with Cross-Linked Polyethylene*. J Bone Joint Surg Am, 2001. **83**(2_suppl_2): p. S116-122.
166. Tipper, J.L., Firkins, P.J., Ingham, E., Fisher, J., Stone, M.H., and Farrar, R., *Quantitative analysis of the wear and wear debris from low and high carbon content cobalt chrome alloys used in metal on metal total hip replacements*. Journal of Materials Science: Materials in Medicine, 1999. **10**(6): p. 353-362.
167. Kamali, A., Hussain, A., Li, C., Pamu, J., Daniel, J., Ziaee, H., and McMinn, D.J.W., *Tribological performance of various CoCr microstructures in metal-on-metal bearings: THE DEVELOPMENT OF A MORE PHYSIOLOGICAL PROTOCOL IN VITRO*. J Bone Joint Surg Br, 2010. **92-B**(5): p. 717-725.
168. De Haan, R., Pattyn, C., Gill, H.S., Murray, D.W., Campbell, P.A., and De Smet, K., *Correlation between inclination of the acetabular component and metal ion levels in metal-on-metal hip resurfacing replacement*. J Bone Joint Surg Br, 2008. **90-B**(10): p. 1291-1297.
169. Hart, A.J., Sabah, S., Henckel, J., Lewis, A., Cobb, J., Sampson, B., Mitchell, A., and Skinner, J.A., *The painful metal-on-metal hip resurfacing*. J Bone Joint Surg Br, 2009. **91-B**(6): p. 738-744.
170. Langton, D.J., Jameson, S.S., Joyce, T.J., Webb, J., and Nargol, A.V.F., *The effect of component size and orientation on the concentrations of metal ions after resurfacing arthroplasty of the hip*. J Bone Joint Surg Br, 2008. **90-B**(9): p. 1143-1151.
171. Langton, D.J., Sprowson, A.P., Joyce, T.J., Reed, M., Carluke, I., Partington, P., and Nargol, A.V.F., *Blood metal ion concentrations after hip resurfacing arthroplasty: A comparative study of articular surface replacement and Birmingham Hip resurfacing arthroplasties*. J Bone Joint Surg Br, 2009. **91-B**(10): p. 1287-1295.
172. Morlock, M.M., Bishop, N., Zustin, J., Hahn, M., Ruther, W., and Amling, M., *Modes of Implant Failure After Hip Resurfacing: Morphological and Wear Analysis of 267 Retrieval Specimens*. J Bone Joint Surg Am, 2008. **90**(Supplement_3): p. 89-95.
173. Smith, S., Dowson, D., and Goldsmith, A., *The effect of femoral head diameter upon lubrication and wear of metal-on-metal total hip replacements*. Proceedings of the Institution of Mechanical Engineers, Part H: Journal of Engineering in Medicine, 2001. **215**(2): p. 161-170.
174. Williams, S., Leslie, I., Isaac, G., Jin, Z., Ingham, E., and Fisher, J., *Tribology and Wear of Metal-on-Metal Hip Prostheses: Influence of Cup Angle and Head Position*. J Bone Joint Surg Am, 2008. **90**(Supplement_3): p. 111-117.
175. Firkins, P., Tipper, J., Ingham, E., Stone, M., Farrar, R., and Fisher, J., *Influence of simulator kinematics on the wear of metal-on-metal hip prostheses*. Proceedings of the Institution of Mechanical Engineers, Part H: Journal of Engineering in Medicine, 2001. **215**(1): p. 119-121.

176. Fisher, J., Hu, X., Tipper, J., Stewart, T., Williams, S., Stone, M., Davies, C., Hatto, P., Bolton, J., Riley, M., Hardaker, C., Isaac, G., Berry, G., and Ingham, E., *An in vitro study of the reduction in wear of metal-on-metal hip prostheses using surface-engineered femoral heads*. Proceedings of the Institution of Mechanical Engineers, Part H: Journal of Engineering in Medicine, 2002. **216**(4): p. 219-230.
177. Ishida, T., Clarke, I.C., Donaldson, T.K., Shirasu, H., Shishido, T., and Yamamoto, K., *Comparing ceramic-metal to metal-metal total hip replacements—A simulator study of metal wear and ion release in 32- and 38-mm bearings*. Journal of Biomedical Materials Research Part B: Applied Biomaterials, 2009. **91B**(2): p. 887-896.
178. Goldsmith, A., Dowson, D., Isaac, G., and Lancaster, J., *A comparative joint simulator study of the wear of metal-on-metal and alternative material combinations in hip replacements*. Proceedings of the Institution of Mechanical Engineers, Part H: Journal of Engineering in Medicine, 2000. **214**(1): p. 39-47.
179. Dowson, D., Hardaker, C., Flett, M., and Isaac, G.H., *A hip joint simulator study of the performance of metal-on-metal joints: Part I: The role of materials*. The Journal of Arthroplasty, 2004. **19**(8, Supplement): p. 118-123.
180. Li, C.X., Hussain, A., and Kamali, A., *A hip simulator study of metal-on-metal hip joint device using acetabular cups with different fixation surface conditions*. Proceedings of the Institution of Mechanical Engineers, Part H: Journal of Engineering in Medicine, 2011. **225**(9): p. 877-887.
181. Kothari, M., Bartel, D.L., and Booker, J.F., *Surface Geometry of Retrieved McKee-Farrar Total Hip Replacements*. Clinical Orthopaedics and Related Research, 1996. **329**: p. S141-S147.
182. *ISO 10360-7:2011. Geometrical product specifications (GPS) -- Acceptance and reverification tests for coordinate measuring machines (CMM) -- Part 7: CMMs equipped with imaging probing systems*.
183. Becker, A., Schollhorn, K., Dirix, Y., and Schmotzer, H., *Metal-on-metal bearings. I. the influence of 3D measurement accuracy on the calculated wear of a ball head using a new mathematical approach*. Proceedings of the 52nd Annual Meeting of the Orthopaedic Research Society, Paper No, 0505, Chicago, 2006.
184. Becker, A. and Dirix, Y., *WEAR MEASUREMENTS ON RETRIEVED METAL-ON-METAL BEARINGS: A HIGH ACCURACY 3D MEASUREMENT APPROACH*. Proceedings of the 55th Annual Meeting of the Orthopaedic Research Society, Poster No 2270, 2009.
185. Morlock, M., Bishop, N., R  ther, W., Delling, G., and Hahn, M., *Biomechanical, morphological, and histological analysis of early failures in hip resurfacing arthroplasty*. Proceedings of the Institution of Mechanical Engineers, Part H: Journal of Engineering in Medicine, 2006. **220**(2): p. 333-344.
186. Bills, P., Blunt, L., and Jiang, X., *Development of a technique for accurately determining clinical wear in explanted total hip replacements*. Wear, 2007. **263**(7-12): p. 1133-1137.
187. Witzleb, W.-C., Hanisch, U., Ziegler, J., and Guenther, K.-P., *In Vivo Wear Rate of the Birmingham Hip Resurfacing Arthroplasty: A Review of 10 Retrieved Components*. The Journal of arthroplasty, 2009. **24**(6): p. 951-956.
188. Morris, B., Zou, L., Royle, M., Simpson, D., and Shelton, J.C., *Quantifying the wear of acetabular cups using coordinate metrology*. Wear, 2011. **271**(7-8): p. 1086-1092.

189. Carmignato, S., Spinelli, M., Affatato, S., and Savio, E., *Uncertainty evaluation of volumetric wear assessment from coordinate measurements of ceramic hip joint prostheses*. *Wear*, 2011. **270**(9-10): p. 584-590.
190. Bills, P.J., Racasan, R., Underwood, R.J., Cann, P., Skinner, J., Hart, A.J., Jiang, X., and Blunt, L., *Volumetric wear assessment of retrieved metal-on-metal hip prostheses and the impact of measurement uncertainty*. *Wear*, 2012. **274-275**(0): p. 212-219.
191. Ong, K., Lau, E., Suggs, J., Kurtz, S., and Manley, M., *Risk of Subsequent Revision after Primary and Revision Total Joint Arthroplasty*. *Clinical Orthopaedics and Related Research*®, 2010. **468**(11): p. 3070-3076.
192. Amstutz, H.C., Wisk, L.E., and Le Duff, M.J., *Sex as a Patient Selection Criterion for Metal-on-Metal Hip Resurfacing Arthroplasty*. *The Journal of Arthroplasty*, 2010. **26**(2): p. 198-208.
193. Nunley, R., Della Valle, C., and Barrack, R., *Is Patient Selection Important for Hip Resurfacing?* *Clinical Orthopaedics and Related Research*®, 2009. **467**(1): p. 56-65.
194. Dowson, D. and Jin, Z.M., *Metal-on-metal hip joint tribology*. *Proceedings of the Institution of Mechanical Engineers, Part H: Journal of Engineering in Medicine*, 2006. **220**(2): p. 107-118.
195. Chan, F.W., Bobyn, J.D., Medley, J.B., Krygier, J.J., and Tanzer, M., *Wear and Lubrication of Metal-on-Metal Hip Implants*. *Clinical Orthopaedics and Related Research*, 1999. **369**: p. 10-24.
196. Joyce, T.J., Langton, D.J., Jameson, S.S., and Nargol, A.V.F., *Tribological analysis of failed resurfacing hip prostheses and comparison with clinical data*. *Proceedings of the Institution of Mechanical Engineers, Part J: Journal of Engineering Tribology*, 2009. **223**(3): p. 317-323.
197. Underwood, R., Matthies, A., Cann, P., Skinner, J.A., and Hart, A.J., *A comparison of explanted Articular Surface Replacement and Birmingham Hip Resurfacing components*. *Journal of Bone & Joint Surgery, British Volume*, 2012. **93-B**(9): p. 1169-1177.
198. Underwood, R.J., Zografos, A., Sayles, R.S., Hart, A., and Cann, P., *Edge loading in metal-on-metal hips: low clearance is a new risk factor*. *Proceedings of the Institution of Mechanical Engineers, Part H: Journal of Engineering in Medicine*, 2012. **226**(3): p. 217-226.
199. Jin, Z., Meakins, S., Morlock, M., Parsons, P., Hardaker, C., Flett, M., and Isaac, G., *Deformation of press-fitted metallic resurfacing cups. Part 1: experimental simulation*. *Proceedings of the Institution of Mechanical Engineers, Part H: Journal of Engineering in Medicine*, 2006. **220**(2): p. 299-309.
200. Unsworth, A., Vassiliou, K., Elfick, A.P.D., Scholes, S., McMinn, D.J.W., and Band, T.J., *Fluid-film lubrication of metal-on-metal hip joints - fact or fiction*. *The International Society for Technology and Arthroplasty Meeting, San Francisco, California, USA, 24-27 September 2003*.
201. Hamrock, B.J. and Dowson, D., *Elastohydrodynamic lubrication of elliptical contacts for materials of low elastic modulus. 1: Fully flooded conjunction*. *Transactions of the ASME. J. Lubr. Technol.*, 1978. **100**: p. 236-245.
202. Johnson, K.L., Greenwood, J.A., and Poon, S.Y., *A simple theory of asperity contact in elastohydro-dynamic lubrication*. *Wear*, 1972. **19**(1): p. 91-108.
203. Bolland, B.J.R.F., Culliford, D.J., Langton, D.J., Millington, J.P.S., Arden, N.K., and Latham, J.M., *High failure rates with a large-diameter hybrid metal-on-metal total hip replacement*. *Journal of Bone & Joint Surgery, British Volume*, 2011. **93-B**(5): p. 608-615.

204. Archard, J.F. and Hirst, W., *The Wear of Metals under Unlubricated Conditions*. Proceedings of the Royal Society of London. Series A. Mathematical and Physical Sciences, 1956. **236**(1206): p. 397-410.
205. De Smet, K., De Haan, R., Calistri, A., Campbell, P.A., Ebramzadeh, E., Pattyn, C., and Gill, H.S., *Metal Ion Measurement as a Diagnostic Tool to Identify Problems with Metal-on-Metal Hip Resurfacing*. J Bone Joint Surg Am, 2008. **90**(Supplement_4): p. 202-208.
206. Berry, D.J., *Periprosthetic fractures associated with osteolysis: A problem on the rise*. The Journal of Arthroplasty, 2003. **18**(3, Supplement 1): p. 107-111.
207. Schmalzried, T.P., Kwong, L.M., Jasty, M., Sedlacek, R.C., Haire, T.C., O'Connor, D.O., Bragdon, C.R., Kabo, J.M., Malcolm, A.J., and Harris, W.H., *The Mechanism of Loosening of Cemented Acetabular Components in Total Hip Arthroplasty: Analysis of Specimens Retrieved at Autopsy*. Clinical Orthopaedics and Related Research, 1992. **274**: p. 60-78.
208. Landgraeber, S., von Knoch, M., LÄ¶er, F., Wegner, A., Tsokos, M., HuÄŸmann, B.r., and Totsch, M., *Extrinsic and intrinsic pathways of apoptosis in aseptic loosening after total hip replacement*. Biomaterials, 2008. **29**(24 - 25): p. 3444-3450.
209. Langton, D.J., Sprowson, A.P., Mahadeva, D., Bhatnagar, S., Holland, J.P., and Nargol, A.V.F., *Cup Anteversion in Hip Resurfacing: Validation of EBRA and the Presentation of a Simple Clinical Grading System*. The Journal of Arthroplasty. **25**(4): p. 607-613.
210. MacDonald, S.J., Brodner, W., and Jacobs, J.J., *A consensus paper on metal ions in metal-on-metal hip arthroplasties*. The Journal of Arthroplasty, 2004. **19**(8, Supplement): p. 12-16.
211. Lord, J.K., Langton, D.J., Nargol, A.V.F., and Joyce, T.J., *Volumetric wear assessment of failed metal-on-metal hip resurfacing prostheses*. Wear, 2011. **272**(1): p. 79-87.
212. Wu, J., Hsu, S.-L., and Chen, J.-H., *Evaluating the accuracy of wear formulae for acetabular cup liners*. Medical and Biological Engineering and Computing, 2009.
213. Coolidge, J.L., *A Historically Interesting Formula for the Area of a Quadrilateral*. The American Mathematical Monthly, 1939. **46**(6): p. 345-347.
214. Allen, M.J., Myer, B.J., Millett, P.J., and Rushton, N., *The Effects of Particulate Cobalt, Chromium and Cobalt-Chromium Alloy on Human Osteoblast-Like Cells In Vitro*. J Bone Joint Surg Br, 1997. **79-B**(3): p. 475-482.
215. Mokhbat, E.A. and Hahn, D.W., *Laser-Induced Breakdown Spectroscopy for the Analysis of CobaltChromium Orthopaedic Wear Debris Particles*. Applied Spectroscopy, 2002. **56**: p. 984-993.
216. *ZYGO NewView 5000 Product Brochure (1998)*. Retrieved April 16, 2012 from <http://www.lambdaphoto.co.uk/pdfs/nv5000en1.pdf>.
217. Mathew, M.T., Runa, M.J., Laurent, M., Jacobs, J.J., Rocha, L.A., and Wimmer, M.A., *Tribocorrosion behavior of CoCrMo alloy for hip prosthesis as a function of loads: A comparison between two testing systems*. Wear, 2011. **271**(9 - 10): p. 1210-1219.
218. Flanagan, S., Jones, E., and Birkinshaw, C., *In vitro friction and lubrication of large bearing hip prostheses*. Proceedings of the Institution of Mechanical Engineers, Part H: Journal of Engineering in Medicine, 2010. **224**(7): p. 853-864.
219. Sariali, E., Stewart, T., Mamoudy, P., Jin, Z., and Fisher, J., *Undetected Fracture of an Alumina Ceramic on Ceramic Hip Prosthesis*. The Journal of Arthroplasty. **25**(4): p. 658.e1-658.e5.

220. Oliveira, A.L.L., Lima, R.G., Cueva, E.G., and Queiroz, R.D., *Comparative analysis of surface wear from total hip prostheses tested on a mechanical simulator according to standards ISO 14242-1 and ISO 14242-3*. *Wear*. **271**(9-10): p. 2340-2345.
221. Leslie, I.J., Williams, S., Brown, C., Anderson, J., Isaac, G., Hatto, P., Ingham, E., and Fisher, J., *Surface engineering: A low wearing solution for metal-on-metal hip surface replacements*. *Journal of Biomedical Materials Research Part B: Applied Biomaterials*, 2009. **90B**(2): p. 558-565.
222. Gadelmawla, E.S., Koura, M.M., Maksoud, T.M.A., Elewa, I.M., and Soliman, H.H., *Roughness parameters*. *Journal of Materials Processing Technology*, 2002. **123**(1): p. 133-145.
223. Wang, A., Essner, A., and Klein, R., *Effect of contact stress on friction and wear of ultra-high molecular weight polyethylene in total hip replacement*. *Proceedings of the Institution of Mechanical Engineers, Part H: Journal of Engineering in Medicine*, 2001. **215**(2): p. 133-139.
224. Jin, Z.M., Stone, M., Ingham, E., and Fisher, J., (v) *Biotribology*. *Current Orthopaedics*, 2006. **20**(1): p. 32-40.
225. Patel, A.B., Wagle, R.R., Usrey, M.M., Thompson, M.T., Incavo, S.J., and Noble, P.C., *Guidelines for Implant Placement to Minimize Impingement During Activities of Daily Living After Total Hip Arthroplasty*. *The Journal of Arthroplasty*, 2010. **25**(8): p. 1275-1281.e1.
226. Barbour, P., Stone, M., and Fisher, J., *A hip joint simulator study using simplified loading and motion cycles generating physiological wear paths and rates*. *Proceedings of the Institution of Mechanical Engineers, Part H: Journal of Engineering in Medicine*, 1999. **213**(6): p. 455-467.
227. Dieter, C., Erwin, C., Oliver, P.G., and Luis, F., *Metal is not inert: Role of metal ions released by biocorrosion in aseptic loosening - Current concepts*. *Journal of Biomedical Materials Research Part A*, 2009. **91A**(4): p. 1252-1262.
228. Reinisch, G., Judmann, K.P., Lhotka, C., Lintner, F., and Zweymüller, K.A., *Retrieval study of uncemented metal-metal hip prostheses revised for early loosening*. *Biomaterials*, 2003. **24**(6): p. 1081-1091.
229. Jacobs, J.J. and Hallab, N.J., *Loosening and Osteolysis Associated with Metal-on-Metal Bearings: A Local Effect of Metal Hypersensitivity?*. *J Bone Joint Surg Am*, 2006. **88**(6): p. 1171-2.
230. Reinisch, G., Judmann, K.P., Lhotka, C., Lintner, F., and Zweymüller, K.A., *Retrieval study of uncemented metal-metal hip prostheses revised for early loosening*. *Biomaterials*, 2003. **24**(6): p. 1081-1091.
231. Griffin, W., Nanson, C., Springer, B., Davies, M., and Fehring, T., *Reduced Articular Surface of One-piece Cups: A Cause of Runaway Wear and Early Failure*. *Clinical Orthopaedics and Related Research®*, 2010. **468**(9): p. 2328-2332.
232. Mellon, S.J., Kwon, Y.M., Simpson, D.J., Murray, D.W., and Gill, H.S., *THE EFFECT OF ACETABULAR COMPONENT ON CONTACT STRESS DURING FUNCTIONAL ACTIVITY IN METAL-ON-METAL HIP RESURFACING*. *Journal of Bone & Joint Surgery, British Volume*, 2012. **94-B**(SUPP XVIII): p. 55.
233. Elkins, J., O'Brien, M., Stroud, N., Pedersen, D., Callaghan, J., and Brown, T., *Hard-on-Hard Total Hip Impingement Causes Extreme Contact Stress Concentrations*. *Clinical Orthopaedics and Related Research®*, 2010. **469**(2): p. 454-463.

234. Skinner, J., Hart, A., Matthies, A., and Knahr, K., *Metal-on-Metal Bearings in Hip Surgery: The London Implant Retrieval Centre Experience*, in *Total Hip Arthroplasty*. 2012, Springer Berlin Heidelberg. p. 73-90.
235. Cohen, D., *How safe are metal-on-metal hip implants?* BMJ, 2012. **344**.
236. Cobb, A.G. and Schmalzreid, T.P., *The clinical significance of metal ion release from cobalt-chromium metal-on-metal hip joint arthroplasty*. Proceedings of the Institution of Mechanical Engineers, Part H: Journal of Engineering in Medicine, 2006. **220**(2): p. 385-398.
237. Vendittoli, P.-A., Amzica, T., Roy, A.G., Lusignan, D., Girard, J., and Lavigne, M., *Metal Ion Release With Large-Diameter Metal-on-Metal Hip Arthroplasty*. The Journal of Arthroplasty, 2011. **26**(2): p. 282-288.
238. Thompson, M., Heneghan, C., Billingsley, M., and Cohen, D., *Medical device recalls and transparency in the UK*. BMJ, 2011. **342**.
239. *MHRA committee on the safety of devices. Meeting minutes, 19 November 2010. Retrieved on 19 June 2012 from <http://www.mhra.gov.uk/home/groups/clin/documents/committeedocument/con105808.pdf>*.
240. Cawley, J., Metcalf, J.E.P., Jones, A.H., Band, T.J., and Skupien, D.S., *A tribological study of cobalt chromium molybdenum alloys used in metal-on-metal resurfacing hip arthroplasty*. Wear, 2003. **255**(7-12): p. 999-1006.
241. Kinbrum, A. and Unsworth, A., *The wear of high-carbon metal-on-metal bearings after different heat treatments*. Proceedings of the Institution of Mechanical Engineers, Part H: Journal of Engineering in Medicine, 2008. **222**(6): p. 887-895.
242. Wang, A., Yue, S., Bobyn, J.D., Chan, F.W., and Medley, J.B., *Surface characterization of metal-on-metal hip implants tested in a hip simulator*. Wear, 1999. **225 - 229**, Part 2(0): p. 708-715.
243. Anissian, H.L., Stark, A., Good, V., Dahlstrand, H., and Clarke, I.C., *The wear pattern in metal-on-metal hip prostheses*. Journal of Biomedical Materials Research, 2001. **58**(6): p. 673-678.
244. Smith, A.J., Dieppe, P., Vernon, K., Porter, M., and Blom, A.W., *Failure rates of stemmed metal-on-metal hip replacements: analysis of data from the National Joint Registry of England and Wales*. The Lancet, 2012.
245. Shareef, N. and Levine, D., *Effect of manufacturing tolerances on the micromotion at the Morse taper interface in modular hip implants using the finite element technique*. Biomaterials, 1996. **17**(6): p. 623-630.
246. Langton, D.J., Sidaginamale, R., Lord, J.K., Nargol, A.V.F., and Joyce, T.J., *Taper junction failure in large-diameter metal-on-metal bearings*. Bone and Joint Research, 2012. **1**(4): p. 56-63.
247. Reikeras, O. and Gunderson, R.B., *Excellent results of HA coating on a grit-blasted stem: 245 patients followed for 8-12 years*. Acta Orthopaedica, 2003. **74**(2): p. 140-145.
248. *The Royal College of Surgeons of England., An Investigation of the Performance of the 3M™ Capital™ Hip System*. 2001.
249. Fraitzl, C.R., Moya, L.E., Castellani, L., Wright, T.M., and Buly, R.L., *Corrosion at the Stem-Sleeve Interface of a Modular Titanium Alloy Femoral Component as a Reason for Impaired Disengagement*. The Journal of Arthroplasty, 2011. **26**(1): p. 113-119.e1.